Diverse Reactivity of Chelating and Xanthine-Derived Copper-*N*-Heterocyclic Carbenes: Catalytic Activity, Electrochemical Reactivity and Non-Innocent Behaviour

Wasupol Rungtanapirom

Submitted in accordance with the requirements for the degree of
Doctor of Philosophy

The University of Leeds

School of Chemistry

May 2018

The candidate confirms that the work submitted is his/her own, except where contribution from others is stated. The candidate confirms that appropriate credit has been given within the thesis where reference has been made to the work of The candidate confirms that the work submitted is his/her own, except where contribution from others is stated. The candidate confirms that appropriate credit has been given within the thesis where reference has been made to the work of others.

Unpublished evaluation of some ligands in chapter 2 was performed by Joseph Sheppard and the computational ligand map was performed by Natalie Fey (Bristol), as stated in the chapter. Assistance with X-ray crystallographic analysis was provided by Dr Christopher Pask in chapter 5.

Acknowledgements

I would firstly like to thank my supervisor, Dr. Charlotte E. Willans for the warm welcome, help, advice, guidance, encouragement and luck wishes throughout years, and for handling my lack of organisation and influence in English. Most of all, I would like to say that I really appreciate that she has shared a lot of her skills and experiences as a researcher, presenter and lecturer, which are tremendously useful that boost my confidence and creativity.

I would like to also thank Professor Patrick McGowan, who always enjoys my presentations in the group meetings and points out all fabulous ideas, Dr. Christopher Pask, who has made crystallography seems so effortless despite my various failure to grown suitable crystals and those weird results, Professor Michaele Hardie for helping me feel confident in the lab and office, Professor Malcolm Halcrow for all the comments from my previous reports, and Dr. Terrence Kee for his calm supports. I would like to extend my gratitude to Professor Ian Fairlamb and Dr Josh Bray, our collaborators in York on ReactIR.

A big thank you is owe to previous members of the office 1.33 and 1.29. Thanks for the Michael-Jordan duo for the lively atmosphere. Michael, I really have to thank you for all your advice on GC, electrochemistry & CV and for your spectacular writing skills. Jordan, thanks for keeping me awake throughout days with his incredible high-pitch laughter and nights with endless mouse clicking, your finger must have been painful writing up the thesis. I must not forget Heba, who shared the bigger and busier end of the lab during my first 2 years and supported me when my mom was in the hospital. Vikki and Flo, thank you for your interests in Thai culture, food and language, and thank you for our good time playing sporcle geography. Laura, the coolest champion who cheered me up all the time, especially when I was nervously shaking presenting my research, and I wish you can now enjoy Eurovision concerts at the venue every year from now on.

I would like to also express my gratitude to the current members of the offices. Firstly, the surviving member of #TeamWillans, Frances, I have to thank this tough lady for her help and support including the climbing experience, which I did enjoy so much. Jonny, Sam O and Ed, the admiring experts in Lord of the Rings, Pokémon, Harry Potter and Game of Thrones. Those are the little things that have made me felt blended in nicely with you guys although we were not on the same team on Pokémon Go, appreciated being bullied by Team Instinct. Hayder, I envy you every time that we have a cheap but massive Iraqi and

Persian meal, while I cannot provide ThaiEdge food likewise. Our neighbouring office, Kay, Iurii, Pablo, Cecilia, Matt, Namrah, Sam G, Raf, Izar, Emma and Becky, together we're the Inorganic team, the most fun gangster to hang out with although I was kinda drifting away lately. I still wanted you guys to know that without any of you, I would not be this full of positive energy.

I would like to extend my thanks to my old and new colleagues at ThaiEdge restaurant, all members of Leeds-Thai student committee and other Thai PhD students. Puttachart Keasarin, thanks for sponsoring my new camera set and various trips in UK and Italy. Pritaporn Kingkaew, my lovely Olaf sis, who has shared the sorrow and happiness of being PhD students and senior workers. You are also the biggest fan of Disney's and Marvel combined that I have ever met, plus you are the expert in photography, providing me with endless tips. My magical sis, Warangkana Napapongs, thank you for all advice and cheering not only my works but also personal life – I have missed you so much since we were departed, and thanks for making me realised I am not the oldest at the restaurant. Thanamon Visessonchoke and Suphatthana Kanjanawibool, your positive energy has driven me this far. Also I can not forget Chalisa Kanjanarat, the drunkard who understands the world more than me. To the committee team, Chen Phanthasa, Kittiyanee Srihiran and Nonthicha Ruenpanich who put a lot of efforts in organising all the events and activities together, we were such a great team. Sophitha Meenmanee, a big fan of Miss Universe and Confit de Canard, I want to thank you for being a good leader in our team, making me realise how strong I am emotionally, and making the journey to York seem like intra-city. Finally, Dr. Gritiya Rattanakantadilok, Dr. Thanisorn Mahatnirunkul, Dr. Benjapor Pongnarisorn and Narongdej Phanthaphoommee, you guys rock my world here!

Unforgettably, I would like to thank the passing Princess Gulyani Vadhana, who was the patron of my scholarship of (Development and Promotion of Science and Technology) and supported me in my musicality in the past. I would like to extend my thank to members of staff at the Office of Educational Affairs and UK Thai Royal Embassy, who support me financially and emotionally.

Most of all, I must thank my parents who have supported me to pursue many life goals, including PhD. Years of long distance has shown me how much you guys have loved and missed me.

Abstract

This thesis involves the preparation and exploration of the reactivity of a variety of organocopper complexes with *N*-heterocyclic carbene (NHC) ligands. The ligands contain either pyridyl/picolyl/allyl *N*-substituents or a xanthine-derived backbone.

Structural modifications were made to the NHC ligands which were investigated for their catalytic activity when coordinated with Cu(I) *in situ* in an Ullmann-type etherification reaction. The ligand found to be the most active in catalysis was 1-allyl-3-picolylbenzimidazol-2-ylidene.

The catalytic reaction was studied in more detail to assess deactivation pathways through reductive elimination of aryl-imidazolium, dehalogenation and/or homocoupling of aryl iodide. In order to quantify the deactivation pathways, the preparation of novel aryl-imidazolium salts *via* C-2 selective arylation of imidazole, and of a biaryl *via* a Pd-catalysed was necessary, which led to more understanding the Cu-catalysed reaction and further side-reactions.

The arylation of NHC-related species was exploited in the C-2-arylation of xanthine-derived compounds. The reactions were investigated *via* Cu-NHC complexes, prepared using an electrochemical method. The kinetics of the arylation of a xanthine-derived Cu-NHC complex were studied using *in situ* ^{1}H NMR and IR spectroscopies. Optimisation and a full understanding of this reaction has potential application in the detection of mismatched DNA bases.

Further to the non-innocent behaviour of NHCs, an unusual Cu-mediated annulation reaction involving an allyl *N*-substituent was investigated. The reaction is proposed to occur *via* oxidative addition of C-Br to a Cu_2Br_2 cluster, Br migration and reductive elimination of the annulated product. Although most of the reactions discussed in this thesis are thought to proceed *via* a Cu(III) intermediate, the isolation of a Cu(III)-NHC has not been achieved to date. Attempts were therefore made to stabilise a Cu(III)-NHC using the macrocyclic effect, which may allow more understanding of the elusive Cu(III)-NHC intermediate in a variety of reactions.

Table of Contents

Lift of Figures

Chapter 1:

Chapter 2:

Chapter 3:

Chapter 4:

List of Schemes

Chapter 2:

Chapter 3:

List of Tables

List of Abbreviations

Å	Angstrom, 1.0×10^{-10} metres
acac	acetylacetonate
acNac	acetyliminate
(under) Ar	argon
ArH	aromatic proton
Br^-	bromide
BzmH	protons attached to an benzimidazole or benzimidazolium ring
$^{13}C\ \{^1H\}$	Proton-decoupled carbon (NMR)
° C	degrees Celcius
Cl^-	chloride
coe	cyclooctadiene
COSY	homonuclear correlation spectroscopy
Cy	cyclohexyl
δ	chemical shift
DCM	dichloromethane
d	doublet resonance (NMR)
d	deuterium
dba	dibenzylideneacetone
DFT	density functional theory
Dipp	2,6-di*iso*propylphenyl
DMAc	*N*,*N*'-dimethylacetamide
DMF	*N*,*N*'-dimethylformamide
DMSO	dimethyl sulfoxide
e.*g*.	*exempli gratia* (for the sake of example)
eq	equivalence
ESI	electrospray ionisation
et al.	*et alia* (and others)

etc.	*et cetera* (and so forth)
Et_2O	diethyl ether
EtOAc	ethyl acetate
G	Gibbs free energy
GC	gas chromatography
^1H	proton (NMR)
HCl	hydrochloric acid
HOMO	highest occupied molecular orbital
HRMS	high resolution mass spectrometry
Hz	Hertz
I	current
I^-	iodide
IAd	1,3-bis(adamantyl)imidazol-2-ylidene
i.e.	*id est* (that is)
IMes	1,3-*bis*(mesityl)imidazol-2-ylidene
imH	protons attached to an imidazole or imidazolium ring
IR	infrared
J	coupling constant (NMR)
kcal	kilocalorie
kJ	kilojoule
LCMS	liquid chromatography – mass spectrometry
LUMO	lowest unoccupied molecular orbital
NHC	*N*-heterocyclic carbene
m	multiplet resonance (NMR)
MeCN	acetonitrile
MECP	minimum energy cross point
MeOH	methanol
m/z	mass to charge ratio
mA	milliamperes

Mes	mesityl (2,4,6-trimethylphenyl)
MHz	Megahertz
m_s	spin quantum number
NBS	*N*-bromosuccinimide
NHC	*N*-heterocyclic carbene
OTf^-	triflate (trifluoromethanesulfonate)
PF_6^-	hexafluorophosphate
PhCN	benzonitrile
ppm	parts per million
pyH	protons attached to a pyridyl ring
pyrrolH	protons attached to a saturated part of a dihydropyrollo-imidazolium
s	singlet resonance (NMR)
Selectfluor	1-chloromethyl-4-fluoro-1,4-diazoniabicyclo[2.2.2]octane *bis*(tetrafluoroborate)
SIMes	1,3-*bis*(mesityl)-4,5-dihydroimidazol-2-ylidene
sept	septet resonance (NMR)
t	triplet resonance (NMR)
Th	thrianthrene
$Th^{\bullet+}$	thrianthrenyl
THF	tetrahydrofuran
THP	tetrahydropyranyl
V	Voltage
$\%V_{bur}$	percentage of buried volume (sterics)
XnH	protons attached to a xanthine or xanthinium ring

Compounds are labelled throughout chapter 1 as **A** – **DD**

Compounds are labelled throughout chapter 2 – 5 as follows:

P#	imidazole (precursor)

L#	ligand
PS#	precursor of substrate
S#	substrate,
Cy#	annulated product,
Ar#, **ArIm**	anisolyl-imidazolium
ArH	anisole
ArNu	1-(4-anisolyl)-3,5-dimethylbenzene
ArAr	bianisolyl
ArI	4-iodoansiole
C#	metal complex of ligand

Chapter 1

Introduction

1.1 Carbenes and electronic states

Carbenes are neutral species which house a divalent carbon centre with six valence electrons (Figure 1-1).[1-4] They are considered to be electron poor due to disobeying the octet rule, hence are highly reactive.[1,2]

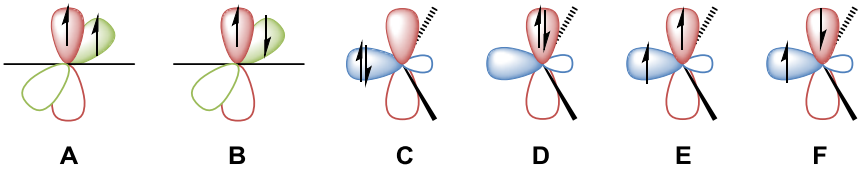

Figure 1-1: Electronic configuration of possible carbenes (**A** – **F**).[1]

A carbene can be linear or bent. The linear type (**A** and **B**, Figure 1-1), a rare case, has a triplet ground state with *sp*-hybridisation. The two degenerate *p*-orbitals are non-bonding, with each possessing an electron in the same spin quantum number, m_s (Figure 1-2).[1,5] The bent carbene centre (**C** – **F**, Figure 1-1) has sp^2-hybridisation which removes the degeneracy of the two non-bonding orbitals. Despite the absence of degeneracy, bent carbenes can exist in either singlet or triplet ground state.[1,4] The multiplicity of a carbene centre is determined by the energy gap between σ and p_π orbitals, which is influenced by the steric and electronic properties of the α-substituents neighbouring the carbene centre.[6] For instance, bulky α-substituents lead to a pseudo linear geometry to minimise the steric interaction, and a triplet carbene is favoured when the energy gap between σ and p_π orbitals is below 1.5 eV (Figure 1-3). A singlet carbene is favoured when the α-substituents are π-donating, which increases the *p*-orbital energy, hence contains a larger energy gap (Figure 1-4).[4]

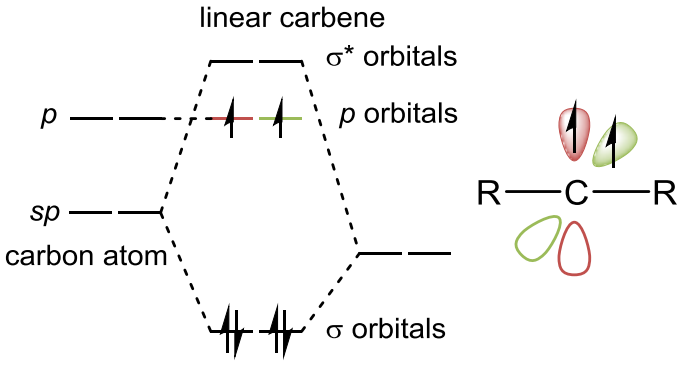

Figure 1-2: Energy diagram for the linear methylene carbene.[1]

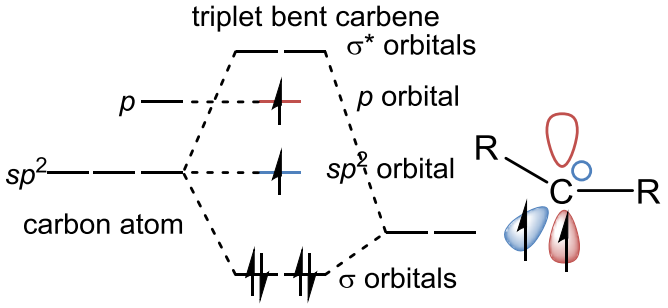

Figure 1-3: Energy diagram for the bent triplet methylene carbene.[1]

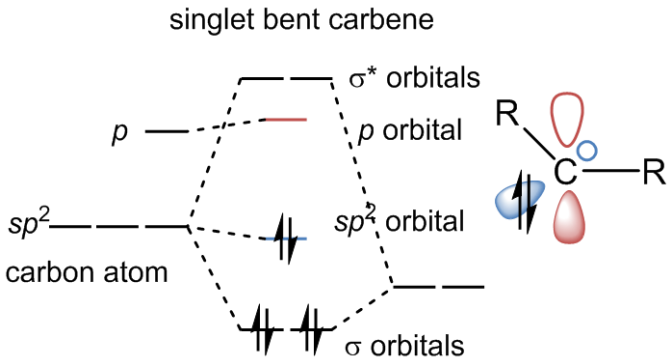

Figure 1-4 Energy diagram for the bent singlet methylene carbene.[1]

1.2 *N*-Heterocyclic carbenes (NHCs)

An *N*-heterocyclic carbene (NHC) is an example of a singlet carbene. It is a ring (usually 5-membered) with a carbene centre having two adjacent π-electron-donating nitrogen atoms.[1] The electronic properties of the nitrogen atoms are the main key to NHC stabilisation. The sp^2-hybridised non-bonding lone pair of an NHC is stabilised by a σ-inductive withdrawing effect from the electronegative nitrogen atoms, thus lowering the HOMO orbital energy.[3,4,7,8] Moreover, the orbital π-interaction of the empty NHC *p*-orbital with two electron lone pairs of two α-amino groups, namely mesomeric effect, raises the LUMO

orbital energy (Figure 1-5).[2-4,7-9] These electronic properties render NHCs stable and strong Lewis base donors.

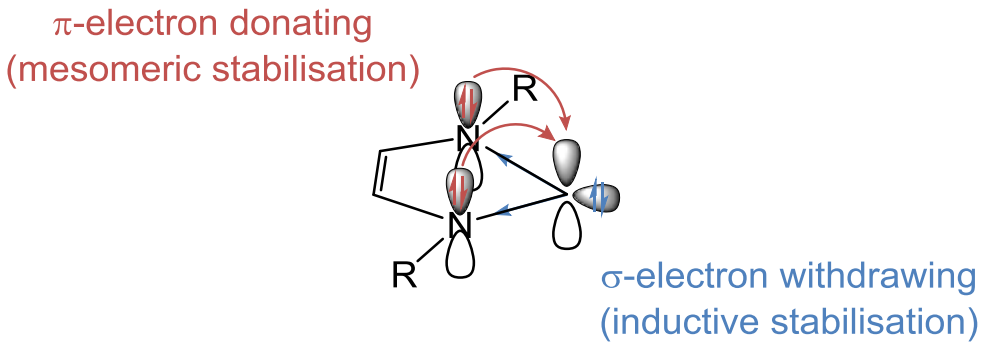

Figure 1-5: Electronic stabilising factors of an NHC.[10]

In addition to the electronic factors, bulky *N*-substituents help stabilise an NHC. For example, bulky adamantyl *N*-substituents make the free NHC more kinetically stable due to steric protection of the carbene centre.[2,4,7,9] The first free (uncoordinated) NHC, 1,3-di(1'-adamantyl)imidazole-2-ylidene (IAd, Scheme 1-1), was established in 1991 by Arduengo,[2,9,11] which sparked a significant amount of interest in NHC research. The persistent NHC was synthesised by deprotonation of its imidazolium precursor using a strong base (NaH).

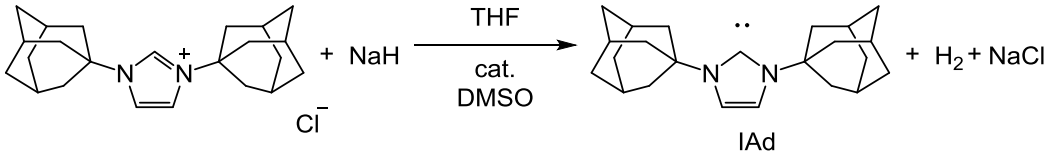

Scheme 1-1: Preparation of IAd, the first isolated free NHC.[9]

1.3 Metal-NHC complexes and their synthesis

The idea of utilising carbenes as ligands was suggested in 1962 by Wanzlick.[12] Although the isolation of a free NHC was not initially reported, the first metal-NHCs were reported in 1968 independently by Öfele[13] and Wanzlick.[14] The real spark for NHCs occurred in 1991 with the first isolation of IAd, which allowed for thorough examination of electronic and steric properties of NHCs.[9] NHCs are strong σ-electron donors, generally stronger than phosphine ligands.[15] Another major difference of NHCs compared to phosphines are the steric properties of the ligand.[2,10] Phosphines have their substituents pointing away from the metal centre, with tetrahedral geometry around the phosphorus atom, which results in a cone shape. NHCs derived from imidazolium salts give an umbrella-shape, with their *N*-substituents pointing towards the metal centre. Tolman angles, θ, are used for phosphine ligands to compare their steric

parameters, while NHC complexes use the percentage of buried volume, $\%V_{bur}$ (Figure 1-6).[16,17] The $\%V_{bur}$ is the percentage of occupied volume by a ligand inside a sphere of 3 Å radius, which is roughly the distance between a metal centre and a nitrogen atom.

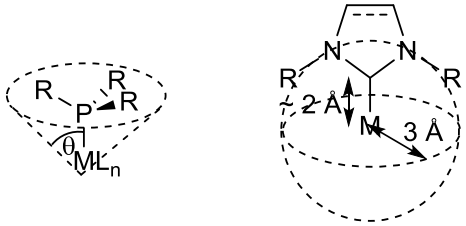

Figure 1-6: Comparison of the different shapes of steric encumbrance imposed by phosphine and NHC ligands.[16]

Several methods can be used to prepare metal-NHC complexes, with the NHC precursor often being an imidazolium salt. Imidazolium salts can be prepared by functionalisation of imidazole derivatives at the N-1 and N-3 positions, building an imidazolium ring *via* condensation reactions or a combination of both methods.[2]

i) Deprotonation of H-imidazolium and metallation

Arduengo employed a strong base to deprotonate an imidazolium salt to give a free NHC,[9] which can subsequently be reacted with a metal salt, or a metal complex bearing a labile ligand, to give a metal-NHC complex. However, a strong base may be unsuitable in the case of some imidazolium salts that have acidic protons other than the H-imidazolium. In addition, isolation of the NHC may be difficult due to instability in the absence of bulky groups. Alternatively, a free NHC can be formed *in situ*, a method that does not require such a strong base. Weaker bases such as K_2CO_3,[18-21] Cs_2CO_3,[22,23] NaOAc[24] and KO*t*Bu,[25,26] which are generally stable to air and moisture, can be used to prepared the complex. As an example, Li *et*. *al*. utilised an imidazolium **G** with K_2CO_3 and $PdCl_2$ in pyridine, which acts as both solvent and ligand, to form the corresponding Pd-NHC complex **H** (Scheme 1-2).[18]

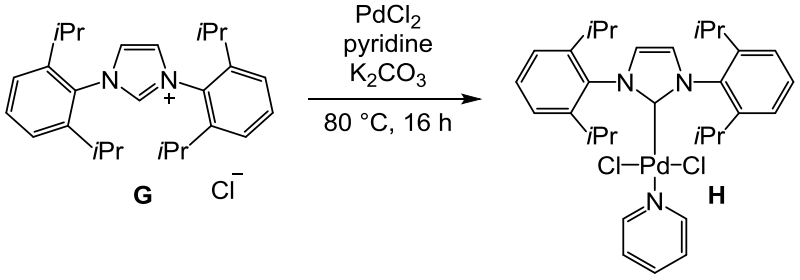

Scheme 1-2: Preparation of a Pd-NHC complex **H** *via in situ* deprotonation.[18]

Another synthetic method uses a basic metal precursor, which combines base and metal source together, and was used by Öfele and Wanzlick to form the first example of metal-NHCs.[13,14] Nowadays, the metal precursors are usually oxide,[27-33] acetate[34,35] or amide[36] salts. For example, Ag_2O is commonly used for the preparation of Ag-NHC complexes, with the solvent used being varied due to the differing solubility of imidazolium precursors (usually DCM, MeOH, MeCN or THF).[37-40] For example, an imidazolium bromide salt **J** is soluble in MeOH, while a PF_6^- salt **K** is soluble in MeCN (Scheme 1-3).[40]

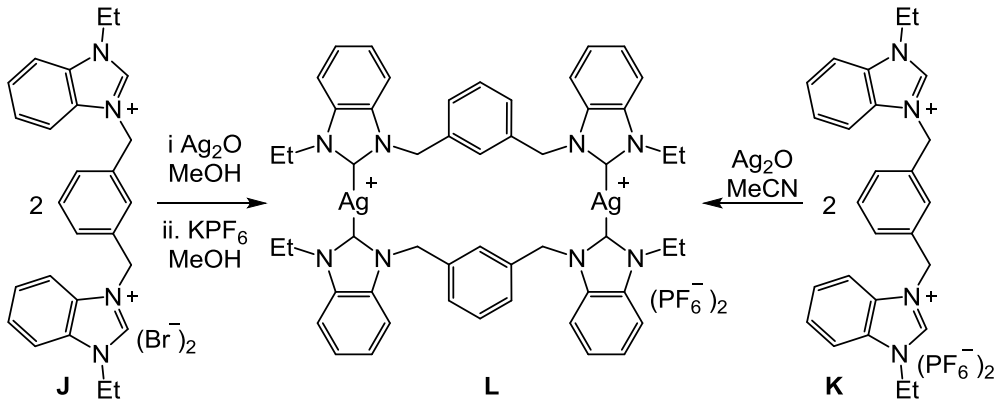

Scheme 1-3: Preparation of a Ag-NHC complex **L** using the basic metal precursor Ag_2O.[40]

ii) Silver transmetallation

Ag-NHC complexes can act as an NHC source, from which the ligand can be transmetallated on to another metal.[24,41-44] The first reported example of this method was the preparation of $PdCl_2(NHC)_2$ **N** and AuBr(NHC) **P** complexes from a Ag-NHC complex **M**, which produced AgBr or AgCl as a by-product (Scheme 1-4).[45] The formation and precipitation of Ag halides makes the transmetallation exothermic and thermodynamically favourable.

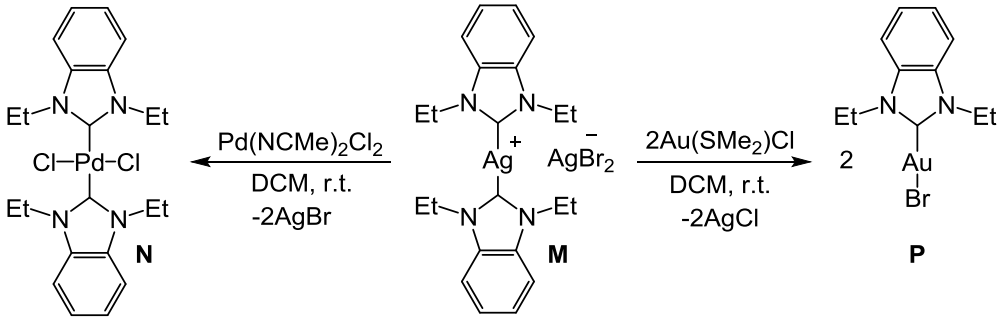

Scheme 1-4: Examples of silver transmetallation.[45]

iii) Oxidative addition

H-imidazolium and halo-imidazolium salts can be activated by transition metals to form metal-NHC complexes with higher oxidation state such as Ni(II), Pd(II) and Pt(II). This method may also be used in catalytic C-H or C-X activation and forms a metal-NHC complex as a reaction intermediate. For example, an H-imidazolium **Q** cation can be activated by a Ni(0) complex **R** and forms a Ni(II)-NHC complex **S** (Scheme 1-5).[46] This is followed by an alkene π-coordination, β-migration and reductive elimination of an alkyl-imidazolium ion product **W**.

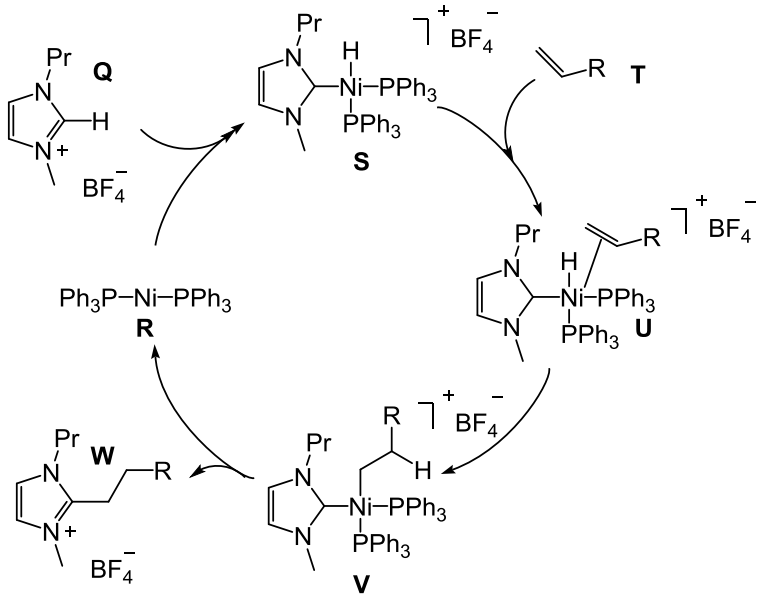

Scheme 1-5: Ni-catalysed reaction between imidazolium (**Q**) and alkene (**T**) *via* Ni-NHC complex intermediates (**S**, **U** and **V**).[46]

Another example of the formation of a metal-NHC through oxidative addition is prepared from an imidazole. A C-H bond of an alkenyl benzimidazole **Z** was oxidatively added to Rh(I) and formed a Rh(III) complex **AA**.[47] This was followed by a proton migration, which reduced the metal centre and oxidised the anionic ligand to form an H-*N*-substituted NHC ligand on a Rh(I) complex **AB**, a rare example of such type (Scheme 1-6).

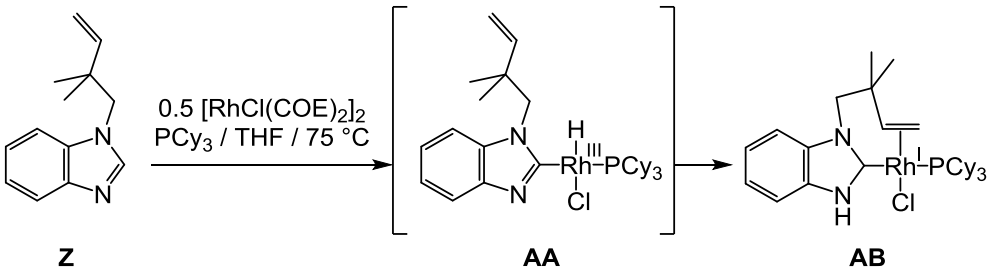

Scheme 1-6: Formation of a Rh-NHC complex *via* oxidative addition of an imidazole and H-migration.[47]

iv) Electrochemical synthesis

For some types of imidazolium *N*-substituents, deprotonation to form free NHC, or metallation with *in situ* deprotonation can be unsuccessful in preparing metal-NHCs, often a result of other acidic protons in the imidazolium precursor.[48,49] Electrolysis can be used as an alternative method to form metal-NHC complexes. At the sacrificial anode, the metal is oxidised to an accessible metal ion, for example Cu(I), Ag(I), Ni(II) and Fe(II), releasing ions into solution.[49,50] Simultaneously, at the cathode, the imidazolium ion is reduced to a free carbene with the release of hydrogen gas. The generated carbene then forms a complex with the metal ions in solution (Scheme 1-7).

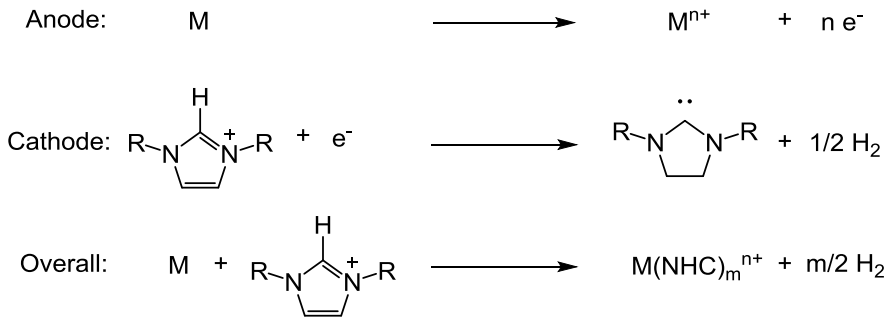

Scheme 1-7: Electrolysis to form metal-NHC complexes.[49]

1.4 Metal-NHC complexes in catalysis

An NHC ligand can be used to improve a ligand-free metal catalyst, and often enhances the reaction over other types of ligands such as phosphines. As a consequence of the strong electron donation of NHCs, the stability of the catalyst may improve.[15,51] Moreover, the steric protection of the metal by the ligand also helps reduce catalyst decomposition.[10] Metathesis reactions,[52-57] catalysed by ruthenium complexes, and cross-coupling reactions[52,58-63] to form C-C, C-B, C-N, C-O, and C-S bonds, catalysed by Pd and other metals, are the most commonly studied reactions by metal-NHC complexes.

An example showing significantly enhanced performance by an NHC ligand is the second generation Grubbs catalyst (Grubbs II) (Figure 1-7).[1,55] Mechanistic studies of Grubbs II catalyst shows that replacing a phosphine ligand (Grubbs I) with SIMes further stabilises the metallacyclobutane intermediate.[16]

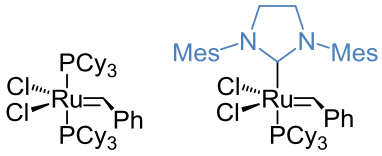

Grubbs I Grubbs II

Figure 1-7: The structure of Grubbs I and Grubbs II catalysts.[55]

1.4.1 Cu-NHC complexes in cross-coupling reactions

Pd complexes have been applied as catalysts in many well-known cross-coupling reactions such as Heck,[64,65] Suzuki[66] and Stille[67] reactions. Cu-catalysed cross-coupling reactions started their history in the early 20th century when Ullmann reported the use of stoichiometric amounts of Cu to prepare diaryl compounds, and later other types of C-X bond couplings *e.g.* C-O, C-N and C-S.[68-70] However, due to the requirement for excess Cu, high reaction temperatures (above 200 °C), harsh bases and limited substrates, the Cu-mediated cross-coupling reactions were not developed at that time. Bidentate ligands such as bipyridines and phenanthrolines were developed as they were found to promote cross-coupling reactions without the need for such harsh conditions.[71,72] The use of Cu in industry has significant advantages over Pd, as it is much more abundant and has lower toxicity. Furthermore, unlike Pd catalysts, which usually require expensive, complicated and air-sensitive ligands, ligands for Cu catalysts are not as complex,[73] such as bipyridine, acac, acNac and NHC ligands. Still, the knowledge of Cu-NHC cross-coupling reactions is limited, as there are few examples of the application.[38,60-64] However, as the electronic and structural properties of NHCs can be easily modified, this provides promise to the field.[41,74-78]

Biffis and co-workers reported the first example of Cu-NHC catalysts for cross-coupling reactions in 2008. A tri-nuclear Cu-NHC complex **AC** was found to be an active catalyst in C-N, C-O and C-C_{alkyne} bond forming reactions, with various aryl halide substrates, at 100 °C using 3 mol % **AC** catalyst (or 9 % equivalents of Cu) (Scheme 1-8).[74,75] It was noted that aryl iodide is more efficient than its aryl bromide counterpart, and that electron-poor aryl iodides lead to a higher conversion to arylated product than electron-rich aryl iodides, which is typical for Cu-catalysed reactions.[79,80]

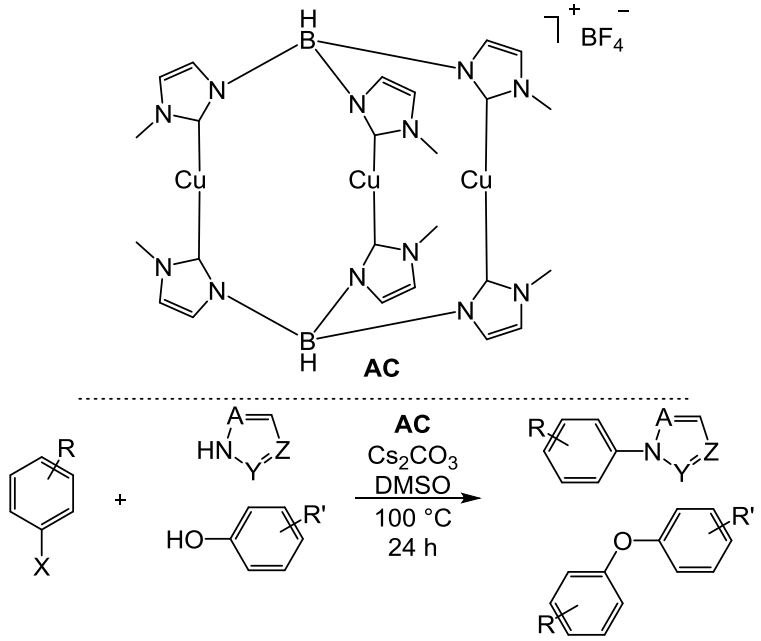

Scheme 1-8: A tri-nuclear Cu-NHC complex and its application as a catalyst in cross-coupling reactions.[74]

In 2014, our group demonstrated that pyridyl-tethered NHC ligands can stabilise Cu(II) bromide complexes despite them being neutral ligands. The Cu(I)-NHC complexes were screened in the etherification of an electron-rich aryl halide with dimethylphenol, at 90 °C in MeCN, which was shown to promote catalytic activity compared to a ligand-free system.[41] It is possible that the chelating NHC can stabilise higher oxidation state intermediates (as demonstrated by the stabilisation of Cu(II)) and also push the substrate into a *cis*-coordination. In 2018, Tahsini showed the application of Cu-NHCs *e.g.* **AD** with pincer ligands in Sonogashira-type reactions, at 140 °C in DMF, using K_2CO_3 as the base.[81] The chelating effect of the ligand leads to a stable complex which enables the reaction to be carried out successfully in air, which gave 80 – 96 % of the coupled products (Scheme 1-9).

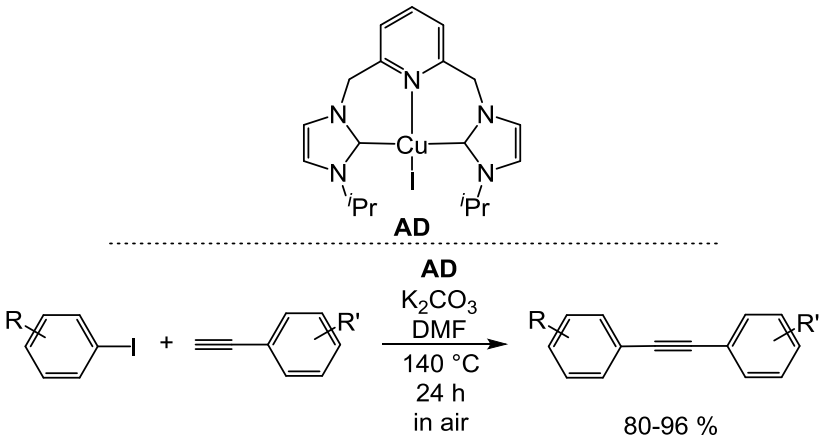

Scheme 1-9: A Cu-NHC pincer complex and its application in a Sonogashira-type reaction.[81]

1.5 Non-innocent activities of NHC ligands at metals

Although metal-NHC bonds are considered strong, there is evidence for the involvement of NHC ligands in reactivity at metals,[82] such as reductive elimination,[34,41,83-91] ligand insertion,[87,92-96] NHC ring opening,[92,97-99] ligand substitution,[100] and *N*-substituent activation.[101]

1.5.1 Reductive elimination of alkyl/aryl-imidazolium salts

i) Observed as side-reactions during catalysis

NHC ligands are most likely to become involved in reductive elimination when they are coordinated to a metal in high oxidation state. Cavell first reported NHC ligands coordinated to Pd(II) undergoing reductive elimination of methyl-imidazolium and forming Pd(0) as a by-product.[102] The Pd(II) complexes **AE** and **AF** are stable at high temperatures and were screened for their catalytic activity in the Heck coupling reaction of 4-bromoacetophenone (**AG**) and *n*-butylacrylate (**AH**) to form *n*-butyl-(E)-4-formylcinnamate (**AJ**), whereas complex **AK** was not stable at 120 °C in DMSO, and led to complex decomposition. The decomposition pathway of complex **AK** was unknown, so it was treated with $AgNO_3$ to remove a chloride ligand, which resulted in complex **AL**. Complex **AL** was found to undergo reductive elimination of methyl-imidazolium nitrate (**AM**) and form Pd(0) species.

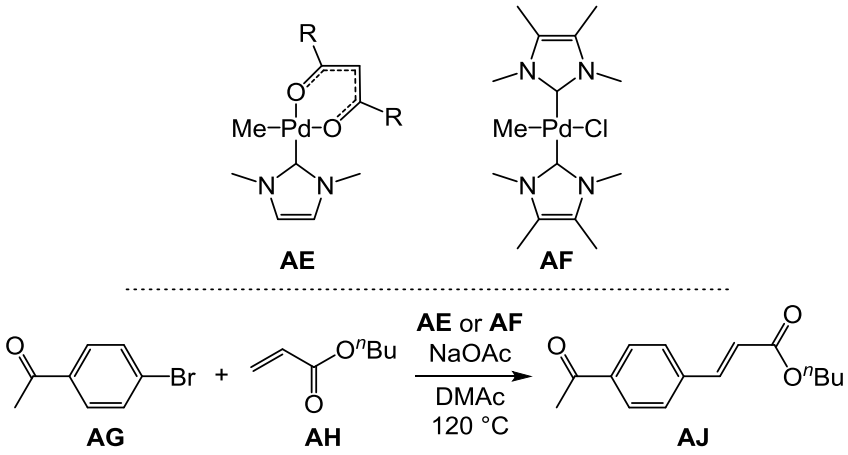

Scheme 1-10: Pd(II)-NHC complexes **AE** and **AF**, and their application in a Heck coupling reaction.[102]

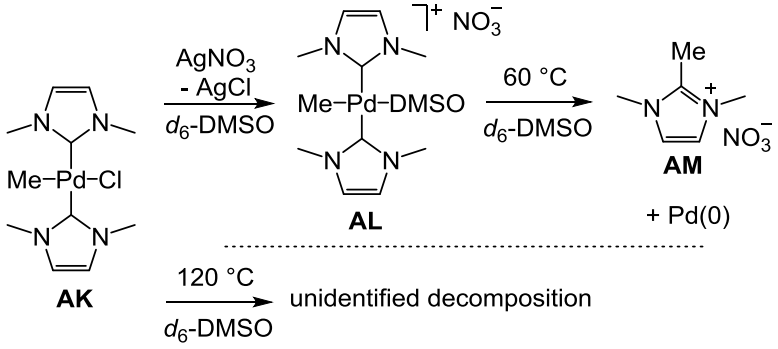

Scheme 1-11: Decomposition of a Pd(II)-NHC complex **AL** *via* reductive elimination of the imidazolium salt **AM**.[102]

Reductive elimination of an NHC can also occur with intramolecular substrates. An imidazolium salt bearing a but-3-enyl *N*-substituent (**AN**) ultimately led to the formation of a 5-membered ring (**AR**) when reacted with Ni(0) (Scheme 1-12).[103] The reaction was suggested to occur *via* the oxidative addition of the H-$C_{imidazolium}$ bond to the Ni(0) centre, with subsequent alkene coordination to form a Ni(II)-NHC complex **AP**. H-insertion of the metal hydride to the alkene to form **AQ**, and reductive elimination would produce the cyclic imidazolium ion **AR**.

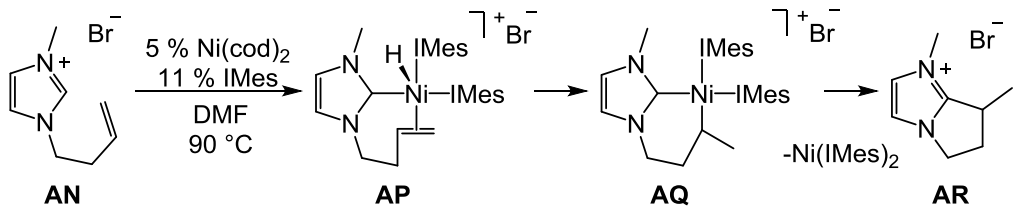

Scheme 1-12: Cyclisation of a but-3-enyl *N*-substituent.[103]

Reductive elimination of a *bis*(imidazolium) ion (**BC**) has been found to occur from a Cu(III) centre, following silver transmetallation of the NHC with one

equivalent of $CuBr_2$. The reaction was found to only occur when the *N*-substituents of the NHC were a mesityl and a 2-pyridyl group (Scheme 1-13).[84] DFT calculations demonstrated that the reaction occurs *via* formation of a Cu(II)-NHC complex **AU**, which reversibly dimerises through halide $(\mu\text{-}Br)_2$-bridges (**AV**). The dimer undergoes disproportionation to a mixed Cu(III)-Cu(I) species (**AW**), followed by reductive elimination at the Cu(III), resulting in formation of a bromoimidazolium salt **AZ** and a Cu(I)-NHC complex **BA** (Figure 1-8). This step is slightly endothermic (+2.2 kJ mol^{-1}).

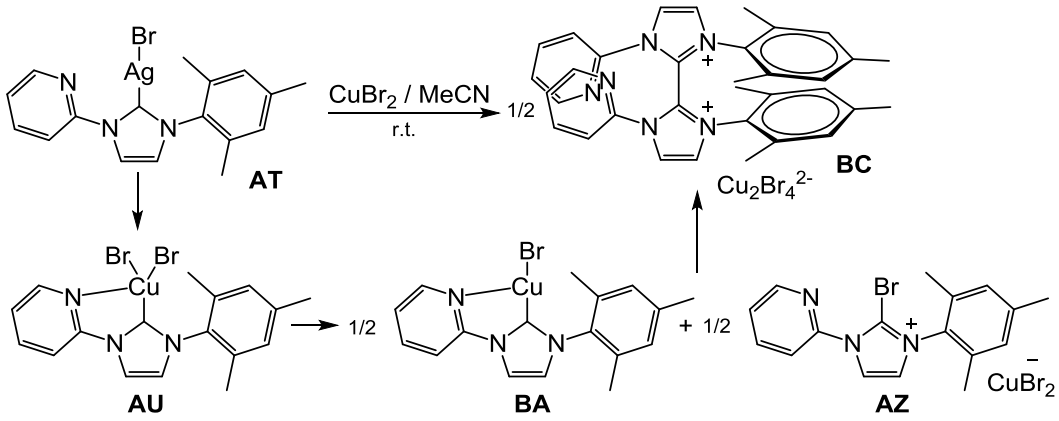

Scheme 1-13: Formation of Cu(II)-NHC containing mesityl and pyridyl *N*-substituents leading to formation of *bis*(imidazolium) cuprate salt.[84]

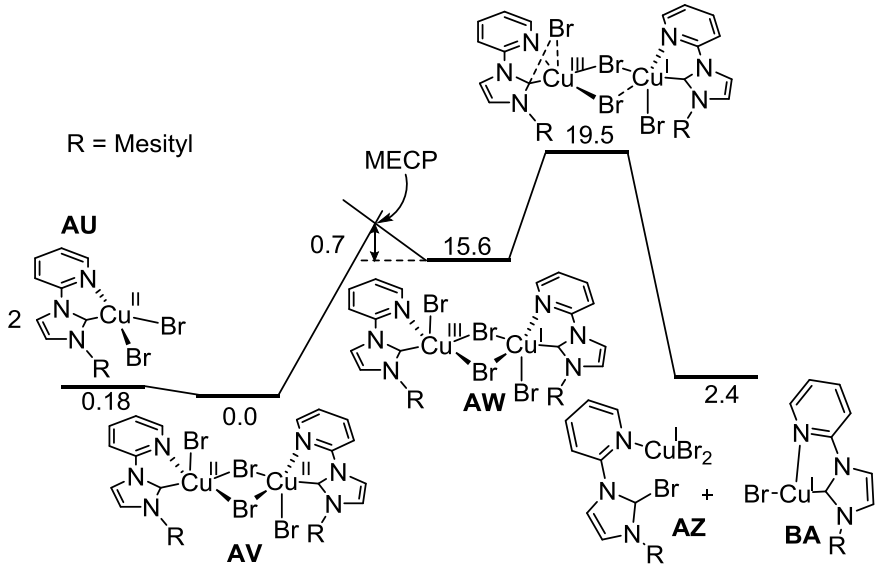

Figure 1-8: DFT calculations for the formation of a bromoimidazolium cuprate salt (**AZ)** and a Cu(I)-NHC (**BA**).[84]

Bromoimidazolium **AZ** is oxidatively added to complex **BA** and forms an octahedral Cu(III)-NHC complex **BB**, which has NHCs *cis* to each other (Figure 1-9). The intermediate **BB** is stabilised by the π-π stacking interaction between the relatively electron rich mesityl *N*-substituents of one ligand and relatively

electron poor pyridyl substituent of the others. Reductive elimination at **BB** occurs with a comparatively low energy barrier ($\Delta G^{\ddagger}$ = 9.4 kcal mol^{-1}) and forms the *bis*(imidazolium) salt **BC**. Overall the reaction is exothermic (-12.4 kJ mol^{-1}) and accessible, likely due to the stabilisation of **BB** and the low energy barrier of the reductive elimination of **BC**.

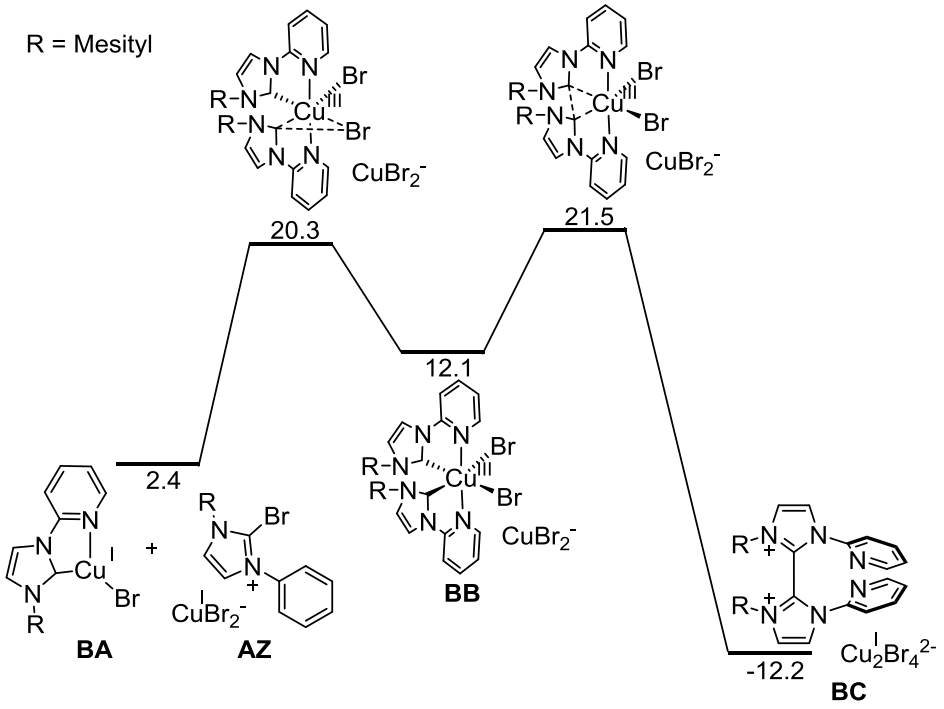

Figure 1-9: DFT calculations for the formation of bis(imidazolium) cuprate salt **BC**.[84]

The involvement of NHCs in reductive elimination becomes an issue when it occurs during catalysis, as it consumes both the substrate and the active metal-NHC catalyst.[104,105] This may also occur when reactions are performed in imidazolium ionic liquids, which can result in arylation of imidazolium, consuming aryl halides.[106]

Efforts have been made to reduce the reactivity of NHCs by using chelating *N*-substituents to block aryl/alkyl substrates coordinating *cis* to the NHC.[90,91,107] Cavell used amino (**BD**) and pyridine (**BF**) groups as *N*-substituents to form tridentate complexes with Pd(II) and a methyl ligand (Scheme 1-14). The stability of the complex **BF** increased tremendously compared to non-chelating Pd(II)-NHC complexes and complex **BD** and slow reductive elimination of **BG** from **BF** only occurred at temperatures above 120 °C.

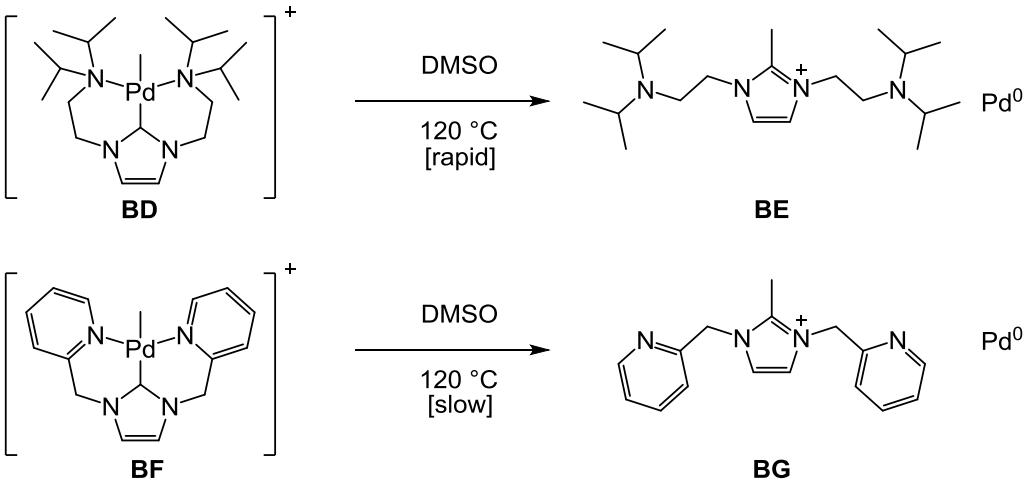

Scheme 1-14: Reductive elimination from a tridentate Pd-NHC complex.[107]

ii) Exploited for synthesis

Cavell and co-workers took advantage of the reductive elimination of a methyl-imidazolium **BJ** from complex **BH** (pre-catalyst) to generate an active bent Pd(0)-diphosphene complex (**BK**) upon heating (Scheme 1-15).[89] **BK** can then undergo oxidative addition with aryl halide, with coupling of substrates to give desired products.

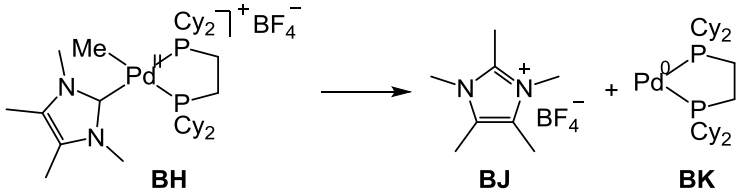

Scheme 1-15: Pd(0) catalyst is generated from reductive elimination of methyl-imidazolium **BJ**.[89]

The reductive elimination of an aryl-imidazolium was used to study the catalytic mechanism of a Heck reaction catalysed by a Pd(0)-*bis*(NHC) complex **BL** (Scheme 1-16).[104] The reaction was proposed to take place *via* oxidative addition of aryl halide to **BL** to form the Pd(II) complex **BM**, followed by insertion of the alkene and β-hydride elimination. To confirm the formation of the intermediate **BM**, $AgBF_4$ was added to the reaction mixture, which removed I^- from **BM** and trapped the reaction (Scheme 1-17), making the Pd complex less stable and resulting in the formation of aryl-imidazolium **BR**, alkyl-imidazolium **BT** and H-imidazolium ions **BV**.

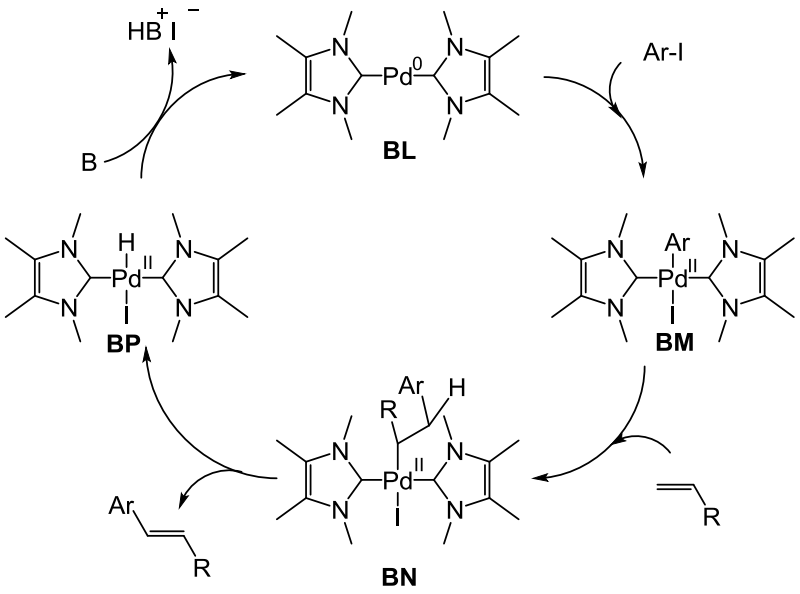

Scheme 1-16: Proposed mechanism of a Heck reaction using Pd(0)-*bis*(NHC) **BL** as the catalyst.[104]

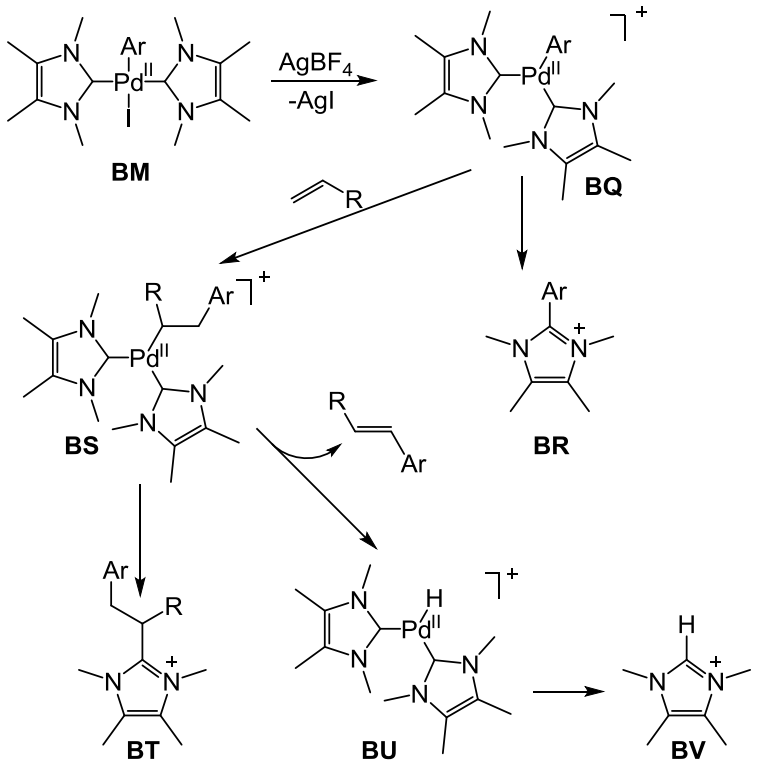

Scheme 1-17: Proposed mechanism in the formation of imidazolium side-products **BR**, **BT** and **BV**.[104]

The aryl/alkyl-imidazolium salts can be used to prepare mesoionic NHC ligands.[108-110] Instead of a coordination site at the C-2 position, the site is blocked and the ligand coordinates at the C-4 or C-5 position. For example, Reichmann demonstrated a coupling reaction between an NHC and aryl halide using a Pd(0) catalyst, followed by metallation with CuI to afford a mesoionic Cu-NHC **CA**

(Scheme 1-18).[111] The mesoionic NHC complex has often outperformed catalytic activities compared to its normal NHC complex.[112-116] For example, mesoionic Ru(II)-NHC complex **CB** has a higher catalytic activity and higher selectivity towards product **CF** than complex **CC** in addition of benzoic acid **CE** to terminal alkyne (phenylacetylene, **CD**).[115]

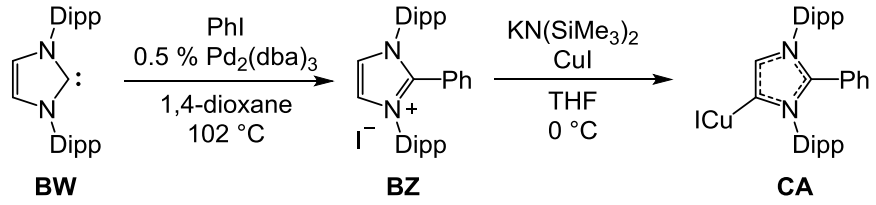

Scheme 1-18: Preparation of a mesoionic Cu-NHC complex.[111]

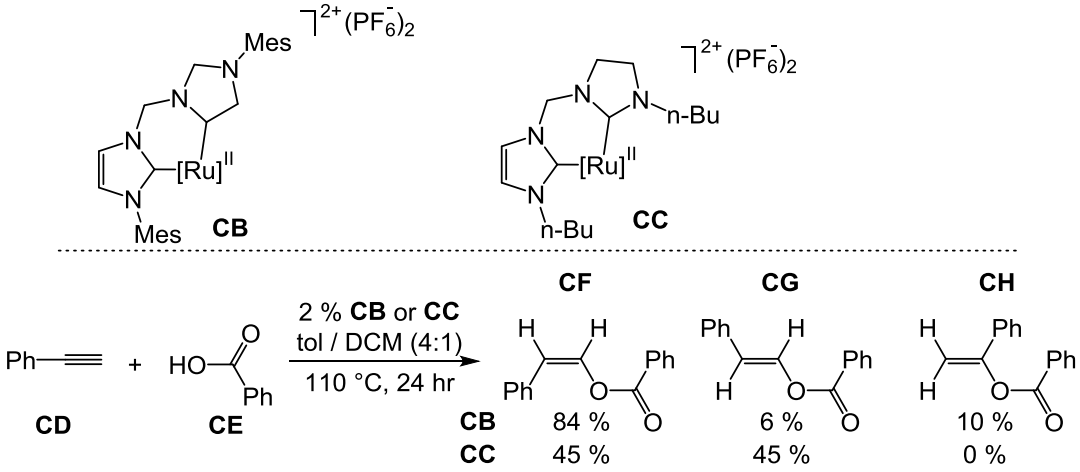

Scheme 1-19: Structures of Ru(II)-NHC **CB** and **CC**, and Ru-catalysed addition of benzoic acid **CE** to phenylacetylene **CD**.[115]

1.5.2 Reductive elimination of halo-imidazolium salts

NHCs are considered soft bases and unsuitable for highly charged metals, hence are likely to take part in reductive elimination. An attempt to prepare a Cu(III)-NHC complex *via* oxidation of a Cu(I)-NHC halide complex using Selectfluor as the oxidant led instead to reductive elimination of a halo-imidazolium salt.[83] In addition to the unsuitable Cu(III)-NHC pairing, Cu(III) compounds are usually unstable and easily reduced to Cu(II) in aqueous solutions ($E_{1/2}$ = +1.57 V).[117]

Although Cu(II) compounds are common, the preparation of Cu(II)-NHCs is more challenging due to the hard acid – soft base interaction. A Cu(II)-NHC acetate **CJ** complex can be prepared and isolated but the preparation of a Cu(II)-NHC bromide complex of the same ligand is not possible.[34] The acetate ligand has an advantage that it is bidentate, which can form a Cu(II) complex that has 19

electrons with two acetate ligands. Similarly, Cu(II)-NHC complexes **CK** and **CL** are examples of Cu(II)-NHC complexes bearing an anionic alkoxy group, which are stable and have 17 electrons.[118,119] A Cu(II)-NHC complex with bromides has only 15 electrons, though can undergo (μ-Br)$_2$ dimerisation to form a 17-electron species **CM**.[34] However, the bridging of **CM** decomposes to **CN** and **CP**, which was proposed to occur *via* disproportionation of the two Cu(II) centres to Cu(I) and Cu(III) and reductive elimination of **CP** at Cu(III). However, the mechanism had not been confirmed in the work.

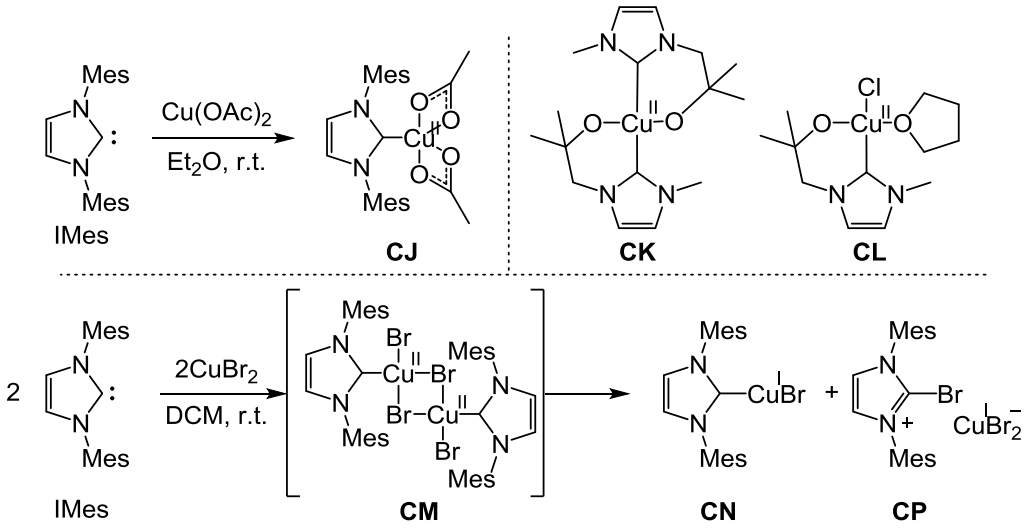

Scheme 1-20: Preparation of a Cu(II)-NHC acetate complex (top left),[34] structure of complexes **CK** and **CL** (top right),[118] and reductive elimination from a Cu-NHC bromide to give a bromo-imidazolium salt (bottom).[34]

Subsequently, our group demonstrated that the preparation of a Cu(II)-NHC bromide **CQ** with a neutral ligand is possible when the *N*-substituent has a coordinating pyridine group.[41] This would help stabilise the Cu(II) centre (17 electrons) and the bridging dimerisation of the complex does not occur. However, when excess $CuBr_2$ is present, (μ-Br)$_2$ bridging does occur with the excess $CuBr_2$, forming **CR** (Scheme 1-21).[84] The bridging leads to disproportionation (**CS**) and reductive elimination of a bromo-imidazolium ion **CT**. DFT calculations also support this observation, which occurs at room temperature. The bridged **CR** forms irreversibly, and disproportionation takes place with a low energy barrier (9.0 kcal mol^{-1}). The low barrier is likely a result of the pyridine group helping stabilise the Cu(III) centre. The reductive elimination of **CT** is also facile, with a calculated energy barrier of 3.0 kcal mol^{-1}.

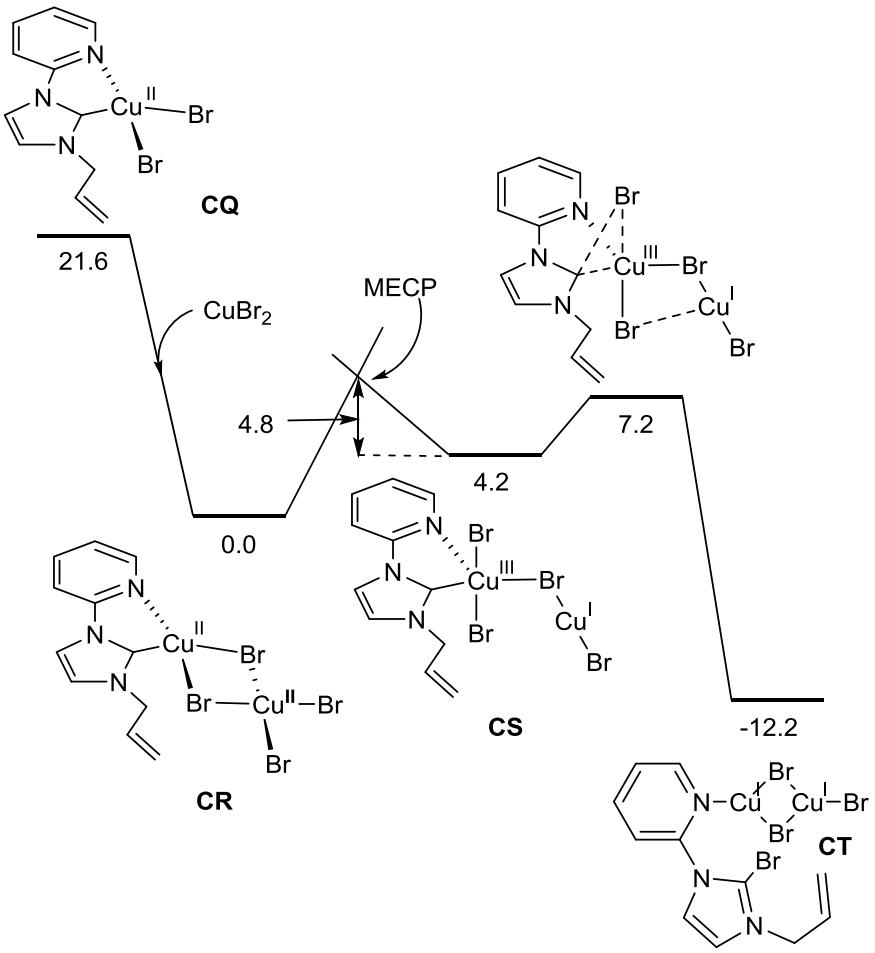

Scheme 1-21: DFT calculations showing favourable reductive elimination of a bromo-imidazolium ion.[84]

1.5.3 Selectivity of reductive elimination

The reductive elimination of C-imidazolium ions has been observed to be more prominent than the reductive elimination of halo-imidazolium ions when both carbon species and halides are present on the metal-NHC.[28,104,120-122] The selectivity of such reactions on Cu were studied by Ariafard using DFT calculations.[123] He showed that the selectivity is due to the stability of the Cu(I) by-product (**CW**), which governs both the kinetics and thermodynamics of the reaction. Hence, soft bases such as halides, CN^- and CF_3^- ions are less likely to cleave as they form more stable Cu(I) salts than hard bases such as alkyls and aryls. The DFT calculations demonstrate that reductive elimination of bromo-imidazolium ions (**CV**) are unfavourable when anionic hydrocarbon ligands are present (Scheme 1-22, Figure 1-10).

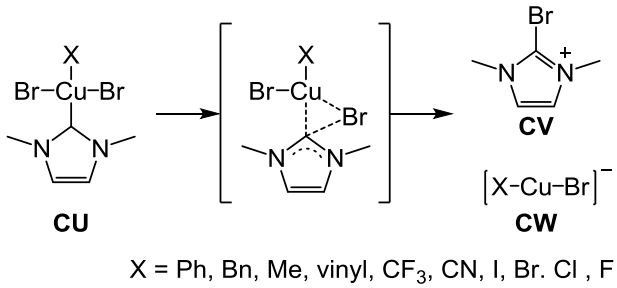

X = Ph, Bn, Me, vinyl, CF_3, CN, I, Br. Cl , F

Scheme 1-22: Reductive elimination of bromo-imidazolium ion (**CV**) from Cu(III) (**CU**) when X is present.

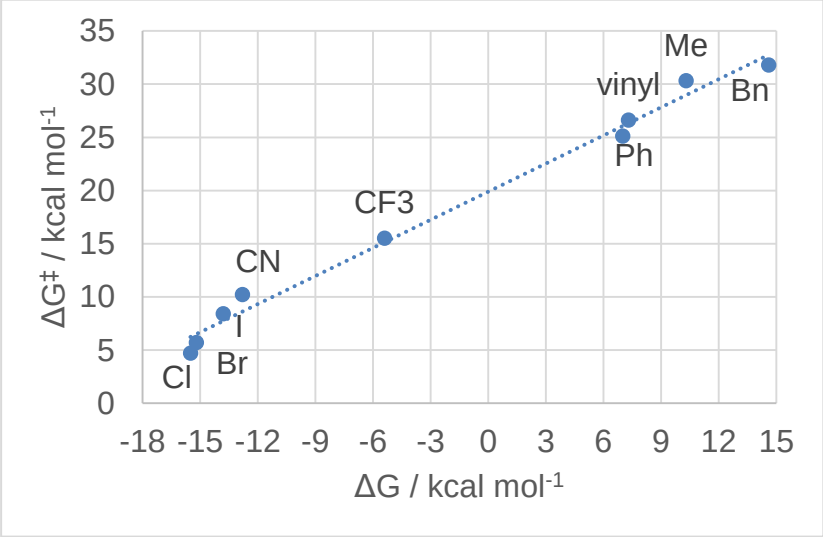

Figure 1-10: Correlation between kinetic and thermodynamic energies in the reductive elimination of **CV** in the presence of an X ligand (X = Cl, I, Br, CN, CF_3, Ph, vinyl, Me and Bn).

1.6 Stable copper(III) complexes

In order to further demonstrate the oxidative addition / reductive elimination mechanism in Cu-catalysed cross-coupling reactions, attempts to synthesise Cu(III) species have been carried out. However, Cu(III) compounds are usually unstable and easily reduced to Cu(II) in aqueous solutions.[117] In addition, the reduction potential of Cu(III) to Cu(II) is +1.57 V. Cu(III) complexes usually have a square planar geometry which is common for d^8 electronic configurations. Square planar Cu(III) complexes are diamagnetic, whereas rare cases of octahedral Cu(III) complexes are paramagnetic.[124,125]

Cu(III) may be stabilised through coordination with oxides and fluorides such as Cs_3CuF_6 and K_3CuF_6, which are paramagnetic octahedral complexes. $KCuO_2$ (**CZ**) and $K_7[Cu(IO_6)_2]$ (**DA**) are examples of diamagnetic square planar Cu(III) complexes (Figure 1-11). Hence, early reported stable Cu(III) complexes are square planar and contain anionic binding sites. Their chelating ligands have

anionic thiolate (**DB**), alkoxide and amide (**DC**) binding sites (Figure 1-12). These complexes showed ligand-dependent reduction potentials of Cu(III) to Cu(II), which decreases to a range of -1.0 to +0.1 V. Therefore, Cu(III) can be stabilised by strong electron donors.

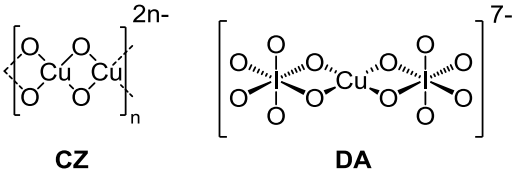

Figure 1-11: Examples of Cu(III) oxide anions[124]

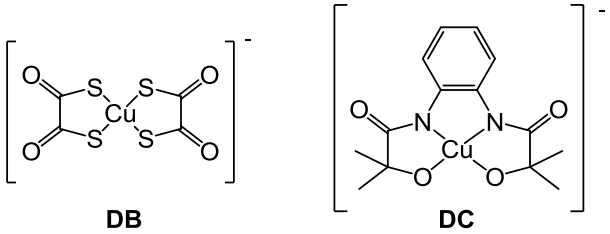

Figure 1-12: Examples of Cu(III) complexes bearing anionic-tethered ligands[124]

Upon attempts to study intermediates in Cu catalysed reactions, the preparation of organo-Cu(III) complexes became an interesting challenge. Ribas used macrocyclic ligands that combine square planar binding sites and an anionic site to successfully isolate complex **DD** (Figure 1-13).[126]

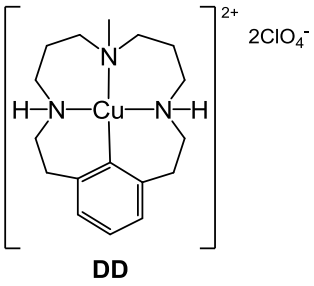

Figure 1-13: A macrocyclic Cu(III) complex[126]

Several mechanisms for the Ullmann reaction have been proposed, including Cu(I)/Cu(II) single electron transfer and atom transfer, and Cu(I)/Cu(III) oxidative addition / reductive elimination.[73,124,127] The most accepted is the latter, and with the demonstration of the macrocyclic aryl-Cu(III) complex **DD**, the mechanism is more convincing. A range of nucleophiles such as carboyxlic acids, amides, alcohols, thiols and halides have been shown to undergo a coupling reaction with the aryl ligand (Scheme 1-23).[128-132] However, the clear evidences of such mechanism are limited to those ligand systems and cannot be used to imply that Cu-catalysed cross-coupling would universally undertake the same mechanism.

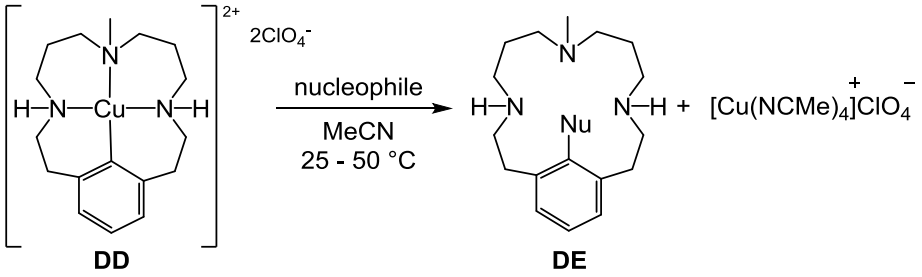

Scheme 1-23: Reductive elimination of aryl-Nu from the macrocyclic aryl-Cu(III) complex.[128-132]

1.7 Project aims

It has been shown in the literature that NHC ligands are able to enhance catalysis in some instances. However, NHC ligands may also become involved in non-innocent reactivity. The aim of this project was to prepare a range of imidazolium salts as NHC ligand precursors, and examine the resulting Cu(I)-NHC complexes as catalysts in an Ullmann-type etherification reaction. Past examples have shown that bidentate *N*,*N*-, *N*,*O*-, *O*,*O*- donor ligands[73,133,134] and pyridyl-tethered NHCs[41] can enhance the catalytic activity of Cu complexes when compared to the ligand free system. Our aim was to extend this by varying the electronic and/or physical properties of NHCs, with both donor and non-donor *N*-substituents and altering the NHC backbones. As Cu complexes formed *in situ* were previously demonstrated to perform as efficiently as the preformed complexes, our focus was on *in situ* formed complexes for catalytic screening and evaluation.

In addition to screening the catalytic competency of the different ligands, another aim was to examine the catalytic species and potential side-reactions that lead to catalyst deactivation. It became evident that reductive elimination of aryl-imidazolium was in operation, hence the synthesis of an aryl-imidazolium salt was desired for calibration to enable quantification of these reactions. Conditions that led to the aryl-imidazolium side-product were to be examined such as type of NHC ligand and equivalents of base, Cu complex and nucleophile. A further objective was to identify other possible side-reactions in these metal-catalysed cross-coupling reactions, with more knowledge in this area enabling the design of more efficient ligands for catalysis.

It was anticipated that the side-reactions of Cu-NHCs through reductive elimination of imidazolium salts may be exploited for synthesis. This part of the project was to focus on the functionalisation of xanthine-derived compounds that are based on imidazole, and can form or react *via* a metal-NHC complex.

Examination of the kinetics of this reaction would aid in the understanding of the mechanism, so that it may be applied to more challenging syntheses such as the arylation of nucleic acid strands.

As the mechanisms of both Cu-NHC catalysed reactions and deactivation reactions are thought to be proceed *via* higher oxidation state Cu, a further part of this project focuses on the stabilisation/isolation and examination of Cu-NHC complexes with higher oxidation states (+2 and +3). The ultimate goal would be to prepare the first example of a Cu(III)-NHC complex.

1.8 References

(1) Clayden, J.; Greeves, N.; Warren, S. *Organic Chemistry*; Oxford University Press: New York, 2012.
(2) Glorius, F. *Top. Organomet. Chem.* **2006**, *21*, 1.
(3) Liddle, S. T.; Edworthy, I. S.; Arnold, P. L. *Chem. Soc. Rev.* **2007**, *36*, 1732.
(4) Bourissou, D.; Guerret, O.; Gabbai, F. P.; Bertrand, G. *Chem. Rev.* **2000**, *100*, 39.
(5) Gleiter, R.; Hoffmann, R. *J. Am. Chem. Soc.* **1968**, 5457.
(6) Harrison, J. F. *J. Am. Chem. Soc.* **1971**, *93*, 4112.
(7) Dixon, D. A.; Arduengo, A. J. *J. Phys. Chem.* **1991**, *95*, 4180.
(8) Arduengo, A. J.; Dias, H. V. R.; Harlow, R. L.; Kline, M. *J. Am. Chem. Soc.* **1992**, *114*, 5530.
(9) Arduengo, A. J.; Harlow, R. L.; Kline, M. *J. Am. Chem. Soc.* **1991**, *1*, 361.
(10) Hopkinson, M.; Richter, C.; Schedler, M.; Glorius, F. *Nature* **2014**, *510*, 485.
(11) Crabtree, R. H. *The Organometallic Chemistry of the Transition Metals*; 5th ed.; Wiley: Hoboken, 2009.
(12) Wanzlick, H. W. *Angew. Chem.* **1962**, *1*, 75.
(13) Öfele, K. *J. Organomet. Chem.* **1968**, *12*, 42.
(14) Wanzlick, H. W.; Schönherr, H. J. *Angew. Chem.* **1968**, *7*, 141.
(15) Herrmann, W. A. *Angew. Chem., Int. Ed.* **2002**, *41*, 1290.
(16) Hillier, A. C.; Sommer, W. J.; Yong, B. S.; Petersen, J. L.; Cavallo, L.; Nolan, S. P. *Organometallics* **2003**, *22*, 4322.
(17) Viciu, M. S.; Navarro, O.; Germaneau, R. F.; III, R. A. K.; Sommer, W.; Marion, N.; Stevens, E. D.; Cavallo, L.; Nolan, S. P. *Organometallics* **2004**, *23*, 1629.
(18) Li, H.; Johansson-Seechurn, C. C. C.; Colacot, T. J. *ACS Catal.* **2012**, *2*, 1147.
(19) Shaw, P.; Kennedy, A. R.; Nelson, D. J. *Dalton Trans.* **2016**, *45*, 11772.
(20) Sarmiento, J. T.; Suarez-Pantiga, S.; Olmos, A.; Varea, T.; Asensio, G. *ACS Catal.* **2017**, *7*, 7146.
(21) Shi, S.; Szostak, M. *Chem. Comm.* **2017**, *53*, 10584.
(22) Lebel, H.; Janes, M. K.; Charette, A. B.; Nolan, S. P. *J. Am. Chem. Soc.* **2004**, *126*, 5046.
(23) Kolli, M. K.; Shaik, N. M.; Chandrasekar, G.; Chidara, S.; Korupolu, R. B. *New J. Chem.* **2017**, *41*, 8187.
(24) Fei, F.; Lu, T.; Chen, X.-T.; Xue, Z.-L. *New J. Chem.* **2017**, *41*, 13442.
(25) Shen, A.; Ni, C.; Cao, Y.-C.; Zhou, H.; Song, G.-H.; Ye, X.-F. *Tetrahedron Lett.* **2014**, *55*, 3278.
(26) Xu, C.; Wang, Z.-Q.; Yuan, X.-E.; Han, X.; Xiao, Z.-Q.; Fu, W.-J.; Ji, B.-M.; Hao, X.-Q.; Song, M.-P. *J. Organomet. Chem.* **2014**, *777*, 1.
(27) Monteiro, D. C. F.; Phillips, R. M.; Crossley, B. D.; Fielden, J.; Willans, C. E. *Dalton Trans.* **2012**, *41*, 3720.
(28) Williams, T. J.; Bray, J. T. W.; Lake, B. R. M.; Willans, C. E.; Rajabi, N. A.; Ariafard, A.; Manzini, C.; Bellina, F.; Whitwood, A. C.; Fairlamb, I. J. S. *Organometallics* **2015**, *34*, 3497.
(29) Touj, N.; Chakchouk-Mtibaa, A.; Mansour, L.; Harrath, A. H.; Al-Tamimi, J. H.; Hamdi, N. *J. Organomet. Chem.* **2017**, *853*, 49.

(30) Lu, H.; Zhou, Z.; Prezhdo, O. V.; Brutchey, R. L. *J. Am. Chem. Soc.* **2017**, *138*, 14844.
(31) Huang, W.-K.; Chen, W.-T.; Hsu, I.-J.; Han, C.-C.; Shyu, S.-G. *RSC Adv.* **2017**, *7*, 4912.
(32) Price, G. A.; Brisdon, A. K.; Randall, S.; Lewis, E.; Whittaker, D. M.; Pritchard, R. G.; Muryn, C. A.; Flower, K. R.; Quayle, P. *J. Organomet. Chem.* **2017**, *846*, 251.
(33) Achar, G.; Agarwal, P.; Brinda, K. N.; Malecki, J. G.; Keri, R. S.; Budagumpi, S. *J. Organomet. Chem.* **2017**, *854*, 64.
(34) Kolychev, E. L.; Shuntikov, V. V.; Khrustalev, V. N.; Bush, A. A.; Nechaev, M. S. *Dalton Trans.* **2011**, *40*, 3074.
(35) Mohamed, H. A.; Lake, B. R. M.; Laing, T.; Phillips, R. M.; Willans, C. E. *Dalton Trans.* **2015**, *44*, 7563.
(36) Grohmann, C.; Hashimoto, T.; Froehlich, R.; Ohki, y.; Tatsumi, K.; Glorious, F. *Organometallics* **2012**, *31*, 8047.
(37) Hindi, K. M.; Panzner, M. J.; Tessier, C. A.; Cannon, C. L.; Youngs, W. J. *Chem. Rev.* **2009**, *109*, 3859.
(38) Siciliano, T. J.; Deblock, M. C.; Hindi, K. M.; Durmus, S.; Panzner, M. J.; Tessier, C. A.; Youngs, W. J. *J. Organomet. Chem.* **2011**, *696*, 1066.
(39) Budagumpi, S.; Haque, R. A.; Endud, S.; Rehman, G. U.; Salman, A. W. *Eur. J. Inorg. Chem.* **2013**, 4367.
(40) Haque, R. A.; Iqbal, M. A.; Budagumpi, S.; Ahamed, M. B. K.; Majid, A. M. S. A.; Hasanudin, N. *Appl. Organomet. Chem.* **2013**, *27*, 214.
(41) Lake, B. R. M.; Willans, C. E. *Organometallics* **2014**, *33*, 2027.
(42) Chardon, E.; Dahm, G.; Guichard, G.; Bellemin-Laponnaz, S. *Inorganica Chim. Acta* **2017**, *467*, 33.
(43) Xiao, X.-Q.; Jin, G.-X. *Dalton Trans.* **2009**, 9298.
(44) Kaloglu, M.; Gurbuz, N.; Semeril, D.; Ozdemir, I. *Eur. J. Inorg. Chem.* **2018**, 1236.
(45) Wang, H. M. J.; Lin, I. J. B. *Organometallics* **1998**, *17*, 972.
(46) Clement, N. D.; Cavell, K. J. *Angew. Chem., Int. Ed.* **2004**, *43*, 3845.
(47) Tan, K. L.; Bergman, R. G.; Ellman, J. A. *J. Am. Chem. Soc.* **2002**, *124*, 3202.
(48) Lake, B. R. M.; Bullough, E. K.; Williams, T. J.; Whitwood, A. C.; Little, M. A.; Willans, C. E. *Chem. Comm.* **2012**, *48*, 4887.
(49) Liu, B.; Zhang, Y.; Xu, D.; Chen, W. *Chem. Comm.* **2011**, *47*, 2883.
(50) Chapman, M. R.; Shafi, Y. M.; Kapur, N.; Nguyen, B. N.; Willans, C. E. *Chem. Comm.* **2015**, *51*, 1282.
(51) Bugaut, X.; Glorius, F. *Chem. Soc. Rev.* **2012**, *41*, 3511.
(52) Schaper, L.-A.; Hock, S. J.; Herrmann, W. A.; Kuehn, F. E. *Angew. Chem., Int. Ed.* **2013**, *52*, 270.
(53) Scholl, M.; Ding, S.; Lee, C. W.; Grubbs, R. H. *Org. Lett.* **1999**, *1*, 953.
(54) Nelson, D. J.; Manzini, S.; Urbina-Blanco, C. A.; Nolan, S. P. *Chem. Comm.* **2014**, *50*, 10355.
(55) Bujok, R.; Bieniek, M.; Masnyk, M.; Michrowska, A.; Sarosiek, A.; Stepowska, H.; Arit, D.; Grela, K. *J. Org. Chem.* **2004**, *69*, 6894.
(56) Keitz, B. K.; Endo, K.; Patel, P. R.; Herbert, M. B.; Grubbs, R. H. *J. Am. Chem. Soc.* **2012**, *134*, 693.
(57) Colacino, E.; Martinez, J.; Lamaty, F. *Coord. Chem. Rev.* **2007**, *251*, 726.
(58) Riener, K.; Haslinger, S.; Raba, A.; Hoegerl, M. P.; Cokoja, M.; Herrmann, W. A.; Kuehn, F. E. *Chem. Rev.* **2014**, *114*, 5215.
(59) Fortman, G. C.; Nolan, S. P. *Chem. Soc. Rev.* **2011**, *40*, 5151.
(60) Egbert, J. D.; Cazin, C. S. J.; Nolan, S. P. *Catal. Sci. Technol.* **2013**, *3*, 912.
(61) Kantchev, E. A. B.; OBrien, C. J.; Organ, M. G. *Angew. Chem., Int. Ed.* **2007**, *46*, 2768.
(62) Prakasham, A. P.; Ghosh, P. *Inorganica Chimica Acta* **2014**.
(63) OBrien, C. J.; Kantchev, E. A. B.; Valente, C.; Hadei, N.; Chass, G. A.; Lough, A.; Hopkinson, A. C.; Organ, M. G. *Chem. Eur. J.* **2006**, *12*, 4743.
(64) Heck, R. F. *J. Am. Chem. Soc.* **1968**, *90*, 5518.
(65) Heck, R. F.; Nolley, J. P. *J. Org. Chem.* **1972**, *37*, 2320.
(66) Miyaura, N.; Suzuki, A. *Chem. Rev.* **1995**, *95*, 2457.
(67) Stille, J. K. *Angew. Chem., Int. Ed.* **1986**, *25*, 508.
(68) Ullmann, F.; Bielecki, J. *Chem. Ber.* **1901**, *34*, 2174.

(69) Ullmann, F. *Chem. Ber.* **1903**, *36*, 2382.
(70) Ullmann, F.; Frentzel, L. *Chem. Ber.* **1905**, *38*, 725.
(71) Ma, D.; Zhang, Y.; Yao, J.; Wu, S.; Tao, F. *J. Am. Chem. Soc.* **1998**, *129*, 12459.
(72) Kelkar, A. A.; Patil, N. M.; Chaudhari, R. V. *Tetrahedron Lett.* **2002**, *43*, 7143.
(73) Sambiago, C.; Marsden, S. P.; Blacker, A. J.; McGowan, P. C. *Chem. Soc. Rev.* **2014**, *43*, 3525.
(74) Tubaro, C.; Biffis, A.; Scattolin, E.; Basato, M. *Tetrahedron* **2008**, *64*, 4187.
(75) Biffis, A.; Tubaro, C.; Scattolin, E.; Basato, M.; Papini, G.; Santini, C.; Alvarez, E.; Conejero, S. *Dalton Trans.* **2009**, 7223.
(76) Ellul, C. E.; Reed, G.; Mahon, M. F.; Pascu, S. I.; Whittlesey, M. K. *Organometallics* **2010**, *29*, 4097.
(77) Borude, V. S.; Shah, R. V.; Shukla, S. R. *Monatsch Chem.* **2013**, *144*, 1663.
(78) Gallop, C. W. D.; Chen, M.-T.; Navarro, O. *Org. Lett.* **2014**, *16*, 3724.
(79) Paine, A. J. *J. Am. Chem. Soc.* **1987**, *109*, 1496.
(80) Wang, D.; Zhang, F.; Kuang, D.; Yu, J.; Li, J. *Green Chem.* **2012**, *14*, 1268.
(81) Domyati, D.; Latifi, R.; Tahsini, L. *J. Organomet. Chem.* **2018**, *860*, 98.
(82) Lake, B. R. M.; Chapman, M. R.; Willans, C. E. *Organometallic Chemistry* **2016**, *40*, 107.
(83) Lin, B.-L.; Kang, P.; Stack, T. D. P. *Organometallics* **2010**, *29*, 3683.
(84) Lake, B. R. M.; Ariafard, A.; Willans, C. E. *Chem. Eur.* **2014**, *20*, 12729.
(85) Campeau, L.-C.; Thansandote, P.; Fagnou, K. *Org. Lett.* **2005**, *7*, 1857.
(86) McGuinness, D. S.; Cavell, K. J.; Yates, B. F.; Skelton, B. W.; White, A. H. *J. Am. Chem. Soc.* **2001**, *123*, 8317.
(87) McGuinness, D. S.; Mueller, W.; Wasserscheid, P.; Cavell, K. J.; Sklelton, B. W.; White, A. H.; Englert, U. *Organometallics* **2002**, *21*, 175.
(88) Normand, A. T.; Stasch, A.; Ooi, L.-L.; Cavell, K. J. *Organometallics* **2008**, *27*, 6507.
(89) Magill, A. M.; Yates, B. F.; Cavell, K. J.; Skelton, B. W.; White, A. H. *Dalton Trans.* **2007**, 3398.
(90) Nielsen, D. J.; Cavell, K. J.; Skelton, B. W.; White, A. H. *Inorg. Chim. Acta.* **2006**, *359*, 1855.
(91) Steinke, T.; Shaw, B. K.; Jong, H.; Patrick, B. O.; Fryzuk, M. D.; Green, J. C. *J. Am. Chem. Soc.* **2009**, *131*, 10461.
(92) Despagnet-Ayoub, E.; Wenling, L. M.; Labinger, J. A.; Bercaw, J. E. *Organometallics* **2013**, *32*, 2934.
(93) Romain, C.; Miqueu, K.; Sotiropoulos, J.-M.; Bellemin-Laponnaz, S.; Dagorne, S. *Angew. Chem., Int. Ed.* **2010**, *49*, 2198.
(94) Danopoulos, A. A.; Tsoureas, N.; Green, J. C.; Hursthouse, M. B. *Chem. Comm.* **2003**, 756.
(95) Becker, E.; Stingl, V.; Dazinger, G.; Puchberger, M.; Mereiter, K.; Kirchner, K. *J. Am. Chem. Soc.* **2006**, *128*, 6572.
(96) Fantasia, S.; Jacobsen, H.; Cavallo, L.; Nolan, S. P. *Organometallics* **2007**, *26*, 3286.
(97) Waltman, A. W.; Ritter, T.; Grubbs, R. H. *Organometallics* **2006**, *25*, 4238.
(98) Campbell, M. G.; Ritter, T. *Chem. Rev.* **2015**, *115*, 612.
(99) Pugh, D.; Boyle, A.; Danopoulos, A. A. *Dalton Trans.* **2008**, 1087.
(100) Allen, D. P.; Crudden, C. M.; Calhoun, L. A.; Wang, R. *J. Org. Chem.* **2004**, *689*, 3203.
(101) Corberan, R.; Sanau, M.; Peris, E. *Organometallics* **2006**, *25*, 4002.
(102) McGuinness, D. S.; Green, M. J.; Cavell, K. J.; Skelton, B. W.; White, A. H. *J. Organomet. Chem.* **1998**, *565*, 165.
(103) Normand, A. T.; Yen, S. K.; Huynh, H. V.; Hor, T. S. A.; Cavell, K. J. *Organometallics* **2008**, *27*, 3153.
(104) McGuinness, D. S.; Cavell, K. J.; Skelton, B. W.; White, A. H. *Organometallics* **1999**, *18*, 1596.
(105) Caddick, S.; Cloke, F. G. N.; Hitchcock, P. B.; Leonard, J.; Lewis, A. K. d. K.; McKerrecher, D.; Titcomb, L. R. *Organometallics* **2002**, *21*, 4318.
(106) Fukuyama, T.; Rahman, M. T.; Mashima, H.; Takahashi, H.; Ryu, I. *Org. Chem. Front.* **2017**, *4*, 1863.
(107) Magill, A. M.; McGuinness, D. S.; Cavell, K. J.; Britovsek, G. J. P.; Gibson, V. C.; White, A. J. P.; Williams, D. J.; White, A. H.; Skilton, B. W. *J. Organomet. Chem.* **2001**, *617-618*, 546.

(108) Ghadwal, R. S.; Lamm, J.-H.; Rottschafer, D.; Schurmann, C. J.; Demeshko, S. *Dalton Trans.* **2017**, *46*, 7664.
(109) Rottschafer, D.; Schurmann, C. J.; Lamm, J.-H.; Paesch, A. N.; Neumann, B.; Ghadwal, R. s. *Organometallics* **2016**, *35*, 3421.
(110) Bidal, Y. D.; Santoro, O.; Melaimi, M.; Cordes, D. B.; Slawin, A. M. Z.; Bertrand, G.; Cazin, C. S. J. *Chem. Eur. J.* **2016**, *22*, 9404.
(111) Sau, S. C.; Roy, S. R.; Sen, T. K.; Mullangi, D.; Mandal, S. K. *Adv. Synth. Catal.* **2013**, *355*, 2982.
(112) Heckenroth, M.; Kluser, E.; Neels, A.; Albrecht, M. *Angew. Chem., Int. Ed.* **2007**, *46*, 623.
(113) Prades, A.; Viciano, M.; Sanau, M.; Peris, E. *Organometallics* **2008**, *27*, 4254.
(114) Lebel, H.; Janes, M. K.; Charette, A. B.; Nolan, S. P. *J. Am. Chem. Soc.* **2004**, *126*, 5046.
(115) Saha, S.; Ghatak, T.; Saha, B.; Doucet, H.; Bera, J. K. *Organometallics* **2012**, *31*, 5500.
(116) Lavallo, V.; Dyker, C. A.; Donnadieu, B.; Bertrand, G. *Angew. Chem., Int. Ed.* **2008**, *47*, 5411.
(117) Popova, T. V.; Aksenova, N. V. *Russian J. Coord. Chem.* **2003**, *29*, 743.
(118) Arnold, P. L.; Rodden, M.; Davis, K. M.; Scarisbrick, C.; Blake, A. J.; Wilson, C. *Chem. Comm.* **2004**, 1612.
(119) VanVeldhuizen, J. J.; Campbell, J. E.; Giudici, R. E.; Hoveyda, A. H. *J. Am. Chem. Soc.* **2005**, *127*, 6877.
(120) Warsink, S.; Boer, S. Y. d.; Jongens, L. M.; Fu, C.-F.; Liu, S.-T.; Chen, J.-T.; Lutz, M.; Spek, A. L.; Elsevier, C. J. *Dalton Trans.* **2009**, 7080.
(121) Lewis, A. K. D. K.; Caddick, S.; Cloke, F. G. N.; Billingham, N. C.; Hitchcock, P. B.; Leonard, J. *J. Am. Chem. Soc.* **2003**, *125*, 10066.
(122) Marshall, W. J.; Grushin, V. V. *Organometallics* **2003**, *22*, 1591.
(123) Younesi, Y.; Nasiri, B.; BabaAhmadi, R.; Willans, C. E.; Fairlamb, I. J. S.; Ariafard, A. *Chem. Comm.* **2016**, *52*, 5057.
(124) Casitas, A.; Ribas, X. *Chem. Sci.* **2013**, *4*, 2301.
(125) Housecroft, C. E.; Sharpe, A. G. *Inorganic Chemistry*; Pearson Education Limited: Harlow, 2008.
(126) Ribas, X.; Jackson, D. A.; Donnadieu, B.; Mahia, J.; Parella, T.; Xifra, R.; Jedman, B.; Hodgson, K. O.; Llobet, A.; Stack, T. D. P. *Angew. Chem., Int. Ed.* **2002**, *41*, 2991.
(127) Casitas, A. *RSC Catalysis Series* **2013**, *11*, 46.
(128) Casitas, A.; King, A. E.; Parella, T.; Costas, M.; Stahl, S. S.; Ribas, X. *Chem. Sci.* **2010**, *1*, 326.
(129) Huffman, L. M.; Stahl, S. S. *J. Am. Chem. Soc.* **2008**, *130*, 9196.
(130) Huffman, L. M.; Casitas, A.; Font, M.; Canta, M.; Costas, M.; Ribas, X.; Stahl, S. S. *Chem. Eur. J.* **2011**, *17*, 10643.
(131) Font, M.; Parella, T.; Costas, M.; Ribas, X. *Organometallics* **2012**, *31*, 7976.
(132) Casitas, A.; Canta, M.; Costas, M.; Sola, M.; Ribas, X. *J. Am. Chem. Soc.* **2011**, *133*, 19386.
(133) Maiti, D.; Buchwald, S. L. *J. Am. Chem. Soc.* **2009**, *131*, 17423.
(134) Yu, H.-Z.; Jiang, Y.-Y.; Fu, Y.; Liu, L. *J. Am. Chem. Soc.* **2010**, *132*, 18078.

Chapter 2

Effects of N-Heterocyclic Carbene Ligand *N*-Substituents on Copper-Catalysed Etherification

2.1 Introduction

Cross-coupling reactions have played a pivotal role in organic synthesis as they allow bond formation for complex molecules, which are widely used in the pharmaceutical industry.[1-5] Different types of bond formation have been achieved with the application of various transition metals, including Pd,[4-9] Au,[10,11] Ag[12-14] and Cu.[15] In the history of Cu catalysts, harsh reaction conditions such as high temperatures and stoichiometric loadings of Cu were required.[16-21] However, the involvement of ligands has played a significant role in development, allowing for lower catalyst loadings and reaction temperatures, shorter reaction times and enabled application of milder bases.[22-24] Some classes of ligands such as bidentate *N*-donors and *O*-donors have been studied for reaction mechanism and selectivity.[25-29] However, knowledge on Cu-NHC cross-coupling catalysts is limited and there are only a few examples of the application of Cu-NHCs in cross-coupling.[30-35]

Recently, our group has observed the noteworthy stability of Cu(I)-NHC and Cu(II)-NHC complexes with pyridine and alkene *N*-substituents.[35] This showed the potential of these ligands for stabilising high oxidation state catalytic intermediates that occur during the proposed Cu(I)/Cu(II) or Cu(I)/Cu(III) pathways (Scheme 2-1). The energy barrier of an aryl-halide bond activation may be reduced and the catalyst decomposition, especially during the high oxidation state, is potentially suppressed. Lake screened a series of Cu(I)-NHC complexes in a challenging etherification reaction using an electron-rich aryl iodide.[35] Such types of aryl iodide are unfavourable to oxidative addition and have given poor conversions to ether product when catalysed by [Cu(IMes)Cl] (15 %) or ligand-free CuI (20 %). From these results it was noted that NHCs bearing pyridine and picolyl *N*-substituents did enhance the product yield compared to the ligand-free system, whereas a mesityl *N*-substituent hindered the reaction, presumably due to it being too bulky and its inability to chelate.

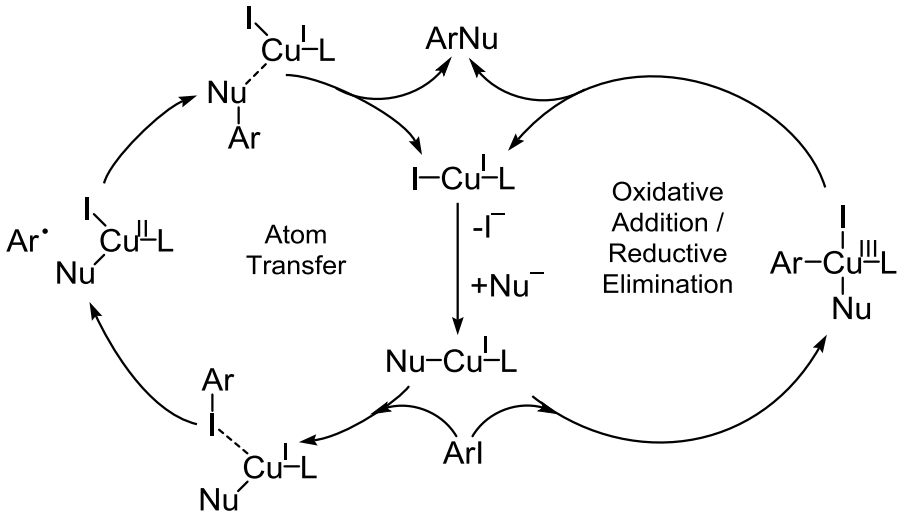

Scheme 2-1: Cu-catalysed cross-coupling reaction *via* atom transfer (Cu^{I}/Cu^{II}) and oxidative addition / reductive elimination (Cu^{I}/Cu^{III}).

This chapter will expand the scope of *N*-substituents, such as methyl, trityl, *t*-butyl and allyl groups, in combination with pyridyl and picolyl groups. The allyl *N*-substituent is a fascinating subject as it was utilised in Lake's work and was observed to be more catalytically active than a mesityl *N*-substituent. Although an intramolecular π-interaction between Cu and alkene was not observed in the solid-state structures of either the Cu(I) or Cu(II) complexes, the alkene group may interact with the Cu centre in the solution phase. This is especially possible during a catalytic cycle, in which the catalytic intermediate has a high oxidation state (Cu(II) or Cu(III)). Further possible NHC variations include changing the NHC ring structure or changing the backbone substituents, which will mainly alter the electronic properties of the NHC.

2.2 Modification of the non-chelating *N*-substituents

Willans demonstrated that an NHC bearing picolyl, allyl *N*-substituents led to higher catalytic activity in an etherification reaction than an NHC bearing pyridyl, allyl *N*-substituents.[35] In this work, the picolyl-tethered NHCs were expanded further (Figure 2-1). To examine the effect of the alkene group, comparison between allyl (**L1**) and propyl (**L2**) groups was undertaken. Variation of the steric bulk of the *N*-substituent was carried out with methyl (**L3**), *t*-butyl (**L4**), chlorotrityl (**L5**) and mesityl (**L6**) groups.

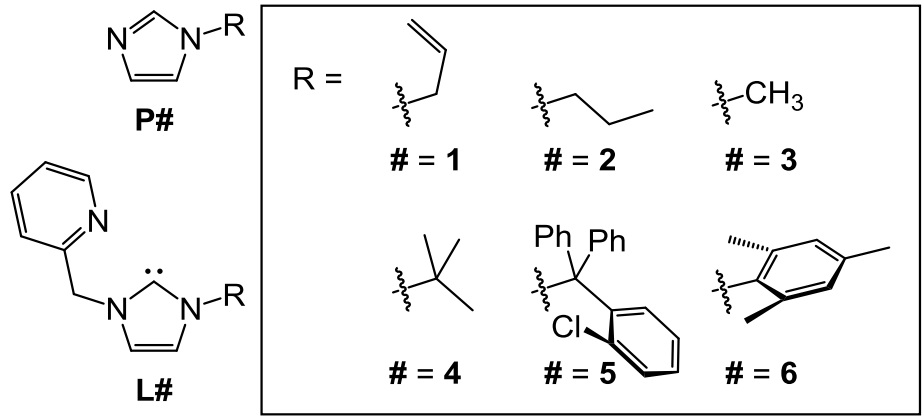

Figure 2-1: Proposed NHC ligands (**L1**-**L6**).

The preparation of the imidazolium precursors to **L1** – **L6** (*i.e.* H**L1**Br – H**L6**Br) requires a nucleophilic substitution of **P1** – **P6** with 2-(bromomethyl)pyridine. **P1** – **P6** were either commercially available or available in the group. H**L2**Br and H**L4**Br were prepared by other group members. H**L1**Br was prepared through reaction of **P1** with the HBr salt of 2-bromomethylpyridine in MeCN at room temperature in the presence of K_2CO_3 (Scheme 2-2). After vigorous stirring for 24 hours, the reaction mixture was filtered and the crude product recrystallised from MeCN / Et_2O and DCM / Et_2O to obtain a dark red oil as the final product. The same procedure was used for the preparation of H**L6**Br.

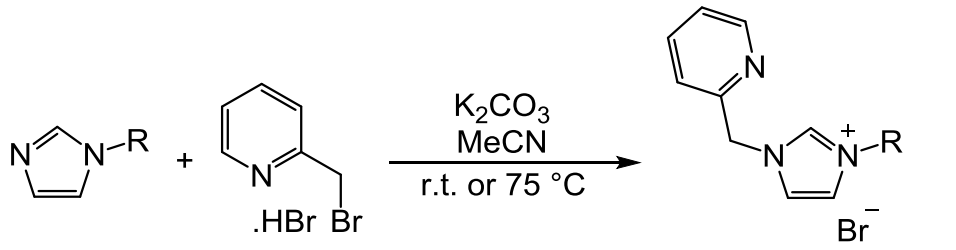

P1; R = allyl
P3; R = Me
P6; R = Mes

H**L1**Br; R = allyl, 77 %
H**L3**Br; R = Me, 46 %
H**L6**Br; R = Mes, 21 %

Scheme 2-2: Preparation of H**L1**Br and H**L6**Br.

Imidazolium precursor H**L3**Br was prepared using the same method as for H**L1**Br and H**L6**Br, but required a higher reaction temperature (75 °C) (Scheme 2-2). During the recrystallisation of H**L3**Br, if **P3** is still present and the mixture contains H-bonding-source water, it became challenging to separate from the imidazolium. Hence, the reaction mixture was dried with Na_2SO_4 prior to recrystallisation.

In the case of a novel trityl,picolyl imidazolium salt (H**L5**Br), clotrimazole (**P5**) was used as the precursor. Attempts were made using 1-tritylimidazole (**P5'**) but

the trityl group was cleaved during the reaction and resulted in a mixture of trityl, picolyl imidazolium and bis(picolyl)imidazolium ions, which were observed in the HR mass spectrum (Scheme 2-3, bottom). The chloride atom in chlorotrityl makes the cation less stable than the trityl cation, and hence the cleavage of the chlorotrityl group is not as facile. To further prevent the dissociation of the chlorotrityl group, the reaction was carried out under anhydrous conditions with molecular sieves (4 Å) to remove the water by-product (Scheme 2-3).

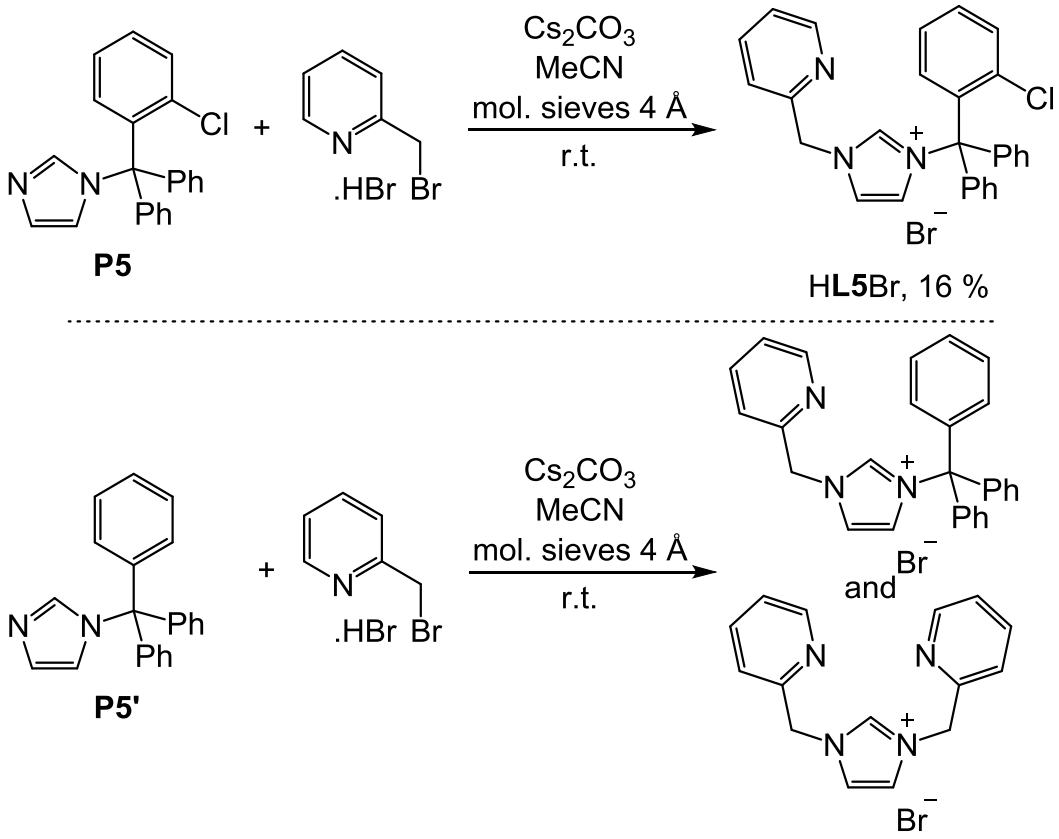

Scheme 2-3: Preparation of H**L5**Br and attempted preparation of H**L5'**Br.

A number of analytical techniques have been used to confirm formation of the desired imidazolium products. Using HRMS, the formation of the imidazolium ion as $[M - X]^+$ can be observed. ^{1}H NMR spectroscopy reveals the H-imidazolium (H_A) signal (singlet or triplet, depending on the strength of the coupling from the backbone protons), the chemical shift of which is more downfield (a range of δ 12 – 8 ppm) than other aromatic proton resonances (δ 7.6 – 6.5 ppm). This is because the positive charge in the proton's environment results in deshielding and a downfield shift. Additionally, the chemical shift of the H-imidazolium may be used to predict the electronic properties of the corresponding NHC ligand as the chemical shift represents the electron density in the region.

For example, H_A of H**L1**Br is at δ 10.46 ppm (Figure 2-2). The H_A proton signal is easily distinguished from the rest of the other aromatic protons, of which the most downfield is H_B at δ 8.56 ppm. The H_B proton signal shows a fascinating splitting pattern, appearing as a ddd with couplings of ^3J = 5 Hz, ^4J = 2 Hz and ^5J = 1 Hz. The aromatic ^3J coupling is normally in the range of 6 – 9 Hz, but this rare coupling of 4 – 6 Hz is characteristic of the doublet coupling to the pyridine ring.[36,37] Furthermore, it can be observed that the H_A peaks of H**L1**Br, H**L3**Br, H**L5**Br and H**L6**Br are at different chemical shifts (δ 10.46, 10.26, 9.55 and 10.43 ppm respectively). This may suggest that **L5** will be the strongest electron donor as H**L5**Br has the least acidic proton. However, the assumption is not truly reliable as the chemical shift may also be affected by the aromaticity of the *N*-substituents. Still, the chemical shift of H_A is one of the factors used in computational experiments to generate a ligand map of chemical space to study the ligand effects,[38] and compare to the experimental results.

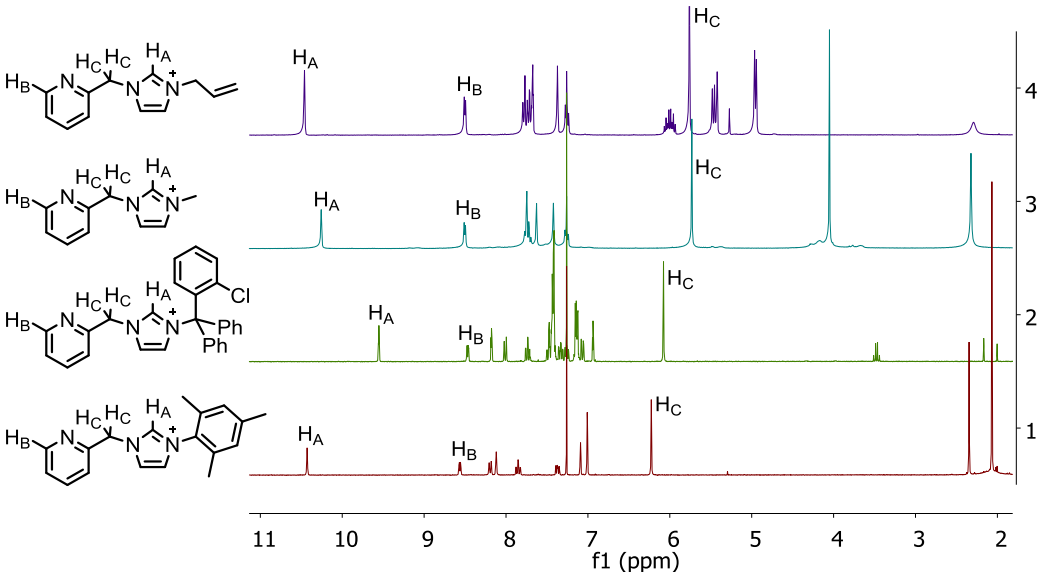

Figure 2-2: ^{1}H NMR spectra (300 MHz, $CDCl_3$) of H**L1**Br, H**L3**Br, H**L5**Br and H**L6**Br (top to bottom).

2.2.1 Ligand evaluation of catalytic activity

To study ligand effects in a Cu-catalysed cross-coupling reaction, the ligands were screened in the etherification reaction of 4-iodoanisole with 3,5-dimethylphenol (Scheme 2-4). Initially the reaction was attempted using 10 mol % of catalyst and 2 equivalents of Cs_2CO_3 under nitrogen, but negligible conversion to ether was attained (0 – 21 %).

The conditions were modified to 4 equivalents of Cs_2CO_3 and the reactions were conducted under argon (Scheme 2-4), which improved the conversion to

36 – 65 % and allowed significant distinction between ligands. The observation is consistent with Lake's work that increasing the base loading can improve the reaction yield.

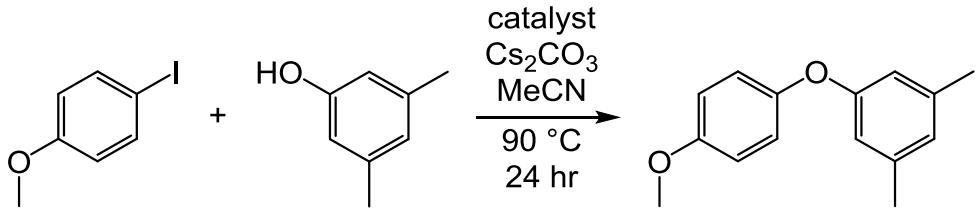

(a) 0.1 eq CuI, 0.1 eq H**L**X or **L**, 2 eq Cs_2CO_3, N_2 (0 - 21 % conversion)
(b) 0.1 eq CuI, 0.1 eq H**L**X or **L**, 4 eq Cs_2CO_3, Ar (25 - 63 % conversion)

Scheme 2-4: Cu-catalysed etherification reaction for the screening of ligand effects.

In situ generated ligands **L1**-**L6** were screened in the etherification of 4-iodoanisole with 3,5-dimethylphenol using 10 mol % of the ligand precursor, 10 mol % of CuI and 4 equivalents of Cs_2CO_3 (Scheme 2-4b). There is a significant difference in the catalytic activities between the Cu catalysts of **L1** and **L2** (63 and 37 % conversion respectively, Table 2-1). **L1** contains an allyl *N*-substituent whereas **L2** contains an *n*-propyl *N*-substituent; this result may indicate that the allyl of **L1** coordinates or interacts with the Cu centre during the catalytic cycle to stabilise higher oxidation state Cu intermediates and prevent catalyst decomposition. Scheme 2-5 shows the stabilisation effects of the allyl group with the speculation that the catalysis takes place *via* oxidative addition / reductive elimination pathway.

Catalyst (10 mol %)	R^1	R^2	NHC ring based on	% conversion
CuI	N/A	N/A	N/A	29
CuI + H**L1**Br	picolyl	allyl	imidazole	63
CuI + H**L2**Br	picolyl	propyl	imidazole	37
CuI + H**L3**Br	picolyl	methyl	imidazole	46
CuI + H**L4**Br	picolyl	*t*-butyl	imidazole	56
CuI + H**L5**Br	picolyl	chlorotrityl	imidazole	61
CuI + H**L6**Br	picolyl	mesityl	imidazole	25
CuI + H**L7**Br	6-methylpicolyl	methyl	imidazole	46

Table 2-1: Ligand screening in the Cu-catalysed etherification reaction of 4-iodoanisole with 3,5-dimethylphenol (conversion determined by GC using *p*-cymene as an internal standard).

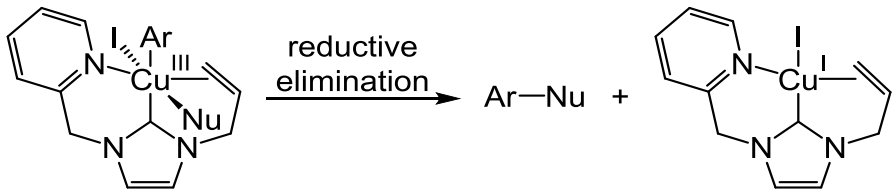

Scheme 2-5: Potential Cu(III) intermediate stabilised by an allyl interaction and reductive elimination of cross-coupled product to regenerate the Cu(I)-NHC catalyst.

Ligands **L3**-**L6** have varying steric bulk in the order **L3** < **L6** < **L4** < **L5** which can be assumed based on the % V_{bur} of related ligands **L3'**, **L4'** and **L6'** (Figure 2-3). These were calculated by Nolan and co-workers to have values of 25.4, 36.2 and 32.7 respectively using a radius of 3.5 Å.[39] Similarly, the catalytic trend was **L6** < **L3** < **L4** < **L5** in the etherification reaction (25, 45, 56 and 61 % conversion to ether respectively). This suggests that the steric protection of NHC ligands is likely to promote the catalytic activity of the Cu complex as the steric bulk can inhibit catalyst decomposition.

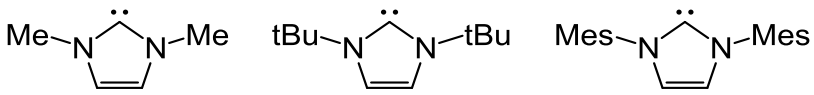

L3' **L4'** **L6'**

$\%V_{bur}$ = 25.4 $\%V_{bur}$ = 36.2 $\%V_{bur}$ = 32.7

Figure 2-3: Structure of **L3'**, **L4'** and **L6'**.[39]

The mesityl group (**L6**) was observed to be deactivating and did not follow the steric trend. Unlike the *t*-butyl and methyl groups, the mesityl group can inductively withdraw electrons from the carbene ring due to the higher electronegativity of sp^2-hybridised carbon than sp^3-hybridised carbon.[40,41] This makes **L6** a weaker donor than **L3**. The electron poor **L6** is evident by ^{1}H NMR spectroscopy, which shows H_A of H**L6**Br more downfield than H_A of H**L3**Br (Figure 2-2). Hence, the steric effects alone cannot be used to determine the catalytic activity, with electronic properties of the NHC also requiring consideration.

In conclusion, varying the second *N*-substituent in picolyl-substituted NHCs demonstrated that an allyl group promotes catalysis when compared to non-coordinating alkyl substituents. The alkene group may play a significant role in Cu-NHC catalysis due to its π-donor ability. Furthermore, steric protection of the *N*-substituents *i.e*. *t*-butyl and chlorotrityl groups also helps promote the catalyst performance. However, the mesityl group is an exception to this rule. It is

proposed that the group makes the NHC a weaker donor and consequently lowers the catalytic activity.

2.3 Modification of the chelating *N*-substituents

A further ligand precursor **(**H**L7**Br) was prepared with a methyl *N*-substituent and a picolyl *N*-substituent bearing a methyl group on the C-6 position of the pyridine ring. The methyl group is electron donating so will increase the Lewis basicity of the pyridyl, and may also have a steric effect at the Cu centre. H**L7**Br was prepared using a similar method to the imidazolium precursors of **L1**-**L6** (Scheme 2-6). In this case a base was not required as the picolyl precursor is in a neutral form rather than the HX salt.

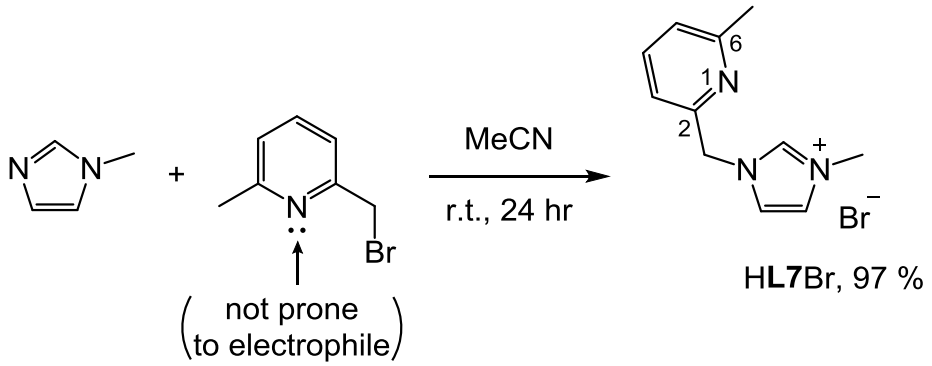

Scheme 2-6: Preparation of H**L7**Br.

The formation of the novel H**L7**Br was confirmed by ^{1}H and ^{13}C {^{1}H} NMR spectroscopy and HRMS. The ^{1}H NMR spectrum was compared to that of H**L3**Br (Figure 2-4) to determine if there is any difference in electronic properties. All of the imidazolium proton peaks of H**L7**Br (H_A, H_B and H_C) are more upfield than H**L3**Br, suggesting that the NHC of **L7** is a stronger donor than **L3**. In addition, the pyridine ring of H**L7**Br is more electron rich than that of H**L3**Br, as all of the pyridine proton peaks of H**L7**Br (H_E, H_F and H_G) are more upfield than their respective peaks of H**L3**Br.

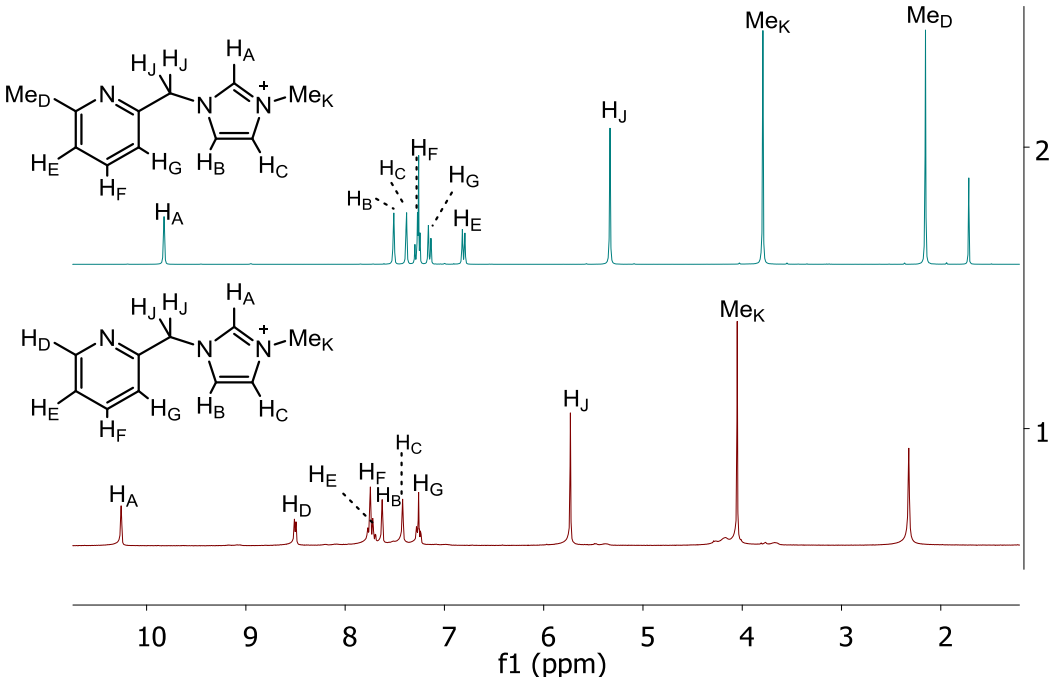

Figure 2-4: ^{1}H NMR spectra (300 MHz, $CDCl_3$) of H**L7**Br (top) and H**L3**Br (bottom).

In situ generated ligands **L3** and **L7** were screened in the same Cu-catalysed etherification reaction as previously, and both gave conversions of 46 % (Table 2-1). Willans previously studied substituents at the C4 position of the pyridyl *N*-substituent, and found that catalytic activity increased Me < H < OMe (Figure 2-5).[35] It is possible that **L7** is electronically deactivating, with the stronger pyridine donor hindering nucleophilic substitution and/or reductive elimination of the cross-coupled product (as proposed in Willans's work). However, **L7** also has added steric protection which may counter the electronic drawback, resulting in the same conversion as when **L3** was used.

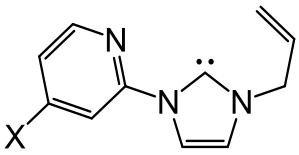

X = Me conversion = 27 %
X = H conversion = 32 %
X = OMe conversion = 34 %

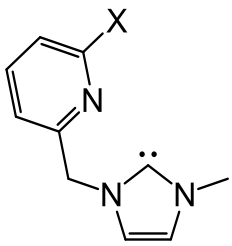

X = H (**L3**) conversion = 46 %
X= Me (**L7**) conversion = 46 %

Figure 2-5: Willans's modified pyridyl-NHC ligands and our modified picolyl-NHC ligands, and % etherification of their Cu-NHC complexes.[35]

The CH_2 linker in picolyl provides flexibility into the ligand and allows for greater steric protection of the metal when compared to a pyridyl substituent. It also hinders the electron-withdrawing effect from the pyridine ring on the carbene centre. To examine the effect of this, pyridyl-substituted ligand precursors H**L8**Br and H**L9**Br were synthesised. **P8** was prepared by a Cu-catalysed coupling reaction between 2-bromopyridine and imidazole in DMSO under basic conditions at 90 °C (Scheme 2-7). DL-proline was used as a ligand in the reaction, and Cs_2CO_3 was used as the base, which has been shown to promote Cu-catalysed reactions compared to K_2CO_3.[42,43] **P8** was allylated to form the desired imidazolium precursor H**L8**Br, which was obtained from recrystallisation using MeCN / Et_2O. The product was characterised by ^{1}H and ^{13}C $\{^{1}H\}$ NMR spectroscopy and HRMS, and the data was consistent with the prior cases.[44] The imidazolium proton resonance appears at δ 11.98 ppm (300 MHz, $CDCl_3$).

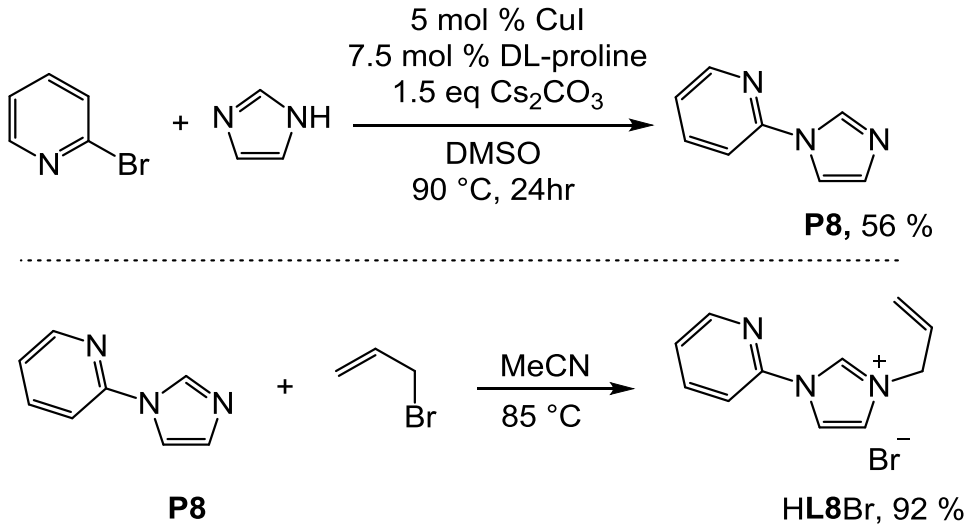

Scheme 2-7: Preparation of **P8** and H**L8**Br.

H**L9**Br was prepared by another group member by heating **P9** with 2-bromopyridine without solvent at 160 °C, *via* a nucleophilic substitution on the S_NAr-capable pyridine ring (Scheme 2-8).[39,44,45]

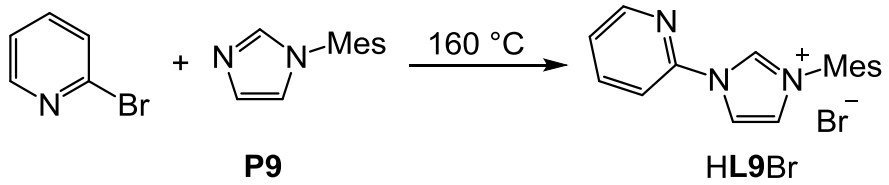

Scheme 2-8: Preparation of H**L9**Br.[44]

Attempts were made to prepare ligand precursors with an aminoethyl *N*-substituent, as this would contain an sp^3 lone-pair which has a higher basicity than the sp^2 lone-pair. Aminoethyl-bearing NHCs have been reported as suitable

ligands for Ag, Au and Pd catalysts for cross-coupling reactions.[45-47] **P1** and **P6** were each added to an HBr salt of 2-bromoethylamine in MeCN. However, the reaction using **P1** resulted in a mixture of H**L10**Br, H**L10***Br and H**L10****Br, as observed in both NMR spectra and the HR mass spectrum (Scheme 2-9). The same was observed when using the **L11** precursor. Unfortunately, H**L10**Br and H**L11**Br cannot be separated from other impurities by recrystallisation or column chromatography.

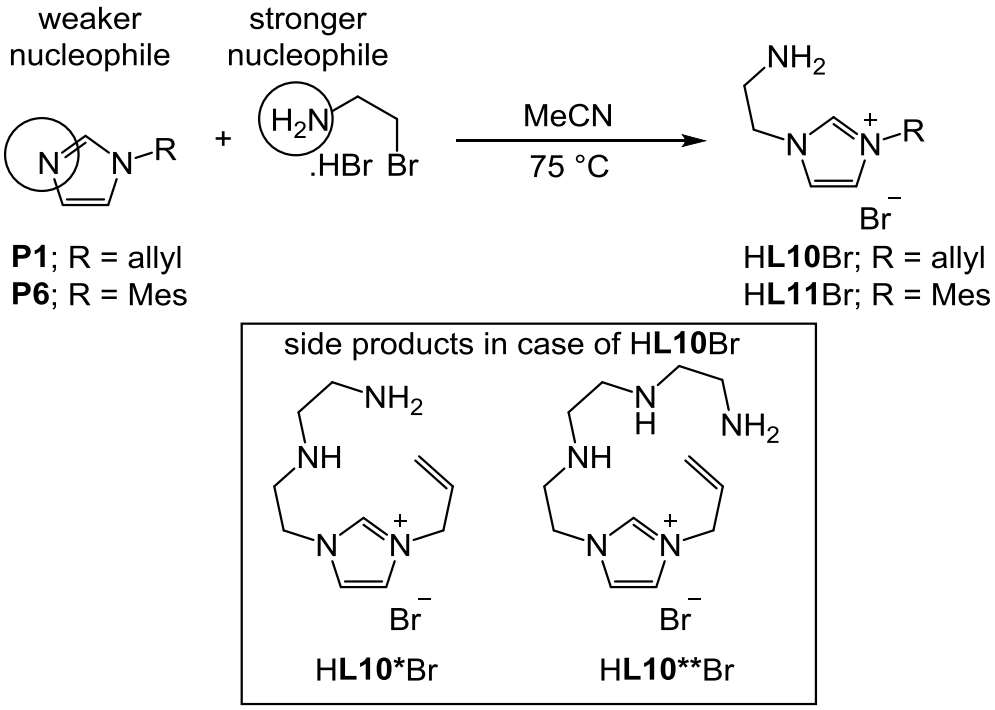

Scheme 2-9: Attempted preparation of H**L10**Br and H**L11**Br.

As the allyl substituent was found to enhance catalytic activity (likely due to the potential of an allyl group coordinating or interacting with the Cu centre), ligand precursors H**L12**Br and H**L13**Br (Figure 2-6) were introduced for screening, and were prepared by other group members.

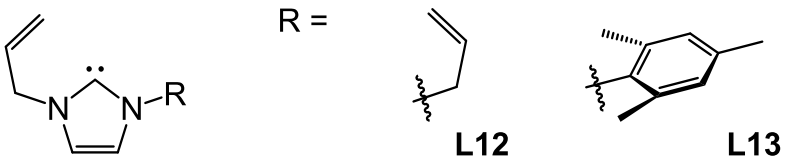

Figure 2-6: Structure of allyl-substituted NHC ligands.

In situ generated ligands **L8**, **L9**, **L12** and **L13** were screened and evaluated for their catalytic activities in the same etherification reaction as previously. In the case of ligands bearing an allyl *N*-substituent, the catalytic activity increased when the second *N*-substituent was modified mesityl (**L13**) < pyridyl (**L8**) < allyl

(**L12**) < picolyl (**L1**) (Table 2-2). The opposite trend was observed in the case of ligands bearing a mesityl *N*-substituent, with the catalytic activity increasing with the second *N*-substituent being picolyl (**L6**) < pyridyl (**L9**) < allyl (**L13**).

Catalyst (10 mol %)	R^1	R^2	NHC ring based on	% conversion
CuI	N/A	N/A	N/A	29
CuI + H**L1**Br	picolyl	allyl	imidazole	63
CuI + H**L6**Br	picolyl	mesityl	imidazole	25
CuI + H**L8**Br	pyridyl	allyl	imidazole	53
CuI + H**L9**Br	pyridyl	mesityl	imidazole	41
CuI + H**L12**Br	allyl	allyl	imidazole	58
CuI + H**L13**Br	allyl	mesityl	imidazole	47

Table 2-2: Ligand screening in the Cu-catalysed etherification reaction of 4-iodoanisole with 3,5-dimethylphenol (conversion determined by GC using *p*-cymene as an internal standard).

L6 was demonstrated to be the least active ligand, performing worse than the ligand free system, which may be due to steric saturation around the metal with the bulky mesityl substituent combined with the picolyl group. Exchanging picolyl for pyridyl (**L9**) improved catalytic activity, despite the fact that the carbene will be a weaker donor when compared to **L6**. This strongly suggests that steric factors have a stronger influence than electronics in this system, with the less bulky (non-coordinating) allyl group (**L13**) improving catalytic activity further.

Ligands bearing an allyl *N*-substituent improve catalytic activity compared to the mesityl *N*-substituent. This may be due to the potential coordination behaviour of the allyl group, inducing stabilisation of Cu intermediates during the catalytic cycle. In addition, the electron withdrawal capability of the mesityl substituent will make the NHC a weaker donor, inhibiting the oxidative addition step and destabilising intermediates. While, the strong coordination ability and flexibility of the picolyl will aid in the stabilisation of catalytic intermediates. Furthermore, the NHC will be a stronger donor when compared to **L8** (with a pyridyl group), which will further stabilise the intermediates and promote oxidation of the Cu(I).

2.4 Modification of the NHC Backbone Substituents

Whilst the *N*-substituents of NHCs tend to have the greatest influence on steric effects of the ligand, modification of the backbone can provide diverse electronic properties.[48] The benzimidazole-based NHC (**L15**) is a weaker σ-donor than the imidazole-based NHC (**L3**) (Figure 2-7). Similarly, changing the backbone substituents from protons to inductively electron-withdrawing chlorine atoms (**L14**) affects the NHC electronic properties.

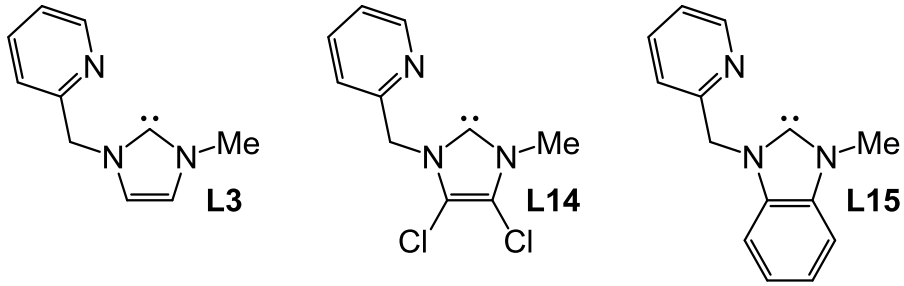

Figure 2-7: Proposed backbone-modified NHCs.

The novel H**L14**X and H**L15**X imidazolium salts can be prepared in a similar way to previous imidazolium salts, with functionalisation of 4,5-dichloroimidazole and benzimidazole with picolyl and methyl groups. It has previously been found that addition of the picolyl group before the methyl group reduces side-product formation. Therefore, 1-picolyl-4,5-dichloroimidazole (**P14***) was synthesised by nucleophilic substitution of 4,5-dichloroimidazole with picolyl bromide.HBr in the presence of base (Scheme 2-10a). However, the methylation of **P14*** led to formation of both H**L14**I and of H**L14***I (Scheme 2-10b), where the major product was the undesired H**L14***I due to the imidazolium ring containing electron-withdrawing chlorine atoms. This lowers the nucleophilicity of the N-imidazole, hence the formation of H**L14**I is less favourable compared to H**L14***I. Instead, H**L14**Br was prepared from reaction of 1-methyl-4,5-dichloroimidazole (**P14**) with picolylbromide.HBr (Scheme 2-10c,d).

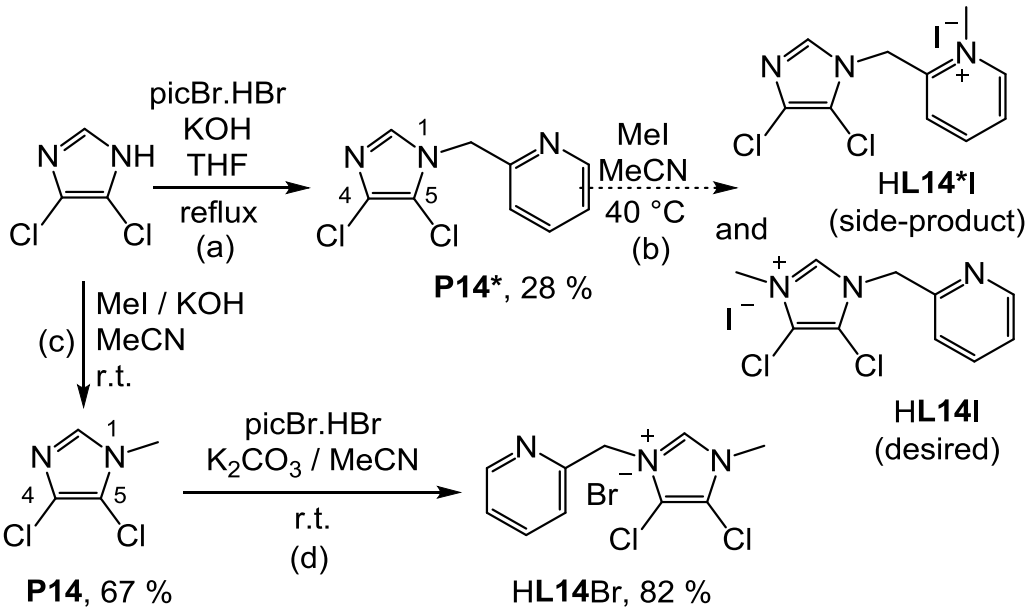

Scheme 2-10: Synthetic routes to imidazolium ligand precursors of **L14**.

The synthetic route *via* 1-methylbenzimidazole (**P15**) was chosen for the preparation of benzimidazolium salt H**L15**Br, to avoid methylation at the pyridine ring (Scheme 2-11). Base is required in the reaction to removed HBr from the picolyl in the imidazolium product. This was added to the reaction mixture after consumption of picolylbromide to prevent the electrophilic bromoalkane attacking the pyridine ring, which would lead to side-products that are hard to separate.

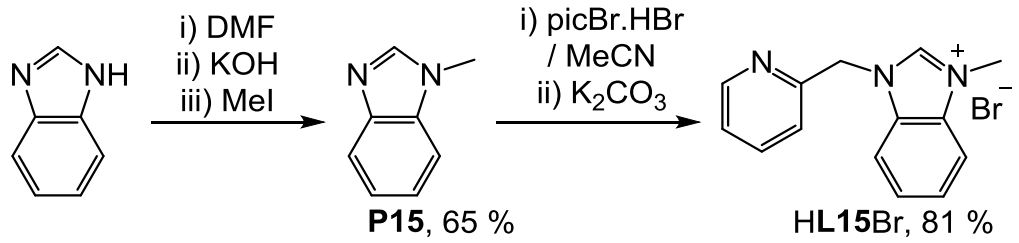

Scheme 2-11: Preparation of **P15** and H**L15**Br.

Both H**L14**Br and H**L15**Br were fully characterised by ^{1}H and ^{13}C {^{1}H} NMR spectroscopy and HRMS. The formation of the imidazolium salt was indicated by the imidazolium proton resonances (11.02 and 11.47 ppm respectively). Theoretically both chlorine atoms and the benzimidazole make the H-imidazolium less basic and a weaker NHC donor. However, the resonances cannot be used to directly compare the electron density between **L14** and **L15** because the chemical shift is heavily affected by the differing aromaticity of the benzimidazolium. The higher aromaticity of benzimidazole can cause the resonance to shift downfield due to the higher magnetic field generated by the π-system, in addition to the σ-electron density of the H-2 imidazolium.

In situ formed Cu(I) complexes of **L14** and **L15** were evaluated in the same etherification reaction as previously (Scheme 2-4), and compared to the ligand-free system and to ligand **L3** (Figure 2-7). Among these 3 ligands, **L15** gave the highest conversion to the ether product (62 %), with **L3** and **L14** being similar to each other (46% and 47% respectively, Table 2-3). The steric and chelating abilities of all three ligands should be similar, hence the difference in conversion is likely to be an electronic effect. The benzimidazole-derived ligand is a weaker donor which will aid in reductive elimination of the ether. However, if this were the main governing factor then **L14** should perform more efficiently than **L15**. This indicates that a fine balance of electronic properties is required; a weaker donor aids the nucleophilic substitution and reductive elimination steps, though if it is too weak the Cu intermediates may not be sufficiently stabilised and oxidative addition may be supressed.

Catalyst (10 mol %)	R^1	R^2	NHC ring based on	% conversion
CuI	N/A	N/A	N/A	29
CuI + H**L3**Br	picolyl	methyl	imidazole	46
CuI + H**L14**Br	picolyl	methyl	4,5-dichloroimidazole	47
CuI + H**L15**Br	picolyl	methyl	benzimidazole	62

Table 2-3: Ligand screening in the Cu-catalysed etherification reaction of 4-iodoanisole with 3,5-dimethylphenol (conversion determined by GC using *p*-cymene as an internal standard).

2.5 Allyl-*N*-substituted NHC ligands

Further studies on picolyl/pyridyl derivatives were carried out in the group by Joseph Sheppard (MChem research project).[49] The same etherification reaction was screened under the same conditions but for 22 hours. Interestingly, in his screen, among the allyl-*N*-substituted NHC ligands, when the second *N*-substituent was a methyl group (**L16**), the ligand performed as effectively as **L1** (picolyl), **L8** (pyridyl) and **L17** (6-methylpyridyl) in the catalysis (39 – 42 % conversion) (Figure 2-8).

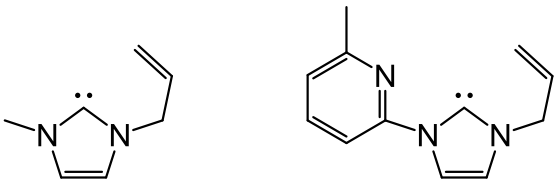

L16 **L17**

Figure 2-8: Structure of **L16** and **L17**.

In this work, we have expanded on this further, with the second *N*-substituent being replaced by sterically bulky groups: trityl and chlorotrityl (Figure 2-9) were chosen.

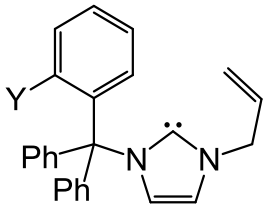

L18; Y = Cl
L19; Y = H

Figure 2-9: Proposed trityl-bearing NHCs.

The preparation of H**L19**Cl was carried out by another group member. The ligand precursor, H**L18**Cl, was prepared by reaction of 2-chlorotritylchloride with 1-allylimidazole in MeCN at 80 °C (Scheme 2-12). The imidazolium salt was purified by recrystallisation and fully characterised using ^{1}H and ^{13}C $\{^{1}H\}$ NMR spectroscopy and HRMS. The imidazolium protons of H**L18**Cl and H**L19**Cl appear at δ 9.23 and 9.62 ppm (300 MHz, $CDCl_3$) respectively in the ^{1}H NMR spectrum.

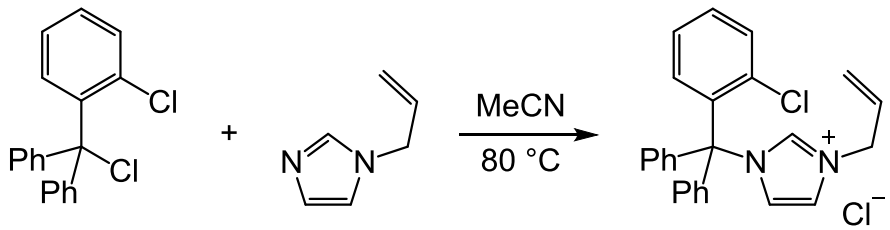

H**L18**Cl, 38 %

Scheme 2-12: Preparation of H**L18**Cl.

The allyl-bearing NHC ligands **L1**, **L8**, **L17**, **L18** and **L19** were compared in the Cu-NHC catalysed etherification reaction. All NHC ligands with an N-donor group performed better than the NHCs without this group (Table 2-4). This illustrates that the N-donor group is more significant than a sterically bulky group in stabilising Cu intermediates during catalysis. Coordination of the picolyl group forces the coordination of aryl and nucleophile reagents to be adjacent to each other so that they can be coupled easily. Contrarily, a bulky group may protect

the Cu centre but does not necessarily force the close proximity of the substrates as the group is not coordinated.

Catalyst (10 mol %)	R^1	R^2	NHC ring based on	% conversion
CuI	N/A	N/A	N/A	23
CuI + H**L1**Br	picolyl	allyl	imidazole	36
CuI + H**L8**Br	pyridyl	allyl	imidazole	31
CuI + H**L17**Br	6-methylpyridyl	allyl	imidazole	36
CuI + H**L18**Cl	chlorotrityl	allyl	imidazole	29
CuI + H**L19**Cl	trityl	allyl	imidazole	27

Table 2-4: Ligand screening in the Cu-catalysed etherification reaction of 4-iodoanisole with 3,5-dimethylphenol (conversion determined by GC using *p*-cymene as an internal standard).

It should be noted that in this catalytic screening and subsequent screens (in sections 2.5 and 2.6), the catalytic performance of the ligand-free system and **L1** and **L8** dropped significantly. This demonstrates the highly sensitive nature of Cu-catalysed reactions, with challenges in reproducibility being common in the field.[50,51] Cu-catalysed reactions are sensitive towards various conditions. Nguyen previously showed that different suppliers of the base Cs_2CO_3 have a large impact on the Cu(I)-catalysed Ullmann-Goldberg C-N coupling reaction.[50] Comparison among milled base supplied by Chemetall, Sigma-Aldrich and Acros Organic, it was observed that the base supplied by Chemetall, which has a smaller particle size and narrower distribution than the base from Sigma-Aldrich, had an induction period and slowed the catalysis. The Acros Organic base has a larger and more evenly distributed particle size and non-porous morphology. It resulted in the fastest reaction.

In our case, Cs_2CO_3 bottles were ordered from just Sigma-Aldrich but with different time of exposure to air, which might the moisture to be trapped in the base and change its morphology or particle size. Contrarily, our MChem student found that storing bases (Cs_2CO_3, K_2CO_3 and K_3PO_4) in an oven cause the % conversion of our model Cu-catalysed etherification to drop significantly (Table 2-5).[49] Other factors might be involved in the greatly sensitive reproducibility, such as the rate of stirring and the time taken for the reaction mixture to reach the desired temperature (90 °C). However, trend across the ligands in the parallel

screen can be compared, as they were observed to have the same trend across the screening *e.g.* **L1** is better than **L3** and **L8**.

base	% conversion	
	normal	stored in an oven
Cs_2CO_3	39	3
K_2CO_3	2	1
K_3PO_4	63	17

Table 2-5: Base screening in the Cu-catalysed etherification reaction of 4-iodoanisole with 3,5-dimethylphenol using L8 as a supporting ligand (conversion determined by GC using *p*-cymene as an internal standard).[49]

2.6 Tridentate ligands

NHC ligands with two strongly coordinating *N*-substituents can coordinate to a metal in a tridentate fashion, with this type of coordination being observed in Pd complexes that are active in Heck coupling of 4-bromoacetophenone with *n*-butyl acrylate[52] and in Cu-(pincer NHC) complexes that are active in Sonogashira-type reactions of aryl iodide and aryl acetylene.[53] The tridentate ligand can prevent reductive elimination of methyl-imidazolium from the Pd centre, which is facile at room temperature,[54] and can be considered as a catalyst deactivation pathway. Tridentate ligand precursors to **L20** and **L21** were prepared, which may coordinate to Cu in a tridentate manner (Figure 2-10).

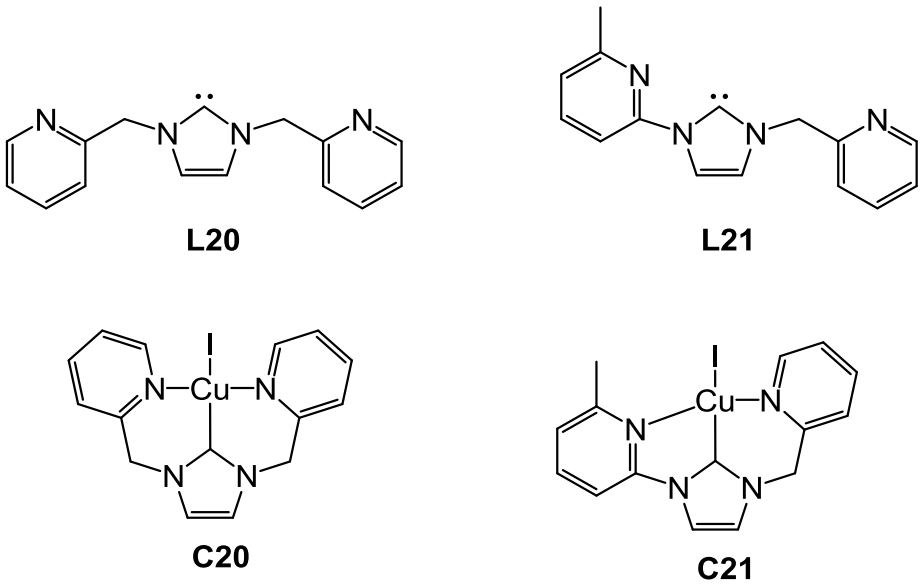

Figure 2-10: Bis(picolyl) and pyridyl-picolyl NHC ligands, and their proposed Cu-NHC complexes.

H**L20**Br is a symmetric imidazolium so can be prepared by heating imidazole with a slight excess of 2-(bromomethyl)pyridine.HBr under reflux in the presence of $NaHCO_3$ in MeOH (Scheme 2-13).

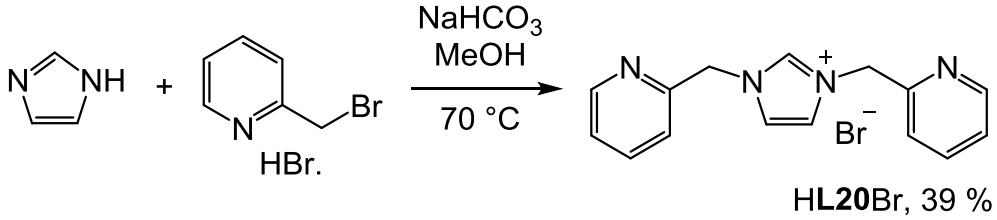

Scheme 2-13: Preparation of H**L20**Br.

H**L21**Br is a novel compound and was prepared in 2 steps (Scheme 2-14), *via* an Ullmann-type coupling reaction to form **P21**, followed by picolylation in MeCN in the presence of a base to give H**L21**Br. Bidentate ligand H**L17**Br was also prepared for comparison in catalysis, through allylation of **P17**. The ^{1}H NMR spectrum of H**L17**Br showed the imidazolium proton signal at δ 11.89 ppm, which is the same as that of H**L21**Br, indicating that the NHCs will have similar donor strengths.

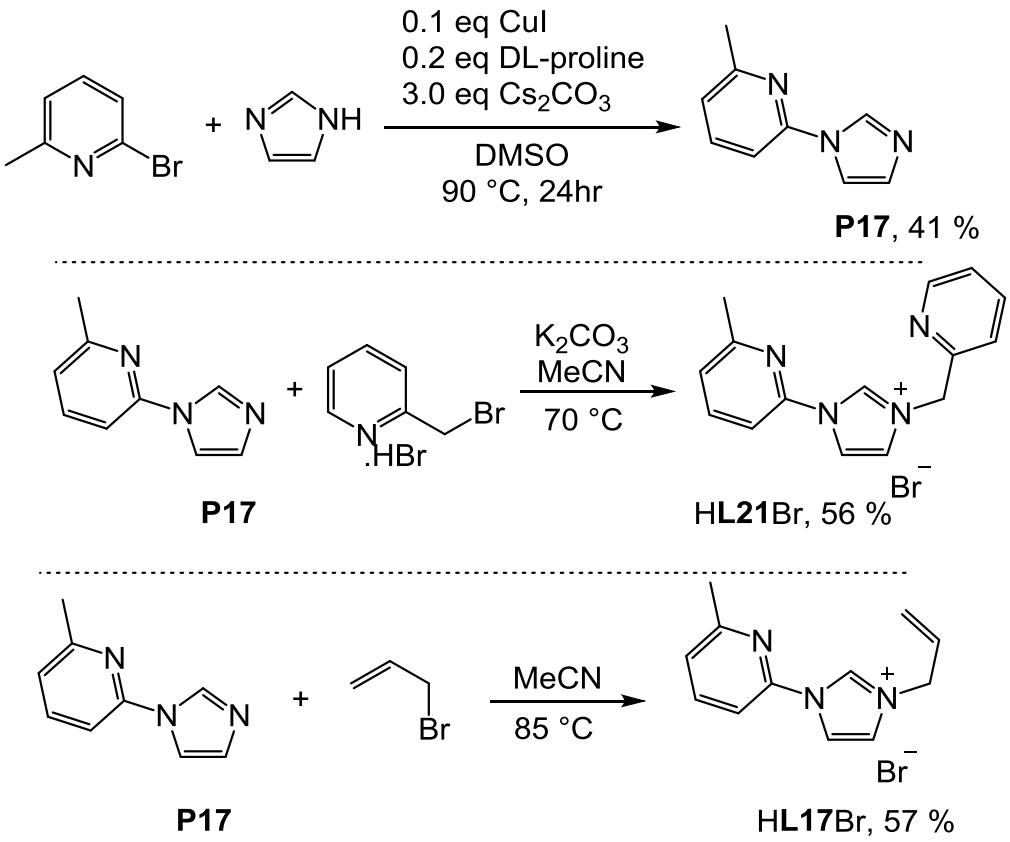

Scheme 2-14: Preparation of **P27**, H**L27**Br and H**L17**Br.

Ligands **L1**, **L17**, **L20** and **L21** were formed *in situ* and examined in the same Cu-catalysed etherification reaction as previously (Scheme 2-4, Table 2-6). Surprisingly, it was observed that the tridentate ligands **L20** and **L21** led to lower conversions (30% and 9% respectively) than the allyl-bearing NHCs **L1** (36 %), **L8** (31 %) and **L17** (36%). This suggests that an allyl group enhances catalysis compared to a picolyl group, when it is on the same NHC as another *N*-donor group. The weak π-donor allows equilibrium coordination so that more suitable sites are available for the cross-coupling reaction. **L21** appears to shut down catalysis which may be due to saturated coordination and sterics.

Catalyst (10 mol %)	R^1	R^2	NHC ring based on	% conversion
CuI	N/A	N/A	N/A	23
CuI + H**L1**Br	picolyl	allyl	imidazole	36
CuI + H**L17**Br	6-methylpyridyl	allyl	imidazole	36
CuI + H**L20**Br	picolyl	picolyl	imidazole	30
CuI + H**L21**Br	6-methylpyridyl	picolyl	imidazole	9

Table 2-6: Ligand screening in the Cu-catalysed etherification reaction of 4-iodoanisole with 3,5-dimethylphenol (conversion determined by GC using *p*-cymene as an internal standard).

Further ligand precursors were prepared which contain a benzimidazole backbone and a combination of allyl and picolyl substituents, as these are the leading *N*-substituents (Figure 2-11).

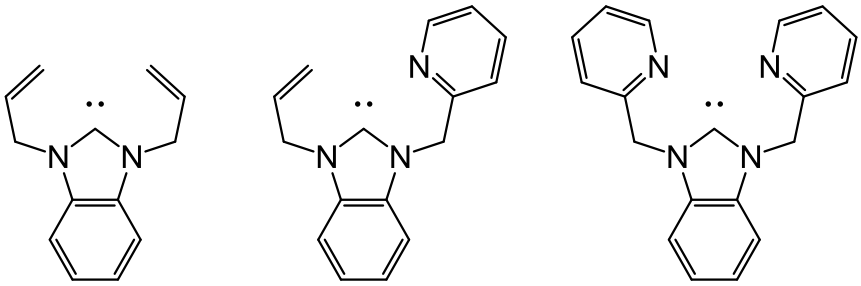

Figure 2-11: Proposed benzimidazole-based NHC ligands

Ligand precursor H**L22**Br was prepared by another group member. A novel compound, H**L23**Br was prepared through nucleophilic substitution of benzimidazole with picolyl bromide, followed by allylation (Scheme 2-15). A novel compound, H**L24**Br was synthesised using the same method as for H**L20**Br.

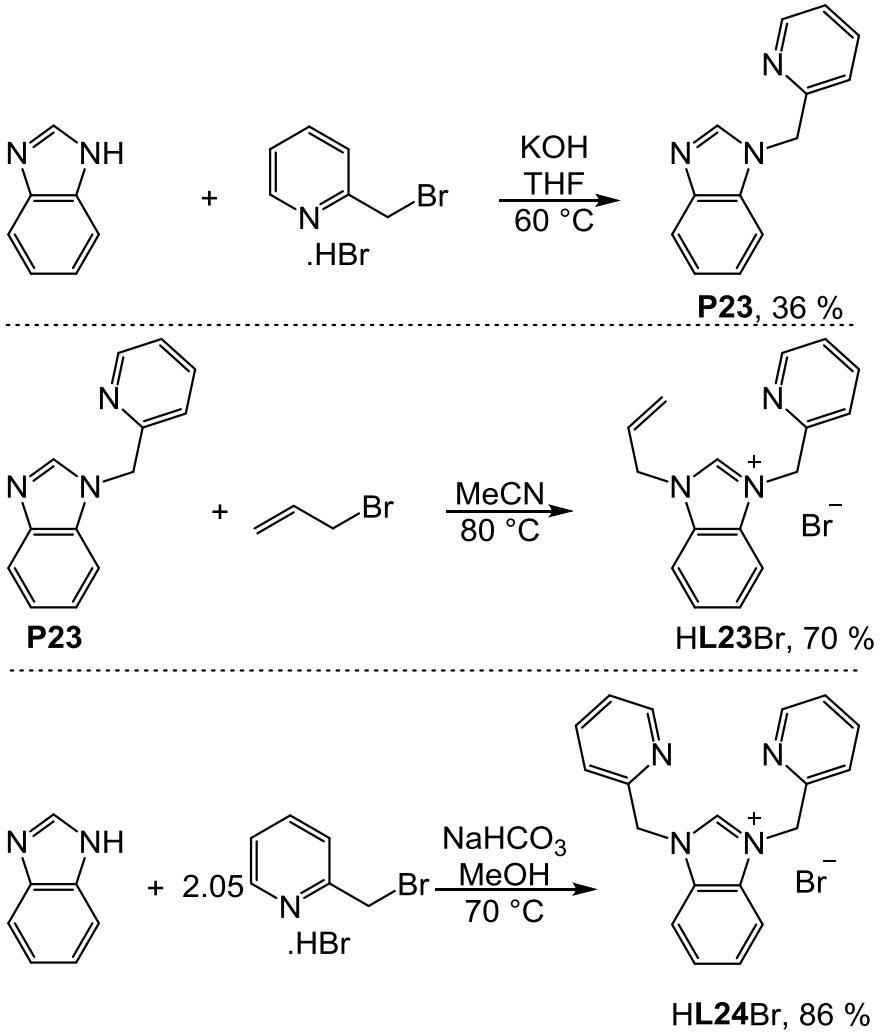

Scheme 2-15: Preparation of **P23**, H**L23**Br and H**L24**Br.

The ligands were screened in the same etherification reaction as previously and compared to the imidazole-based ligands (Table 2-7). Ligand **L23**, with a combination of allyl and picolyl substituents, led to the highest conversion. This is in keeping with the previous observations with **L1** and **L23**, in which a mixed allyl/picolyl NHC is more active ligand in catalysis. Comparing NHCs of the same *N*-substituents shows that benzimidazole-based NHCs **L23** and **L24** exhibit higher catalytic activity than the imidazole derivatives **L1** and **L20**. This observation is consistent with previous results, which found the benzimidazole ligand **L15** to be more catalytically active than the imidazole derivative **L3**. This may be due to the benzimidazole-based ligands being weaker donors, leading to faster reductive elimination of the cross-coupled product.

Catalyst (10 mol %)	R^1	R^2	NHC ring based on	% conversion
CuI	N/A	N/A	N/A	23
CuI + H**L22**Br	allyl	allyl	benzimidazole	27
CuI + H**L1**Br	picolyl	allyl	imidazole	36
CuI + H**L23**Br	picolyl	allyl	benzimidazole	52
CuI + H**L20**Br	picolyl	picolyl	imidazole	30
CuI + H**L24**Br	picolyl	picolyl	benzimidazole	43

Table 2-7: Ligand screening in the Cu-catalysed etherification reaction of 4-iodoanisole with 3,5-dimethylphenol (conversion determined by GC using *p*-cymene as an internal standard).

To summarise, a benzimidazole backbone on the NHC benefits the catalytic activity of Cu-NHCs in the etherification reaction studied, indicating that a weaker donor ligand is more advantageous. The *N*-substituents that enhance catalytic activity are picolyl and allyl groups, especially when both of them are cooperated on the same NHC ligand. The picolyl group is a strong donor and is likely to promote nucleophilic substitution and oxidative addition of an aryl halide, while the weak π-donor allyl group may not provide an active site at the metal centre but stabilise Cu intermediates when required.

2.7 Comparison with Other Bidentate Ligands

There are many literature examples of *N*-donor and *O*-donor ligands that were found effective in enhancing Ullmann reactions.[28,29] To compare these to the NHC ligands, *N*-donor ligands 2,2'-bipyridyl (**L25**), 1,10-phenanthroline (**L26**) and *N*,*N*,*N*',*N*'-tetramethyl ethylenediamine (**L27**) were examined in the etherification reaction studied in this chapter. The electron lone pairs of **L25** and **L26** are in sp^2 orbitals, while the nitrogen atoms of **L27** have sp^3 configurations. *O*-donor ligands that were examined are dimethoxyethylene (**L28**), glycolate (**L29**), ketocyclohexanone (**L30**) and acetyl acetonate (**L31**) (Figure 2-12).

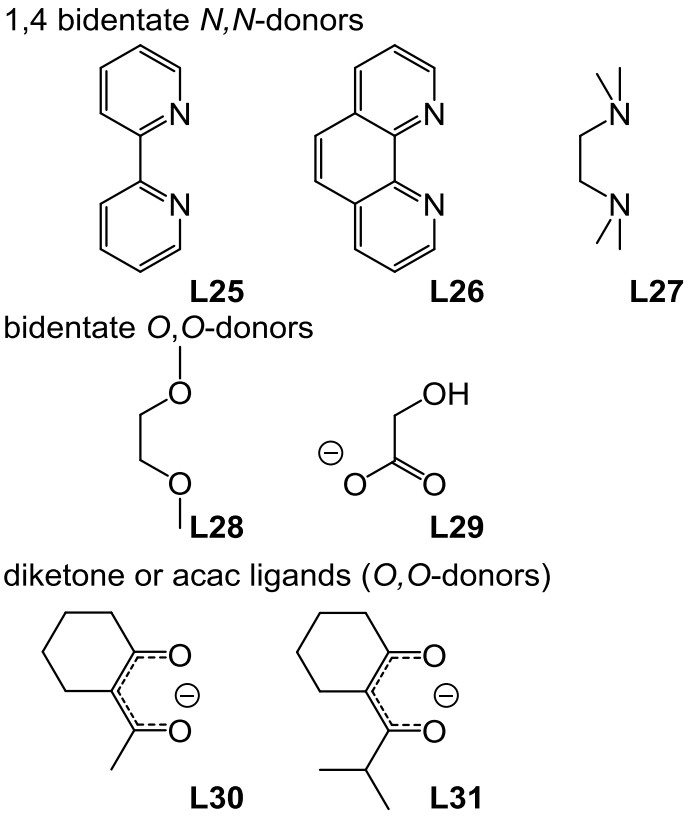

Figure 2-12: Ligands with *O*,*O'*-donors or *N*,*N'*-donors

In general, the trend in ligand performance follows acac-type (**L30** and **L31**) > *N*,*N'*-donors (**L25**, **L26** and **L27**) > neutral *O*,*O'*-donor (**L28**) > glycolate (**L29**) (Table 2-8). Acac-type ligands have been demonstrated to be selective towards C-N coupling over C-O coupling, as the electron rich ligands disfavour the coordination of the *O*-nucleophile.[28,29] However, the ligands did show reasonable activity in the etherification reaction, as the negative charge is likely to stabilise high oxidation-state intermediates enhancing catalytic activity more than neutral *N*,*N'*-donors. **L31** showed higher activity than **L30**, likely due to the steric effect of the *iso*propyl group, which probably protects the Cu centre from decomposition.

Catalyst (10 mol %)	% conversion
CuI	29
CuI + H**L1**Br	63
CuI + **L25**	46
CuI + **L26**	49
CuI + **L27**	50
CuI + **L28**	35
CuI + **L29**	24
CuI + **L30**	55
CuI + **L31**	61

Table 2-8: Ligand screening in the Cu-catalysed etherification reaction of 4-iodoanisole with 3,5-dimethylphenol (conversion determined by GC using *p*-cymene as an internal standard).

N,*N*′-donor ligands (**L25**, **L26** and **L27**) were found to improve catalytic activity over dme (**L28**) ligand. When both N and O atoms are neutral, N can denote more electron density than O because of lower electronegativity. The stronger donor helps promote the nucleophilic substitution step and stabilise the Cu intermediate. Moreover, **L27** gave the highest conversion among its group because its lone pair lies in an sp^3 orbital, which has higher energy and is more electron donating than an sp^2 orbital. Glycolate (**L29**) was the least active ligand despite bearing a negative charge, which should benefit the stabilisation of higher oxidation state Cu intermediates. However, unlike the acac-type ligands, glycolate contains 2 nucleophilic sites: carboxylate and hydroxyl groups, both of which may compete with the phenol. If both sites react with the aryl iodide, they can consume up to 20% of the aryl iodide. The side-reaction is also deactivating as it transforms the negatively charged ligand to a neutral *O*-donor ligand (aryl glycolate), which is less electron donating and hence less catalytically active.

To summarise, the acac-type diketonic ligands and *N*,*N*′-donors were demonstrated to enhance Cu-catalysed etherification and hence their Cu complexes have been used in cross-coupling reactions.[28,29] In this work, electron rich ligands generally lead to higher catalytic activity with the exception of **L29**, which can compete as a nucleophile. In addition, the amine sp^3 donor may enhance the catalytic activity compared to the pyridine sp^2 donor. Hence, it is

possible that an NHC with this substituent (*i.e*. **L10** or a derivative) would perform better than their pyridyl/picolyl derivatives.

2.8 Conclusions

A range of NHC ligands, *N*,*N′*-donors and *O*,*O′*-donors have been evaluated for their activity in the Cu-catalysed Ullmann-type etherification of 4-iodoanisole with 3,5-dimethylphenol. The ligands that were found to show good activity are **L1**, **L5**, **L23**, **L27** and **L31**. Overall, increased steric bulk was observed to enhance the catalytic activity in the case of bidentate ligands **L5** and **L31**. Bidentate ligands are more active than tridentate and non-chelating ligands as they afford the non-strained close proximity of the aryl and nucleophile. Electron-rich ligands favour nucleophilic substitution and are likely to stabilise the Cu(III) intermediates. Contrarily, electron poor NHCs can be beneficial for the coordination of the nucleophile and reductive elimination of the cross-coupled product. Hence, **L23**, which contains both picolyl and allyl *N*-substituents on a benzimidazole-based NHC, was found to have the greatest catalytic activity.

2.9 Future work

The *N*,*N′*-donors are selective for C-O bond formation, whereas acac-type ligands are selective for C-N bond formation.[28,29,55] From the selectivity, it was proposed that *O*-nucleophilic substitution occurs prior to nucleophile deprotonation, followed by oxidative addition in the case of *N*,*N′*-donors. In the case of acac-type ligands, the catalytic cycle steps are proposed to be halide dissociation, oxidative addition, coordination of *N*-nucleophile, deprotonation of nucleophile and reductive elimination. Since, NHC ligands are comparable to *N*,*N′*-donors and acac-type ligands, screening Cu-NHC complexes with amino-alcohol groups such as aminoethanol in C-O and C-N bond formation would allow us to predict the mechanism of the catalytic cycle by comparing the selectivity.

Furthermore, it is desirable to numerically correlate the performance and properties of NHC ligands for comparison. Comparison of electronic, geometric and steric properties of ligands can be challenging when more than one component has been modified, especially comparing across different types of ligands (*e.g.* NHCs, *N*,*N*- and *N*,*O*-donors). A computational ligand map can be used to numerically distinguish these differences,[38,56-58] which is a multi-dimensional plot of principle component (PC) scores. The role of PC analysis is

to include as many differences in the data as possible but in a few numbers of dimensions (or PCs). As a result, each PC score is generated by different loadings or coefficients of each descriptor. Descriptors are physical properties such as energies of HOMO and LUMO of the free ligand, proton affinity, metal-ligand bond lengths, etc. Due to different loadings of descriptors, each PC can be dominated by certain properties such as steric effects, metal-ligand interactions (σ and π), or electronic and geometric differences of ligands. Utilising the ligand map may help us reveal any correlations between ligand properties and catalytic activities and enable improved ligand design and predictability through a more knowledge-based approach. A ligand map has been calculated in collaboration with Dr Natalie Fey (Bristol). Currently, there are not enough data points to establish statistically significant correlation between the ligand map and the catalytic activity (Figure 2-13).

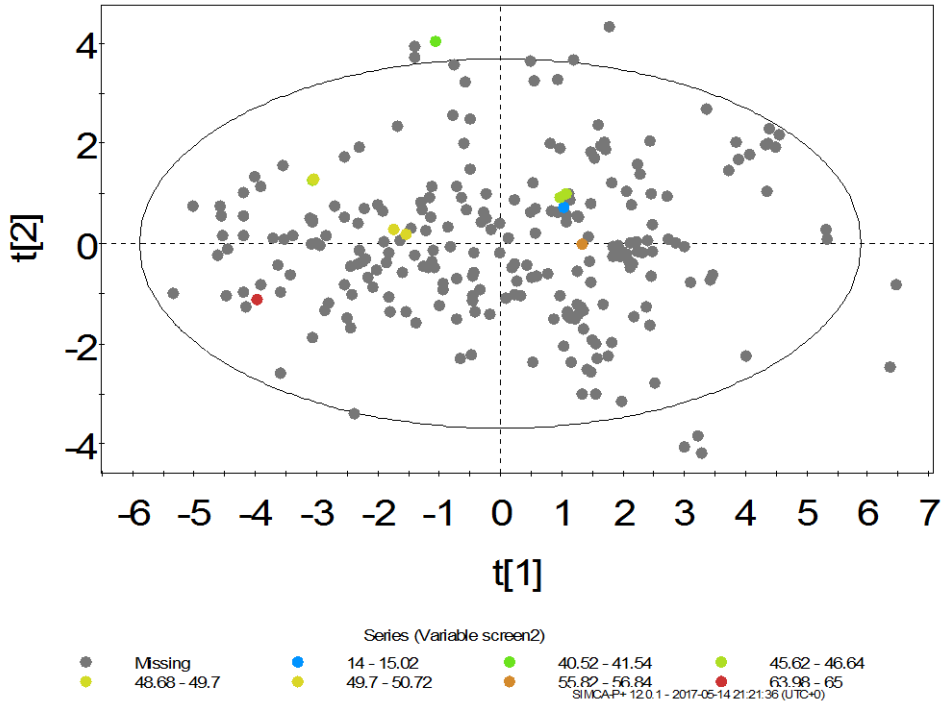

Figure 2-13: Ligand map of NHC ligands with % conversion in the Cu-catalysed etherification reaction.

2.10 Experimental

2.10.1 General considerations

General considerations are applied to experimental throughout this thesis.

Unless otherwise stated, manipulations were performed using standard Schlenk line and Glovebox techniques. N_2 was passed through a twin-column drying

apparatus containing molecular sieves (4Å) and phosphorus pentoxide. Anhydrous solvents were prepared by passing the solvent over activated alumina to remove water, *via* the Dow-Grubbs solvent system. Anhydrous CD_3CN, $CDCl_3$ and d_6-DMSO were dried over CaH_2, cannula filtered or distilled, and then freeze-pump-thaw degassed or bubbled by Ar prior to use. All other chemicals were obtained from commercial sources and used as received. Cu foil (99.9 % purity) was used as electrode surface directly without further purification (purchased from Goodfellow Cambridge Ltd).

^1H and ^{13}C {^1H NMR spectra were recorded by automated procedures on either a Bruker Avance (500/126 MHz) or DPX (300/75 MHz) NMR spectrometer, using the residual solvent as an internal standard. The values of chemical shift are reported in parts per million (ppm) with the multiplicities of the spectra assigned as follows: singlet (s), doublet (d), triplet (t), quartet (q), septet (sept) and multiplet (m), values for coupling constants (J) are assigned in Hz.

High-resolution electrospray mass spectra (ESI-MS) were measured on an open-access Bruker Daltonics (micro TOF) instrument operating in the electrospray mode. Samples were injected directly from feed solutions and acquired over the *m/z* range 50 – 4000. All spectra were recorded using an MeCN / water mix as the eluent and a sodium formate solution as a calibrant.

LC-MS analyses were conducted on a Thermo Scientific Ultimate 3000 using UHPLC+ technology. All experiments were run through a Kinetix C-18 50×2.1 mm LC-Column, 2.6 µm particle size, using a 5-95 % gradient (MeCN:water, 0.1 % formic acid) over 1.7 min. Samples were ionised by electrospray.

Samples for microanalysis were dried under vacuum prior to analysis and the elemental composition determined by Ms. Tanya Marinko-Covell of the University of Leeds or by Mr Stephen Boyer at London Metropolitan University.

Fourier-transform IR spectra were recorded as solid phase or in MeCN or DMF phase on a Perkin-Elmer Spectrum One spectrophotometer. Reactions were monitored in situ using a Mettler Toledo ReactIR ic_{10} with K6 conduit SiComp (silicon) probe and MCT detector.

Thin-layer chromatography (TLC) was carried out using Merck S554 aluminum-backed silica plates (silica gel 60 F254), and spots were visualised by UV light (at 254 nm). Flash and fractional column chromatography was performed using Merck 60 silica gel (particle size 40 – 63 µm) and a solvent system as reported in the text.

Electrochemical measurements were conducted using an Autolab PGSTAT204 voltammetric analyser under an Ar atmosphere, solvated in pre-dried MeCN containing 0.10 M [*n*-Bu_4N](PF_6) as a supporting electrolyte. Voltammetric experiments utilised a Pt disk working electrode, a Pt rod auxiliary electrode and a Ag/AgCl reference electrode. All potentials quoted are referenced to an internal ferrocene/ferrocenium standard.

Single crystal X-ray diffraction data were collected on an Agilent SuperNova diffractometer fitted with an Atlas CCd detector with Mo Kα radiation (λ = 0.7107 Å) or Cu Kα radiation (λ = 1.5418 Å). Crystals were mounted under oil on nylon fibres. Crystals were held at 120 K using an Oxford Cryosystems low temperature device during unit cell determination and data collection. Data sets were corrected for absorption using a multiscan method, and the structures were solved by direct methods using SHELXS-97 or SHELXT and refined by full-matrix least squares on F2 using ShelXL-97, interfaced through the program Olex2. Molecular graphics for all structures were generated using POV-RAY in the X-Seed program.

GC analyses were performed using a Bruker 430-GC equipped with a CP-8400 autosampler and a BR-5 column (30 m × 0.25 mm (ID) × 0.25 μm film thickness) with carrier gas flow rate of 2.0 mL min^{-1} and a temperature ramp from 50 → 310 °C at 20 °C min^{-1}. The injection volume was 1.0 μL with a split ratio of 10. The response factors for the internal standard (p-cymene), substrate and authentic product were calculated using an appropriate calibration for this GC, method and column.

2.10.2 Preparation of imidazoles

i) Preparation of **P5'**

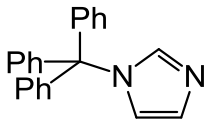

Imidazole (1.47 g, 21.52 mmol) was added to a three-necked round-bottomed flask. Trityl chloride (2.00 g, 7.17 mmol) was added to a Schlenk flask. DMF (18 mL) was added to both flasks *via* syringe and stirred until full dissolution. The trityl chloride solution was transferred to a dropping funnel attached to the three-necked flask *via* syringe and added dropwise to the reaction vessel, and the resulting solution stirred for 24 hours. The solution turned cloudy after 2-3 hours of mixing. The reaction mixture was partitioned between water (100 mL) and chloroform (100 mL), and the aqueous layer was extracted with $CHCl_3$ (3 × 100 mL). The combined organic phase (including first partition) were washed with water (100 + 5 × 50 mL), dried over Na_2CO_3, and the solvent removed *in vacuo*.

The extraction and washing steps were repeated to give a white solid. The crude product was dissolved in hot MeCN, and the solvent was allowed to slowly evaporate until a solid precipitated. The mixture was cooled in an ice bath to yield more white precipitate, which was collected by filtration and was washed with cold MeCN. Yield: 1.23 g, 3.96 mmol, 55 %.

^{1}H NMR (300 MHz, $CDCl_3$) δ (ppm) 7.48 (t, *J* = 1.4 Hz, 1H, imH-2), 7.38 – 7.33 (m, 9H, Trt), 7.20 – 7.13 (m, 6H, Trt), 7.09 (t, *J* = 1.4 Hz, 1H, imH), 6.85 (t, *J* = 1.4 Hz, 1H, imH). ^{13}C {^{1}H} NMR (75 MHz, $CDCl_3$) δ (ppm) 142.5 (C), 129.8 (CH), 128.3 (CH), 128.0 (CH), 127.9 (CH), 121.8 (CH), 75.2 (C). HRMS (ESI^+): *m/z* 311.1538 $[M + H]^+$, calculated $[M + H]^+$ 311.1543.

Consistent with data previously reported.[35]

ii) Preparation of **P8**

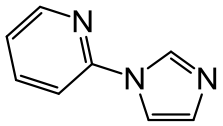

Imidazole (3.93 g, 57.7 mmol), Cs_2CO_3 (10.87 g, 78.7 mmol), CuI (0.50 g, 2.6 mmol), and DL-proline (0.45 g, 3.9 mmol) were added to a Schlenk flask and placed under Ar. 2-Bromo-pyridine (5.0 mL, 52.4 mmol) and anhydrous DMSO (10 mL) were added to the flask, and the mixture was stirred at 100 ºC for 22 hours. After cooling to room temperature, DCM (100 mL) was added and the suspension was filtered through Celite. The filtrate was washed with water (100 mL) and the aqueous layer was extracted with DCM (3 × 100mL). The combined organic phase was reduced *in vacuo* to give a green liquid, which was dissolved in DCM (100 mL) and washed with water (3 × 100 mL) and the aqueous layers were combined and extracted with $CHCl_3$ (3 × 100 mL). The organic layers were combined, washed with water (6 × 100 mL), and the solvent removed *in vacuo*. The green liquid was dissolved in DCM (100 mL) and washed with saturated EDTA solution (3 × 100 mL), water (3 × 100 mL) and brine (100 mL), dried over Na_2SO_4, and the solvent was removed *in vacuo* to give a yellow oil. The crude product was purified by flash column chromatography (silica gel), eluting with EtOAc / petroleum ether (50: 50) → EtOAc / petroleum ether / MeOH (45: 45: 10). The pure product was obtained as an orange oil. Yield: 4.25 g, 29.3 mmol, 56 %.

^{1}H NMR (300 MHz, $CDCl_3$) δ (ppm) 8.47 (ddd, *J* = 4.9, 1.9, 0.8 Hz, 1H, pyH-6), 8.33 (t, *J* = 1.4 Hz, 1H, imH), 7.81 (ddd, *J* = 8.2, 7.5, 1.9 Hz, 1H, pyH-4), 7.63 (t, *J* = 1.4 Hz, 1H, imH), 7.35 (dt, *J* = 8.2, 0.8 Hz, 1H, pyH-3), 7.23 (ddd, *J* = 7.5, 4.9, 0.9 Hz, 1H, pyH-5), 7.18 (t, *J* = 1.4 Hz, 1H, imH). ^{13}C {^{1}H} NMR (75 MHz, $CDCl_3$) δ (ppm) 149.3 (CH), 149.2 (C), 139.1 (CH), 135.1 (CH), 130.7 (CH),

122.2 (CH), 116.3 (CH), 112.5 (CH). HRMS (ESI$^+$): *m/z* 146.0744 [M + H]$^+$, calculated [M + H]$^+$ 146.0713.

Consisted with data previously reported.[44,52]

iii) Preparation of **P14***

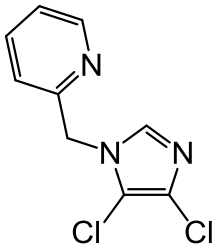

4,5-Dichloroimidazole (0.50 g, 3.65 mmol), 2-(bromomethyl)pyridine.HBr (0.92 g, 3.65 mmol) and KOH (0.82 g, 14.6 mmol) were placed in a round-bottomed flask and THF (20 mL) was added. The mixture was heated to 60 ºC for 24 hours under N_2 and hydrous conditions then allowed to cool to room temperature and the solvent removed *in vacuo*. The crude mixture was partitioned between DCM (50 mL) and water (50 mL) and the aqueous layer was extracted with DCM (2 × 50 mL). The organic layers were combined, dried over Na_2SO_4 and the solvent removed *in vacuo*. The dark oil was dissolved in Et_2O (50 mL), filtered, and the filtrate was reduced *in vacuo* to obtain an orange oil. Yield: 0.23 g, 1.00 mmol, 28%.

^{1}H NMR (300 MHz, CDCl3) δ (ppm) 8.55 (ddd, *J* = 4.8, 1.7, 0.8 Hz, 1H, pyH-6), 7.66 (td, *J* = 7.7, 1.7 Hz, 1H, pyH-4), 7.51 (s, 1H, imH), 7.23 (ddd, *J* = 7.7, 4.8, 0.8 Hz, 1H, pyH-5), 7.02 (dt, *J* = 7.7, 0.8 Hz, 1H, pyH), 5.17 (s, 2H, N**CH$_2$**-py). ^{13}C {^{1}H} (75 MHz, $CDCl_3$) δ (ppm) 154.1, 149.9, 137.5, 135.1, 126.4, 123.4, 121.5, 113.6, 51.1. HRMS (ESI$^+$): *m/z* 228.0107 [M + H]$^+$, calculated [M + H]$^+$ 228.0090.

iv) Preparation of **P14**

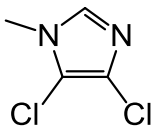

4,5-Dichloroimidazole (0.30 g, 2.19 mmol) was dissolved in MeCN (15 mL). KOH (0.54 g, 9.64 mmol) was added, and the mixture was stirred at room temperature for 2 hours under N_2 and hydrous conditions. The reaction mixture was filtered and iodomethane (0.136 mL, 2.19 mmol) was added to the light brown filtrate. The reaction mixture was stirred for 24 hours. The white precipitate was filtered off, and the solvent was removed from the filtrate *in vacuo*. The crude oil was dissolved in DCM (50 mL) and washed with water (3 × 50 mL). The aqueous layers were combined and back-extracted with DCM (3 × 50 mL). All organic layers were combined, dried over Na_2SO_4 and the solvent removed *in vacuo*. The product was obtained as a yellow solid. Yield: 0.22 g, 1.46 mmol, 67%.

^{1}H NMR (300 MHz, $CDCl_3$) δ (ppm) 7.34 (s, 1H, imH), 3.59 (s, 3H, N**CH_3**). ^{13}C {^{1}H} NMR (75 MHz, CDCl3) δ (ppm) 134.61, 125.9, 113.9, 32.6. HRMS (ESI^+): *m/z* 150.9826 $[M + H]^+$, calculated $[M + H]^+$ 150.9824.

v) Preparation of **P15**

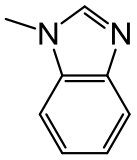

Benzimidazole (1.0 g, 8.46 mmol) and KOH (0.95 g, 16.93 mmol) were stirred in DMF (10 mL) for 3 hours. MeI (0.53 mL, 8.46 mmol) was added, and the reaction mixture was stirred for 18 hours under N_2 and hydrous conditions. The mixture was partitioned between water (25 mL) and $CHCl_3$ (10 mL). The aqueous layer was extracted with $CHCl_3$ (3 × 10 mL). The combined organic layers were washed with water (3 × 50 mL), which were combined and extracted with $CHCl_3$ (3 × 30 mL). All organic layers were combined, dried over $MgSO_4$ and the solvent removed *in vacuo* to give a colourless oil. Yield: 0.73 g, 5.52 mmol, 65%.

^{1}H NMR (300 MHz, $CDCl_3$) δ (ppm) 7.81 (s, 1H, BzmH), 7.79 – 7.75 (m, 1H, BzmH), 7.37 – 7.32 (m, 1H, BzmH), 7.32 – 7.27 (m, 1H, BzmH), 7.26 – 7.20 (m, 1H, BzmH), 3.78 (s, 3H, N**CH_3**). ^{13}C {^{1}H} NMR (75 MHz, $CDCl_3$) δ (ppm) 143.8, 143.5, 134.6, 122.9, 122.1, 120.3, 109.3, 31.0. HRMS (ESI^+): *m/z* 133.0767 $[M + H]^+$, calculated $[M + H]^+$ 133.0760.

vi) Preparation of **P17**

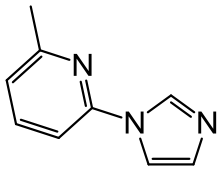

DL-proline (0.10 g, 0.9 mmol), Cs_2CO_3 (4.0 g, 13 mmol), CuI (0.084 g, 0.45 mmol) and imidazole (0.38 g, 5.3 mmol) were added to a Schlenk flask. DMSO (5 mL) was added, followed by 2-bromo-6-methylpyridine (0.5 mL, 4.4 mmol). The reaction mixture was stirred at 90 °C for 23 hours under Ar. The mixture was allowed to cool to room temperature and DCM (50 mL) was added and the mixture filtered through Celite. The filtrate was washed with water (4 × 50 mL) and the aqueous layers were combined and extracted with DCM (4 × 150 mL). The extracted organic layers were combined and the volume reduced to about 50 mL *in vacuo*. The washing/extracting steps were repeated twice. These organic layers were combined, dried over Na_2SO_4 and the solvent removed *in vacuo* to obtain a brown liquid. The crude product was purified by flash column chromatography (silica gel), eluting with EtOAc / hexane (1: 2) → EtOAc / petroleum ether / MeOH (40: 50: 10). The pure product was obtained as a colourless oil. Yield: 0.29 g, 1.82 mmol, 41 %.

^{1}H NMR (300 MHz, $CDCl_3$) δ (ppm) 8.37 (s, 1H, imH), 7.71 (dd, *J* = 8.1, 7.6 Hz, 1H, pyH-4), 7.67 (s, 1H, imH), 7.22 (s, 1H, imH), 7.17 (d, *J* = 8.1 Hz, 1H, pyH-5), 7.11 (d, *J* = 7.6 Hz, 1H, pyH-3), 2.59 (s, 3H, py**CH_3**). ^{13}C {^{1}H} NMR (75 MHz, $CDCl_3$) δ (ppm) 158.8, 139.0. 121.5, 109.2, 24.3. HRMS (ESI^+): *m/z* 160.0870 $[M + H]^+$, calculated $[M + H]^+$ 160.0869.

vii) Preparation of **P23**

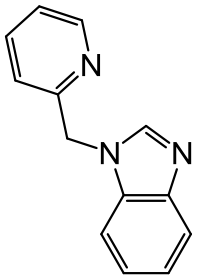

KOH (0.52 g, 9.3 mmol) was dissolved in THF (20 mL) and the reaction mixture stirred for 15 minutes. Benzimidazole (0.5 g, 4.2 mmol) was added and the mixture was heated to 60 °C under N_2 and hydrous conditions. 2-(Bromomethyl)pyridine.HBr (1.12 g, 4.4 mmol) was added to the heating solution and the reaction mixture was held at reflux for 27 hours. The mixture was allowed to cool to room temperature, filtered, and the filtrate reduced *in vacuo*. EtOAc (50 mL) was added and washed with water (3 × 50 mL). The aqueous layers were combined and extracted with DCM (3 × 100 mL). All organic layers were combined, dried over Na_2SO_4, and the solvent removed *in vacuo*. The crude brown oil was sonicated in Et_2O (50 mL) for 30 minutes, filtered and the filtrate was reduced *in vacuo* to obtain a brown solid. Yield: 0.32 g, 1.5 mmol, 36 %.

^{1}H NMR (300 MHz, $CDCl_3$) δ (ppm) 8.64 (ddd, *J* = 5.1, 1.8, 0.7 Hz, 1H, pyH-6), 8.08 (s, 1H, BzmH-2), 7.86 (ddd, *J* = 6.3, 2.1, 0.8 Hz, 1H, BzmH), 7.62 (td, J = 7.7, 1.8 Hz, 1H, pyH-4), 7.36 – 7.30 (m, 3H, BzmH), 7.24 (ddd, J = 7.7, 5.1, 1.5 Hz, 1H, pyH-5), 6.93 (ddd, J = 7.7, 0.7, 1.5 Hz, pyH-3), 5.52 (s, 2H, N**CH_2**-py). ^{13}C {^{1}H} NMR (75 MHz, $CDCl_3$) δ (ppm) 155.5 (C), 149.8 (CH), 143.9 (C), 143.4 (CH), 137.2 (CH), 133.9 (C), 123.2 (CH), 123.0 (CH), 122.4 (CH), 121.1 (CH), 120.5 (CH), 110.0 (CH), 50.6 (CH_2). HRMS (ESI^+): *m/z* 210.1031 $[M + H]^+$, calculated $[M + H]^+$ 210.1026.

2.10.3 Preparation of imidazolium salts

i) Preparation of H**L1**Br

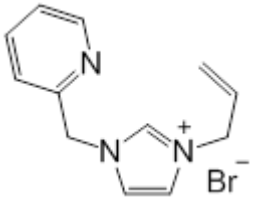

2-(Bromomethyl)pyridine.hydrobromide (2.50 g, 9.88 mmol) and K_2CO_3 (0.68 g, 4.94 mmol) were added to a round-bottomed flask, followed by addition of MeCN (160 mL) and dropwise addition of N-allyl imidazole (1.15 mL, 10.67 mmol). The resulting pale red mixture was stirred at room temperature under N_2 for 24 hours, over which time a colour change from red to yellow was observed. The yellow solution was dried over

$CaCl_2$ and the volume reduced *in vacuo* to 10 mL. Et_2O (150 mL) was added to precipitate a dark yellow-brown oil. The oil was washed with Et_2O (2 × 100 mL). Yield: 2.14 g, 7.63 mmol, 77 %.

^{1}H NMR (300 MHz, $CDCl_3$) δ (ppm) 10.46 (t, *J* = 1.7 Hz, 1H, imH-2), 8.56 (ddd, *J* = 4.9, 1.8, 1.1 Hz, 1H, pyH-6), 7.93 (dt, *J* = 7.7, 1.1 Hz, 1H, pyH-3), 7.80 (td, *J* = 7.7, 1.8 Hz, 1H, pyH-4), 7.70 (t, *J* = 1.7 Hz, 1H, imH), 7.33 (ddd, *J* = 7.7, 4.9, 1.1 Hz, 1H, pyH-5), 7.21 (t, *J* = 1.7 Hz, 1H, imH), 6.02 (ddt, *J* = 16.7, 10.3, 6.5 Hz, 1H, **CH**=CH_2), 5.83 (s, 2H, N**CH_2**-py), 5.54 – 5.44 (m, 2H, CH=**CH_2**), 4.94 (dt, *J* = 6.5, 1.3 Hz, 2H, N**CH_2**-vinyl). ^{13}C {^{1}H} NMR (75 MHz, $CDCl_3$) δ (ppm) 152.1 (C), 149.4 (CH), 138.3 (CH), 137.7 (CH), 129.3 (CH), 124.6 (CH), 124.3 (CH), 123.2 (CH), 123.0 (CH), 120.9 (CH_2), 53.7 (CH_2), 52.4 (CH_2). HRMS (ESI$^+$): *m/z* 200.1214 [M – Br]$^+$, calculated [M – Br]$^+$ 200.1182.

Consistent with data previously reported.[35,59]

ii) Preparation of H**L3**Br

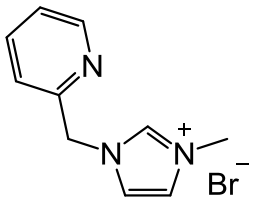

1-Methylimidazole (1.7 mL, 21.7 mmol) was dissolved in MeCN (100 mL), 2-(bromomethyl)pyridine.hydrobromide (5.0 g, 19.8 mmol) was added and stirred vigorously, followed by Na_2CO_3 (1.05 g, 9.9 mmol). The red reaction mixture was then heated and stirred at 80 °C under N_2 for 24 hours. The mixture was allowed to cool to room temperature, dried over Na_2SO_4, filtered and the volume reduced to about 5 mL. Et_2O (150 mL) was added to precipitate a dark red-brown oil. The oil was dissolved in MeOH (20 mL), dried over Na_2SO_4, the volume reduced to 5 mL and EtOAc (100 mL) was added to precipitate a dark red-brown oil. Yield: 2.29 g, 9.0 mmol, 46 %.

^{1}H NMR (300 MHz, $CDCl_3$) δ (ppm) 10.26 (s, 1H, imH-2), 8.50 (d, *J* = 4.7 Hz, 1H, pyH-6), 7.79 – 7.68 (m, 2H, pyH), 7.63 (s, 1H, imH), 7.42 (s, 1H, imH), 7.29 – 7.23 (m, 1H, pyH), 5.73 (s, 2H, N**CH_2**-py), 4.05 (s, 3H, N**CH_3**). ^{13}C {^{1}H} NMR (101 MHz, $CDCl_3$) δ (ppm) 152.5 (C), 149.9 (CH), 149.4 (CH), 137.9 (CH), 137.8 (CH), 124.1 (CH), 122.9 (CH), 122.8 (CH), 54.0 (CH_2), 36.8 (CH_3). HRMS (ESI$^+$): *m/z* 174.1025 [M – Br]$^+$, calculated [M – Br]$^+$ 174.1026.

Consistent with data previously reported.[60,61]

iii) Attempted synthesis of H**L5'**Br

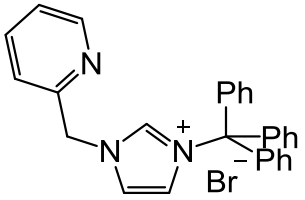

To freshly activated 4Å molecular sieves, 2-(bromomethyl)pyridine hydrobromide (0.045 g, 0.177 mmol) and Cs_2CO_3 (0.029 g, 0.089 mmol) were added. MeCN (10 mL) was transferred into the flask *via* cannula. The resulting mixture was stirred at room temperature for 3 hours. **P5'** (0.050 g, 0.161 mmol) was added and the reaction mixture stirred at room temperature for 24 hours. The yellow mixture was filtered and the filtrate volume was reduced *in vacuo* to 2 mL. A mixture of Et_2O and pentane (50 mL) was added, which precipitated a pale orange solid and the solid was collected from filtration. Yield: 0.0061 g.

HRMS (ESI$^+$): *m/z* 160.0869 [picolyl imidazole + H]$^+$, calculated [picolyl imidazole + H]$^+$ 160.0869; 243.1184 [tritryl]$^+$, calculated [trityl]$^+$ 243.1168; 251.1292 [dipicolyl imidazolium]$^+$, calculated [dipicoly imidazolium]$^+$ 251.1291; 402.1970 [M - Br]$^+$, calculated [M - Br]$^+$ 402.1965; 553.2645 [ditrityl imidazolium]$^+$ calculated [ditrityl imidazolium]$^+$ 553.2638. From the MS data it is clear that a mixture of products were formed in this reaction.

iv) Preparation of H**L5**Br

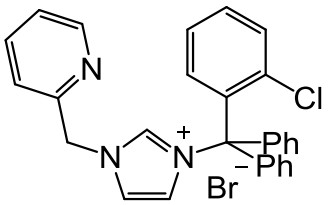

To freshly activated 4Å molecular sieves, 2-(bromomethyl)pyridine hydrobromide (1.00g, 3.95 mmol) and caesium carbonate (1.35 g, 4.15 mmol) were added,. MeCN (10 mL) was transferred into the flask *via* cannula. The resulting mixture was stirred at room temperature for 3 hours. Clotrimazole (1.43 g, 4.15 mmol) was added and the reaction mixture stirred at room temperature for 18 hours. The yellow mixture was filtered and the filtrate volume was reduced *in vacuo* to 2 mL. Et_2O (50 mL) was added to precipitate a pale orange solid. The solid was washed with Et_2O (2 × 50 mL). Yield: 0.32 g, 0.62 mmol, 16 %.

^{1}H NMR (300 MHz, $CDCl_3$) δ (ppm) 9.55 (t, *J* = 1.8 Hz, 1H, imH-2), 8.47 (ddd, *J* = 4.9, 1.8, 0.9 Hz, 1H, pyH-6), 8.18 (t, *J* = 1.8 Hz, 1H, imH), 8.01 (dt, *J* = 7.8, 1.0 Hz, 1H), 7.73 (td, *J* = 7.7, 1.8 Hz, 1H, pyH-4), 7.51 – 7.38 (m, 8H), 7.33 (ddd, *J* = 8.0, 7.0, 2.0 Hz, 1H), 7.29 – 7.23 (m, 1H), 7.17 – 7.10 (m, 4H, Trt), 7.07 (dd, *J* = 8.0, 1.4 Hz, 1H), 6.94 (t, *J* = 1.8 Hz, 1H, imH), 6.08 (s, 2H, im-**CH_2**-py). ^{13}C {^{1}H} NMR (75 MHz, $CDCl_3$) δ (ppm) 152.7, 149.4, 138.3, 138.2, 138.1, 137.7, 137.4, 135.3, 132.9, 131.5, 131.3, 129.8, 129.4, 129.0, 127.8, 124.7, 123.9, 123.4, 122.7, 54.2. HRMS (ESI$^+$): *m/z* 436.1604 [M - Br]$^+$, calculated [M - Br]$^+$ 436.1575.

Analysis Calculated for $C_{28}H_{23}N_3ClBr$ $0.8H_2O$: C, 63.30; H 4.67; N, 7.91. Found: C, 63.30; H, 4.45, N, 7.70.

v) Preparation of H**L6**Br

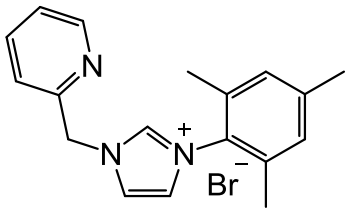

1-Mesitylimidazole (0.20 g, 1.07 mmol) and 2-(bromomethyl)pyridine.HBr (0.25 g, 0.98 mmol) were dissolved and stirred in MeCN (5 mL) for 24 hours under N_2. K_2CO_3 (0.067 g, 0.49 mmol) was added and the mixture stirred for a further 1 hour. The reaction mixture was filtered, and the filtrate reduced *in vacuo*. The resulting mixture was recrystallised from MeCN / Et_2O to give a red brown solid. Yield: 0.073 g, 0.20 mmol, 21 %.

^{1}H NMR (300 MHz, $CDCl_3$) δ (ppm) 10.43 (t, J = 1.7 Hz, 1H, imH-2), 8.57 (ddd, J = 4.9, 1.8, 0.7 Hz, 1H, pyH-6), 8.19 (dt, J = 7.8, 0.7 Hz, 1H, pyH-4), 8.12 (t, J = 1.7 Hz, 1H, imH), 7.85 (td, J = 7.7, 1.7 Hz, 1H, pyH-3), 7.37 (ddd, J = 7.6, 4.9, 0.9 Hz, 1H, pyH-5), 7.09 (t, J = 1.7 Hz, 1H, imH), 7.01 (s, 2H, MesH), 6.23 (s, 2H, im-**CH_2**-py), 2.35 (s, 3H, Mes-**CH_3**), 2.07 (s, 6H, Mes-**$2CH_3$**).^{13}C {^{1}H} NMR (75 MHz, $CDCl_3$) δ (ppm) 152.2, 148.8, 141.6, 139.2, 138.5, 137.5, 134.4, 130.1, 124.6, 123.9, 122.6, 53.2 (CH_2), 21.2 (CH_3), 17.8 (CH_3). HRMS (ESI^+): *m/z* 278.1664 $[M - Br]^+$, calculated $[M - Br]^+$ 278.1652.

Consistent with data previously reported.[62]

vi) Preparation of H**L7**Br

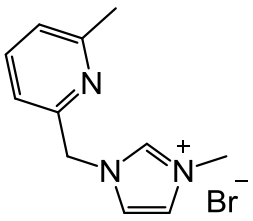

2-(Bromomethyl)-6-methylpyridine (0.50 g, 2.69 mmol) was dissolved in MeCN (50 mL). 1-methylimidazole (0.22 mL, 2.82 mmol) was added, and the pale red solution was stirred at room temperature under N_2 for 24 hours. The volume was reduced *in vacuo* to 5 mL. Et_2O (75 mL) was added to precipitate brown oil, which was sonicated in Et_2O (2 × 75 mL) to obtain a light orange-brown oil. Yield: 0.70 g, 2.61 mmol, 97 %.

^{1}H NMR (300 MHz, $CDCl_3$) δ (ppm) 9.82 (t, *J* = 1.7 Hz, 1H, imH-2), 7.51 (t, *J* = 1.7 Hz, 1H, imH), 7.38 (t, *J* = 1.7 Hz, 1H, imH), 7.27 (t, *J* = 7.6 Hz, 1H, pyH-4), 7.15 (d, *J* = 7.6 Hz, 1H, pyH-3), 6.81 (d, *J* = 7.7 Hz, 1H, pyH-5), 5.33 (s, 2H, N-**CH_2**-im), 3.79 (s, 3H, im-**CH_3**), 2.15 (s, 3H, py-**CH_3**). ^{13}C {^{1}H} NMR (75 MHz, $CDCl_3$) δ (ppm) 156.8, 149.4, 135.5, 134.8, 121.6, 121.5, 120.6, 118.33, 51.8 (CH_2), 34.6 (im-**CH_3**), 22.2 (py-**CH_3**). HRMS (ESI^+): *m/z* 188.1189 $[M - Br]^+$,

calculated $[M - Br]^+$ 188.1182. Analysis Calculated for $C_{11}H_{14}BrN_3$ $2.25H_2O$: C, 42.80; H 6.04; N, 13.61. Found: C, 42.80; H, 5.90, N, 13.80.

vii) Preparation of H**L8**Br

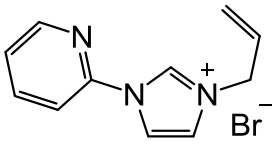

1-(2-Pyridyl)imidazole (**P8**, 1.50 g, 10.3 mmol) was dissolved in MeCN (100 mL). Allyl bromide (4.5 mL, 51.7 mmol) was added to the solution, and the solution was stirred at 85 ºC under N_2 for 24 hours. Additional allyl bromide (0.5 mL, 5.8 mmol) was added and the reaction heated for a further 1 hour. The volume was reduced *in vacuo* to 10 mL, and Et_2O (150 mL) was added slowly to precipitate a white solid. The solid was collected by filtration and repeatedly recrystallised in MeCN / Et_2O. The solid collected was then suspended in Et_2O (150 mL) for 1 hour, and the solid was collected from filtration, washed repeatedly with Et_2O, and dried *in vacuo* to give a white solid. Yield: 2.54 g, 9.54 mmol, 92.4 %.

^{1}H NMR (300 MHz, $CDCl_3$) δ (ppm) 11.98 (d, *J* = 1.9 Hz, 1H. imH-2), 8.52 (dt, *J* = 8.3, 0.9 Hz, 1H, pyH-3), 8.46 (ddd, *J* = 4.9, 1.9, 0.9 Hz, 1H, pyH-6), 8.23 (t, *J* = 1.9 Hz, 1H, imH), 8.01 (ddd, *J* = 8.3, 7.5, 1.9 Hz, 1H, pyH-4), 7.41 (ddd, *J* = 7.5, 4.9, 0.9 Hz, 1H, pyH-5), 7.27 (d, *J* = 1.9 Hz, 1H, imH), 6.05 (ddt, *J* = 16.7, 10.1, 6.6 Hz, 1H, **CH**=CH_2), 5.57 – 5.45 (m, 2H, CH=**CH_2**), 5.17 (dt, *J* = 6.6, 1.3 Hz, 2H, N**CH_2**-vinyl). ^{13}C {^{1}H} NMR (75 MHz, $CDCl_3$) δ (ppm) 149.0, 140.7, 136.0, 129.5, 125.2, 123.4, 121.8, 118.9, 115.1, 52.7. HRMS (ESI^+): *m/z* 186.0845 $[M - Br]^+$, calculated $[M - Br]^+$ 186.1031. Analysis Calculated for $C_{11}H_{12}BrN_3$: C, 49.64; H 4.54; N, 15.79. Found: C, 49.40; H, 4.50, N, 15.70.

Consisted with data previously reported.[44]

viii) Attempted synthesis of H**L10**Br

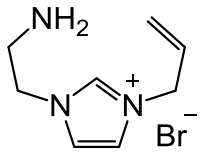

2-Bromoethylamine.HBr (0.50 g, 2.44 mmol) was dissolved in MeOH or MeCN (5 mL) and 1-allylimidazole (0.29 mL, 2.68 mmol) was added. The reaction solution was stirred in a closed ampoule for 16 hours under N_2 at 75 ºC. A pale brown precipitate was observed in the case of MeCN. The crude products were obtained after solvent removal *in vacuo*. They were recrystallised in MeOH / Et_2O.

ix) Attempted synthesis of H**L14**I *via* **P14'**

P14' (0.1 g, 0.44 mmol) was dissolved in MeCN (2 mL). MeI (30 µL, 0.48 mmol) was added to the solution. The solution was stirred at 30 ºC under N_2 and

hydrous conditions for 24 hours. More MeI (60 µL, 0.96 mmol) was added. A pale white solid precipitated in the reaction vessel. Et_2O (70 mL) was added to the reaction mixture. The precipitate was collected *via* filtration and washed with Et_2O (3 × 25 mL). Yield: 0.18 g.

x) Preparation of H**L14**Br

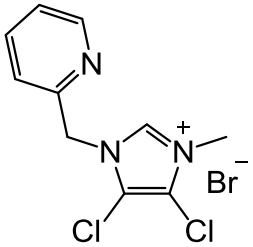

P14 (0.05 g, 0.33 mmol) and 2-(bromomethyl)pyridine.HBr (0.08 g, 0.32 mmol) were dissolved in MeCN (15 mL) and heated under reflux under N_2 and hydrous conditions for 24 hours. The reaction mixture volume was reduced *in vacuo* to 5 mL. Et_2O (70 mL) was added to precipitate the product, which was isolated by filtration. Yield: 0.088 g, 0.27 mmol, 82%.

^{1}H NMR (300 MHz, $CDCl_3$) δ (ppm) 11.02 (s, 1H, imH), 8.48 (dd, *J* = 4.7, 1.7 Hz, 1H, pyH-6), 7.76 (td, *J* = 7.8, 1.7 Hz, 1H, pyH-4), 7.58 (d, *J* = 7.8 Hz, 1H, pyH-3), 7.28 (dd, *J* = 7.8, 4.7 Hz, 1H, pyH-5), 5.82 (s, 2H, N**CH_2**-py) 4.08 (s, 3H, N**CH_3**). ^{13}C {^{1}H} NMR (75 MHz, $CDCl_3$) δ (ppm) 151.0, 150.0, 138.7, 137.7, 124.1, 122.9, 52.9, 34.5. HRMS (ESI^+): *m/z* 242.0247 $[M + H]^+$, calculated $[M + H]^+$ 242.0246.

xi) Preparation of H**L15**Br

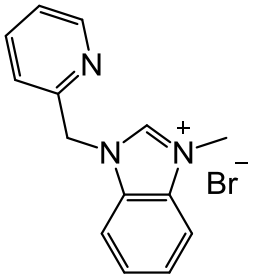

P15 (0.29 g, 2.17 mmol) was dissolved in MeCN (5 mL). 2-(Bromomethyl)pyridine.HBr (0.50 g, 1.98 mmol) was added and the solution stirred for 2 hours under N_2 and hydrous conditions. K_2CO_3 (0.14 g, 0.99 mmol) was added and the reaction mixture was stirred for further 18 hours. The mixture was filtered, and the filtrate volume reduced *in vacuo* to 2 mL. Et_2O (50 mL) was added to precipitate an orange solid. The solid was recrystallised from MeCN / Et_2O. The orange brown solid was collected *via* filtration and dried *in vacuo*. Yield: 0.54 g, 1.77 mmmol, 81%.

^{1}H NMR (300 MHz, $CDCl_3$) δ (ppm) 11.47 (s, 1H, BzmH-2), 8.47 (ddd, *J* = 4.9, 1.6, 0.9 Hz, 1H, pyH-6), 7.92 – 7.86 (m, 2H), 7.77 – 7.64 (m, 3H), 7.63 – 7.56 (m, 2H), 7.23 (ddd, *J* = 7.5, 4.9, 1.0 Hz, 1H, pyH-5), 6.03 (s, 2H, im-**CH_2**-py), 4.26 (s, 3H, N**CH_3**). ^{13}C {^{1}H} NMR (75 MHz, $CDCl_3$) δ (ppm) 152.4 (C), 149.7 (CH), 143.5 (CH), 137.7 (CH), 131.9 (C), 131.6 (C), 127.2 (CH), 127.2 (CH), 124.0 (CH), 123.9 (CH), 114.5 (CH), 112.5 (CH), 52.4 (CH_2), 33.8 (CH_3). HRMS (ESI^+): *m/z* 224.1186 $[M - Br]^+$, calculated $[M - Br]^+$ 224.1182.

xii) Preparation of H**L17**Br

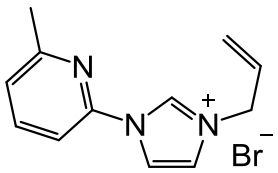

P17 (0.1 g, 0.6 mmol) was dissolved in MeCN (5 mL) and allyl bromide (0.1 mL, 1.2 mmol) was added. The solution was stirred at 75 °C under N_2 and hydrous conditions for 24 hours and the reaction mixture was allowed to cool to room temperature. Et_2O (100 mL) was added to precipitate a light brown-grey solid, which was collected by filtration and dried *in vacuo*. Yield: 0.10 g, 0.36 mmol, 57 %.

^{1}H NMR (400 MHz, $CDCl_3$) δ (ppm) 11.87 (s, 1H, imH-2), 8.24 (d, *J* = 7.9 Hz, 1H, pyH), 8.23 (s, 1H, imH), 7.85 (t, *J* = 7.9 Hz, 1H, pyH), 7.26 (s, 1H, imH), 7.23 (d, *J* = 7.9 Hz, 1H, pyH), 6.03 (ddd, *J* = 16.5, 10.1, 6.5 Hz, 1H, **CH**=CH_2), 5.51 (d, *J* = 16.5 Hz, 1H, CH=**CH**$_2$ *cis*), 5.47 (d, *J* = 10.1 Hz, 1H, CH=**CH**$_2$ *trans*), 5.17 (d, *J* = 6.5 Hz, 2H, N**CH$_2$**-vinyl), 2.53 (s, 3H, **CH$_3$**-py). ^{13}C {^{1}H} NMR (101 MHz, $CDCl_3$) δ (ppm) 159.0 (C), 140.8 (CH), 136.3 (C), 129.6 (CH), 124.8 (CH), 123.3 (CH_2), 121.2 (CH), 118.9 (CH), 112.0 (CH), 52.7 (CH_2), 42.1 (CH_3). HRMS (ESI$^+$): *m/z* 200.1180 [M – Br]$^+$, calculated [M – Br]$^+$ 200.1182.

xiii) Preparation of H**L18**Cl

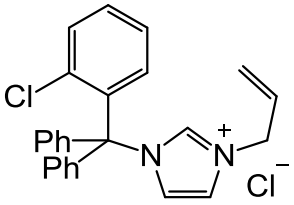

2-Chlorotrityl chloride (0.093 g, 0.3 mmol) was dissolved in MeCN (5 mL) and 1-allylimidazole (34 µL, 0.315 mmol) was added. The yellow solution was stirred at 80 °C for 18 hours. The volume was reduced to about 1 mL *in vacuo*, and Et_2O (50 mL) was added to precipitate a pale yellow oil. The crude oil was recrystallised from DCM (1 mL) / Et_2O (50 mL) and dried *in vacuo* to obtain a pale-yellow sticky solid. Yield: 0.048 g, 0.11 mmol, 38 %

^{1}H NMR (300 MHz, $CDCl_3$) δ (ppm) 9.23 (s, 1H, imH), 7.49 – 7.28 (m, 13H), 7.15 – 7.08 (m, 2H), 6.70 (dd, *J* = 7.9, 1.5 Hz, 1H), 6.00 (ddt, *J* = 17.0, 10.1, 6.3 Hz, 1H, **CH**=CH_2), 5.51 (d, *J* = 10.1 Hz, 1H, CH=**CH**$_2$ *trans*), 5.43 (d, *J* = 17.0 Hz, 1H, CH=**CH**$_2$ *cis*), 4.91 (d, *J* = 6.3 Hz, 2H, N**CH$_2$**-vinyl). HRMS (ESI$^+$): *m/z* 385.1457 and 387.1442 [M - Br]$^+$, calculated [M - Br]$^+$ 385.1466 and 387.1437; 277.0788 and 279.0754 [chlorotrityl]$^+$, calculated [chlorotrityl]$^+$ 277.0779 And 279.0749.

Consistent with data previously reported.[63]

xiv) Preparation of H**L20**Br

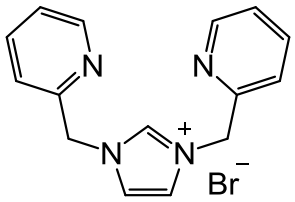

In air, imidazole (0.068 g, 1 mmol) and $NaHCO_3$ (0.256 g, 3.05 mmol) were dissolved in MeOH (10 mL) and stirred. 2-(Bromomethyl)pyridine.HBr (0.518 g, 2.05 mmol) was added and the mixture was stirred at 70 °C under hydrous conditions for 18 hours. The solvent was removed *in vacuo*. DCM (50 mL) was added, the mixture filtered, and the filtrate dried with $MgSO_4$, and the solvent removed *in vacuo*. The crude red liquid was triturated in THF (50 mL) to give a red-brown oil. The oil was recrystallised from DCM (5 mL) / Et_2O (70 mL) twice, to obtain a sticky red-brown solid. Yield: 0.13 g, 0.39 mmol, 39 %

^{1}H NMR (300 MHz, $CDCl_3$) δ (ppm) 10.65 (s, 1H, imH), 8.54 (d, *J* = 4.7 Hz, 2H, pyH-6), 7.79 – 7.73 (m, 4H, pyH), 7.57 (s, 2H, imH), 7.29 (dd, *J* = 8.3, 4.3 Hz, 2H, pyH-5), 5.68 (s, 4H, N**CH$_2$**-py). ^{13}C {^{1}H} NMR (75 MHz, $CDCl_3$) δ (ppm) 152.3 (C), 149.9 (CH), 137.9 (CH), 124.2 (CH), 124.1 (CH), 122.4 (CH), 110.0 (CH), 54.2 (CH_2). HRMS (ESI$^+$): *m/z* 251.1295 [M - Br]$^+$, calculated [M - Br]$^+$ 251.1291.

Consisted with data previously reported.[61]

xv) Preparation of H**L21**Br

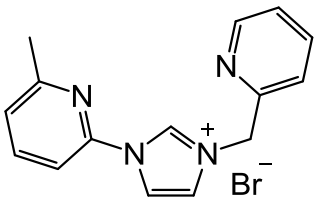

P17 (0.1 g, 0.6 mmol) and was stirred in MeCN (5 mL) and heated to 50 °C. 2-(Bromomethyl)pyridine.HBr (0.16 g, 0.6 mmol) was added and stirred at 50 °C under N_2 and hydrous conditions for 8 hours. The reaction mixture was allowed to cool to room temperature, stirred with K_2CO_3 (0.17 g, 1.2 mmol) for 30 minutes and filtered. The filtrate was reduced *in vacuo* and the resulting oil was dissolved in DCM (20 mL), dried over $MgSO_4$ and filtered. The volume was reduced to about 3 mL, and Et_2O (50 mL) was added to precipitate a dark brown oil. Yield: 0.11 g, 0.35 mmol, 56 %.

^{1}H NMR (300 MHz, $CDCl_3$) δ (ppm) 11.95 (s, 1H, imH-2), 8.56 (ddd, *J* = 4.8, 1.8, 0.8 Hz, 1H, picH-6), 8.21 (s, 1H, imH), 8.14 (d, *J* = 7.9 Hz, 1H, pyH), 7.99 (d, *J* = 7.9 Hz, 1H, pyH), 7.89 (t, *J* = 7.9 Hz, 1H, pyH), 7.77 (td, *J* = 7.7, 1.8 Hz, 1H, picH-4), 7.74 (s, 1H, imH), 7.31 (ddd, *J* = 7.7, 4.8, 0.8 Hz, 1H, picH-5), 7.26 (dt. *J* = 7.7, 0.8 Hz, picH-3), 5.91 (s, 2H, N**CH$_2$**-py), 2.58 (s, 3H, py**CH$_3$**). ^{13}C {^{1}H} NMR (75 MHz, $CDCl_3$) δ (ppm) 159.0 (C), 152.3 (C), 152.2 (C), 149.8 (CH), 145.2 (C), 140.7 (CH), 137.9 (CH), 136.0 (CH), 124.7 (CH), 124.2 (CH), 122.7 (CH), 120.6 (CH), 118.2 (CH), 111.6 (CH), 111.3 (CH), 54.4 (CH_2), 24.1 (CH_3). HRMS (ESI$^+$): *m/z* 251.1286 [M – Br]$^+$, calculated [M – Br]$^+$ 251.1291.

xvi) Preparation of H**L23**Br

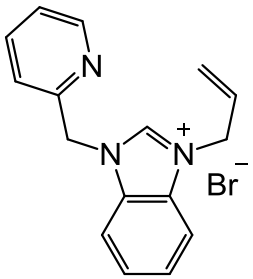

P23 (0.10 g, 0.5 mmol) was dissolved in MeCN (5 mL) and allyl bromide (0.1 mL, 1.2 mmol) was added. The yellow reaction mixture was held at reflux under N_2 and hydrous conditions for 24 hours. The reaction mixture was allowed to cool to room temperature and Et_2O (100 mL) was added to precipitate a brown solid, which was collected by filtration and dried *in vacuo*. Yield: 0.11 g, 0.33 mmol, 70 %.

^{1}H NMR (300 MHz, $CDCl_3$) δ (ppm) 11.49 (s, 1H, BzmH-2), 8.43 (dd, *J* = 4.6, 1.7 Hz, 1H, pyH-6), 7.91 – 7.83 (m, 2H, BzmH), 7.70 (td, *J* = 7.7, 1.7 Hz, 1H, pyH-4), 7.65 – 7.50 (m, 4H, pyH and BzmH), 6.15 – 6.02 (m, 1H, **CH**=CH_2), 6.00 (s, 2H, N**CH_2**-py), 5.48 – 5.40 (m, 2H, CH=**CH_2**), 5.18 (d, *J* = 6.0 Hz, 2H, N**CH_2**-vinyl). ^{13}C {^{1}H} NMR (75 MHz, $CDCl_3$) δ (ppm) 152.3 (C), 149.6 (CH), 143.2 (CH), 137.8 (CH), 129.2 (CH), 127.2 (CH), 127.1 (CH), 124.0 (CH), 122.2 (CH), 114.7 (CH), 113.6 (CH_2), 113.2 (CH), 52.43 (CH_2), 50.20 (CH_2). HRMS (ESI$^+$): *m/z* 250.1338 [M – Br]$^+$, calculated [M – Br]$^+$ 250.1339.

xvii) Preparation of H**L24**Br

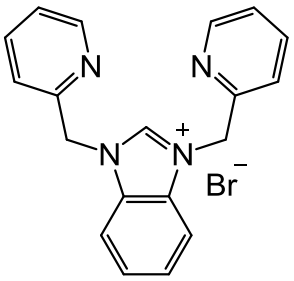

Benzimidazole (0.24 g, 2 mmol) and $NaHCO_3$ (0.60 g, 7.1 mmol) were dissolved in MeOH (10 mL). 2-(Bromomethyl)pyridine.HBr (1.1 g, 4.1 mmol) was added and the mixture was stirred at 70 °C under N_2 and hydrous conditions for 18 hours. The solvent was removed *in vacuo*. DCM (50 mL) was added, the solution filtered, dried with $MgSO_4$ and the solvent removed *in vacuo*. The crude red liquid was triturated in THF (50 mL) to give a red-brown oil. The oil was recrystallised from DCM (5 mL) / Et_2O (70 mL) twice, to obtain a sticky dark red-brown solid. Yield: 0.49 g, 1.7 mmol, 86 %.

^{1}H NMR (300 MHz, $CDCl_3$) δ (ppm) 11.68 (s, 1H, BzmH-2), 8.45 (ddd, *J* = 4.6, 1.9, 1.0 Hz, 2H, pyH-6), 7.82 – 7.76 (m, 4H, BzmH and pyH-5), 7.69 (td, *J* = 7.6 1.9 Hz, 2H, pyH-4), 7.48 (dd, *J* = 6.3, 2.2 Hz, 2H, BzmH), 7.21 (dd, *J* =7.3, 1.0 Hz, pyH-3), 5.90 (s, 2H, N**CH_2**-py). ^{13}C {^{1}H} NMR (75 MHz, $CDCl_3$) δ (ppm) 152.2 (C), 149.7 (CH), 143.4 (CH), 137.8 (CH), 131.7 (C), 127.1 (CH), 124.0 (CH), 123.8 (CH), 114.2 (CH), 52.7 (CH_2). δ. HRMS (ESI$^+$): *m/z* 301.1449 [M – Br]$^+$, calculated [M – Br]$^+$ 301.1448.

Consistent with data previously reported.[61]

2.10.4 Cu-catalysed etherification reaction for ligand screening and evaluations

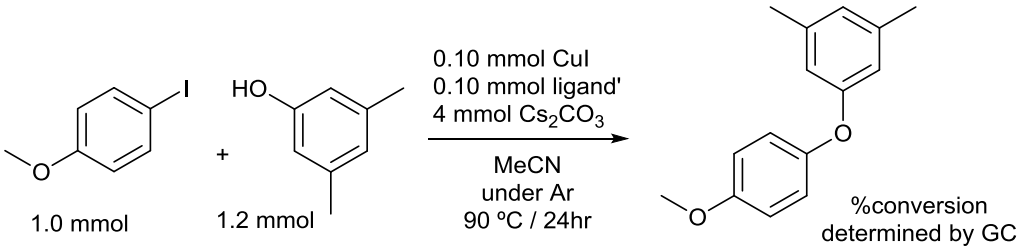

3,5-Dimethylphenol (0.1465 g, 1.2 mmol), 4-iodoanisole (0.2340 g, 1.0 mmol), CuI (0.0190g, 0.10 mmol), Cs_2CO_3 (1.3033 g, 4.0 mmol) and ligand (0.10 mmol) were placed in a carousel tube and under Ar. To this was added anhydrous MeCN (5 mL) *via* syringe. The resulting mixture was heated with stirring at 90 °C for 24 hours under Ar. After this time, the mixture was cooled to room temperature and a 100 µL aliquot was withdrawn from the reaction mixture and added to 2 mL of a 10 mM stock solution of p-cymene (internal standard) in DCM. The solution containing the reaction mixture and internal standard was filtered through Celite and subsequently analysed by GC.

2.11 References

(1) Lee, D. Y. W.; He, M. *Curr. Top. Med. Chem.* **2005**, *5*, 1333.
(2) Carey, J. S.; Laffan, D.; Thomsom, C.; Williams, M. T. *Org. Biomol. Chem.* **2006**, *4*, 2337.
(3) Torborg, C.; Beller, M. *Adv. Synth. Catal.* **2009**, *351*, 3027.
(4) Shaughnessy, K. H. *Molecules* **2015**, *20*, 9419.
(5) Froese, R. D. J.; Lombardi, C.; Pompeo, M.; Rucker, R. P.; Organ, M. G. *Acc. Chem. Res.* **2017**, *50*, 2244.
(6) Baba, S.; Negishi, E. *J. Am. Chem. Soc.* **1976**, *98*, 6729.
(7) Heck, R. F. *J. Am. Chem. Soc.* **1968**, *90*, 5518.
(8) Ruiz-Castillo, P.; Buchwald, S. L. *Chem. Rev.* **2016**, *116*, 12564.
(9) Chen, X.; Engle, K. M.; Wang, D.-H.; Yu, J.-Q. *Angew. Chem., Int. Ed.* **2009**, *48*, 5094.
(10) Tamaki, A.; Kochi, J. K. *J. Organomet. Chem.* **1974**, *64*, 411.
(11) Cai, R.; Lu, M.; Aguilera, E. Y.; Xi, Y.; Akhmedox, N. G.; Peterson, J. L.; Chen, H.; Shi, X. *Angew. Chem., Int. Ed.* **2015**, *54*, 8772.
(12) Li, P.; Wang, L. *Synlett* **2006**, *14*, 2261.
(13) Font, M.; Acuna-Pares, F.; Parella, T.; Serra, J.; Luis, J. M.; Lloret-Fillol, J.; Costas, M.; Ribas, X. *Nature Commun.* **2014**, *5*.
(14) Das, R.; Manhal, M.; Chakraborty, D. *Asian J. Org. Chem.* **2013**, *2*, 579.
(15) Gilman, H.; Jones, R. G.; Woods, L. A. *J. Org. Chem.* **1952**, *17*, 1630.
(16) Ullmann, F.; Bielecki, J. *Chem. Ber.* **1901**, *34*, 2174.
(17) Ullmann, F. *Chem. Ber.* **1903**, *36*, 2382.
(18) Ullmann, F.; Frentzel, L. *Chem. Ber.* **1905**, *38*, 725.
(19) Goldberg, I. *Chem. Ber.* **1906**, *39*, 1691.
(20) Fanta, P. E. *Synthesis* **1974**, *1*, 9.
(21) Lindley, J. *Tetrahedron* **1984**, *40*, 1433.
(22) Weingarten, H. *J. Org. Chem.* **1964**, *29*, 3624.
(23) Kiyomori, A.; Marcoux, J.-F.; Buchwald, S. L. *Tetrahedron Lett.* **1999**, *40*, 2657.
(24) Kelkar, A. A.; Patil, N. M.; Chaudhari, R. V. *Tetrahedron Lett.* **2002**, *43*, 7143.
(25) Ma, D.; Zhang, Y.; Yao, J.; Wu, S.; Tao, F. *J. Am. Chem. Soc.* **1998**, *120*, 12459.

(26) Job, G. E.; Buchwald, S. L. *Org. Lett.* **2002**, *4*, 3703.
(27) Shafir, A.; Lichtor, P. A.; Buchwald, S. L. *J. Am. Chem. Soc.* **2007**, *129*, 3490.
(28) Maiti, D.; Buchwald, S. L. *J. Am. Chem. Soc.* **2009**, *131*, 17423.
(29) Yu, H.-Z.; Jiang, Y.-Y.; Fu, Y.; Liu, L. *J. Am. Chem. Soc.* **2010**, *132*, 18078.
(30) Tubaro, C.; Biffis, A.; Scattolin, E.; Basato, M. *Tetrahedron* **2008**, *64*, 4187.
(31) Biffis, A.; Tubaro, C.; Scattolin, E.; Basato, M.; Papini, G.; Santini, C.; Alvarez, E.; Conejero, S. *Dalton Trans.* **2009**, 7223.
(32) Ellul, C. E.; Reed, G.; Mahon, M. F.; Pascu, S. I.; Whittlesey, M. K. *Organometallics* **2010**, *29*, 4097.
(33) Borude, V. S.; Shah, R. V.; Shukla, S. R. *Monatsch Chem.* **2013**, *144*, 1663.
(34) Gallop, C. W. D.; Chen, M.-T.; Navarro, O. *Org. Lett.* **2014**, *16*, 3724.
(35) Lake, B. R. M.; Willans, C. E. *Organometallics* **2014**, *33*, 2027.
(36) Castellano, S.; Sun, C.; Kostelnik, R. *J. Chem. Phys.* **1967**, *46*, 327.
(37) Reich, H. J. *https://www.chem.wisc.edu/areas/reich/nmr/h-data/hdata.htm*.
(38) Fey, N.; Harvey, J. N.; Lloyd-Jones, G. C.; Murray, P.; Orpen, A. G.; Osborne, R.; Purdie, M. *Organometallics* **2008**, *27*, 1372.
(39) Viciu, M. S.; Navarro, O.; Germaneau, R. F.; III, R. A. K.; Sommer, W.; Marion, N.; Stevens, E. D.; Cavallo, L.; Nolan, S. P. *Organometallics* **2004**, *23*, 1629.
(40) Brown, M. G. *Trans. Faraday Soc.* **1959**, *55*, 694.
(41) Bent, H. A. *J. Chem. Edu.* **1960**, *37*, 616.
(42) Marcoux, J.-F.; Doye, S.; Buchwald, S. L. *J. Am. Chem. Soc.* **1997**, *119*, 10539.
(43) Li, Z.; Ke, F.; Deng, H.; Xu, H.; Xiang, H.; Zhou, X. *Org. Biomol. Chem.* **2013**, *11*, 2943.
(44) Lake, B. R. M.; Willans, C. E. *Chem. Eur. J.* **2013**, *19*, 16780.
(45) Flahaut, A.; Baltaza, J.-P.; Roland, S.; Mangeney, P. *J. Organomet. Chem.* **2006**, *691*, 3498.
(46) Tsai, C.-C.; Shih, W.-C.; Fang, C.-H.; Li, C.-Y.; Ong, T.-G.; Yap, G. P. A. *J. Am. Chem. Soc.* **2010**, *132*, 11887.
(47) Huang, H.-J.; Lee, W.-C.; Yap, G. P. A.; Ong, T.-G. *J. Organomet. Chem.* **2014**, *761*, 64.
(48) Hopkinson, M.; Richter, C.; Schedler, M.; Glorius, F. *Nature* **2014**, *510*, 485.
(49) Sheppard, J. F., University of Leeds, 2016.
(50) Sherbourne, G. J.; Adomeit, S.; Menzel, R.; Rabeah, J.; Bruckner, A.; Fielding, M. R.; Willans, C. E.; Nguyen, B. N. *Chem. Sci.* **2017**, *8*, 7203.
(51) sung, S.; Sale, D.; Braddock, D. C.; Armstrong, A.; Brennan, C.; Davies, R. P. *ACS Catal.* **2016**, *6*, 3965.
(52) Wang, J.; Liu, S.; Xu, S.; Zhao, F.; Xia, H.; Wang, Y. *J. Organomet. Chem.* **2017**, *846*, 351.
(53) Domyati, D.; Latifi, R.; Tahsini, L. *J. Organomet. Chem.* **2018**, *860*, 98.
(54) Magill, A. M.; McGuinness, D. S.; Cavell, K. J.; Britovsek, G. J. P.; Gibson, V. C.; White, A. J. P.; Williams, D. J.; White, A. H.; Skilton, B. W. *J. Organomet. Chem.* **2001**, *617-618*, 546.
(55) Sambiago, C.; Marsden, S. P.; Blacker, A. J.; McGowan, P. C. *Chem. Soc. Rev.* **2014**, *43*, 3525.
(56) Fey, N.; Haddow, M. F.; Harvey, J. N.; McMullim, C. L.; Orpen, a. G. *Dalton Trans.* **2009**, 8183.
(57) Fey, N. *Chemistry Central Journal* **2015**, *9*.
(58) Fey, N.; Papadouli, S.; Pringle, P. G.; Ficks, A.; Fleming, J. T.; Higham, L. J.; Wallis, J. F.; Carmichael, D.; Mezailles, N.; Muller, C. *Phosphorus, Sulfur, and Silicon* **2016**, *190*, 706.
(59) Ibrahim, H.; Bala, M. D. *New J. Chem.* **2016**, *40*, 6986.
(60) Barczak, N. T.; Grote, R. E.; Jarvo, E. R. *Organometallics* **2007**, *26*, 4863.
(61) Beillard, A.; Golliard, E.; Gillet, V.; Bantreil, X. *Chem. Eur.* **2015**, *21*, 17614.
(62) Warsink, S.; Aubel, C. M. S. v.; Weigand, J. J.; Liu, S.-T.; Elsevier, C. J. *Eur. J. Inorg. Chem.* **2010**, *35*, 5556.
(63) Abdelgawad, H., University of Leeds, 2016.

Chapter 3

Non-Innocent Activity of NHCs During Cu-Catalysed Coupling Reactions

3.1 Introduction

There are many examples in the literature of reductive elimination of alkyl-imidazolium,[1-9] allyl-imidazolium[10] and aryl-imidazolium salts,[11-15] particularly at group 10 metals. Some have demonstrated the reaction as a method to activate a catalyst, as the metal is subsequently reduced to the active oxidation state by the reductive elimination.[5,7] Others have considered the reaction as a catalyst deactivation pathway in metal-catalysed coupling reactions.[16,17] The reductive elimination of aryl-imidazolium consumes both starting material and supporting ligand (NHC) (Scheme 3-1).[18] This leads to a decrease in catalyst efficiency due to the loss of the supporting ligand, leaving the metal centre more exposed and less stable.

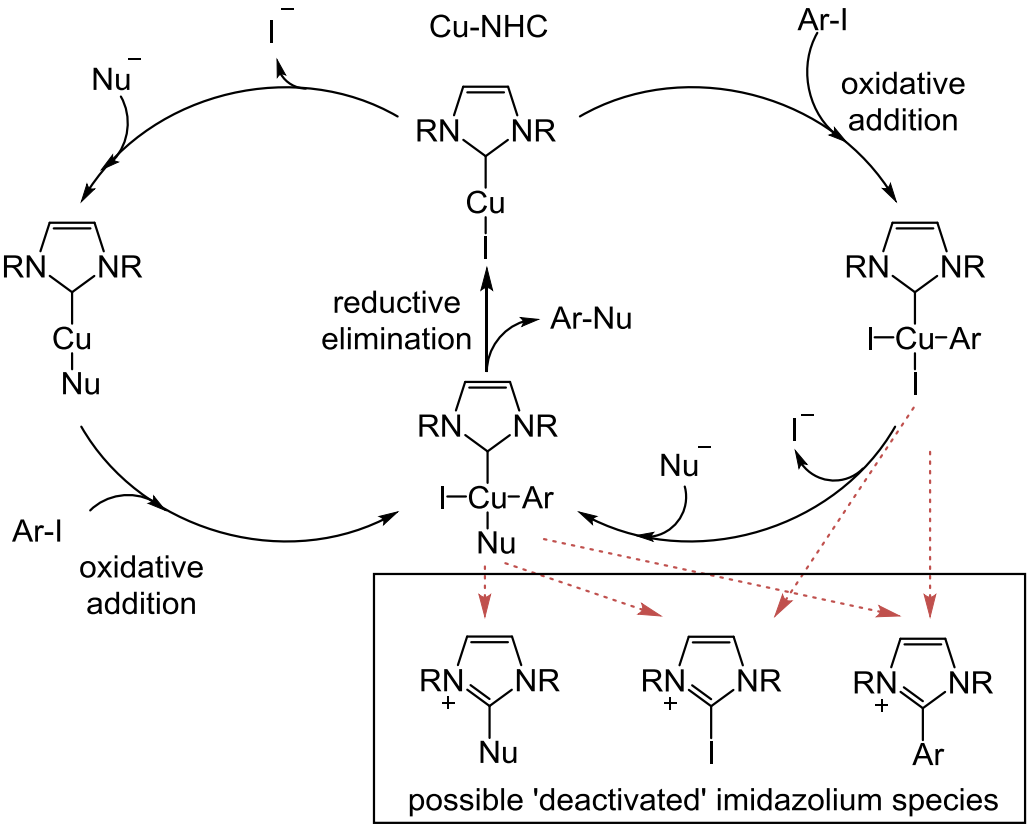

Scheme 3-1: Representation of a coupling reaction *via* oxidative addition / reductive elimination, and potential deactivation pathway steps.

Previous studies in the Willans group have utilised Cu-NHC complexes as cross-coupling catalysts[19,20] (also discussed in Chapter 2), during which the formation of aryl-imidazolium cations was observed.[20] The arylated imidazolium was observed in the HR mass spectrum of the reaction mixture that used an *in situ* formed catalyst through addition of CuI and 1-(but-3-enyl)-3-picolylimidazolium bromide (Scheme 3-2). The detected species was proposed to have the aryl group substituted at the C-2 position of the imidazolium, which was likely co-ordinated to the metal centre in the active species.

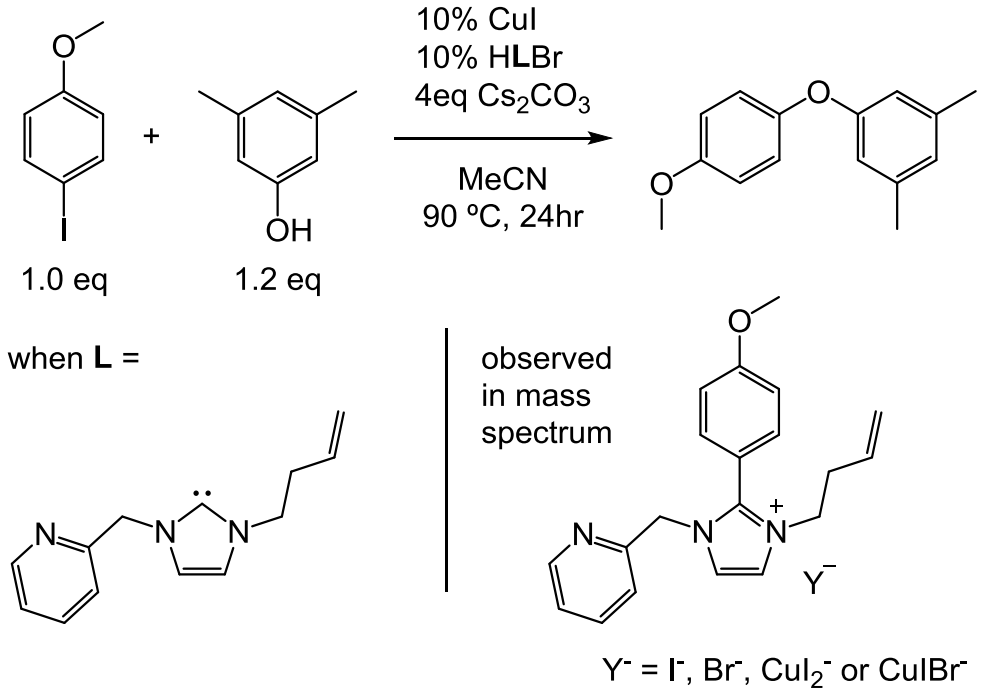

Scheme 3-2: Observation of aryl-imidazolium formation in an Ullmann-type etherification reaction.[20]

This part of the project is focused on understanding the reductive elimination of aryl-imidazolium which appears to occur during the Cu-NHC-catalysed etherification reaction. Other potential reductive elimination reactions were also considered *e.g.* X-imidazolium, Nu-imidazolium, Nu-X.

3.2 Examination of varying ligand precursors for aryl-imidazolium formation

The coupling reaction of 4-iodoanisole and 3,5-dimethylphenol was carried out in the presence of Cs_2CO_3 and CuI/imidazolium bromide (10 mol%) (Scheme 3-3). Reactions were carried out at 90 °C for 24 hours. Each reaction mixture was quenched by filtration through Celite and was examined for the reductive elimination of aryl-imidazolium and other possible species using HRMS. When

ligands **L1** – **L4**, **L8** and **L9** were examined, X-imidazolium or Nu-imidazolium ions were not observed in any entries. This supports the DFT theory that reductive elimination on a Cu metal centre tends to involve strongly nucleophilic ligands (section 1.5.3).[21] Hence the aryl group, which is the most nucleophilic, participates in the reductive elimination more readily. The observed species in these reactions were H-imidazolium (HL) ion, imidazolone (from oxidation or hydrolysis of the NHC), the cross-coupled ether product and, in some cases, aryl-imidazolium ion.

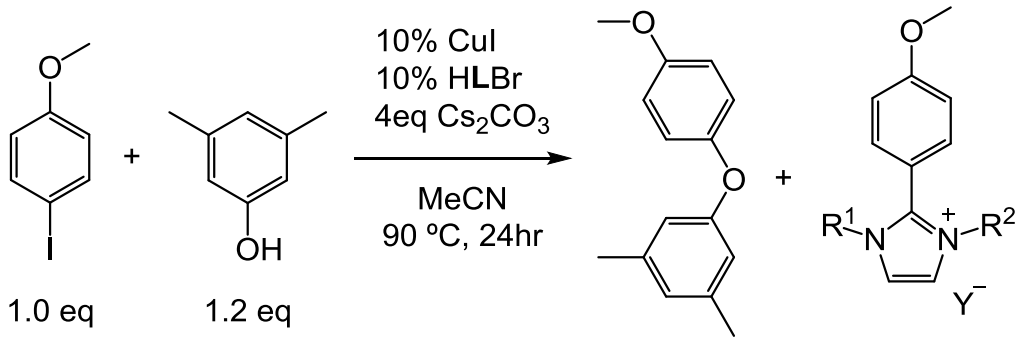

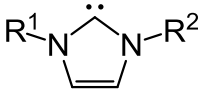

L1: R^1 = picolyl, R^2 = allyl
L2: R^1 = picolyl, R^2 = propyl
L3: R^1 = picolyl, R^2 = methyl
L4: R^1 = picolyl, R^2 = t-butyl
L8: R^1 = pyridyl, R^2 = allyl
L9: R^1 = pyridyl, R^2 = mesityl

Scheme 3-3: Ligand screening for reductive elimination of aryl-imidazolium.

Aryl-imidazolium was observed in the HRMS in the cases of **L2**, **L3** and **L4** (Table 3-1). The conversions to ether (determined by GC using *p*-cymene as an internal standard) in these reactions were 37 %, 46 % and 56 % respectively. Conversion to the ether product when using ligands **L8** and **L9** was also in the same range, at 53 % and 41 % respectively; however, no aryl-imidazolium was observed in these cases. This indicates that the efficiency of the reaction is not only governed by catalyst deactivation *via* aryl-imidazolium formation. Other factors such as the steric and electronic effects of the NHC ligands are also important (as discussed in Chapter 2). Nevertheless, it cannot be concluded from these results that the picolyl *N*-substituent consistently leads to the aryl-imidazolium deactivation as there was no aryl-imidazolium observed in the case of **L1**. The etherification reaction catalysed by a Cu complex of **L1** gave the highest conversion (63 %), which may be linked to no aryl-imidazolium being formed.

Ligand	R^1	R^2	% ether	aryl-imidazolium
L1	picolyl	allyl	63	not observed
L2	picolyl	propyl	37	observed
L3	picolyl	methyl	46	observed
L4	picolyl	t-butyl	56	observed
L8	pyridyl	allyl	53	not observed
L9	pyridyl	mesityl	41	not observed

Table 3-1: Etherification (% determined by GC using *p*-cymene as an internal standard) and aryl-imidazolium formation (observed by HRMS). Reaction conditions as shown in Scheme 3-3.

Another ligand (**L38**) was introduced to the investigation to see if there are any correlations between catalytic activity of a Cu-NHC complex and the aryl-imidazolium formation (Scheme 3-4). **L38** had previously been found to perform poorly in the etherification reaction (14 % conversion),[19] hence it might be expected that catalyst deactivation may occur *via* aryl-imidazolium formation. The ligand precursor H**L38**Br was prepared in a similar fashion to H**L8**Br (Scheme 3-4) with analysis by ^{1}H and ^{13}C $\{^{1}H\}$ NMR spectroscopy and HRMS being consistent with previous reported data.[19]

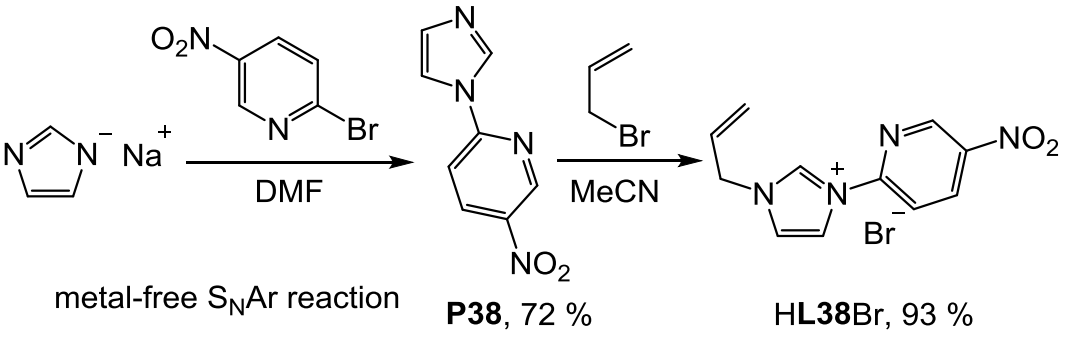

Scheme 3-4: Preparation of **P8** (for comparison), **P38** and H**L38**Br.

To investigate directly the competing reaction between ether and aryl-imidazolium formation, stoichiometric reactions were carried out in which the CuI and HLBr were increased to 100 mol% (Scheme 3-5). In addition to **L38**, investigations were carried out using **L3**, which had led to the formation of **Ar3** in previous catalytic reactions, and **L1** and **L8**, which had not led to the side-reaction. In the stoichiometric reactions, both picolyl-bearing ligands (**L1** and **L3**) led to aryl-imidazolium formation although **Ar1** was not observed previously (Table 3-2). However, **L8** with a pyridyl *N*-substituent still did not result in aryl-

imidazolium formation. The stoichiometric reaction with **L38**, which had not performed well in the cross-coupling reaction in the past (14 % compared to 20 % in the ligand-free system),[19] also did not lead to aryl-imidazolium formation. Therefore, it was concluded that the aryl-imidazolium side-reaction does not correlate with the catalytic activity of Cu-NHC complexes, and it appears that ligands with a picolyl *N*-substituent leads to aryl-imidazolium formation, whereas ligands with a pyridyl *N*-substituent do not. In addition, X-imidazolium and Nu-imidazolium were not observed in any cases, which is consistent with the observation in the catalytic reactions.

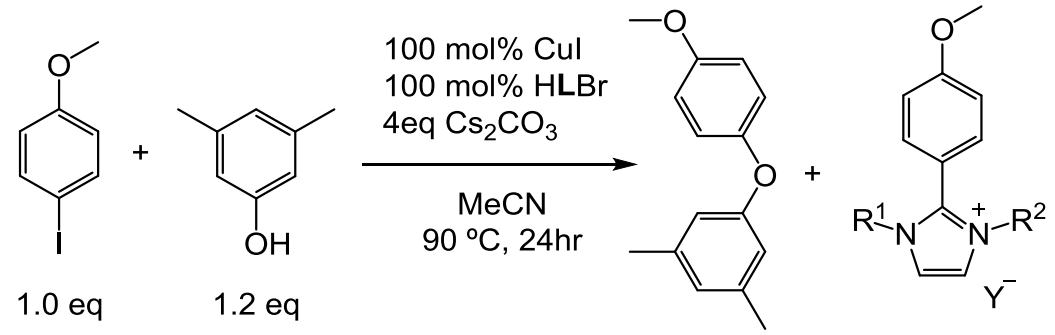

L1: R^1 = picolyl, R^2 = allyl
L3: R^1 = picolyl, R^2 = methyl
L8: R^1 = pyridyl, R^2 = allyl
L38: R^1 = 5-nitropyridyl, R^2 = allyl

Scheme 3-5: Competing reactions using stoichiometric amount of CuI and imidazolium salt.

ligand	R^1	R^2	10 mol % CuI + HLBr		100 mol % CuI + HLBr
			% ether	ArIm	ArIm
L1	picolyl	allyl	63	not observed	observed
L3	picolyl	methyl	46	observed	observed
L8	pyridyl	allyl	53	not observed	not observed
L38	5-nitro pyridyl	allyl	N/A (< 29)	N/A	not observed

Table 3-2: Results of screening using 10 and 100 mol % CuI/imidazolium bromide (aryl-imidazolium side-product observed by HRMS).

We have observed that C-2 arylation of an NHC occurs when it contains a picolyl *N*-substituent, whereas replacing this with a pyridyl group inhibits arylation of the

NHC. There are several different possibilities for why this is the case. The physical difference between these groups is the flexibility of the linkage between the pyridine ring and the carbene ring. The pyridyl group has a rigid $C_{pyridine}$-N_{NHC} bond whereas the picolyl group has a flexible methylene spacer between the rings. The distance of the pyridine ring of the picolyl group is further away from the carbene, as previously observed in the crystal structures of Cu(I)-NHC-Br (**C1** and **C8**) where the angle of C_{NHC}-Cu-$N_{pyridine}$ increases from 81.5 ° in **C8** to 92.2 ° in **C1** (Figure 3-1).[19,22] The higher steric encumbrance by **L1** may promote the catalytic activity of this complex by pushing the substrates into closer proximity but, at the same time, increase the energy barrier for nucleophilic substitution and increase the opportunity for aryl-imidazolium formation. However, we postulate that the presence of the nucleophile is essential in the formation of aryl-imidazolium (section 3.3.3) and therefore sterics should not affect the nucleophilic substitution, and it is more likely that the electronic differences cause the aryl-imidazolium in the case of picolyl-NHCs.

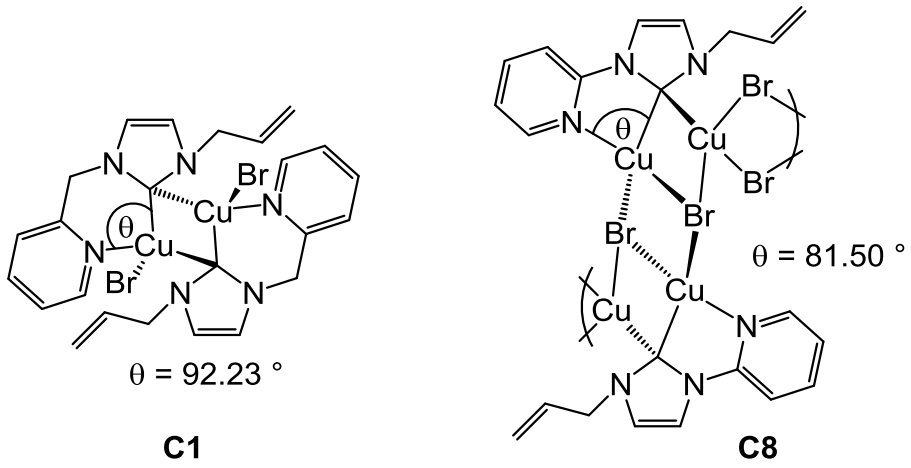

Figure 3-1: Structure of **C1** and **C8**.[19,22]

^{1}H NMR spectra of imidazolium salts can be used to study the electronic properties of the ligands. Considering H**L1**Br, H**L8**Br and H**L38**Br, which all have the same second *N*-substituent (*i.e.* an allyl group), it can be seen that the imidazolium ring of H**L1**Br is the most electron rich. The ^{1}H NMR spectrum of H**L1**Br shows the imidazolium peak (H_A) at δ 10.46 ppm, which is more upfield than the H_A peaks of H**L8**Br (δ 11.98 ppm) and H**L38**Br (δ 12.28 ppm) (Figure 3-2). The imidazolium backbone (H_B and H_C) of H**L1**Br (δ 7.70 and 7.21 ppm) are also slightly more upfield than H**L8**Br (δ 8.23 and 7.27 ppm) and H**L38**Br (δ 8.33 and 7.37 ppm). The *N*-picolyl-bearing NHC has more electron density at the NHC ring than the *N*-pyridyl analogue, due to the methylene linkage which lowers the electron withdrawal by the pyridine ring. Therefore, **L1** may perform

better in catalysis due to greater stabilisation of the Cu(III) intermediate by the stronger base under the assumption that the catalytic cycle proceed *via* such intermediate. However, when the stoichiometric reaction was performed, which would also proceed *via* a Cu(III) intermediate, formation of aryl-imidazolium became a competing factor.

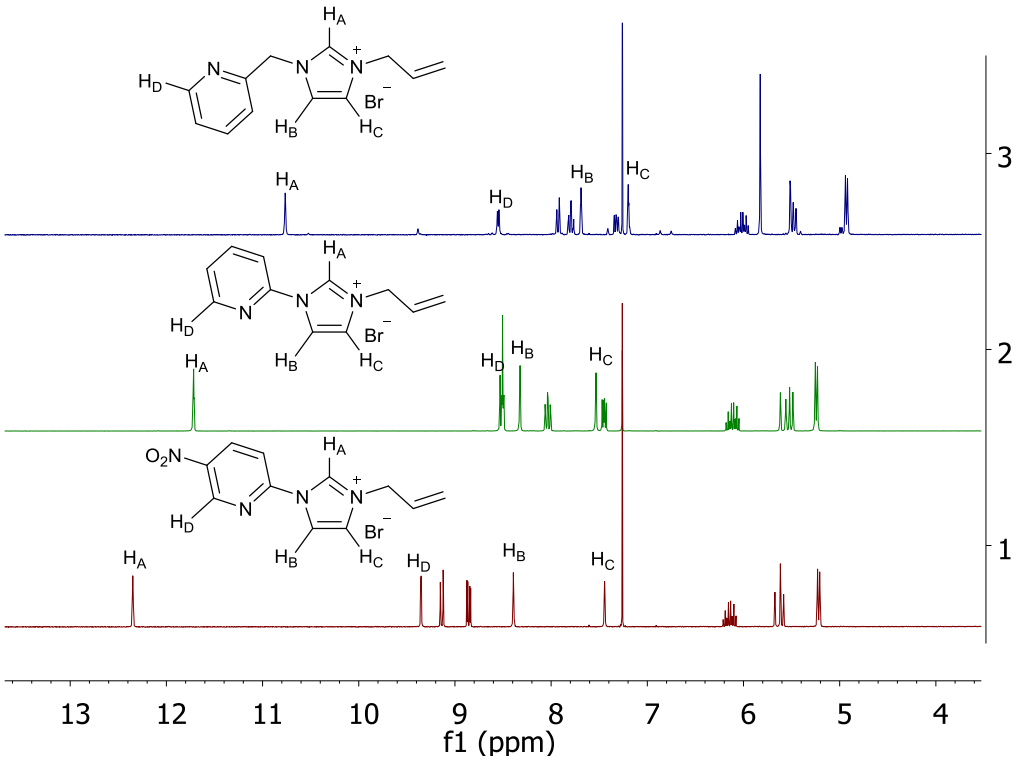

Figure 3-2: ^{1}H NMR spectra (300 MHz, $CDCl_3$) of H**L1**Br (top), H**L8**Br (middle) and H**L38**Br (bottom).

It is thought that aryl-imidazolium formation occurs only with picolyl-substituted NHCs due to the stability of the regenerated Cu(I)-NHC complex, which governs the rate of the reductive elimination of the cross-coupled product. The ΔG of reductive elimination from a Cu centre was proposed by Ariafard to rely on the stability of the resulting Cu anion [X-Cu-Br]$^-$ (Scheme 3-6).[21] Furthermore, the less negative ΔG leads to the higher ΔG‡ and hence lengthens the lifetime of the Cu(III) intermediate (Figure 3-3).

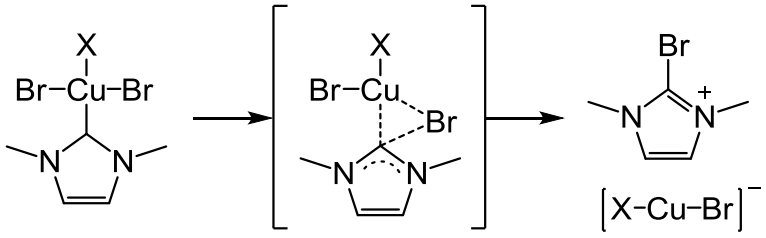

Scheme 3-6: Reductive elimination of bromo-imidazolium, forming [X-Cu-Br]$^-$

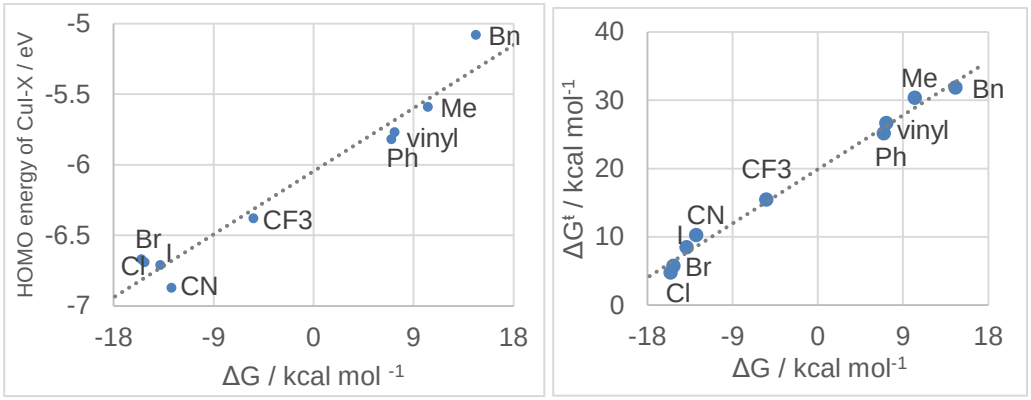

Figure 3-3: Plot of HOMO energy of Cu-X versus ΔG (left) and $\Delta G^{\ddagger}$ versus ΔG (right) for reductive elimination of bromo-imidazolium from *trans*-(NHC)Cu(Br)$_2$X complexes.[21]

The same principle may be applied in the case of the reductive elimination of the ether product. A more electron rich ligand makes the Cu(I)-NHC complex less stable and increases the stability of the Cu(III) intermediate. The ΔG of the reductive elimination of the ether product, in the case of **L1**, is likely to be less negative than **L8** and **L38**. As the Cu(III) intermediate is prolonged, the chance of the competing reductive elimination of aryl-imidazolium increases (Scheme 3-7). Therefore, considering the electronic properties, picolyl-NHCs are more likely to lead to the reductive elimination of aryl-imidazolium during an Ullmann-type cross-coupling reaction than pyridyl-NHCs.

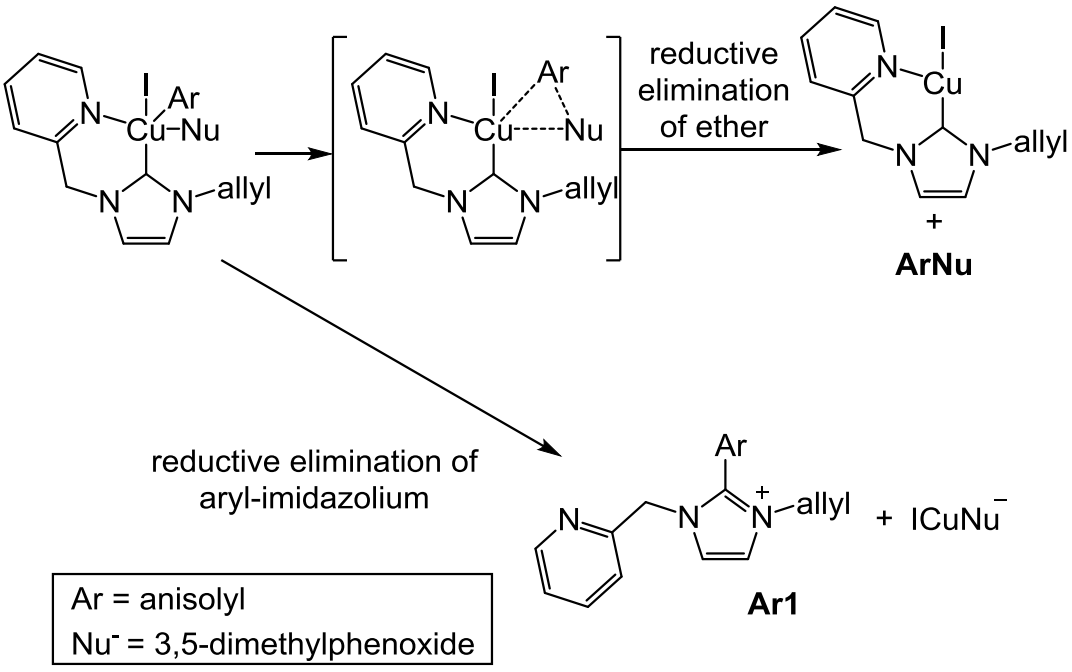

Scheme 3-7: Reductive elimination of **ArNu** or **Ar1**

We have demonstrated that picolyl-substituted NHCs partake in reductive elimination of aryl-imidazolium during an Ullmann-type cross-coupling reaction. Both physical and electronic properties of the picolyl *N*-substituent have been considered. However, the above screening reactions are qualitative and cannot be used to compare other factors that may affect the competing reactions such as the second *N*-substituents (*e.g.* difference between **L1** and **L3**), base, nucleophile and catalyst loadings.

3.3 Quantification of the arylation reaction

3.3.1 Preparation of aryl-imidazolium salts

The previous reactions which examined aryl-imidazolium formation during the etherification reaction detected the products using HRMS. Attempts were made to use ^{1}H NMR spectroscopy to analyse and quantify each species in the quenched reaction mixtures, but this proved futile as the Cu-catalysed reactions resulted in a number of different species (Figure 3-4). For example, the methoxy singlet peak of 4-iodoanisole resonates at δ 3.76 ppm, but in the reaction mixture, there are 6 overlapping peaks between δ 3.90 – 3.72 ppm. This indicates that the fate of the anisolyl is not just restricted to the starting material, the cross-coupled ether product and the aryl-imidazolium ion.

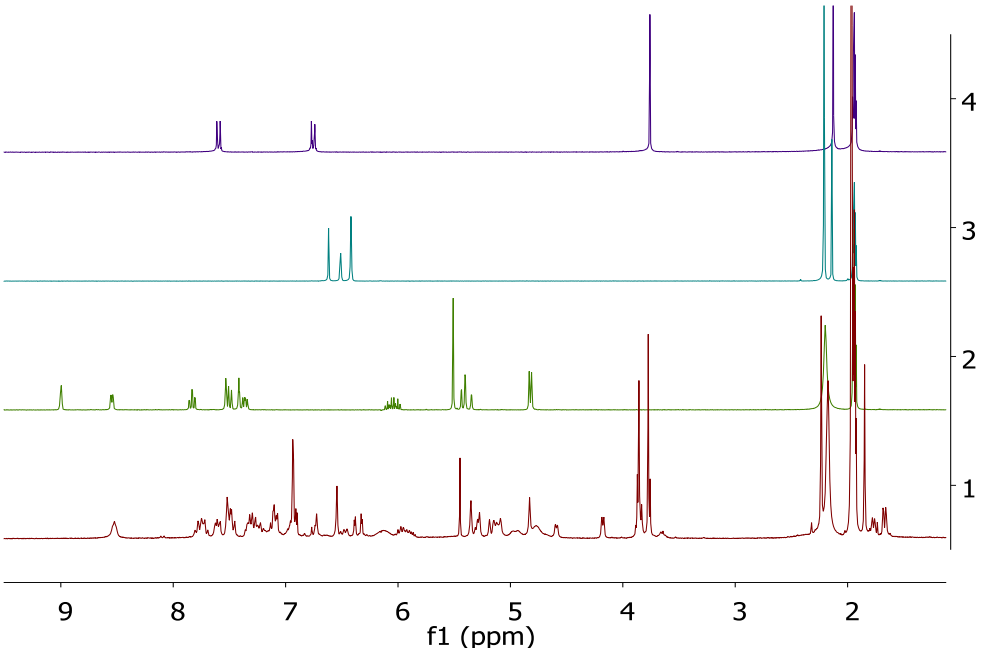

Figure 3-4: ^{1}H NMR spectra (300 MHz, CD_3CN) of 4-iodoanisole (4), 3,5-dimethylphenol (3), H**L1**Br (2) and the quenched mixture following an etherification using stoichiometric amounts of H**L1**Br and CuI (1).

In order to quantify formation of the different species, an analytical technique that separates the reaction mixture (*i.e.* chromatography) would be beneficial, though this requires calibration using authentic material. Attempts were therefore made to prepare aryl-imidazolium salts **Ar1** and **Ar3** to enable calibration and quantification (Figure 3-5).

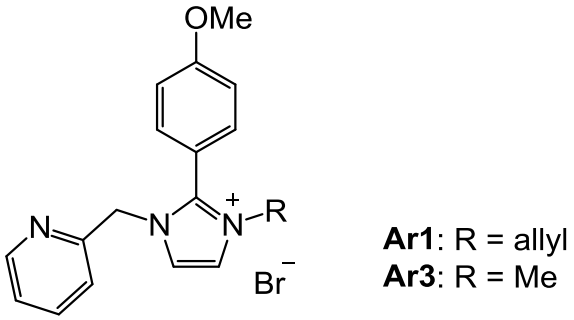

Figure 3-5: Structures of target arylated imidazolium salts.

Several synthetic routes have been attempted for the preparation of **Ar1**. Bellina and co-workers demonstrated the C-2 arylation of imidazoles through reaction with aryl iodide in the presence of 0.05 equivalents of $Pd(OAc)_2$ and 2 equivalents of CuI, in anhydrous DMF at 140 °C (Scheme 3-8a).[23-27] A similar reaction was carried out starting from 1-allylimidazole; however, arylation occurred on the allyl and resulted in the formation of **39** (Scheme 3-8b). The ^{1}H NMR spectrum showed that the C-2 proton (H_A) had not been substituted, with the resonance still present at δ 7.54 ppm (Figure 3-6). Furthermore, the chemical shifts and *J*-couplings of the allylic group are significantly different from the starting imidazole. The *trans* CH=**CH**$_2$ proton (H_E, at δ 5.00 ppm in the starting material), which has a $^3J_{cis}$ coupling constant of 10.2 Hz with the vinylic proton, was no longer observed in the spectrum of the product. The vinylic protons (H_D), allylic protons (H_B) and the *cis* proton (H_C) shifted downfield due to the newly introduced aryl group, with the *trans* proton being most downfield as it is closest to the aryl group. The NMR data indicates that the arylation occurred at the terminal alkene and results in a *trans*-alkene.

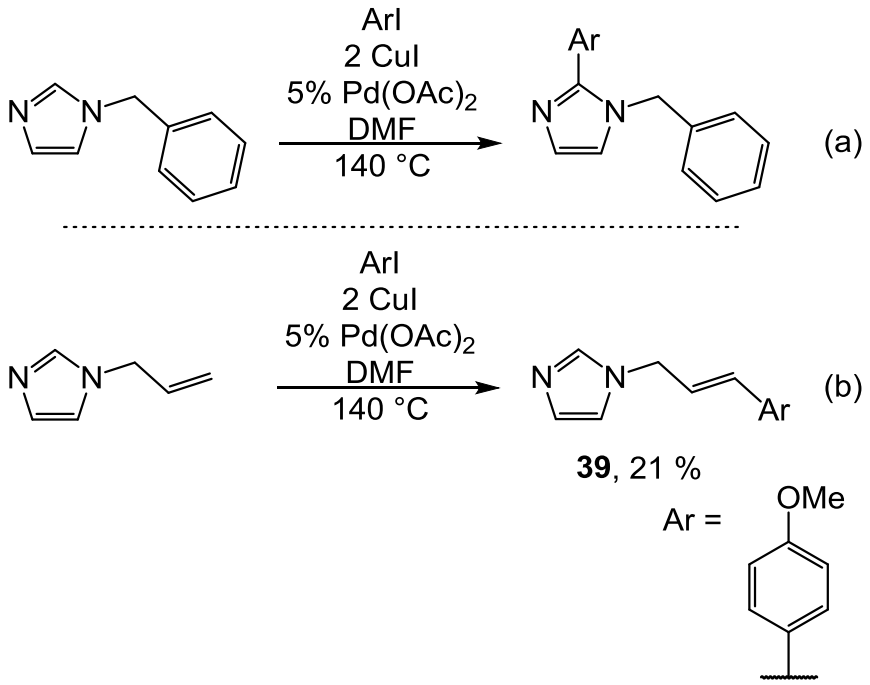

Scheme 3-8: Arylation of 1-benzylimidazole[23] and 1-allylimidazole.

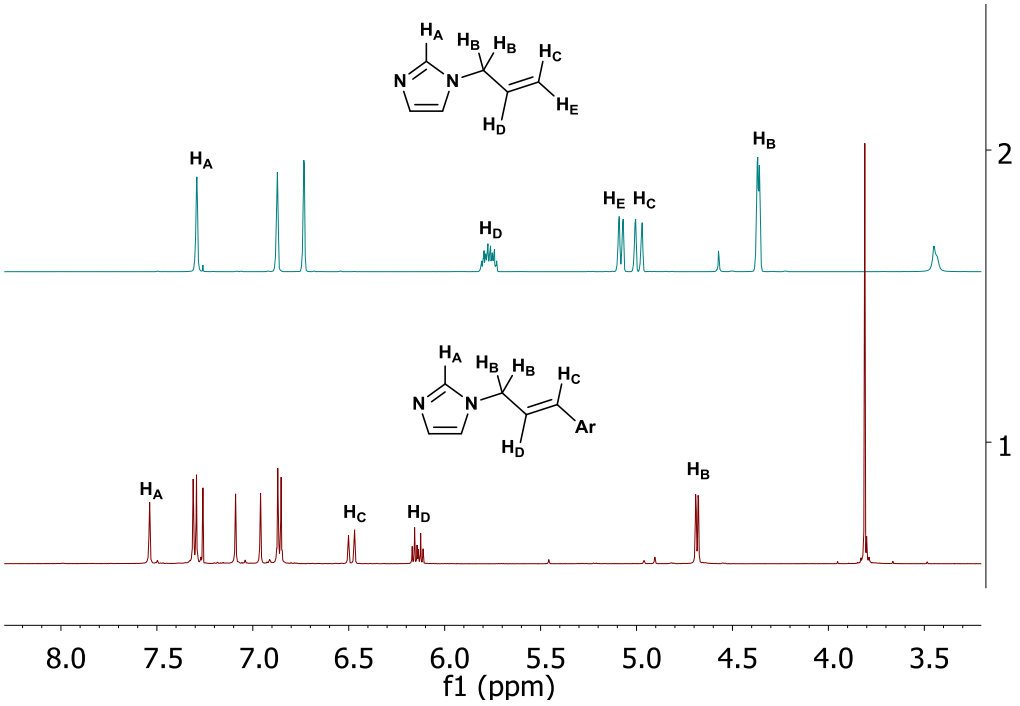

Figure 3-6**:** ^{1}H NMR spectra (500MHz, $CDCl_3$) of 1-allylimidazole (top) and the arylated product (bottom).

1-Picolylimidazole (**P1**) was synthesised by nucleophilic substitution of imidazole with picolyl bromide.HBr in the presence of base, with the aim of arylating this precursor (Scheme 3-9).

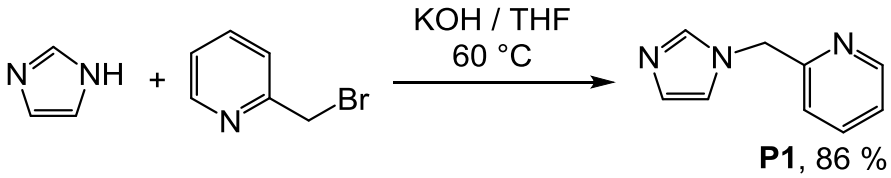

Scheme 3-9: Preparation of **P1**.

P1 was arylated using Bellina's method (Scheme 3-10). The arylated imidazole **40** was obtained in very low isolated yield (1%), even though this was observed as a major product in both the crude ^{1}H NMR spectrum and the HR mass spectrum. It is therefore proposed that **40** is lost during the work-up, which requires removal of Cu species by washing with EDTA solution. As **40** can coordinate to Cu, it is possible that it was removed through coordination.

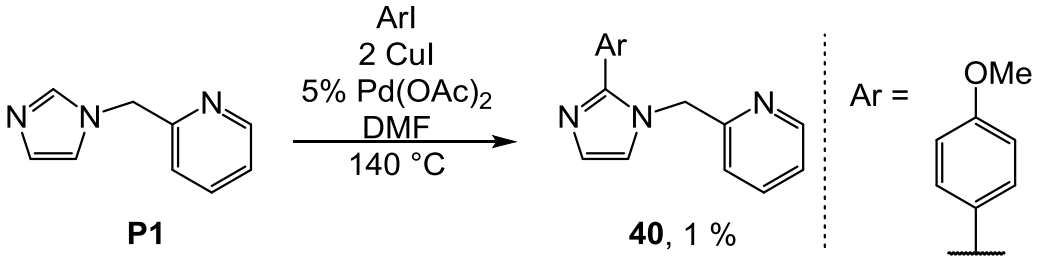

Scheme 3-10: Arylation of **P1**.

Arylation of unsubstituted imidazole was carried out, with the aim of functionalisation after arylation. The C-2 arylated imidazole (**41**) was successfully synthesised and isolated in a high yield (95%) using Bellina's procedure for arylation of imidazole.[23] Then *N*-allylation of **41** was attempted (to prepare **42**), though several products involving *bis*- and *tris*-allylated imidazole were observed, and difficult to separate. Hence, the picolyl group was added first to give **40**, followed by allylation to prepare the desired **Ar1**. **Ar1** was purified by recrystallisation in MeCN / Et_2O in the same manner as H-imidazolium salts. The H-imidazolium resonance was absent in ^{1}H NMR spectrum of **Ar1**, with a ratio of imidazolium / picolyl / anisolyl / allyl resonances of 1: 1: 1: 1, indicating the successful addition of the 3 desired groups on to the imidazole ring (Figure 3-7). The $^{13}C\{^{1}H\}$ NMR spectrum shows 6 resonances corresponding to the aromatic protons of the anisolyl group, with the *ortho*- and *meta*- carbon pairs being inequivalent due to asymmetric *N*-substituents on the imidazolium (Figure 3-8). The imidazolium cation formation can also be confirmed using HRMS (*m/z* [**Ar1** – Br]$^{+}$ 306.1617, calculated 306.1606).

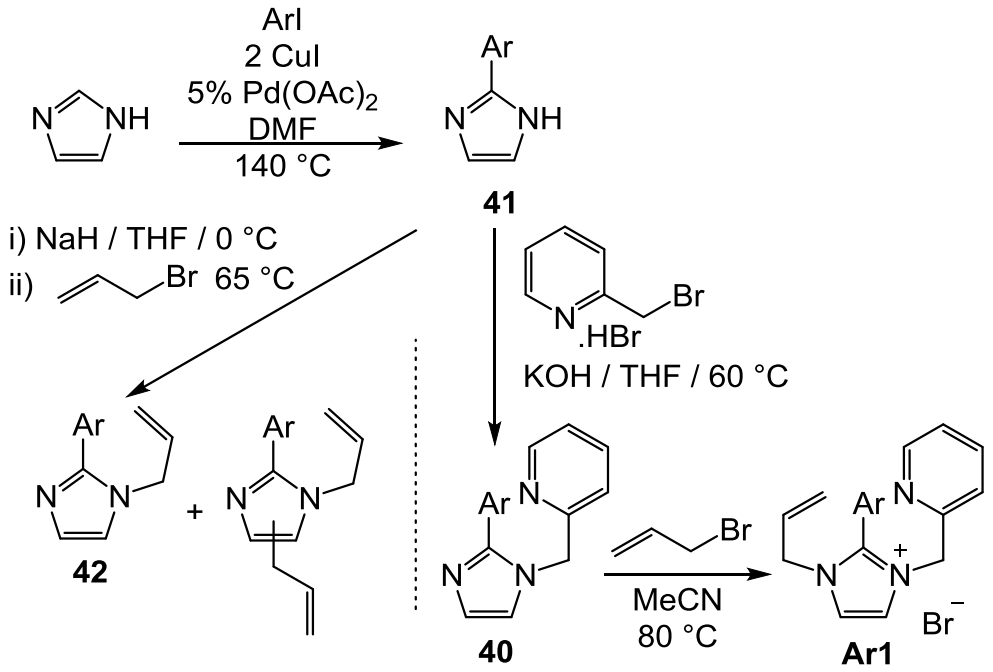

Scheme 3-11: Preparation of arylated imidazolium **Ar1**.

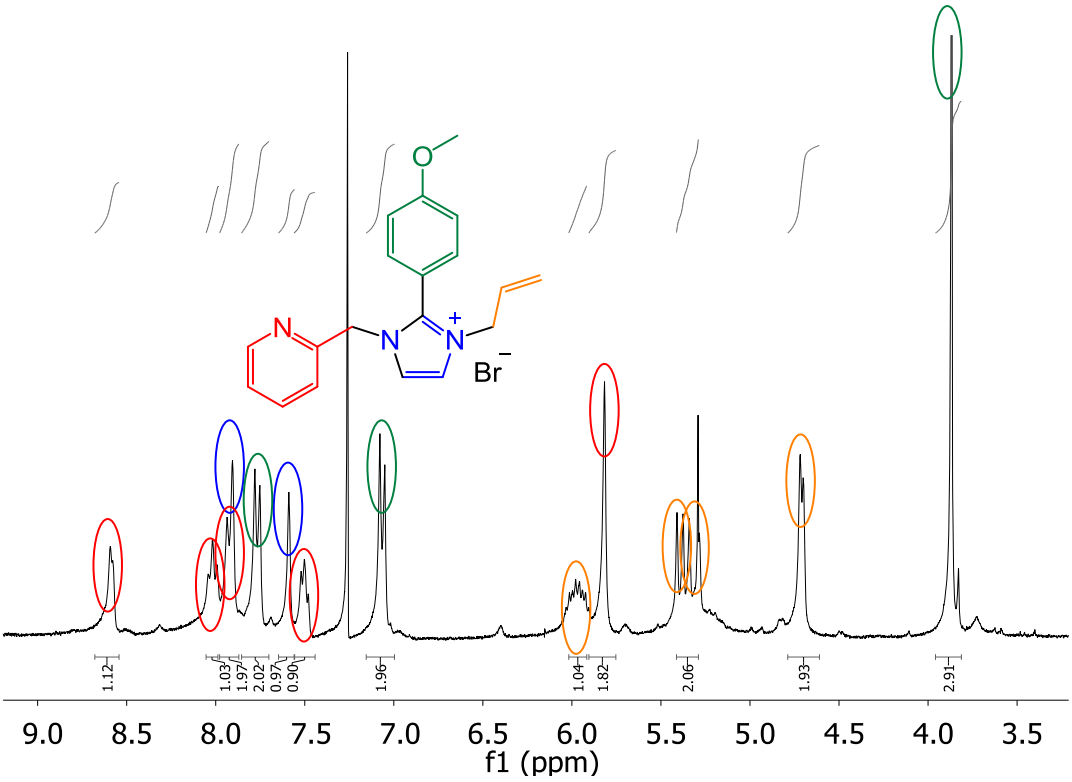

Figure 3-7: ^{1}H NMR spectrum (300 MHz, $CDCl_3$) of **Ar1**.

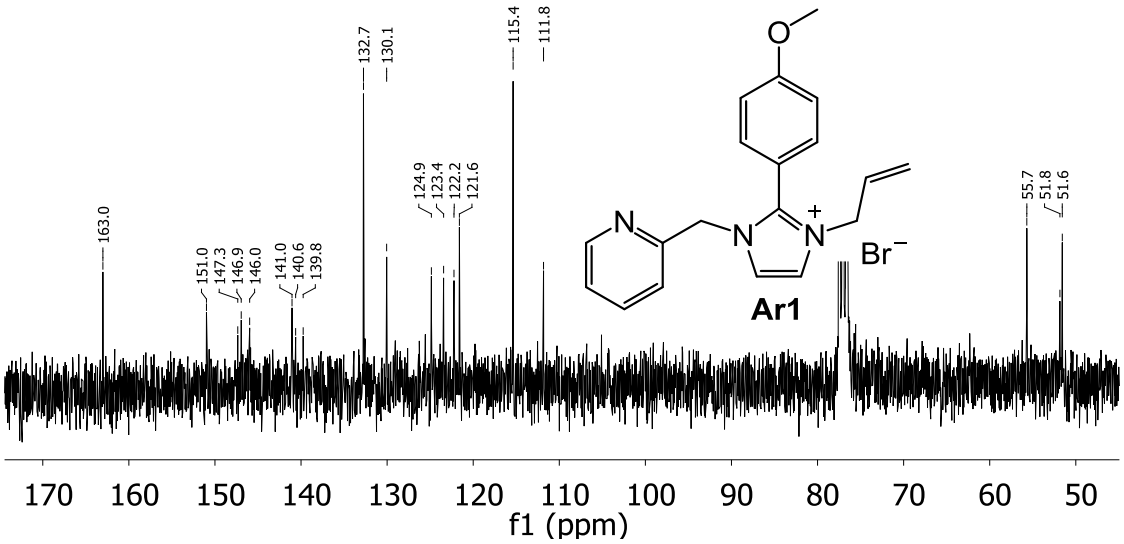

Figure 3-8**:** ^{13}C {^{1}H} NMR spectrum (75 MHz, $CDCl_3$) of **Ar1**.

To prepare **Ar3**, 1-methylimidazole was arylated at the C2 position. Reaction with picolyl bromide resulted in successful formation of arylated imidazolium **Ar3**, which was characterised using ^{1}H and ^{13}C {^{1}H} NMR spectroscopies and HRMS. As with **Ar1**, the asymmetry of the anisolyl group was observed in the $^{13}C\{^{1}H\}$ NMR spectrum of **Ar3**, with 16 carbon peaks being observed in the aromatic region (Figure 3-9).

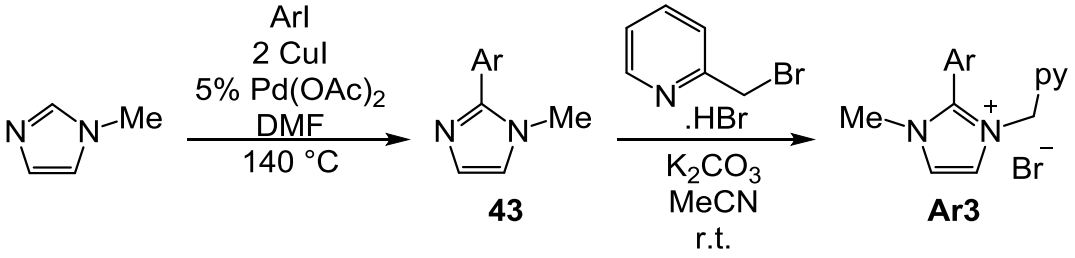

Scheme 3-12: Preparation of **Ar3**.

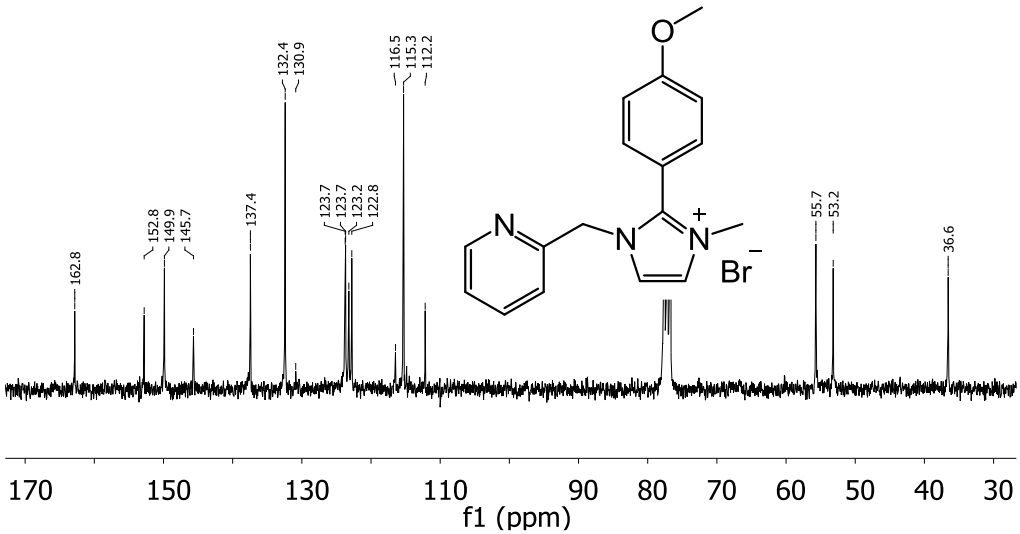

Figure 3-9: ^{13}C {^{1}H} NMR spectrum (75 MHz, $CDCl_3$) of **Ar3**.

3.3.2 Preparation of other potential deactivated species

In addition to examining the reductive elimination of the aryl-imidazolium cation, other potential side-reactions involving the aryl iodide species have been considered. Possible products of these side-reactions include homo-coupled biaryl (**ArAr**) and dehalogenated anisole (**ArH**). Starting aryl-iodide or a different aryl-halide (as a result of reductive elimination) and the desired cross-coupled product may also be observed (Scheme 3-13).[28-32]

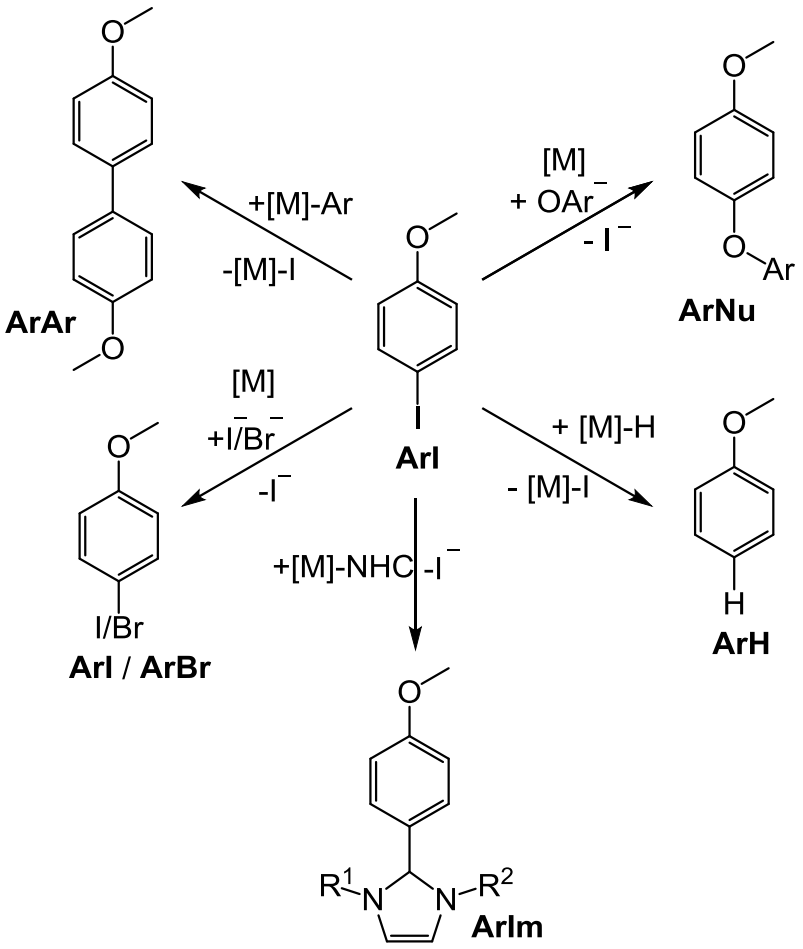

Scheme 3-13: Potential products from the aryl-iodide in metal-catalysed cross coupling reactions.

To be able to quantify individual products, the arylated species were prepared separately so that calibration and quantification could be carried out using GC-UV and HPLC-MS. The 4-iodoanisole (**ArI**) and anisole (**ArH**) are commercially available, with the ether product (**ArNu**) and the biaryl (**ArAr**) being synthesised.

The ether product **ArNu** was prepared using an Ullmann-type etherification reaction and a CuI/acac catalyst that derived from *iso*-butyryl cyclohexanone (Scheme 3-14, section 2.7). The pure product was obtained after column chromatography as an off-white solid. The product was fully characterised by ^{1}H (Figure 3-10) and ^{13}C $\{^{1}H\}$ NMR spectroscopy and HRMS.

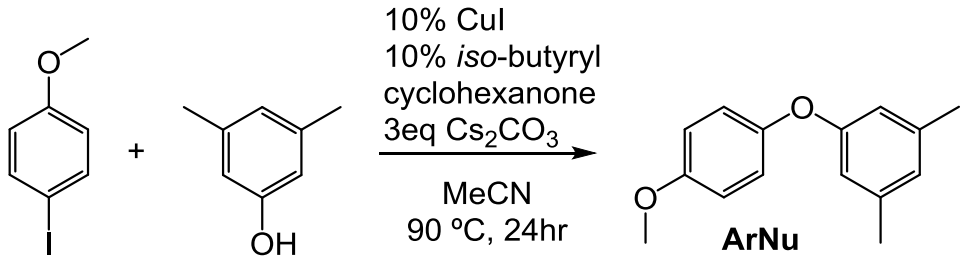

Scheme 3-14: Preparation of **ArNu**.

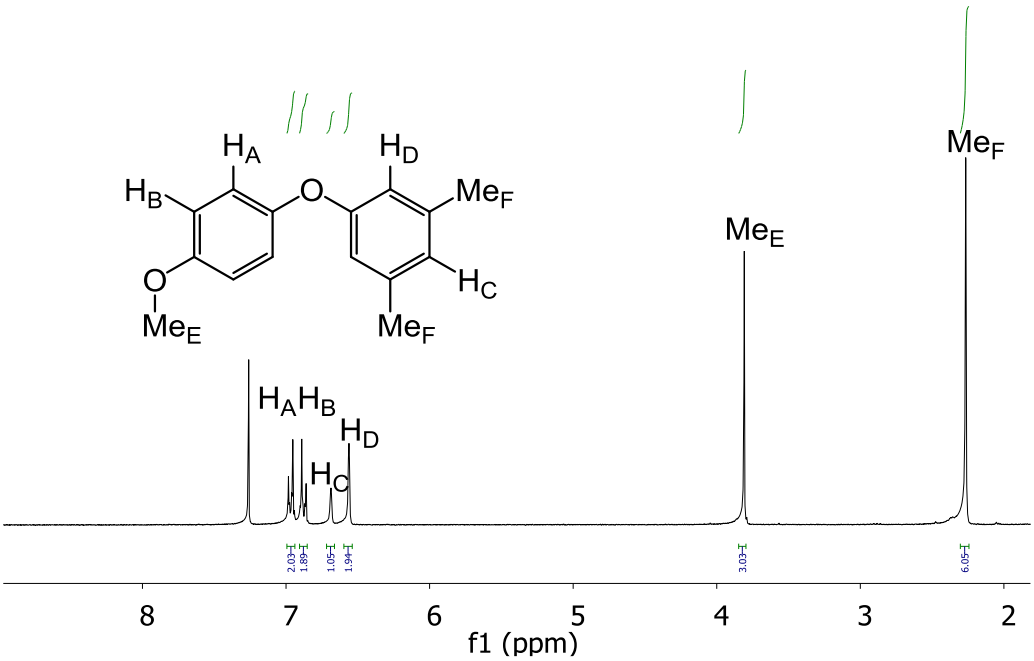

Figure 3-10: ^{1}H NMR spectrum (300 MHz, $CDCl_3$) of **ArNu**.

Similar to the preparation of the ether, the biaryl was prepared by a metal-catalysed coupling reaction using an organometallic aryl. The **ArI** was stirred with *n*-BuLi to generate aryl-lithium (**ArLi**). The organometallic compound was then transferred into a reaction mixture of **ArI** and a Pd catalyst (Scheme 3-15). The crude reaction mixture was partitioned in NH_4Cl solution and Et_2O, and extracted by Et_2O. Column chromatography (silica gel) was then used to purify the crude mixture and the product was obtained in 16 % yield. **ArAr** was characterised by ^{1}H and ^{13}C {^{1}H} NMR spectroscopy. However, the product was not observed in the HR mass spectrum (ESI) as it is unlikely to be ionised by electron spray.

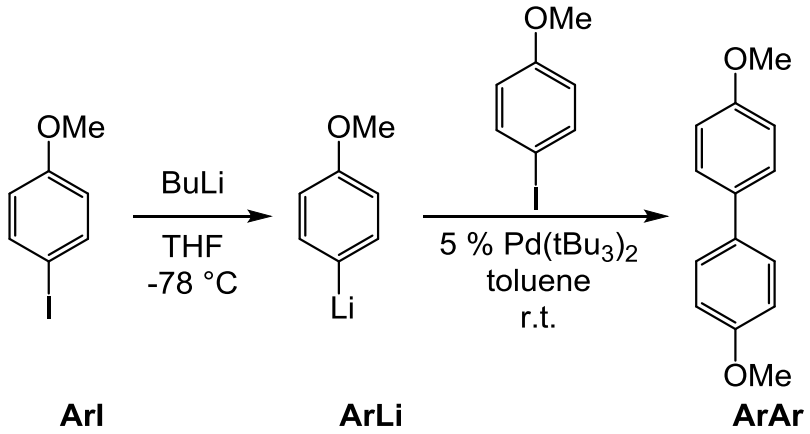

Scheme 3-15**:** Preparation of **ArAr**.

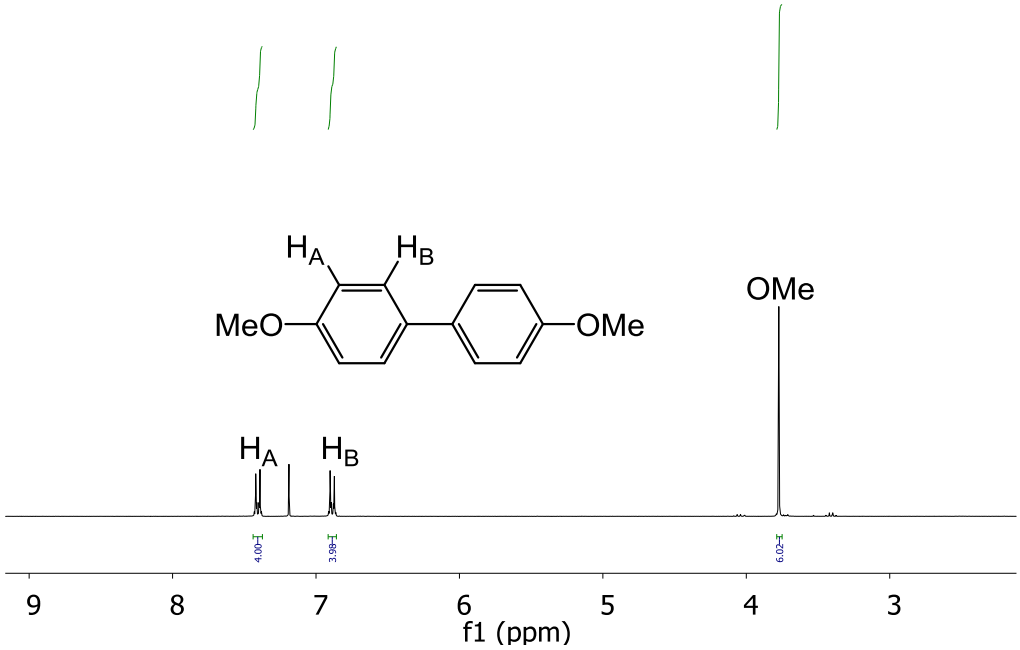

Figure 3-11: ^{1}H NMR spectrum (300 MHz, $CDCl_3$) of **ArAr**.

3.3.3 Conditions that affect Ullmann-type etherification and competing reactions

In the previous sections, it was observed that aryl-imidazolium **Ar1** (derived from **L1**) formed only when using stoichiometric amount of metal and ligand, whereas **Ar3** (derived from **L3**) was observed at 10 mol% of the catalyst. In addition to quantifying this data, other factors such as nucleophile, base and catalyst loadings can also be studied to see how they affect competing reactions.

i) Nucleophile equivalents

The first factor to be examined was equivalents of nucleophile (*i.e.* 3,5-dimethylphenol). Ullmann-type etherification reactions were carried out using a stoichiometric amount of the *in situ* formed Cu complex from **L1** (Table 3-3). The cross-coupled ether product (**ArNu**), as expected, increased when the nucleophile loadings were higher. The aryl-imidazolium (**ArIm**) formation also increased upon increasing amounts of nucleophile, with similar quantities of **ArNu** and **ArIm** with up to 1.2 equivalents of 3,5-dimethylphenol. This suggests that either the nucleophile or the imidazolium could act as supporting ligand with the other reductively eliminating under the speculation that the reaction occurs *via* Cu(III) intermediates. It is therefore likely that nucleophile substitution occurs prior to oxidation (Scheme 3-16).

L	Cu/L eq	3,5-dimethylphenol (H**Nu**) eq	**ArI**	**ArNu**	**ArH**	**ArAr**	**ArIm***
L1	1	0	69	0	6	0	<1
		0.6	57	7	5	4	8
		1.2	49	13	6	5	18
		2.4	29	32	11	5	12
L3	0.1	0	100	0	0	0	<1
		0.6	91	3	0	0	<1
		1.2	47	42	6	5	9
		2.4	70	13	0	0	3

Table 3-3: % formation of different aryl species. Reaction conditions: 1.0 mmol 4-iodoanisole, 0 – 2.4 mmol 3,5-dimethylphenol, 1.0 mmol of CuI/H**L1**Br or 0.1 mmol of CuI/H**L3**Br, 3.0 mmol Cs_2CO_3, 5 mL MeCN, 90 °C, 24hr. Yields were determined by GC using *p*-cymene as an internal standard. * Yields were determined by HPLC-MS spiking. <1 = the species was observed but calculated to be less than 1%.

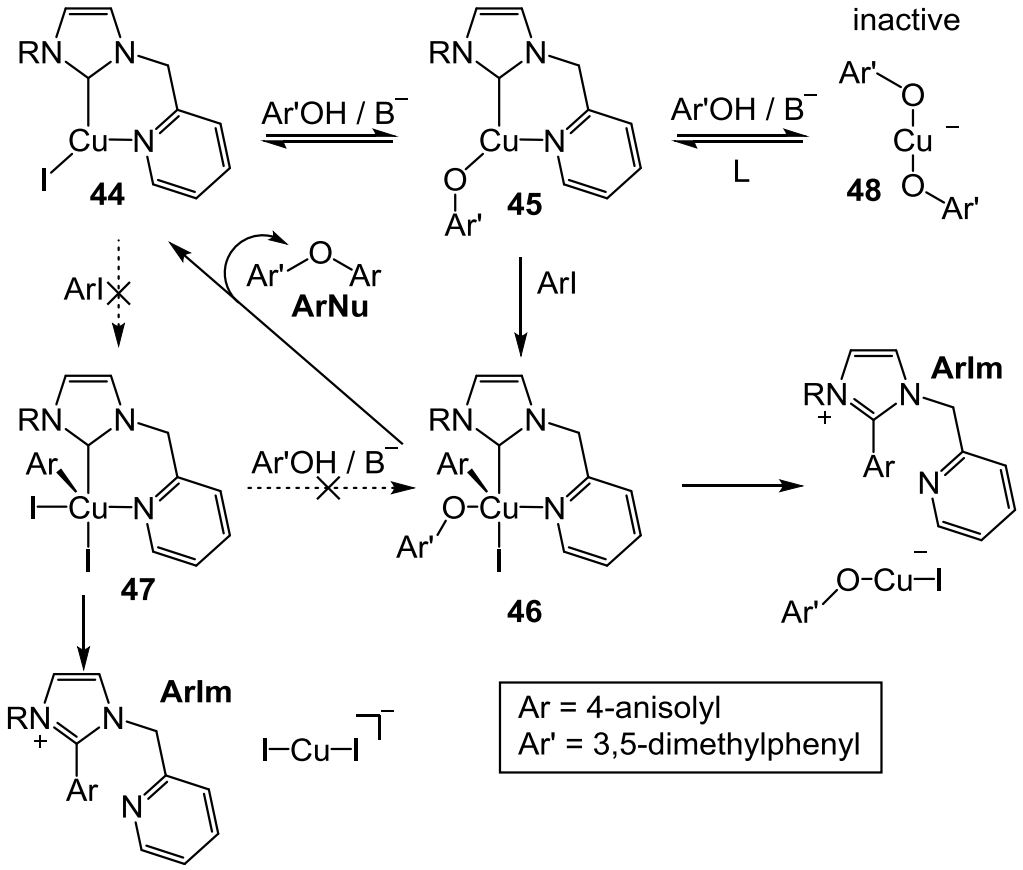

Scheme 3-16: Simplified competing reactions and deactivation pathways

However, when the equivalents of nucleophile was increased to 2.4, the **ArIm** formation decreased slightly whilst the **ArNu** formation continued to increase. The same trend for **ArIm** formation was observed in the case of using catalytic amount of the *in situ* formed Cu complex from **L3**. However, increasing the nucleophile equivalents in this case from 1.2 to 2.4, the % conversion to **ArNu** decreased from 42 to 13. This is possibly due to another deactivation pathway involving a *bis*-nucleophile complex (**48**) formation (Scheme 3-16), which has been observed as a resting state in reported Cu-catalysed C-N bond formation reactions.[33,34]

ii) Base equivalents

The amount of base, ranging from 0-4 equivalents Cs_2CO_3, was also examined in the reaction (Table 3-4). Increasing the base loading increased formation of **ArNu**, with the optimum appearing to be 3 equivalents for **L1**, and 2 equivalents for **L3** (stoichiometric metal). It has previously been reported that increasing the base loading can raise the catalytic activity. As previously shown, increasing the base equivalents from 2 to 4 was demonstrated to promote the catalytic yield of the etherification model using **L1** as a ligand from 42 % to 58 %.[19] Furthermore,

a base is essential for the deprotonation of imidazolium ligand precursor and nucleophile (either before or after ligand substitution) (Scheme 3-17). Hence, higher base equivalents would give higher conversions to the desired product.

L	Cu/L eq	base eq	**ArI**	**ArNu**	**ArH**	**ArAr**	**ArIm***
L1	1	0	106	10	none	none	<1
		2**	14	23	9	75	27
		3	none	43	22	9	7
		4	none	44	21	2	<1
L3	1	0	94	8	none	none	<1
		2	42	50	8	none	3
		3	9	50	15	none	5
		4	none	53	13	none	3
	0.1	0	96	none	none	none	<1
		2	57	32	6	none	<1
		3	45	44	6	none	<1
		4	42	53	6	none	<1

Table 3-4: % formation of different aryl species. Reaction conditions: 1.0 mmol 4-iodoanisole, 1.2 mmol 3,5-dimethylphenol, 1.0 mmol of CuI/H**L1**Br/H**L3**Br or 0.1 mmol of CuI/H**L3**Br, 0 – 4.0 mmol Cs_2CO_3, 5 mL MeCN, 90 °C, 24hr. Yields were determined by GC using *p*-cymene as an internal standard. * Yields were determined by HPLC-MS spiking. <1 = the species was observed but calculated to be less than 1%. ** 48% over theoretical mass balance, error in GC calibration at higher concentration.

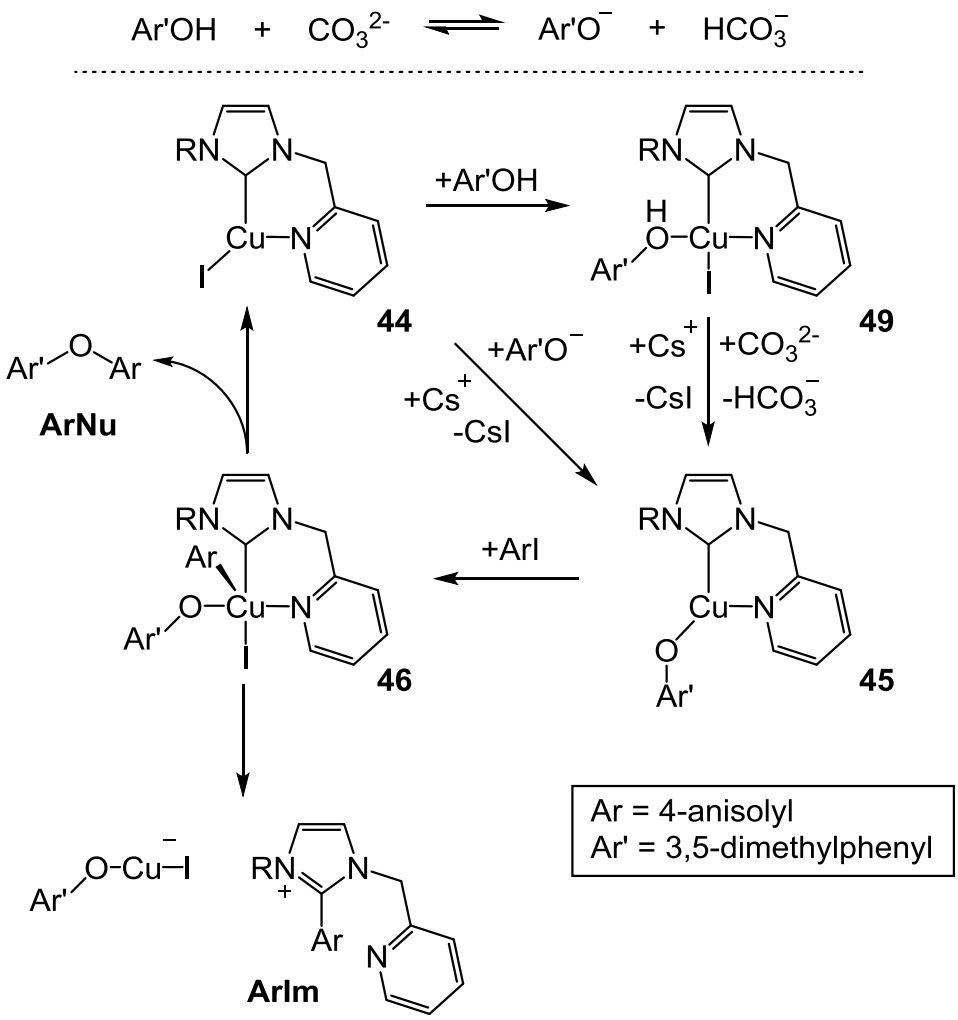

Scheme 3-17: Base-involved etherification and aryl-imidazolium formation, with the proposal that both reactions take place *via* the oxidative addition / reductive elimination pathway

The effect of base equivalents on dehalogenation has been reported in the Suzuki coupling of bromo-pyrazole and aryl boronic acid (Scheme 3-18).[35,36] It was proposed that the side-reaction of dehalogenation is base induced (8, 59 and 63 % using 2, 3 and 4 equivalents of K_2CO_3 respectively). The deprotonation of pyrazole was implicated in the dehalogenation reaction (Scheme 3-19). It is possible that dehalogenation of 4-iodoanisole takes place *via* similar mechanism (Scheme 3-20), though in this case deprotonation is not required so base loading should not affect formation. **ArH** formation was found to increase in the case of stoichiometric CuI + imidazolium salt loadings up to 22 % (**L1**) and 15 % (**L3**) with 3 equivalents of base. The increase of base equivalents may be involved in the removal of the iodine atom (as either iodine cation or iodine anion).

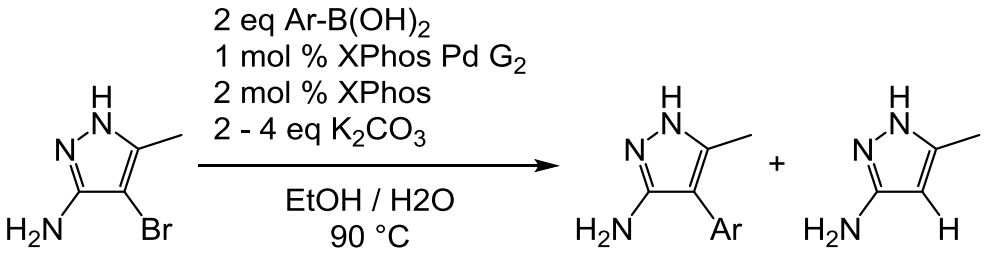

Scheme 3-18: Suzuki coupling reaction of bromo-pyrazole and aryl boronic acid, and a side-reaction of hydrodehalogenation.[36]

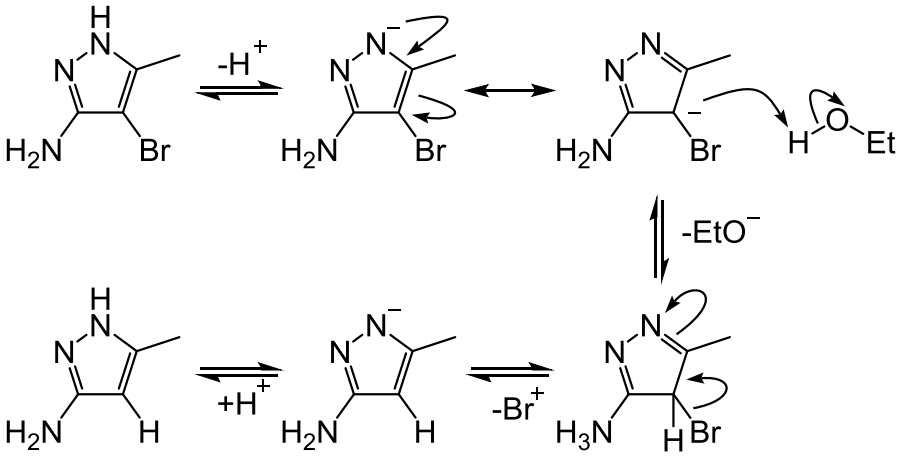

Scheme 3-19: The mechanism of dehalogenation of bromo-pyrazole, proposed by Jedinak.[36]

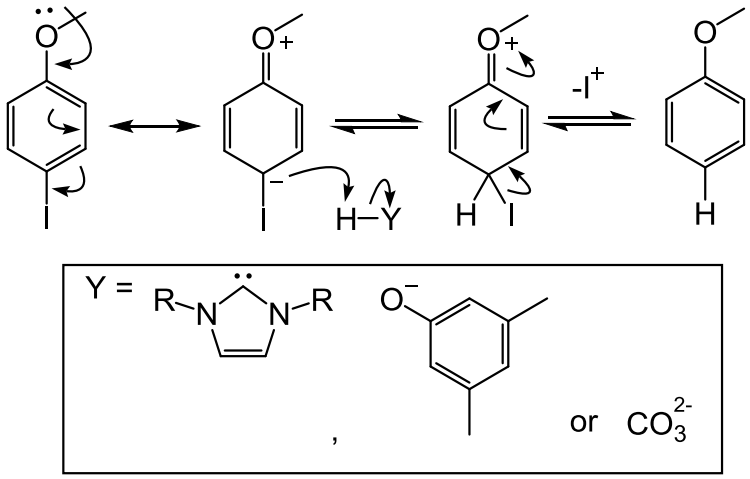

Scheme 3-20: A proposed mechanism of dehalogenation of 4-iodoanisole.

Another side-reaction observed was homocoupling (**ArAr**), which happened only in the case of **L1** under stoichiometric conditions. It is not clear why **L1** leads to **ArAr** formation, though this decreases upon increasing base loading, likely as a result of competing reactions such as etherification being able to take place. Increasing the Cs_2CO_3 can drive etherification by providing sufficient amounts of nucleophile. A similar observation was reported in the literature in a Pd-catalysed

arylation reaction, in which sufficient amount of active nucleophile leads to the successful suppression of homocoupling.[37]

Upon increasing the base loading, it was found that aryl-imidazolium formation decreased particularly in the case of **L1** under stoichiometric conditions (27 % with 2 equivalent, decreasing to 7 % with 3 equivalents and negligible with 4 equivalents, Table 3-4). Decrease in **ArIm** formation is again likely due to the competing cross-coupling reaction (**ArNu**).

iii) Metal complex loadings

Metal/ligand loadings were varied, ranging from a catalytic amount (10 %) to an excess amount (200 %) (Table 3-5). The homocoupling (**ArAr** formation) still occurred in the case of **L1**, which was enhanced by higher catalyst loadings (> 100 %). It appears that etherification dominates under catalytic conditions, reaching its highest efficiency at 0.5 equivalents. However, as the metal/ligand loadings are increased further, reductive elimination of ArIm started to occur at high metal/ligand loadings due to higher concentration of NHC in the reaction system. Similarly, the homocoupling reaction started to occur at high metal/ligand loadings as there is a higher chance of aryl transmetallation due to more populated metal species, and the amount of nucleophile substrate to the metal centre became insufficient.

In addition, comparing **L1** and **L3** in **ArIm** formation, **L3** led to the reductive elimination of **ArIm** (**Ar3**) at lower catalyst loadings (10%), while **Ar1** started to be discovered at 50% catalyst loadings. This is consistent with the earlier observation (section 3.2) that **Ar1** was not observed when a catalytic amount of catalyst was used, but was detected in the reaction with a stoichiometric amount of catalyst.

L	Cu/L eq	**ArI**	**Ether**	**ArH**	**Ar-Ar**	**Ar-im***
L1	0	94	none	none	none	none**
	0.1	52	42	6	none	none**
	0.5	12	61	15	none	<1
	1	none	32	19	21	11
	1.5	7	20	18	29	26
	2	17	17	6	56	25
L3	0	93	none	none	none	none**
	0.1	45	43	7	none	<1
	0.5	10	67	14	none	<1
	1	7	36	13	none	4
	1.5	9	37	13	none	5
	2	9	52	16	none	9

Table 3-5: % formation of different aryl species. Reaction conditions: 1.0 mmol 4-iodoanisole, 1.2 mmol 3,5-dimethylphenol, 0 – 2.0 mmol of CuI/imidazolium salt', 3.0 mmol Cs_2CO_3, 5 mL MeCN, 90 °C, 24hr. Yields were determined by GC using p-cymene as an internal standard. * Yields were determined by HPLC-MS spiking. **No formation was confirmed by HRMS. <1 = the species was observed but calculated to be less than 1%

Overall, **ArNu** was generally the major product in these reactions, even when stoichiometric amounts of metal/ligand were applied. The homocoupled side-product **ArAr** was the least formed except when the metal/ligand loadings were used in huge excess. Furthermore, the **ArIm** was not the major side-product, even in the presence of stoichiometric metal/ligand. Instead, formation of the dehalogenated product (**ArH**) appeared to be the major deactivation pathway of the aryl iodide starting material in the reaction.

3.4 Conclusions

A range of picolyl/pyridyl/allyl-bearing NHC ligands have been used to examine the competing reactions in an Ullmann-type etherification reaction. Only ligands with a picolyl *N*-substituent afford the aryl-imidazolium side-product, with its formation generally increasing **ArNu** formation. This is likely due to strongly basic NHC ligand being able to stabilise higher oxidation state Cu intermediates, with reductive elimination of **ArNu** and **ArIm** taking place.

The results from varying nucleophile, base and metal/ligand concentrations show that etherification is favoured by a sufficient amount of nucleophile and metal/ligand, and can be promoted with excess base. However, unlike the **ArNu**, the **ArIm** reductive elimination can be increased by a sufficient amount of nucleophile, excess metal/ligand, but minimal base. Furthermore, the higher metal/ligand loadings promote other side-reactions, including dehalogenation (**ArH**) and homocoupling (**ArAr**).

3.5 Future Work

The field of Cu-NHC catalysed cross-coupling reactions is still very much in its infancy. Cu is more uncontrolled when compared to precious metal such as Pd and Rh, hence the outcome of reactions is very difficult to predicet. The more knowledge that can be added to understanding the reactivity of Cu the better ligand and reaction design will become to enable Cu to be applied more broadly. In this specific study, other variables that may contribute to reaction outcome include other types of bases (K_3PO_4, K_2CO_3 and CsF), type of nucleophiles (phenols, anilines, aryl lithiums), ligand:Cu ratios (2:1 *versus* 1:1), types of counter anions and solvents (DMF, DMAc and DMSO). Furthermore, other instruments may be adapted and applied to track the reactions in real time.

3.6 Experimental

3.6.1 Preparation of imidazole

i) Preparation of **P38**

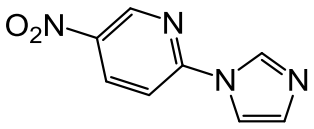

2-Bromo-5-nitropyridine (2.0 g, 9.8 mmol) and imidazolyl sodium (0.99 g, 11 mmol) were added to a Schlenk flask. DMF (40 mL) was transferred into the flask *via* syringe resulting in a dark red-orange mixture. The mixture was stirred at room temperature for 3 hours. Water (150 mL) was added resulting in precipitation of the product, which was collected as light orange-brown solid by filtration and washed with water (3 × 25 mL). The solid was dissolved in hot MeCN (100 mL), filtered and dried over Na_2SO_4. The solvent was removed *in vacuo* to give a brown solid. Yield: 1.35 g, 0.71 mmol, 72%.

^{1}H NMR (300 MHz, $CDCl_3$) δ (ppm) 9.33 (d, *J* = 2.7 Hz, 1H, pyH-6), 8.63 (dd, *J* = 8.9, 2.7 Hz, 1H, pyH-4), 8.46 (s, 1H, imH), 7.70 (s, 1H, imH), 7.50 (d, *J* = 8.9 Hz, 1H, pyH-3), 7.26 (s, 1H, imH). ^{13}C {^{1}H} NMR (75 MHz, $CDCl_3$) δ (ppm) 152.2

(C), 145.7 (CH), 142.3 (C), 135.6 (CH), 134.7 (CH), 132.1 (CH), 116.2 (CH), 111.5 (CH). HRMS (ESI$^+$): *m/z* 191.0640 $[M + H]^+$, calculated $[M + H]^+$ 191.0564.

Consistent with data previously reported.[38]

ii) Preparation of **P1**

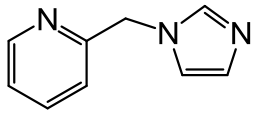

In air, imidazole (0.27 g, 3.95 mmol) and KOH (0.89 g, 15.8 mmol) were added to a round-bottomed flask, followed by THF (20 mL) and stirred for 20 minutes at room temperature. 2-(bromomethyl)pyridine.HBr (1.0 g, 3.95 mmol) was added and stirred at 60 °C for 48 hours. The mixture was allowed to cool to room temperature and the solvent removed *in vacuo*. The crude mixture was partitioned in DCM (100 mL) and water (100 mL). The water layer was extracted with DCM (2 × 100 mL). The organic layers were combined, washed with brine (100 mL), dried with Na_2SO_4 and solvent removed *in vacuo*. The dark oil was dissolved and sonicated in Et_2O (50 mL), filtered, and the solvent removed *in vacuo* to obtain a dark orange oil. Yield: 0.54 g, 3.40 mmol, 86%.

^{1}H NMR (300 MHz, $CDCl_3$) δ (ppm) 8.55 (ddd, *J* = 4.9, 1.7, 0.8 Hz, 1H, pyH-6), 7.62 (td, *J* = 7.7, 1.8 Hz, 1H, pyH-4), 7.57 (s, 1H, imH-2), 7.22 – 7.16 (m, 1H, pyH-5), 7.07 (s, 1H, imH), 6.95 (s, 1H, imH), 6.91 (d, *J* = 7.8 Hz, 1H, pyH-3), 5.21 (s, 2H, N**CH_2**-py). ^{13}C {^{1}H} NMR (75 MHz, $CDCl_3$) δ (ppm) 156.1 (C), 149.7 (CH), 137.6 (CH), 137.3 (CH), 129.8 (CH), 123.0 (CH), 121.2 (CH), 119.5 (CH), 52.5 (CH_2). HRMS (ESI$^+$): *m/z* 160.0881 $[M + H]^+$, calculated $[M + H]^+$ 160.0869.

Consistent with data previously reported.[39,40]

3.6.2 Preparation of imidazolium salts

i) Preparation of H**L38**Br

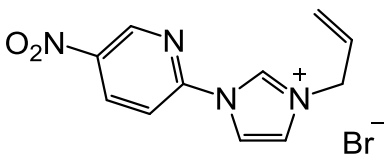

In air, **P38** (1.0 g, 5.25 mmol) was added to a round-bottom flask followed by MeCN (150 mL). The mixture was heated to 80 °C to fully dissolve **P38**. Allyl bromide (2.3 mL, 26 mmol) was added dropwise to the solution and the mixture was heated to 80 °C and held at reflux for 24 hours. The volume was reduced to ca. 30 mL *in vacuo*. Slow addition of Et_2O (150 mL) induced the precipitation of a light brown solid, which was filtered and dried in air. Yield: 1.52 g, 4.89 mmol, 93 %.

^{1}H NMR (300 MHz, $CDCl_3$) δ (ppm) 12.28 (dd, *J* = 1.8, 1.6 Hz, 1H, imH-2), 9.29 (dd, *J* = 2.6, 0.6 Hz, 1H, pyH-6), 9.07 (dd, *J* = 9.0, 0.6 Hz, 1H, pyH-3), 8.79 (dd, *J* = 9.0, 2.6 Hz, 1H, pyH-4), 8.33 (dd, *J* = 2.1, 1.8 Hz, 1H, imH), 7.37 (dd, *J* = 2.1,

1.6 Hz, 1H, imH), 6.08 (ddt, *J* = 16.7, 10.1, 6.6 Hz, 1H, **CH**=CH_2), 5.55 (m, 2H, CH=**CH_2**), 5.15 (d, *J* = 6.6 Hz, 2H, N**CH_2**-vinyl). ^{13}C {^1H} NMR (75 MHz, $CDCl_3$) δ (ppm) 148.9 (C), 144.9 (CH), 144.6 (C), 137.6 (CH), 128.9 (CH), 124.2 (CH), 122.1 (CH_2), 119.2 (CH), 116.3 (CH), 53.1 (CH_2). HRMS (ESI^+): *m/z* 231.0882 $[M - Br]^+$, calculated $[M - Br]^+$ 231.0882.

Consistent with data previously reported.[22]

3.6.3 Preparation of arylated imidazoles/imidazoliums

i) Arylation of 1-allylimidazole, synthesis of **39**

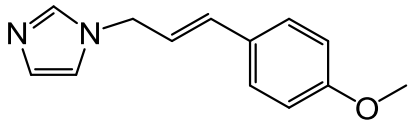

4-Iodoanisole (0.27 g, 1.16 mmol), $Pd(OAc)_2$ (0.010 g, 0.046 mmol) and CuI (0.35 g, 1.85 mmol) were added to a Schlenk flask. DMF (5 mL) was added, followed by 1-allylimidazole (0.10 mL, 0.92 mmol). The reaction mixture was stirred at 140 °C for 48 hours, cooled to room temperature, diluted in EtOAc (30 mL), and poured into a saturated solution of NH_4Cl (100 mL) and stirred for 30 mins. The organic layer was separated, and the aqueous layer was extracted with EtOAc (5 × 30 mL). All organic layers were combined, dried with $MgSO_4$ and the solvent removed *in vacuo*. The crude brown product was purified with fractional column chromatography, eluting with EtOAc / petroleum ether (40-60 °) / methanol (45: 45: 10). The pure product was obtained as a pale brown solid. Yield: 0.42 g, 0.20 mmol, 21%.

^1H NMR (500 MHz, $CDCl_3$) δ (ppm) 7.54 (s, 1H, imH-2), 7.30 (d, *J* = 8.8 Hz, 2H, ArH), 7.09 (s, 1H, imH), 6.96 (s, 1H, imH), 6.86 (d, *J* = 8.8 Hz, 2H, ArH), 6.49 (dt, *J* = 15.8, 1.2 Hz, 1H, CH=**CH**Ar), 6.14 (dt, *J* = 15.8, 6.3 Hz, 1H, **CH**=CHAr), 4.68 (dd, *J* = 6.3, 1.2 Hz, 2H, N**CH_2**-vinyl), 3.81 (s, 3H, OCH_3). ^{13}C {^1H} NMR (126 MHz, CDCl3) δ (ppm) 159.8 (CH), 137.1 (CH), 133.3 (CH), 129.6 (CH), 128.5 (C), 127.9 (CH), 127.0 (C), 121.3 (CH), 119.0 (CH), 114.2 (CH), 114.1 (CH), 55.33 (CH_2), 49.1 (CH_3). HRMS (ESI^+): *m/z* 215.1184 $[M + H]^+$, calculated $[M + H]^+$ 215.1179.

ii) Preparation of **40** *via* C-2 arylation of **P1**

4-Iodoanisole (0.38 g, 1.25 mmol), $Pd(OAc)_2$ (0.010 g, 0.046 mmol) and CuI (0.49 g, 2.57 mmol) were added to a Schlenk flask. DMF (5 mL) was added, followed by **P1** (0.20g, 1.25 mmol) and the mixture was stirred at 140 °C under Ar for 24 hours. The mixture was allowed to cool to room temperature, transferred into EtOAc (100 mL) and stirred with a saturated solution of EDTA / NH_4Cl (100 mL) for 1 hour. The organic layer was collected, and the aqueous

layer was extracted with EtOAc (3 × 50 mL). The organic layers were combined and volume reduced to 50 mL *in vacuo*, washed with water (3 × 50 mL) and back-extracted into EtOAc (3 × 100 mL). The product was purified by fractional column chromatography eluting with DCM / methanol (95: 5) to obtain a brown sticky solid. Yield: 0.005 g, 0.018 mmol, 1.4 %.

HRMS (ESI$^+$): *m/z* 266.1290 [M + H]$^+$, calculated [M + H]$^+$ 266.1288. ^{1}H and ^{13}C {^{1}H} NMR spectroscopies were performed later when **40** was synthesised with an alternative route.

iii) Preparation of **41**

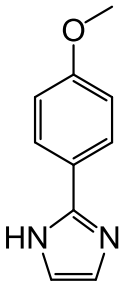

Imidazole (0.20 g, 2.94 mmol), 4-iodoanisole (0.86 g, 3.7 mmol), $Pd(OAc)_2$ (0.033 g, 0.15 mmol) and CuI (1.12 g, 5.88 mmol) were added to a Schlenk flask. DMF (5 mL) was added and the mixture stirred at 140 °C under Ar for 48 hours. After cooling to room temperature to room temperature, the mixture was poured into EtOAc (30 mL) and stirred with a saturated solution of EtOAc / NH_4Cl (100 mL) for 30 minutes. The organic layer was collected, while the aqueous layer was extracted with EtOAc (5 × 50 mL). All organic layers were combined, dried with $MgSO_4$ and the solvent removed *in vacuo*. The crude brown sticky solid was purified by fractional column chromatography eluting with DCM / methanol (95: 5) to obtain a dark orange sticky solid. Yield: 0.49 g, 2.81 mmol, 95%.

^{1}H NMR (300 MHz, $CDCl_3$) δ 7.81 – 7.74 (m, 2H, ArH), 7.10 (s, 2H, imH), 6.93 – 6.86 (m, 2H, ArH), 3.81 (s, 3H, OCH_3). ^{13}C NMR (75 MHz, $CDCl_3$) δ 160.8 (C), 146.5 (C), 127.4 (CH), 121.7 (C). 120.8 (CH), 114.5 (CH), 55.4 (CH_3). HRMS (ESI$^+$): *m/z* 175.0864 [M + H]$^+$, calculated [M + H]$^+$ 175.0866.

Consistent with data previously reported.[41]

iv) Attempted preparation of **42**

NaH (15 mg, 0.63 mmol) and **41** (0.10 g, 0.57 mmol) were added to an ampoule. The mixture was cooled to 0 ºC, then THF (3 mL), also cooled to 0 °C, was added *via* syringe and the reaction mixture was stirred for 1 hour. Allyl bromide (60 µL, 0.69 mmol) was added and the reaction mixture was heated to 65 ºC and stirred for 4 hours. The mixture was allowed to cool to room temperature, DCM (50 mL) was added to dilute and washed by water (3 × 50 mL). The organic layer was dried with Na_2SO_4 and the solvents removed *in vacuo*. Several allylated species were observed in the HR mass spectrum, including *tris*-allylated and *tetrakis*-allylated species.

v) Preparation of **40** *via* **41**

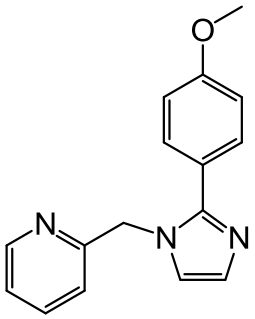

In air, **41** (0.1 g, 0.5 mmol) was dissolved in THF (20 mL). KOH (0.129 g, 2.3 mmol) and 2-(bromomethyl)pyridine.HBr (0.145 g, 0.5 mmol) were added and the reaction stirred at 60 °C for 48 hours. The mixture was allowed to cool to room temperature and the solvent was removed *in vacuo*. The crude mixture was partitioned in water (50 mL) and DCM (50 mL), with the aqueous layer being extracted by DCM (3 x 50 mL). The combined organic layers were dried with $MgSO_4$ and solvent removed *in vacuo*. The crude product was purified by fractional column chromatography eluting with EtOAc / petroleum ether (40 – 60 °) (4: 1). The final product was obtained as pale brown sticky solid. Yield: 0.050 g, 0.19 mmol, 33%.

^{1}H NMR (300 MHz, $CDCl_3$) δ (ppm) 8.53 (d, *J* = 4.4 Hz, 1H, pyH-6), 7.58 (t, *J* = 7.7 Hz, 1H, pyH-4), 7.42 (d, *J* = 8.5 Hz, 2H, ArH), 7.21 – 7.12 (m, 1H, pyH-5), 7.11 (s, 1H, imH), 6.96 (s, 1H, imH), 6.84 (d, *J* = 8.5 Hz, 2H, ArH), 6.81 (d, *J* = 7.7 Hz, 1H, pyH-3), 5.24 (s, 2H, N**CH_2**-py), 3.74 (s, 3H, OCH_3). ^{13}C {^{1}H} NMR (75 MHz, $CDCl_3$) δ (ppm) 159.1 (C), 156.0 (C), 148.8 (CH), 147.3 (C), 136.2 (CH), 129.1 (CH), 128.0 (CH), 121.8 (CH), 120.1 (CH), 120.0 (CH), 119.8 (CH), 113.0 (CH), 54.3 (CH_3), 51.1 (CH_2). HRMS (ESI^+): *m/z* 266.1297 $[M + H]^+$, calculated $[M + H]^+$ 266.1288.

vi) Preparation of **Ar1**

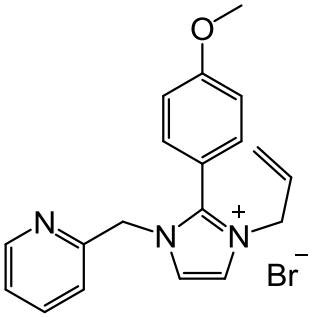

In air, **40** (50 mg, 0.19 mmol) was dissolved in MeCN (10 mL) and allyl bromide (0.2 mL, 2.3 mmol) was added. The reaction solution was stirred at 80 ºC for 24 hours. The mixture was allowed to cool to room temperature and the solvent volume was reduced to 1 mL *in vacuo*. Et_2O (50 mL) was added to precipitate a light brown solid, which was recrystallised in MeCN / Et_2O. Yield: 41.4 mg, 0.11 mmol, 57 %.

^{1}H NMR (300 MHz, $CDCl_3$) δ (ppm) 8.59 (d, *J* = 4.4 Hz, 1H, pyH-6), 8.00 (t, *J* = 7.7 Hz, 1H, pyH-4), 7.92 (d, *J* = 7.7 Hz, 1H, pyH-3), 7.91 (s, 1H, imH), 7.77 (d, *J* = 8.2 Hz, 2H, ArH), 7.59 (s, 1H, imH), 7.50 (dd, *J* = 7.7, 4.4 Hz, 1H, pyH-5), 7.06 (d, *J* = 8.2 Hz, 2H, ArH), 5.97 (ddt, *J* = 16.6, 10.3, 5.7 Hz, 1H, **CH**=CH_2), 5.82 (s, 2H, N**CH_2**-py), 5.39 (d, *J* = 10.3 Hz, 1H, CH=**CH_2** *trans*), 5.31 (d, *J* = 16.6 Hz, 1H, CH=**CH_2** *cis*), 4.71 (d, *J* = 5.7 Hz, 2H, N**CH_2**-vinyl), 3.87 (s, 3H, OCH_3). ^{13}C {^{1}H} NMR (75 MHz, $CDCl_3$) δ (ppm) 163.0 (C), 151.0 (CH), 147.4 (C), 147.0 (CH),

146.0 (C), 141.1 (CH), 140.6 (CH), 139.8 (CH), 132.7 (CH), 130.1 (CH), 124.9 (CH), 123.4 (CH), 122.2 (CH), 121.6 (CH2), 115.4 (CH), 111.8 (CH), 55.7 (CH_3), 51.8 (CH_2), 51.6 (CH_2). HRMS (ESI^+): *m/z* 306.1617 $[M - Br]^+$, calculated $[M - Br]^+$ 306.1601.

vii) Preparation of **43**

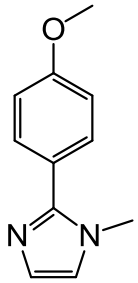

4-Iodoanisole (1.06 g, 4.52 mmol), $Pd(OAc)_2$ (42 mg, 0.19 mmol) and CuI (1.43 g, 7.53 mmol) were added to a Schlenk flask. Anhydrous DMF (3 mL) and 1-methyl imidazole (0.3 mL, 3.76 mmol) were added *via* syringe. The reaction mixture was stirred at 140 ºC under N_2 for 24 hours. The resulting mixture was diluted in EtOAc and stirred with an aqueous solution of EDTA / NH_4Cl (100 mL) for 1 hour. The organic layer was collected, while the aqueous layer was extracted with ethyl acetate (3 × 50 mL). The organic layers were combined and the solvent removed *in vacuo*. The crude product was purified using fractional column chromatography eluting with DCM / methanol (96: 4) to give a brown oil. Yield: 0.15 g, 0.80 mmol, 21%.

^1H NMR (300 MHz, $CDCl_3$) δ (ppm) 7.53 (d, *J* = 8.5 Hz, 2H, ArH), 7.07 (s, 1H, imH), 6.99 – 6.88 (m, 3H, ArH and imH), 3.80 (s, 3H, CH_3), 3.70 (s, 3H, CH_3). $^{13}C\{^1H\}$ NMR (75 MHz, $CDCl_3$) δ (ppm) 159.9 (C), 130.4 (CH), 130.0 (CH), 123.1 (CH), 122.0 (CH), 113.9 (CH), 55.3 (CH_3), 34.4 (CH_3). HRMS (ESI^+): *m/z* 189.1020 $[M + H]^+$, calculated $[M + H]^+$ 189.1022.

Consistent with data previously reported.[24,42]

viii) Preparation of **Ar3**

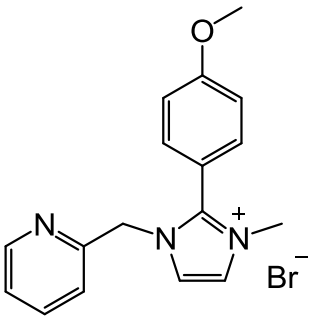

43 (0.020 g, 0.11 mmol) was dissolved in MeCN (20 mL). K_2CO_3 (0.0073 g, 0.053 mmol) and 2-(bromomethyl) pyridine.HBr (0.026 g, 0.11 mmol) were added and the reaction mixture was stirred at 75 ºC for 24 hours. The mixture was allowed to cool to room temperature and filtered. The filtrate volume was reduced to about 2 mL *in vacuo* and Et_2O (50 mL) was added to precipitate a brown solid. The crude solid was recrystallised in MeCN / Et_2O and DCM / Et_2O to give a brown solid. Yield: 0.0309 g, 0.086 mmol, 81 %.

^1H NMR (300 MHz, $CDCl_3$) δ (ppm) 8.45 (d, *J* = 4.3 Hz, 1H, pyH-6), 7.90 (s, 1H, imH), 7.73 (s, 1H, imH), 7.66 (t, *J* = 7.7 Hz, 1H, pH-4), 7.62 (d, *J* = 8.8 Hz, 2H, ArH), 7.45 (d, *J* = 7.7 Hz, 1H, pyH-3), 7.21 (dd, *J* = 7.7, 4.3 Hz, 1H, pyH-5), 7.03 (d, *J* = 8.8 Hz, 2H. ArH), 5.45 (s, 2H, N**CH_2**-py), 3.84 (s, 3H, CH_3), 3.83 (s, 3H,

CH_3). ^{13}C {^1H} NMR (75 MHz, $CDCl_3$) δ (ppm) 162.8 (C), 152.8 (C), 149.9 (CH), 137.4 (C), 132.4 (CH), 130.9 (C), 123.7 (CH), 123.6 (CH), 123.2 (CH), 122.8 (CH), 116.5 (CH), 115.3 (CH), 112.2 (CH), 55.7 (CH_3), 53.2 (CH_2), 36.6 (CH_3). HRMS (ESI^+): *m/z* 280.1451 $[M - Br]^+$, calculated $[M - Br]^+$ 280.1444.

3.6.4 Preparation of other aryl species

i) Preparation of 4-(3,5-dimethylphenoxy)anisole (**ArNu**)

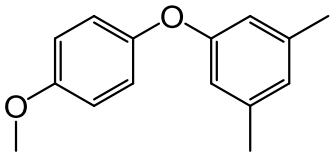

4-Iodoanisole (1.6 g, 6.8 mmol), 3,5-dimethylphenol (1.0 g, 8.1 mmol), CuI (0.26 g, 1.4 mmol), *iso*butyryl cyclohexanone (0.22 mL, 1.4 mmol) and Cs_2CO_3 (6.6 g, 20 mmol) were added to an ampoule. MeCN (5 mL) was added and the reaction mixture stirred at 90 °C for 24 hours under Ar. The crude mixture was diluted in DCM (50 mL), filtered through Celite and washed with EDTA solution (3 × 50 mL), water (3 × 50) and dried with $MgSO_4$. The crude product was purified by fractional column chromatography (silica gel), eluting with ethyl acetate / hexane (1:20). The product was obtained as an off-white solid. Yield: 0.12 g, 0.53 mmol, 25%.

^1H NMR (300 MHz, $CDCl_3$) δ (ppm) 7.00 – 6.94 (m, 2H, ArH), 6.91 – 6.85 (m, 2H, ArH), 6.69 (t, *J* = 0.5 Hz, 1H, ArH), 6.56 (d, *J* = 0.5 Hz, 2H, ArH), 3.81 (s, 3H, OCH_3), 2.27 (s, 6H, CH_3). ^{13}C {^1H} NMR (75 MHz, $CDCl_3$) δ (ppm) 158.6 (C), 155.9 (C), 150.4 (C), 139.6 (C), 124.3 (CH), 120.9 (CH), 115.4 (CH), 114.9 (CH), 55.8 (CH_3), 21.4 (CH_3). HRMS (ESI^+): *m/z* 229.1223 $[M + H]^+$, calculated $[M + H]^+$ 229.1223.

ii) Preparation of Bianisolyl (**ArAr**)

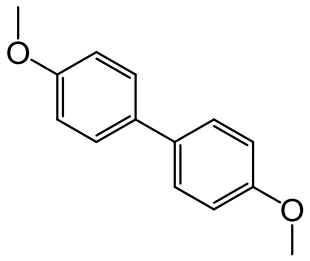

4-iodoanisole (0.30 g, 1.3 mmol) was added to an ampoule. THF (3 mL) was added and the solution cooled to - 78 °C under Ar. *n*-BuLi (1.4 mL, 1.2 M, 1.7 mmol) was added dropwise into the stirring solution and stirred at - 78°C for 30 minutes. In another ampoule, 4-iodoanisole (0.20 g, 0.85 mmol) and *bis*(tri-(*t*-butyl)-phosphine)Pd(0) (22 mg, 0.043 mmol) were added, followed by toluene (5 mL). The first solution was allowed to warm to room temperature then transferred to the Pd mixture dropwise *via* syringe. The reaction mixture was stirred at room temperature for 3 hours. A saturated solution of NH_4Cl (30 mL) was added and then extracted with Et_2O (3 × 50 mL). The crude product was purified by fractional column chromatography (silica gel), eluting with ethyl acetate / hexane (1:9). Yield: 0.03 g, 0.1 mmol, 16%.

^{1}H NMR (300 MHz, $CDCl_3$) δ (ppm) 7.44 – 7.37 (m, 4H, ArH), 6.92 – 6.86 (m, 4H, ArH), 3.77 (s, 6H, OCH_3). ^{13}C {^{1}H} NMR (75 MHz, $CDCl_3$) δ (ppm) 158.7 (C), 133.5 (CH), 127.7 (C), 114.2 (CH), 55.4 (CH_3).

Consistent with data previously reported.[43]

3.7 References

(1) Clement, N. D.; Cavell, K. J. *Angew. Chem., Int. Ed.* **2004**, *43*, 3845.
(2) Tan, K. L.; Park, S.; Ellman, J. A.; Bergman, R. G. *J. Org. Chem.* **2004**, *69*, 7329.
(3) Normand, A. T.; Hawkes, K. J.; Clement, N. D.; Cavell, K. J.; Yates, B. F. *Organometallics* **2007**, *26*, 5352.
(4) Nielsen, D. J.; Magill, A. M.; Yates, B. F.; Cavell, K. J.; Skelton, B. W.; White, A. H. *Chem. Comm.* **2002**, 2500.
(5) McGuinness, D. S.; Green, M. J.; Cavell, K. J.; Skelton, B. W.; White, A. H. *J. Organomet. Chem.* **1998**, *565*, 165.
(6) Cavell, K. J.; McGuinness, D. S. *Coord. Chem. Rev.* **2004**, *248*, 671.
(7) Magill, A. M.; McGuinness, D. S.; Cavell, K. J.; Britovsek, G. J. P.; Gibson, V. C.; White, A. J. P.; Williams, D. J.; White, A. H.; Skilton, B. W. *J. Organomet. Chem.* **2001**, *617-618*, 546.
(8) Nielsen, D. J.; Cavell, K. J.; Skelton, B. W.; White, A. H. *Inorg. Chim. Acta.* **2006**, *359*, 1855.
(9) Steinke, T.; Shaw, B. K.; Jong, H.; Patrick, B. O.; Fryzuk, M. D.; Green, J. C. *J. Am. Chem. Soc.* **2009**, *131*, 10461.
(10) Normand, A. T.; Stasch, A.; Ooi, L.-L.; Cavell, K. J. *Organometallics* **2008**, *27*, 6507.
(11) Ho, N. K. T.; Neumann, B.; Stammler, H.-G.; Silva, V. H. M. d.; Watanabe, D. G.; Braga, A. A. C.; Ghadwal, R. S. *Dalton Trans.* **2017**, *46*, 12027.
(12) Astakhov, A. V.; Khazipov, O. V.; Chernenko, A. Y.; Pasyukov, D. V.; Kashin, A. S.; Gordeev, E. G.; Khrustalev, V. N.; Chernyshev, V. M.; Ananikov, V. P. *Organometallics* **2017**, *36*, 1981.
(13) Williams, T. J.; Bray, J. T. W.; Lake, B. R. M.; Willans, C. E.; Rajabi, N. A.; Ariafard, A.; Manzini, C.; Bellina, F.; Whitwood, A. C.; Fairlamb, I. J. S. *Organometallics* **2015**, *34*, 3497.
(14) Ghadwal, R. S.; Reichmann, S. O.; Herbst-Irmer, R. *Chem. Eur. J.* **2015**, *21*, 4247.
(15) McGuinness, D. S.; Cavell, K. J.; Skelton, B. W.; White, A. H. *Organometallics* **1999**, *18*, 1596.
(16) Campeau, L.-C.; Thansandote, P.; Fagnou, K. *Org. Lett.* **2005**, *7*, 1857.
(17) McGuinness, D. S.; Cavell, K. J.; Yates, B. F.; Skelton, B. W.; White, A. H. *J. Am. Chem. Soc.* **2001**, *123*, 8317.
(18) Sambiago, C.; Marsden, S. P.; Blacker, A. J.; McGowan, P. C. *Chem. Soc. Rev.* **2014**, *43*, 3525.
(19) Lake, B. R. M.; Willans, C. E. *Organometallics* **2014**, *33*, 2027.
(20) Hemming, O.; University of Leeds: 2014.
(21) Younesi, Y.; Nasiri, B.; BabaAhmadi, R.; Willans, C. E.; Fairlamb, I. J. S.; Ariafard, A. *Chem. Comm.* **2016**, *52*, 5057.
(22) Lake, B. R. M.; Willans, C. E. *Chem. Eur. J.* **2013**, *19*, 16780.
(23) Bellina, F.; Cauterccio, S.; Fiore, A. D.; Marchetti, C.; Rossi, R. *Tetrahedron* **2008**, *64*, 6060.
(24) Bellina, F.; Cauteruccio, S.; Rossi, R. *Eur. J. Org. Chem.* **2006**, 1379.
(25) Bellina, F.; Calandri, C.; Cauteruccio, S.; Rossi, R. *Tetrahedron* **2007**, *63*, 1970.
(26) Bellina, F.; Rossi, R. *Adv. Synth. Catal.* **2010**, *352*, 1223.
(27) Pivsa-Art, S.; Satoh, T.; Kawamura, Y.; Miura, M.; Nomura, M. *Bull. Chem. Soc. Jpn.* **1998**, *71*, 467.
(28) Yagyu, T.; Hamada, M.; Osakada, K.; Takakazu, Y. *Organometallics* **2001**, *20*, 1087.
(29) Liu, Q.; Lan, Y.; Liu, J.; Li, G.; Wu, Y.-D.; Lei, A. *J. Am. Chem. Soc.* **2009**, *131*, 10201.

(30) Liu, Q.; Duan, H.; Luo, X.; Tang, Y.; Li, G.; Huang, R.; Lei, A. *Adv. Synth. Catal.* **2008**, *350*, 1349.
(31) Ozawa, F.; Fujimori, M.; Yamamoto, T.; Yamamoto, A. *Organometallics* **1986**, *5*, 2144.
(32) Orbach, M.; Choudhury, J.; Lahav, M.; Zenkina, O. V.; Diskin-Posner, Y.; Leitus, G.; Iron, M. A.; Boom, M. E. v. d. *Organometallics* **2012**, *31*, 1271.
(33) Strieter, E. R.; Blackmond, D. G.; Buchwald, S. L. *J. Am. Chem. Soc.* **2005**, *127*, 4120.
(34) Sherbourne, G. J.; Adomeit, S.; Menzel, R.; Rabeah, J.; Bruckner, A.; Fielding, M. R.; Willans, C. E.; Nguyen, B. N. *Chem. Sci.* **2017**, *8*, 7203.
(35) Handy, S. T.; Bregmann, H.; Lewis, J.; Zhang, X.; Zhang, Y. *Tetrahedron Lett.* **2003**, *44*, 427.
(36) Jedinak, L.; Zatopkova, R.; Zemankova, H.; Sustkova, A.; Cankar, P. *J. Org. Chem.* **2017**, *82*, 157.
(37) Kuwabara, J.; Fujie, Y.; Maruyama, K.; Yasuda, T.; Kanbara, T. *Macromolecules* **2016**, *49*, 9388.
(38) McPhillie, M. J.; Trowbridge, R.; Mariner, K. R.; ONeill, A. J.; Johnson, A. P.; Chopra, I.; Fishwick, C. W. G. *ACS Med. Chem. Lett.* **2011**, *2*, 729.
(39) Chiu, P. L.; Lai, C.-L.; Chang, C.-F.; Hu, C.-H.; Lee, H. M. *Organometallics* **2005**, *24*, 6169.
(40) Su, W.; Younus, H. A.; Zhou, K.; Khattak, Z. A. K.; Chaemcheun, S.; Chen, C.; Verpoort, F. *Catal. Sci. Technol.* **2017**, *7*, 387.
(41) Lau, G. P. S.; Schreier, M.; Vasilyev, D.; Scopelliti, R.; Gratzel, M.; Dyson, P. J. *J. Am. Chem. Soc.* **2016**, *138*, 7820.
(42) Miller, R. D.; Lee, V. Y.; Moylan, C. R. *Chem. Mater.* **1994**, *6*, 1023.
(43) Giannerini, M.; Fananas-Mastral, M.; Feringa, B. L. *Nature Chem.* **2013**, *5*, 667.

Chapter 4

Selective Arylation of Xanthine-Derived Imidazolium Salts

4.1 Introduction

Following the deactivation of Cu-NHC catalysts *via* the reductive elimination of a C-2 arylated imidazolium ion (Chapter 3), we were keen to examine if the reaction could be exploited to develop the selective arylation of natural compounds such as xanthine, guanine and adenine (Figure 4-1). These compounds have an imidazole ring incorporated into their structures and may potentially be functionalised *via* a Cu-NHC complex. The Cu-mediated reaction would replace multiple-step organic synthetic methods, which involve formation of imidazoles *via* condensation reactions instead of functionalisation of an imidazole ring (Scheme 4-1).[1-4] Furthermore, the modified arylated products will be fluorescent,[5] allowing a method to detect xanthine-derived compounds in biology (*e.g*. DNA bases) if the synthetic methods could be extended to these systems.

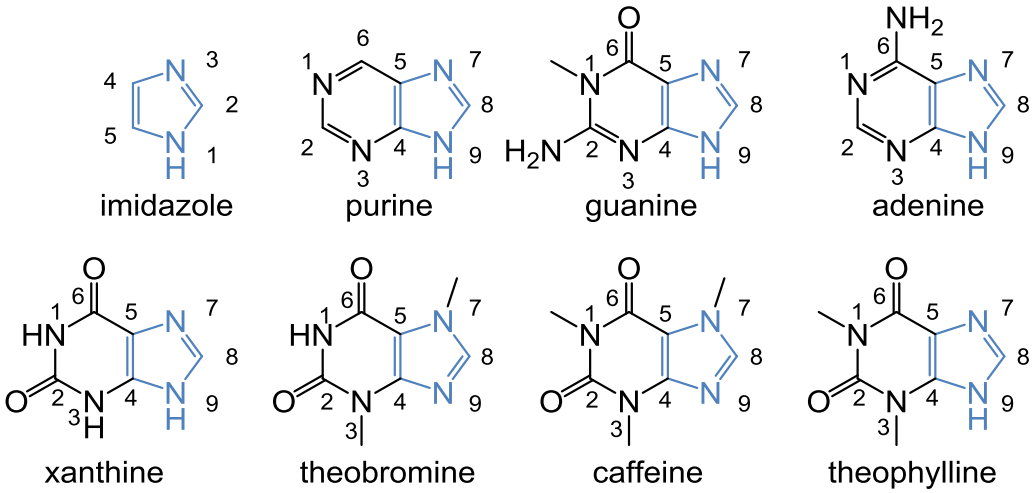

Figure 4-1: Structure of imidazole and purine-based compounds.

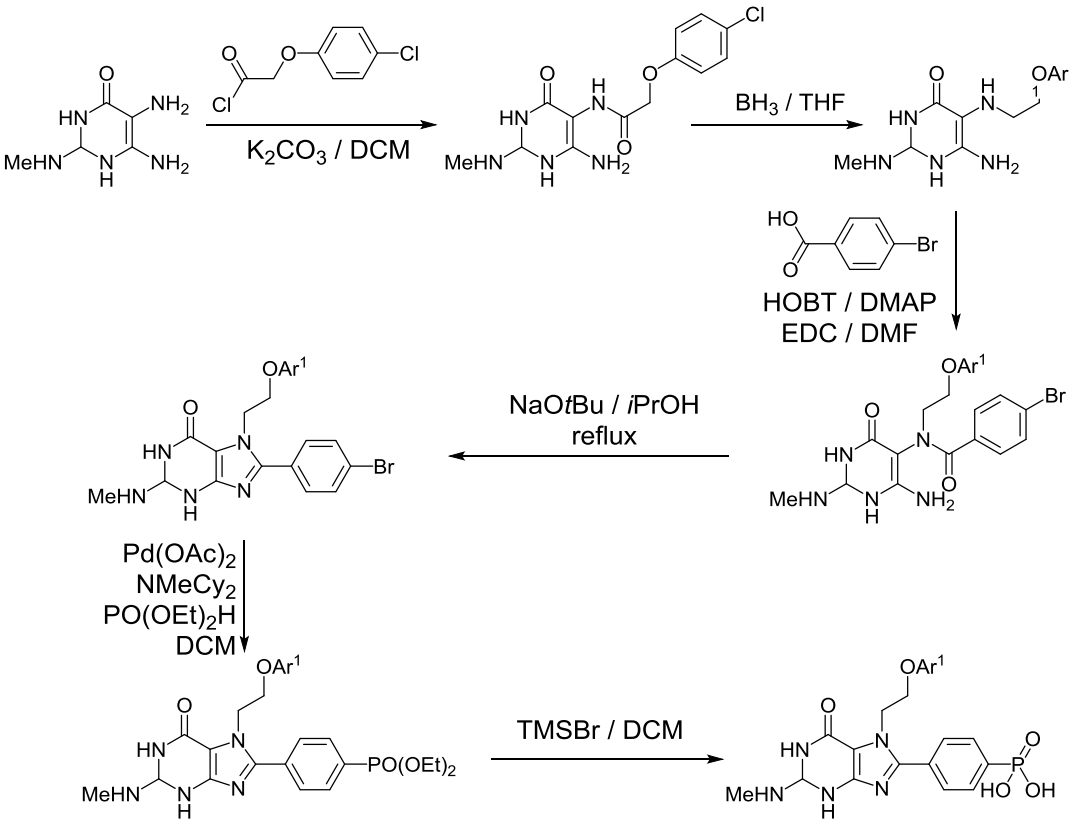

Scheme 4-1: Preparation of C-8 functionalised xanthine derivative *via* condensation reactions to form an imidazole ring.[3]

Understanding the methodology for selective functionalisation of such heterocycles under mild conditions may enable selective modification of natural compounds such as DNA strands, which comprise adenine and guanine groups (*i.e*. xanthine derivatives). The ability to selectively arylate adenine and guanine could be very powerful and may lead to the ability to alternatively distinguish between pyrimidine- and purine-derived bases in nucleic acid strands by fluorescence (Figure 4-2).[6]

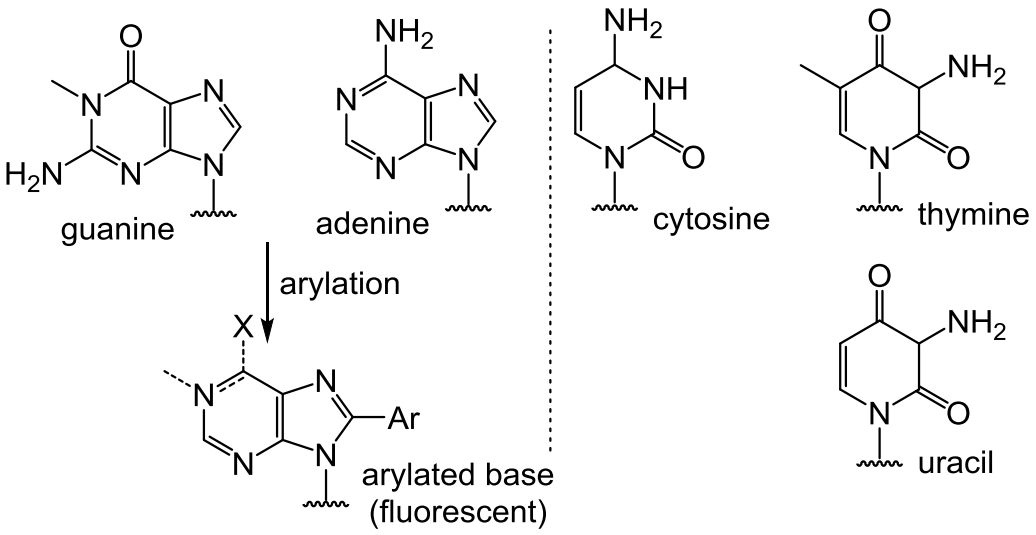

Figure 4-2: Purine and pyrimidine nucleobases.

Many approaches to the selective arylation of imidazole and its derivatives have been developed and studied. In 1998, Nomura showed that 1-methylimidazole can be selectively functionalised at either the C-2 or the C-5 position using different metal catalysts.[7] In the presence of a catalytic amount of Pd, the coupling reaction between phenyl iodide and 1-methylimidazole led to the formation of **I** and **II** (Scheme 4-2A). However, there was no formation of **I** when an excess amount of Cu and catalytic amount of Pd were used in the reaction. Instead, **III** was formed along with **II** (Scheme 4-2B). Furthermore, with an excess amount of Cu but in the absence of Pd, the coupling reaction led to the formation of **III** only (Scheme 4-2C). Similarly, 2-aryl imidazole can be prepared when an excess amount of CuI is used with Pd or Co as a co-catalyst. Application of Cu and a Pd co-catalyst was essential for the formation of the reductively eliminated aryl-imidazolium side-product in the etherification reaction (Chapter 3).

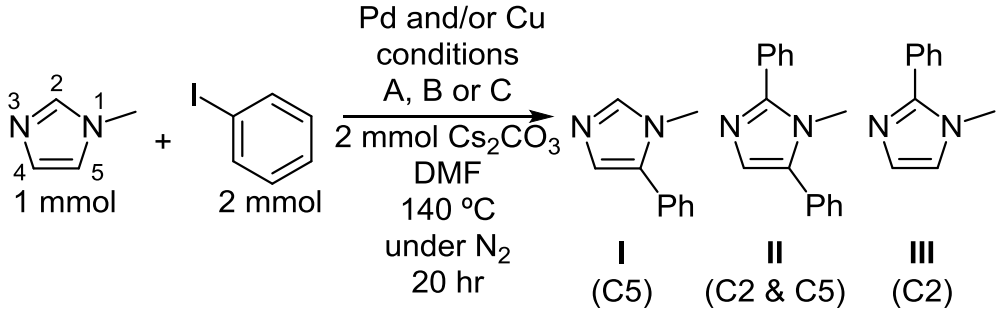

conditions	$Pd(OAc)_2$	CuI	PPh_3	yield **I**	yield **II**	yield **III**
A	0.1 mmol	-	0.2 mmol	54	24	-
B	0.1 mmol	2 mmol	0.2 mmol	-	40	37
C	-	2 mmol	0.6 mmol	-	-	37

Scheme 4-2 Arylation of 1-methylimidazole in the presence of different amounts of metals.[7]

The regioselectivity of the Pd-catalysed reaction shows the same preference as observed in electrophilic substitution.[8] Therefore, it is possible that the Pd(II) intermediate, resulting from oxidative addition of aryl iodide to Pd(0), may act as an electrophile towards imidazole species (Scheme 4-3).[9]

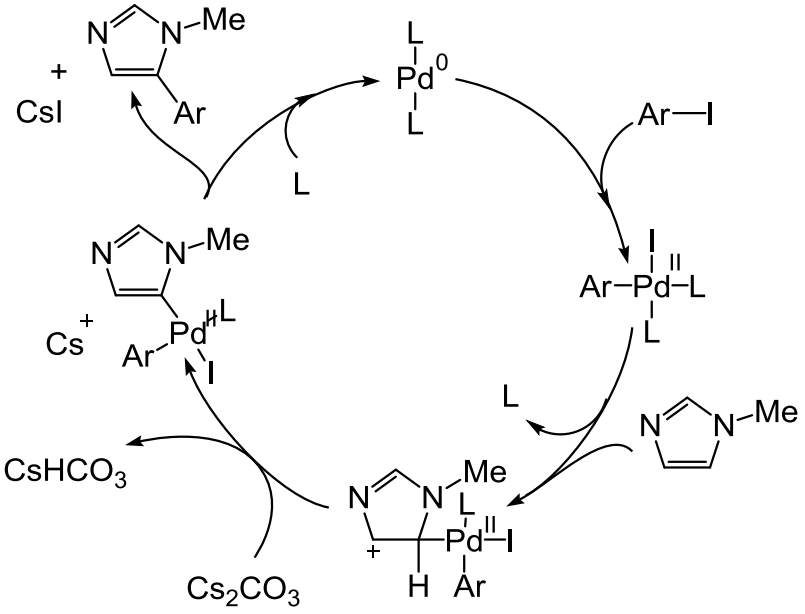

Scheme 4-3 Modified proposed mechanism for the Pd-catalysed arylation of 1-methylimidazole.[7]

However, when Cu is present, the arylation occurs at the C-2 position instead.[7,10,11] It was thought that the reaction involved deprotonation at the C-2 position, which is the most acidic proton.[8] The necessity of Cu was later explained by the reaction possibly occurring *via* the formation of a Cu(I)-NHC

complex.[12] Cu(I)-NHC complexes have been observed to react with aryl iodide to give aryl-imidazolium salts (Scheme 4-4). The oxidative addition of imidazole to Cu(I) and proton migration, leading to formation of a Cu(I)-NHC intermediate, is possibly a key factor in the C-2 selectivity of imidazole arylation (Scheme 4-5).

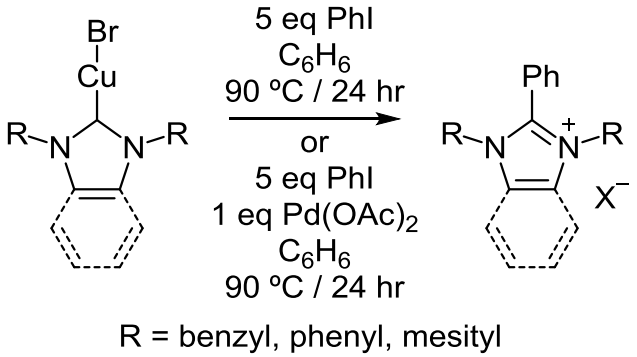

Scheme 4-4 Arylation of Cu-NHC complexes.[12]

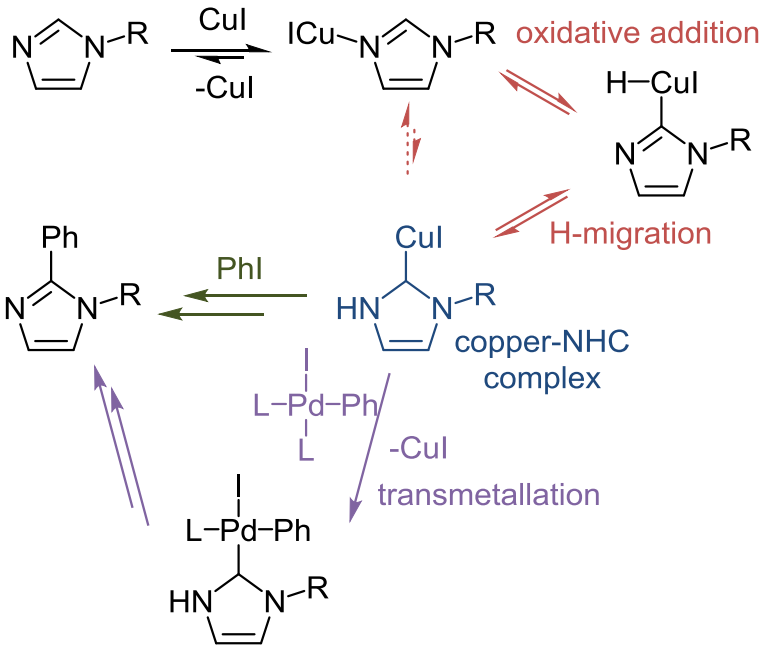

Scheme 4-5 Suggested mechanism of Cu-mediated arylation of imidazole in the absence and presence of Pd.[12]

This chapter focuses on the arylation of xanthine-derived imidazolium salts. The key factors for the reaction are examined and discussed, such as activation of the C-H bond of the imidazolium salts, necessity of Cu and optimisation of reaction conditions. Kinetics of the arylation of Cu-NHCs were studied and compared to theoretical computational data.

4.2 Preparation of xanthine-derived copper-*N*-heterocyclic carbene) complexes

Previously, our group have utilised natural xanthines to prepare imidazolium salts, Ag-NHC and Cu-NHC complexes. The Ag-NHC complexes were screened for anticancer properties,[13] and the Cu-NHC complexes were examined as anticancer agents and as catalysts in the etherification reaction (discussed in Chapter 2). The Cu complexes were observed to be stable in air, which is highly unusual for Cu(I)-NHCs with non-bulky *N*-substituents (methyl groups in this case). These complexes gave negligible catalytic activity (3 % conversion, Scheme 4-6), similar to CuI in the absence of a ligand (5 %).[13]

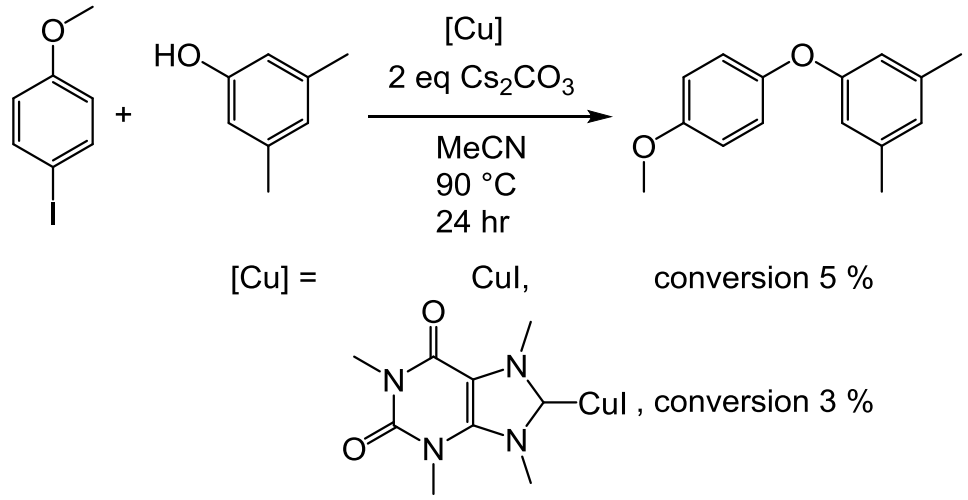

Scheme 4-6: Etherification reaction attempted using xanthine-derived NHCs.

Within this study, it became evident that a major by-product of the reactions was C-2 arylated imidazolium compounds, hence the C-2 arylation was investigated further using ligands with different N-substituents. Fairlamb and coworkers proposed that the C-2 selective arylation of imidazole where excess amount of CuI is required for the C-H activation (Scheme 4-5).[12] The reaction is thought to proceed *via* a Cu-NHC complex with the proton *N*-substituent as a resting state prior to oxidative addition of aryl iodide and reductive elimination of C-2 aryl imidazole. A methyl group is the smallest carbon substituent and most comparable to the proton *N*-substituent, hence was used in this study.

Theophylline (**44**) was reacted with one equivalent of 1-bromobutane under basic conditions to afford **P45** in 69% yield (Scheme 4-7). Methylation of **P45** and caffeine (**P46**) to form imidazolium salts H**L45**I and H**L46**I were carried out using methyl iodide.

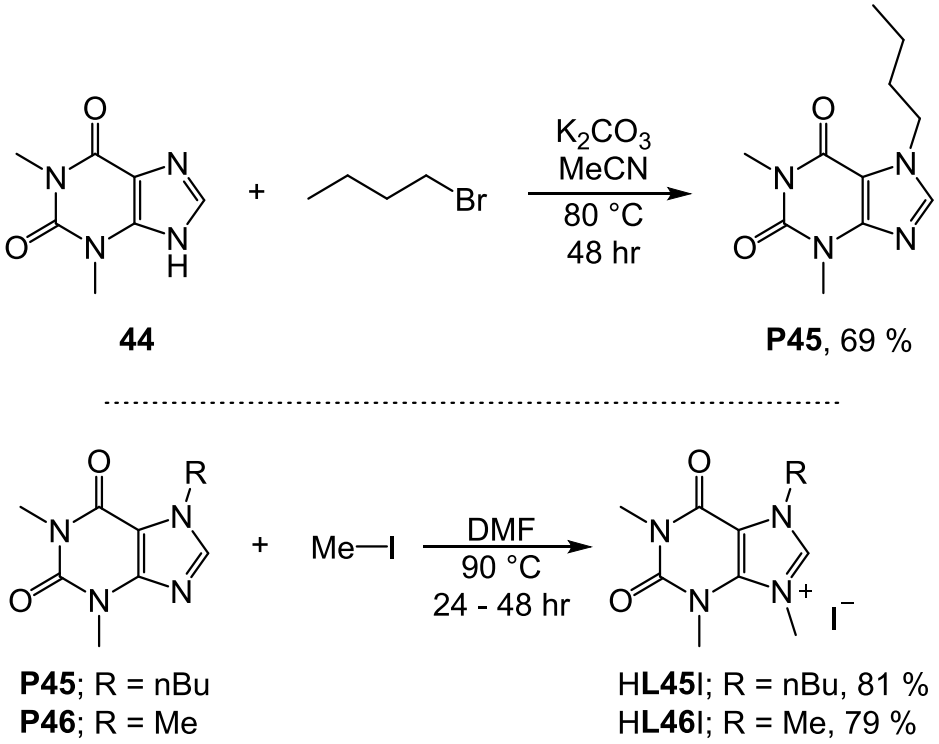

Scheme 4-7: Preparation of **P45**, H**L45**I and H**L46**I.

As discussed in Chapter 1, imidazolium salts are used as NHC ligand precursors through deprotonation at the C-2 position, or C-H bond activation by either oxidative addition to a metal centre or reduction by electrolysis. An electrochemical method developed in our laboratory[14,15] was used to prepare Cu-NHCs **C45** and **C46** using Cu electrodes in MeCN (Scheme 4-8). MeCN is generally used as the solvent for the electrochemical method as it can stabilise free Cu(I) ions which are generated at the anode prior to NHC coordination. Reduction of the imidazolium to form a free NHC is a result of the other half-reaction occurring at the cathode. A potential was applied to maintain a constant current of 30 mA throughout the reaction. The theoretical time was calculated from the equation ($t = \frac{n \times mol \times F}{I}$), where n = 1, as 0.47 hours for the preparation of **C45** (0.53 mmol) and 2.26 hours for the preparation of **C46** (2.54 mmol). However, as it has previously been found in the group that the reactions do not operate at 100% faradaic efficiency, the actual times were doubled. **C45** was isolated in 77 % yield (36 % faradaic efficiency) and **C46** was isolated in 69 % yield (31 % faradaic efficiency).

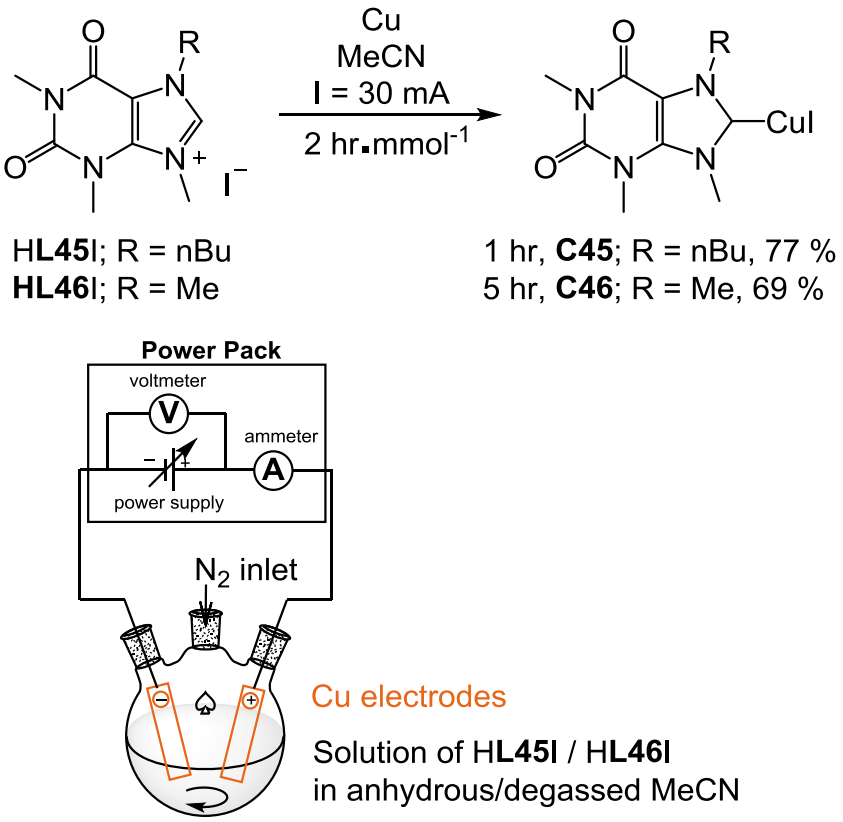

Scheme 4-8: Preparation of **C45** and **C46** *via* an electrochemical method.

Formation of both **C45** and **C46** was confirmed using ^{1}H NMR spectroscopy (300 MHz, d_6-DMSO) by the absence of the imidazolium NC*H*N resonance (δ 8.7 – 9.0 ppm). However, the high resolution mass spectra did not show any Cu-related species and only the corresponding imidazolium ions were observed, hence MS appears to be unsuitable for monitoring these complexes. **C45** is more soluble in MeCN than **C46**, with both being more soluble in MeCN at higher temperature (75 °C). In addition, both complexes are completely soluble in dipolar aprotic solvents (DMF and DMSO) and poorly soluble in non-polar solvents (toluene, hexane).

4.3 Arylation of xanthine-derived copper-*N*-heterocyclic carbene) complexes

C45 and **C46** were reacted with 4-iodoanisole to examine the formation of aryl-imidazoliums. Heating **C45** and **C46** with excess 4-iodoanisole (5 equivalents) in DMF at 140 °C under N_2 afforded novel aryl-imidazolium **Ar45** and **Ar46** respectively (Scheme 4-9). EtOAc was added to the reaction mixture, which precipitated the product. **Ar46** was found to be pure by ^{1}H (Figure 4-3) and

^{13}C {^{1}H} NMR spectroscopy, HRMS, elemental analysis and IR spectroscopy. **Ar45** was characterised by ^{1}H NMR spectroscopy and HRMS.

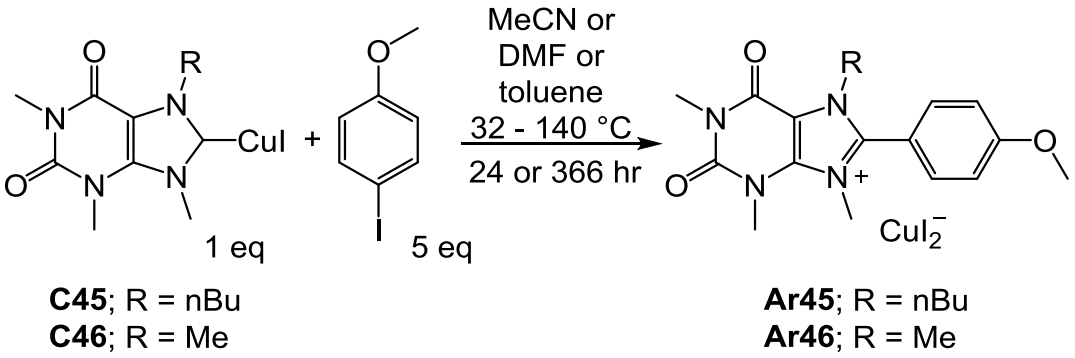

C45; R = nBu
C46; R = Me

Ar45; R = nBu
Ar46; R = Me

Scheme 4-9: Arylation of **C45** and **C46.**

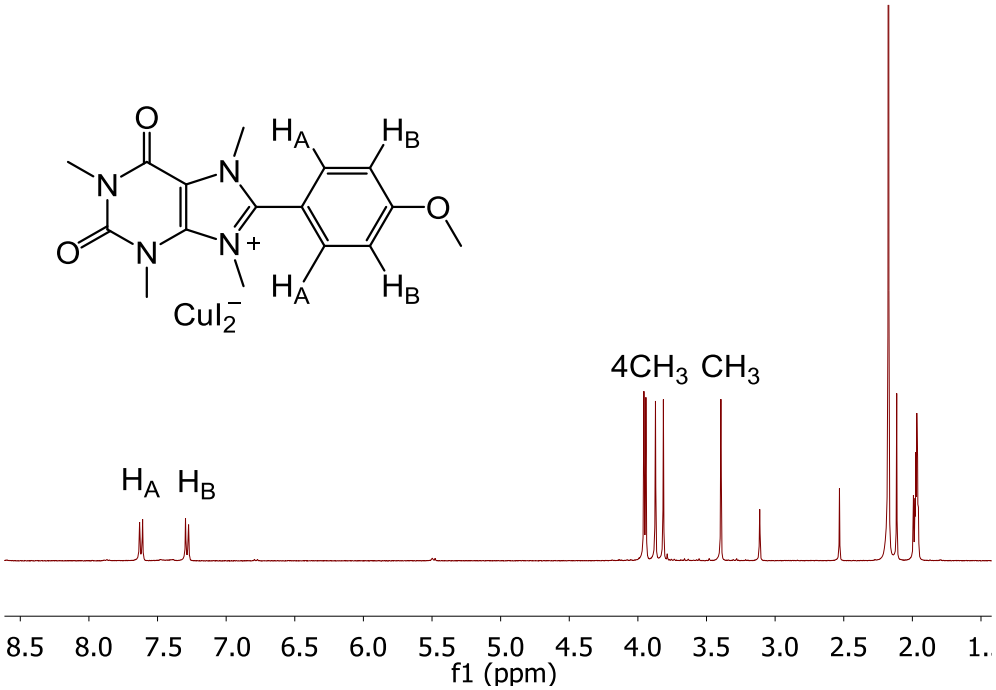

Figure 4-3: ^{1}H NMR (300 MHz, CD_3CN) of **Ar46**.

The complete conversion of **C46** to **Ar46** was successful at 140 °C, though our ultimate goal is to arylate natural compounds such as nucleobases, with these reaction conditions being too harsh and would result in deformation of DNA strands. Therefore, lower reaction temperatures (90 – 32 °C) were investigated. It should be noted that in some cases, **C46** and **Ar46** were isolated as a mixture as they are not possible to separate (by addition of EtOAc to DMF or recrystallisation in MeCN / Et_2O). Hence, % net yield was calculated based on the % of product in the recrystallised mixture (according to ^{1}H NMR analysis, Figure 4-4) and the total mass of the recrystallised mixture. At 90 °C, >99 % purity and 55 % net yield of **Ar46** was observed in DMF, whereas only 50 %

purity and 23 % net yield was observed in MeCN, with no reaction taking place in toluene (Table 4-1). The yield appears to correlate with the solubility of **C46**, which fully dissolved in DMF, partly dissolved in MeCN and did not dissolve in toluene.

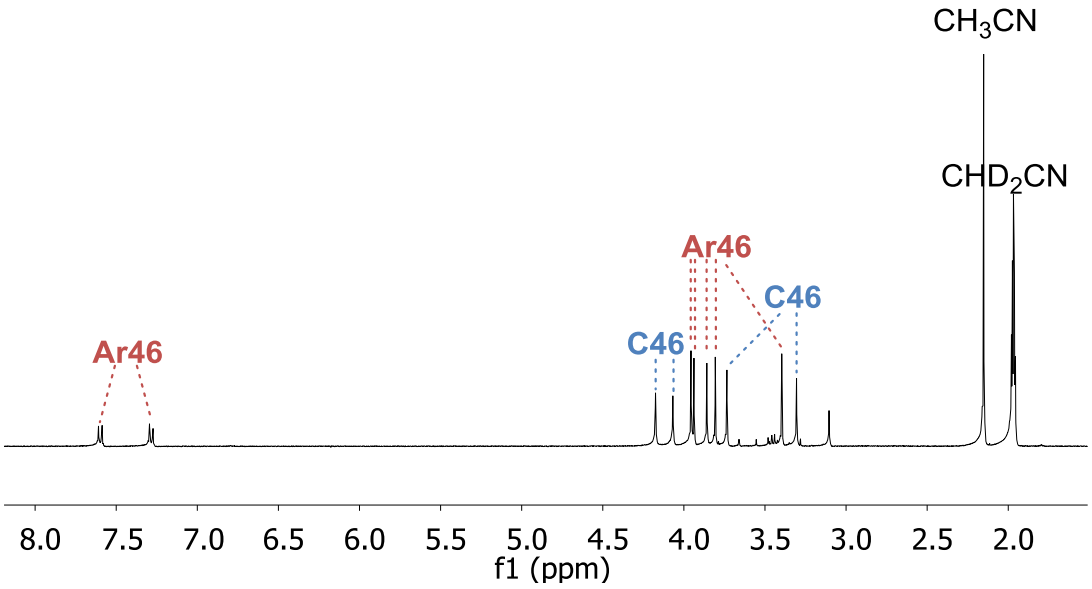

Figure 4-4: ^{1}H NMR spectrum (300 MHz, CD_3CN) of a mixture of **Ar46** and **C46** from the reaction of **C46** and 4-iodoanisole in MeCN at 90 °C (entry3)

entry	Cu-NHC	solvent	T / °C	time / hr	**Ar45** or **Ar46** (% purity)*	**Ar45** or **Ar46** (% net yield)**
1	**C46**	DMF	140	24	>99	80
2	**C46**	DMF	90	24	>99	55
3	**C46**	MeCN	90	24	50	23
4	**C46**	toluene	90	24	0	0
5	**C46**	DMF	32	24	10	6
6	**C46**	DMF	35	366	75	14
7	**C45**	DMF	140	24	>99	60

Table 4-1: Results of the arylation of **C45** and **C46** to afford **Ar45** and **Ar46** under different reaction conditions. *calculated from average integration in ^{1}H NMR resonances: **Ar46** δ 7.62, 7.28, 3.96, 3.94, 3.87, 3.81, 3.40 ppm, **C46** δ 4.17, 4.07, 3.73, 3.31. **based on mass and % purity of the recrystallised product

The reaction was also observed to occur at low temperature (32 °C, 6 % net yield after 24 h), hence was followed for a longer period of time. It was found that after heating at 35 °C for 2 weeks, the % purity of the recrystallised product increases to 75 % but the yield was very low (14 %). The low isolated yield is likely due to decomposition of **C46** during the reaction over a prolonged period, which would result in relatively high **Ar46** ratio in the isolated mixture (75 %) but low % mass recovery.

In addition to **C46** and **Ar46**, another product with *m/z* = 252.1460 was observed in the HR mass spectra of entries 1, 2, 5 and 6, where the reaction was performed in DMF. The mass of the side-product corroborates with dimethylamino-imidazolium **47** (Scheme 4-10), which is a result of the DMF becoming involved in the reaction (calculated *m/z* = 252.1455). However, this side-product was not observed in any ^{1}H NMR spectra, indicating that **47** was formed in very low amounts which could not be detected by ^{1}H NMR spectroscopy. Therefore, the formation of the amino side-product was not considered a factor that contributed to the low isolated yield.

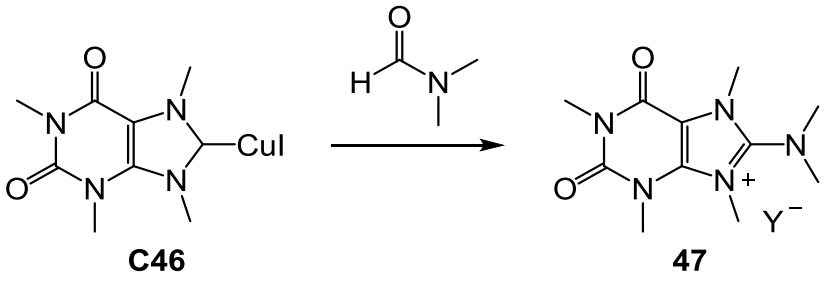

C46 **47**

Scheme 4-10: Amination of **C46** in DMF.

Reaction of **C46** with DMF was further examined in the absence of aryl iodide. **C46** (0.075 mmol) was heated in anhydrous, degassed DMF (3 mL) for 196 hours (Scheme 4-11), resulting in a mixture of H**L46**Y, **C46** and **47**, with a ratio of 2:2:1, determined by ^{1}H NMR spectroscopy. In addition to acting as a source of dimethylamino group, the DMF may also act as a proton source to form H**L46**Y.

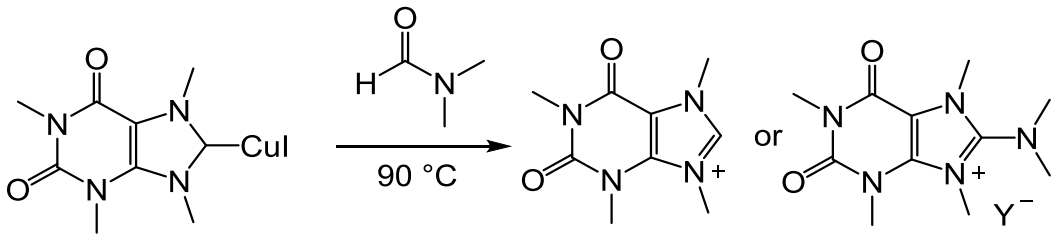

C46 H**L46**Y, 40 % **47**, 20%

Scheme 4-11: Reaction of **C46** with DMF in the absence of ArI.

The formation of amino-imidazolium occurs at 100 °C and even as low as 35 °C in the arylation reaction mixture, while the DMF thermal decomposition to carbon monoxide and dimethylamine normally occurs at high temperature (350 °C).[16] Hence, the DMF possibly oxidatively adds to the Cu centre of **C46** either through $C_{carbonyl}$-N or $C_{carbonyl}$-H bonds (Scheme 4-12). H-migration or amino migration would then form $[Cu(NHC)(CO)(NMe_2)H]^+$ with reductive elimination resulting in **47** or H**L46**. $C_{carbonyl}$-N bond activation using a Ni catalyst has recently been observed.[17,18] Amide, despite being considered an inert substrate due to resonance stabilisation,[19] can be used as an acyl building block upon C-N bond cleavage. In addition, DMF has been used as a cheap CO source in Pd-catalysed reactions.[20,21] The reactions can be carried out under relatively mild conditions, hence DMF $C_{carbonyl}$-N bond oxidative addition is more likely to take place than the $C_{carbonyl}$-H bond.

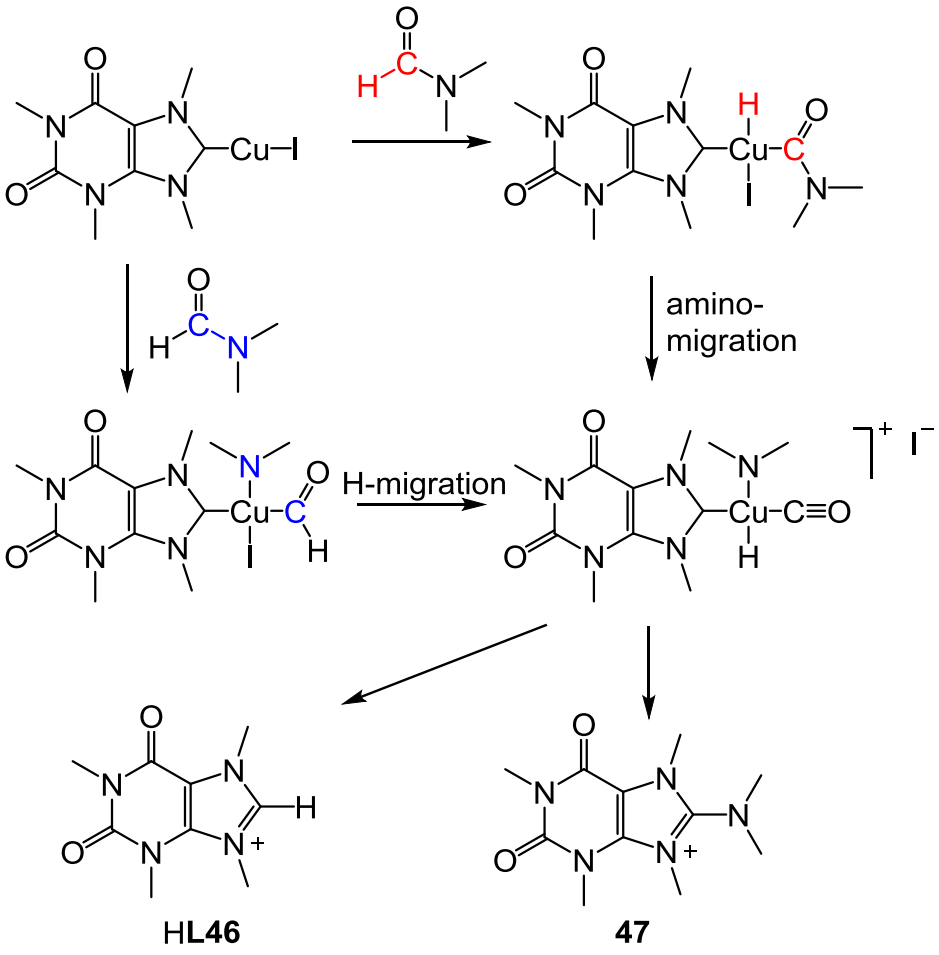

Scheme 4-12: Proposed mechanism of DMF amination of **C46**.

Further studies into the arylation of **C46** were carried out using PhCN as a solvent, which has a high boiling point (191 °C) but is easily removed *in vacuo*. **C46** was heated at 120 °C with 4-iodoanisole in PhCN for 12 hours, at which

time the [H**L46**]$^{+}$ fragment of **C46** was no longer observed in the HR mass spectrum. The solvent and 4-iodoansiole were removed *in vacuo* for 2 hours to afford a crude product. The ^{1}H NMR spectrum (300 MHz, d_6-DMSO) of the collected product showed a mixture of **Ar46** and a second product. The crude mixture was purified by recrystallisation from MeCN/Et_2O, with the precipitate being identified as pure **Ar46** (63 % yield). The solvent of the filtrate was removed *in vacuo* and the solid was characterised by ^{1}H and ^{13}C {^{1}H} NMR spectroscopy and HR mass spectrometry. The solid was found to be the novel demethylated imidazole compound **48** (37 % yield) (Scheme 4-13).

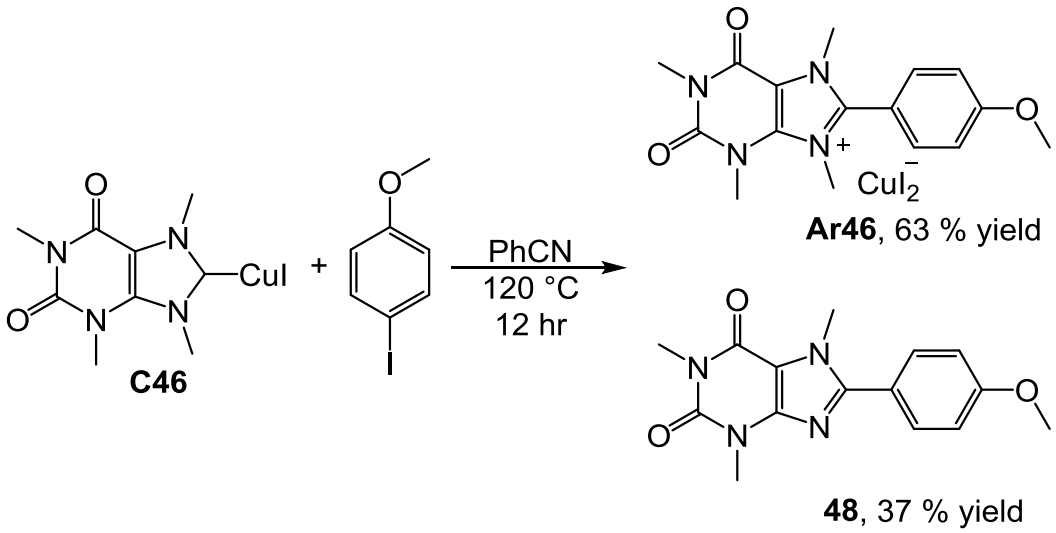

Scheme 4-13: Arylation of **C46** in PhCN at 120 °C.

The *N*-demethylation reaction was further investigated on an NMR scale (0.05 mmol). **Ar46** was heated in CD_3CN at 110 °C, which showed 9 % conversion to **48** after 20 hours. Following further heating at 110 °C, the reaction reached 20 % conversion after 38 hours and 60 % conversion after 97 hours. Furthermore, in the presence of 1 and 2 equivalents of 4-iodoanisole, **Ar46** was heated at 110 °C giving the same result as in the absence of 4-iodoanisole, suggesting that 4-iodoanisole has no effect on the demethylation reaction. To examine if the presence of Cu affects the reaction, H**L46**I was heated at 110 °C in the presence and absence of CuI. In each case, demethylation was observed. Another factor to consider is the iodide counter ion, which was examined by heating H**L46**PF_6 under the same conditions. The demethylation was not observed in this case, therefore it is proposed that the iodide ion is essential as a nucleophile on the methyl *N*-substituent and iodomethane is formed as the side-product although MeI was not observed in ^{1}H NMR spectra.

Although the demethylation is a side-reaction in these investigations (which is subsequently removed through recrystallisation), it leads to imidazole species, which is our ultimate goal. However, the demethylation requires high temperatures (110 °C). As the temperature is unsuitable for DNA and other natural compounds, further development is still needed to achieve the ultimate goal of DNA functionalisation.

4.4 Utilising trimethylsilyl protecting group to afford aryl-imidazole

The selective C-2 arylation of *N*-substituted imidazole has been shown to require high temperatures *via* either Bellina's method (140 °C) or Cu-mediated arylation (90 °C) and demethylation (110 °C). An alternative route was proposed using trimethylsilyl (TMS) as a protecting group (Scheme 4-14) instead of the methyl *N*-substituent with the aim of removal under ambient conditions, which would be more suitable for DNA and other natural compounds. The TMS group can be cleaved using a fluoride salt at room temperature or under reflux in alcohol.[22-25]

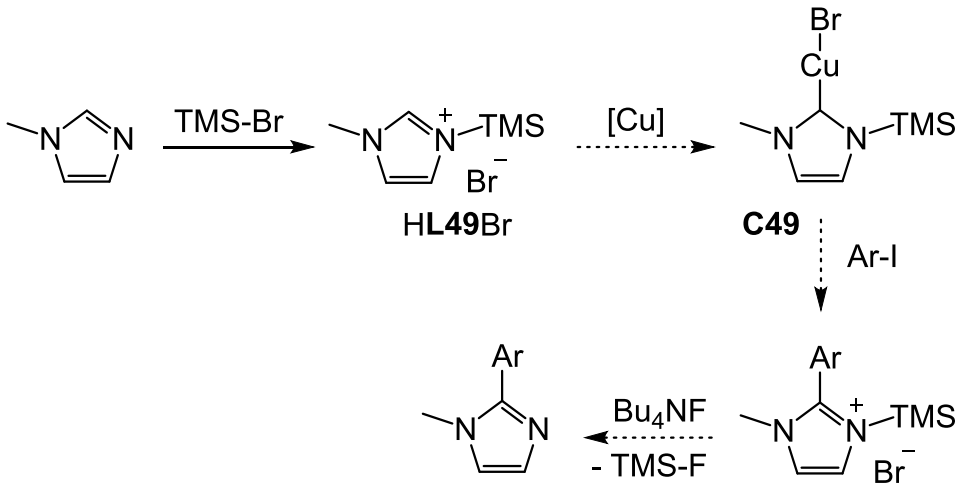

Scheme 4-14: A proposed alternative C-2 arylation of imidazole using a trimethylsilyl protecting group.

H**L49**Br was prepared by dropwise addition of freshly distilled 1-methylimidazole to an anhydrous solution of bromotrimethylsilane in Et_2O under an inert atmosphere (Scheme 4-15). A colourless solid formed immediately which was collected by filtration and characterised using ^{1}H and $^{13}C\{^{1}H\}$ NMR spectroscopy (Figure 4-5). The TMS peak appears upfield (^{1}H δ 0.58 and ^{13}C δ -0.9 ppm) due to the low electronegativity of Si.

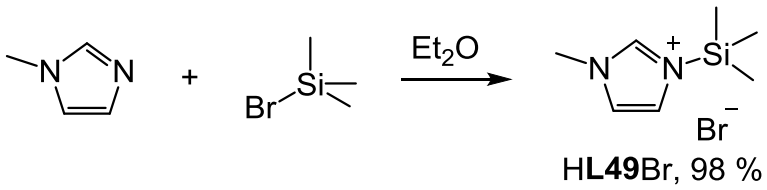

Scheme 4-15: Preparation of H**L49**Br.

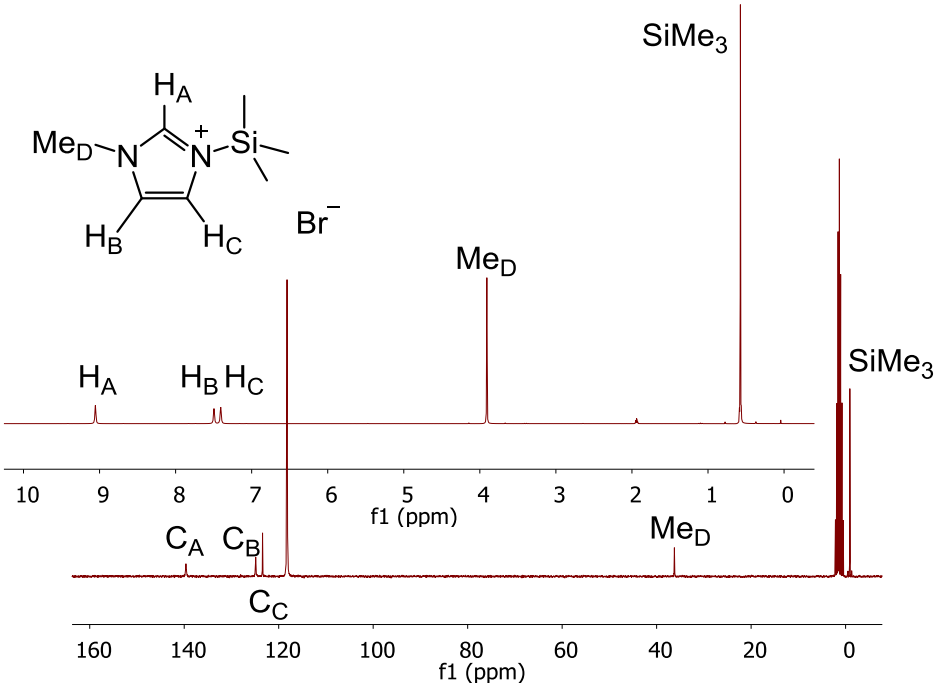

Figure 4-5: ^{1}H and ^{13}C {^{1}H} NMR (300 MHz and 75 MHz, CD_3CN) spectra of H**L49**Br

Preparation of **C49** was attempted using the electrochemical method to reduce the imidazolium ion, however, this resulted in cleavage of the TMS group. The product was characterised by ^{1}H NMR spectroscopy (Figure 4-6) and HRMS. The TMS peak was absent in the ^{1}H NMR spectrum and the mass ratios (*m/z* = 227.0348 (^{63}Cu) and 229.0329 (^{65}Cu)) were observed to be [**C50** – Br]$^{+}$. Another attempt at complex synthesis was carried out using Ag_2O and CuI to form an *in situ* Ag-NHC complex and transmetallation to Cu. The ^{1}H NMR spectrum shows 1-methylimidazole, whereas the TMS peak was absent. The [**C50** – Br]+ was observed in the HR mass spectrum. In the electrochemical method, the TMS group is possibly reduced to a trimethylsilyl radical which dimerises to give hexamethyldisilane, whereas the basicity of Ag_2O may react with the TMS group to give trimethylsilanol or hexamethyldisiloxane. However, these TMS derivatives were not observed in any ^{1}H NMR spectra, likely due to their volatility

(b.p. hexamethyldisilane = 113 °C, trimethylsilanol = 99 °C and hexamethyldisiloxane = 101 °C) and being removed *in vacuo* during work-up.

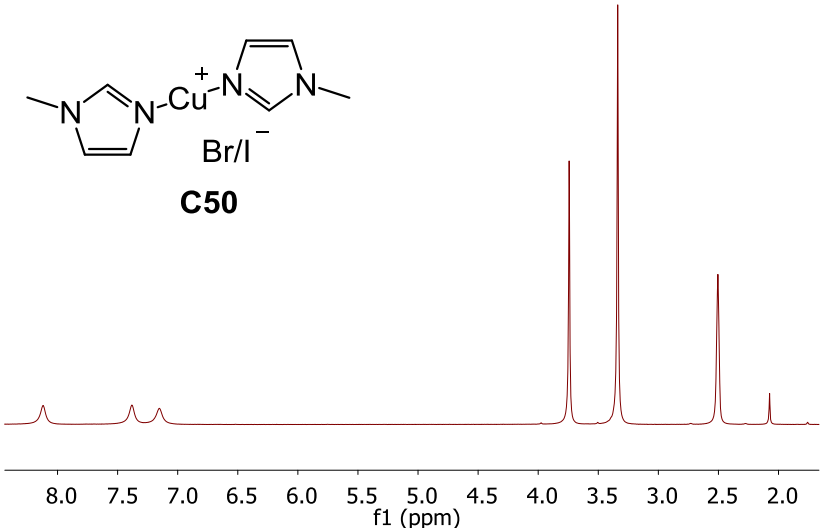

Figure 4-6: ^{1}H NMR spectrum (300 MHz, d_6-DMSO) of the product following electrolysis of H**L49**Br in the presence of Cu.

4.5 Kinetic study on the arylation of copper-*N*-heterocyclic carbene using NMR spectroscopy

To further understand the arylation of a xanthine-based NHC coordinated to Cu, kinetic studies were carried out. Monitoring the reaction at varying reactant stoichiometries, solvents and temperatures allows us to gain more knowledge on how the Cu-NHC and aryl iodide are involved in the arylation reaction. Activation energy of the reaction can be calculated from the reactions at varying temperatures using an Arrhenius plot, and compared to computational studies on potential reaction mechanisms. Moreover, we hope to understand which factors are contributed to the activation energy and how this might be decreased so that the arylation can take place at ambient temperature.

The arylation of **C46** was carried out in an NMR tube and monitored using ^{1}H NMR spectroscopy with *m*-xylene as an internal standard. The reaction was performed at 120 °C initially in CD_3CN, but the low solubility of **C46** in this solvent rendered quantification inaccurate. Therefore reactions were conducted in d_7-DMF, with heating in the NMR spectrometer to avoid delay in transferring the reaction vessels from the oil bath (Scheme 4-16). Although the temperature is limited to 70 °C using this technique (to prevent degradation of a NMR tube

holder), the data can be taken more accurately and frequently allowing more data points for the reaction profile. A solution of 0.006 M **C46**, 0.10 M 4-iodoanisole and 0.08 M *m*-xylene in 0.4 mL d_7-DMF was prepared and heated in the NMR spectrometer at 70 °C for 16 hours, and the data collected at intervals of 15 minutes. The concentration of each species was worked out by the average of several integrals: *m*-xylene δ 7.13, 6.99 ppm; **C46** δ 4.30, 4.12, 3.31 ppm; 4-iodoanisole δ 7.62, 6.82 ppm; Ar46 δ 7.82, 7.37, 4.13, 4.08, 3.40 ppm. From the concentration profile, it is difficult to determine the rate order of the reaction (Figure 4-7). The rate order with respect to **C46** can be determined by comparing [**C46**], ln[**C46**] and 1/[**C46**] (Figure 4-7, Figure 4-8 & Figure 4-9). The most linear plot is ln[**C46**] (R^2 = 0.96), which gives a pseudo 1st order rate constant (k'; rate = k'[**C46**]) of 1.17 × 10^{-5} s^{-1} and 2nd order rate constant (k; rate = k[**C46**][ArI]) of 1.17 × 10^{-4} $M^{-1}s^{-1}$.

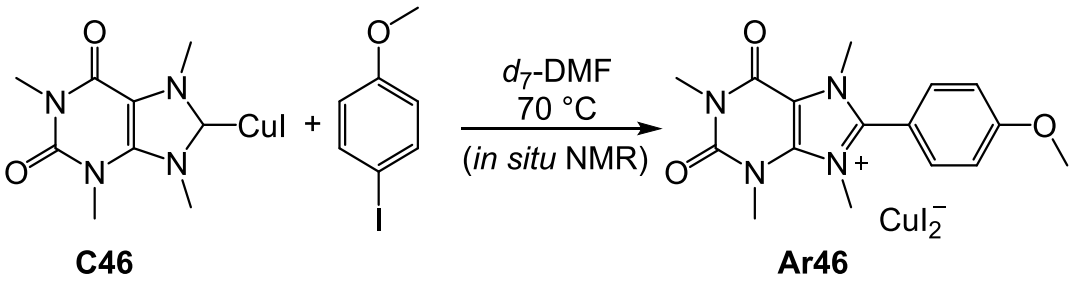

Scheme 4-16: Arylation of **C46** in an *in situ* ^{1}H NMR spectroscopy in d_7-DMF at 70 °C

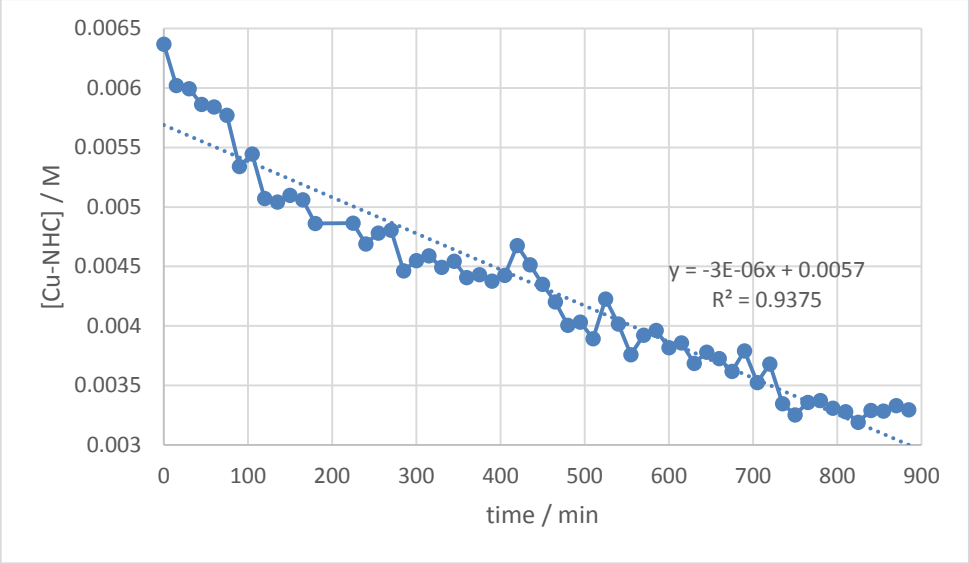

Figure 4-7: Concentration profile of **C46** and pseudo 0th order plot for **C46** in d_7-DMF at 70 °C derived from ^{1}H NMR integration using *m*-xylene as an internal standard: *m*-xylene δ 7.13, 6.99 ppm; **C46** δ 4.30, 4.12, 3.31 ppm; 4-iodoanisole δ 7.62, 6.82 ppm; and **Ar46** δ 7.82, 7.37, 4.13, 4.08, 3.40 ppm.

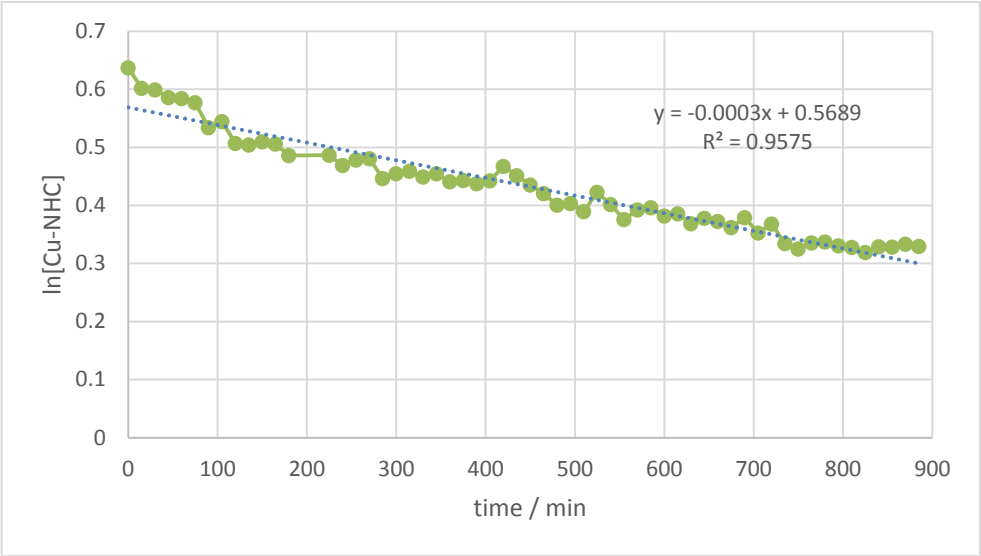

Figure 4-8: Pseudo 1st order plot for **C46** in d_7-DMF at 70 °C.

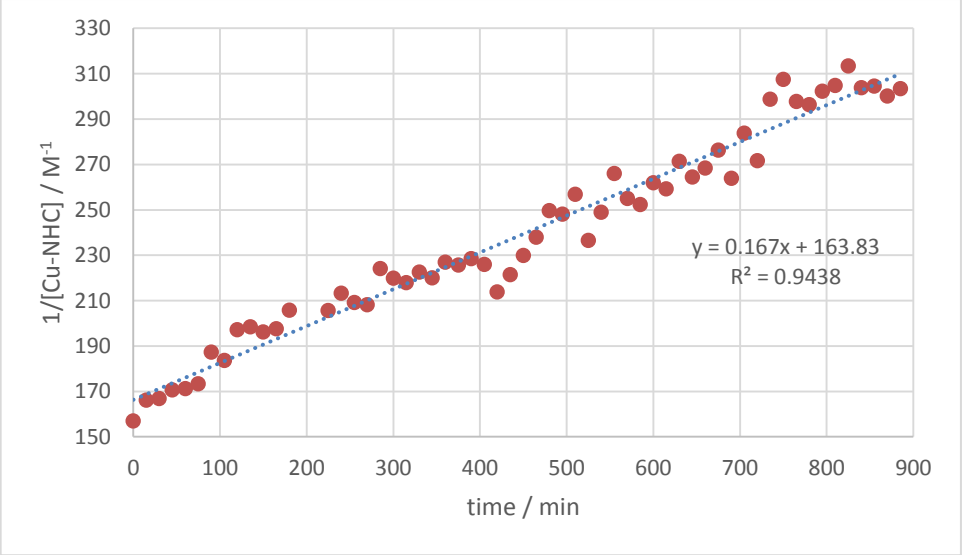

Figure 4-9: Pseudo 2nd order plot for **C46** in d_7-DMF at 70 °C.

4.6 Kinetic study on the arylation of copper-*N*-heterocyclic carbene using *in situ* IR spectroscopy

Due to the temperature limit of monitoring the arylation reaction using NMR spectroscopy (mainly the high temperature limit), an alternative technique was desired which would allow the reaction to be screened at higher temperature. *In situ* IR spectroscopy was therefore used to monitor the reaction, as reflux temperatures can be used. The reaction was performed using 0.05 M **C46** and 0.25 M ArI in MeCN at 78 °C (reflux temperature) (Scheme 4-17).

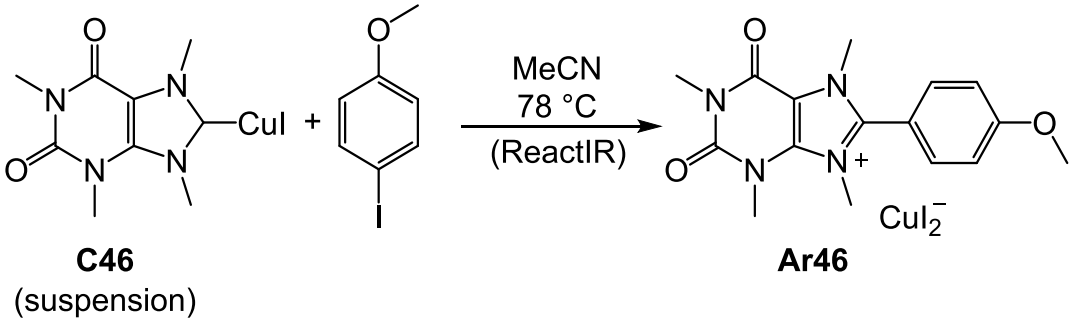

C46
(suspension)

Ar46

Scheme 4-17: Arylation of **C46** in an *in situ* IR spectroscopy in MeCN at 78 °C

Data between 1750 – 1220 cm^{-1} was acquired at 1 minute time intervals over 17 hours using ReactIR. The frequencies used for monitoring were 1287 cm^{-1} for the 4-iodoanisole, 1715 cm^{-1} for the C=O of **C46**, 1536 cm^{-1} for **Ar46** and 1712 cm^{-1} for the C=O of **Ar46**. However, as the peaks are 3 cm^{-1} apart from each other, the overlapping peaks were further investigated with normalised absorption graph (Figure 4-10), which visualises the absorption increases at 1712 cm^{-1} and the decrease at 1715 cm^{-1}. The 2nd derivative data of both points were performed to confirm the change on both sides of the peak resulted from the overlap of those 2 peaks.

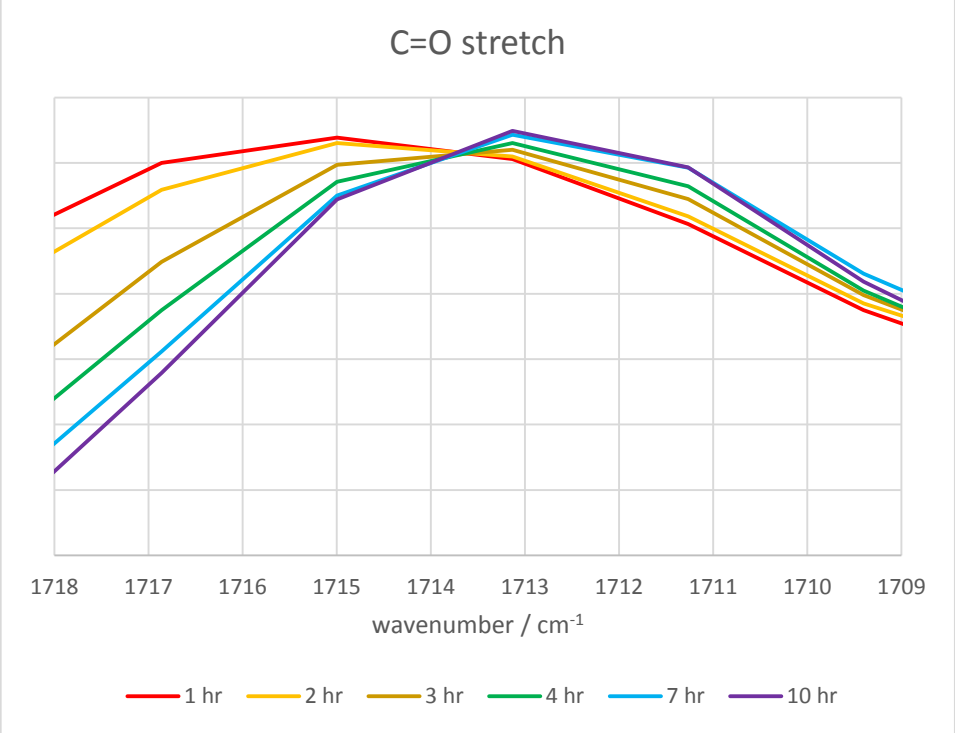

Figure 4-10: IR spectra change between 1718 – 1709 cm^{-1}; 0.05 M **C46** and 0.25 M 4-iodoanisole in MeCN at 78 °C.

A ^{1}H NMR spectrum of the crude mixture after 17 hours reaction time shows 39 % **C46** converted to **Ar46**. The concentration changes of **C46** and **Ar46** over

time are shown in Figure 4-11. The arylation reaction appeared to have an induction period (sigmoidal curve), which is likely the result of incomplete solubility of **C46** under the reaction conditions. Furthermore, the solid-state structure of **C46** was found to be a dimer,[13] which must cleave to form monomers in the solution phase which act as an active form of the complex (Scheme 4-18).

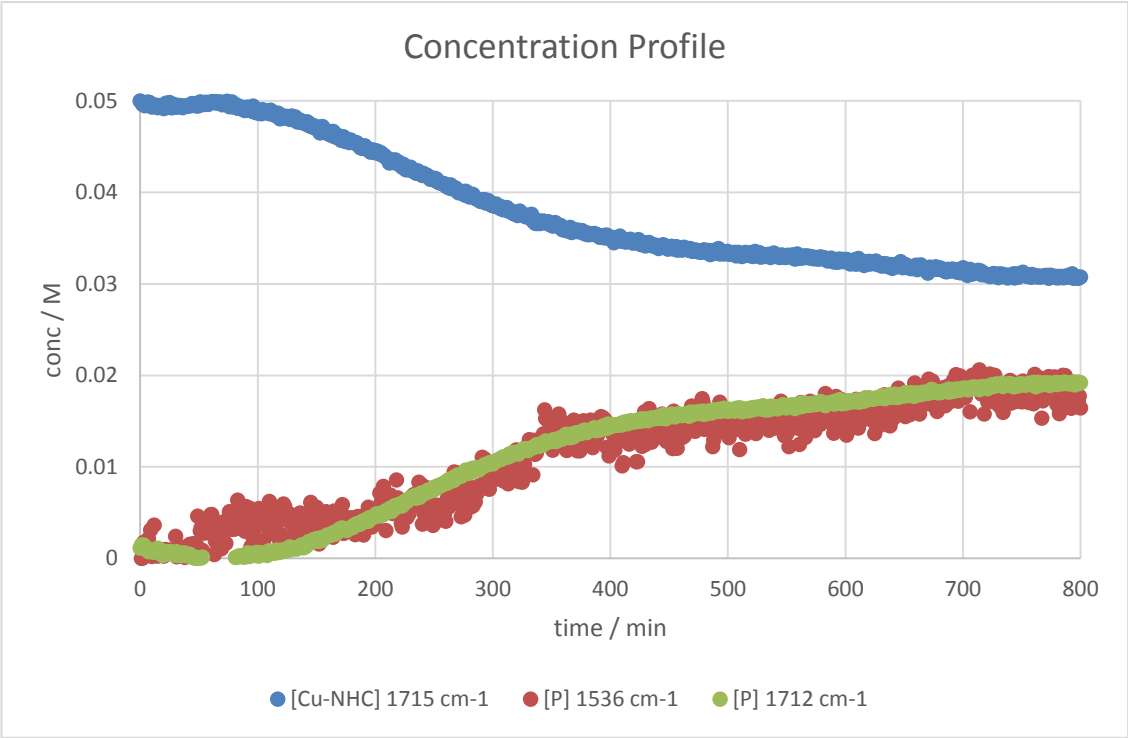

Figure 4-11: Concentration profile of **C46** (blue) and **Ar46** (red and green) in MeCN at 78 °C derived from the IR absorptions at 1715 (**C46**), 1536 and 1712 (**Ar46**) cm^{-1}.

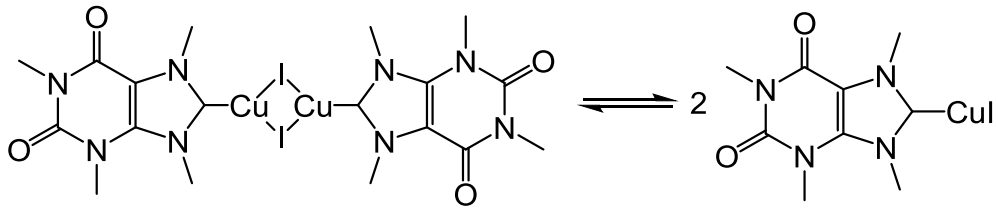

C46 solid **C46** solution

Scheme 4-18: Cleavage of **C46** dimer.

The concentration changes of **C46** and **Ar46** can then be used to plot ln[**C46**] vs time based on a pseudo-1st and 2nd order (rate = k'[**C46**] = k[**C46**][ArI]) using the data points from 200 – 450 min, which is after the initiation period. The slope of the pseudo 1st order plot of ln[**C46**] vs time is -0.00109 min^{-1}, which can be derived as k = 7.30 × 10^{-4} $M^{-1}s^{-1}$ (Figure 4-12, Table 4-2). Other k values were derived from [**Ar46**] using pseudo 1st order plot of ln(1-20[**Ar46**]) vs time (see Appendix), which are 7.62 and 7.32 × 10^{-4} $M^{-1}s^{-1}$. The 2nd order calculations were

derived from the plot of 5ln(5+(1/[**C46**])) and 5ln(5+4/(4[**Ar46**]-1)) vs time (see Appendix, Figure 4-13), resulting in rate constants = 7.65, 7.97 and 7.63 × 10^{-4} $M^{-1}s^{-1}$.

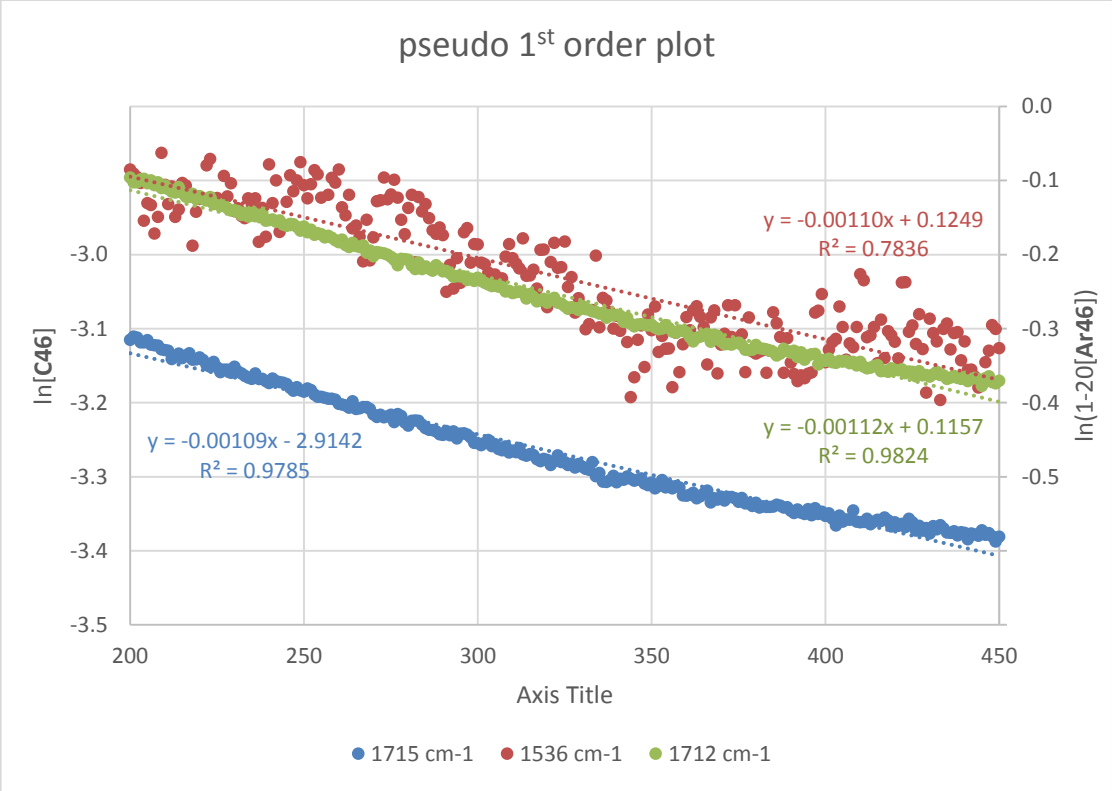

Figure 4-12: Pseudo 1st order plots: ln[**C46**] (blue) and ln(1-20[**Ar46**]) (red and green) vs time of the arylation in MeCN at 78.0 °C, probed by ReactIR.

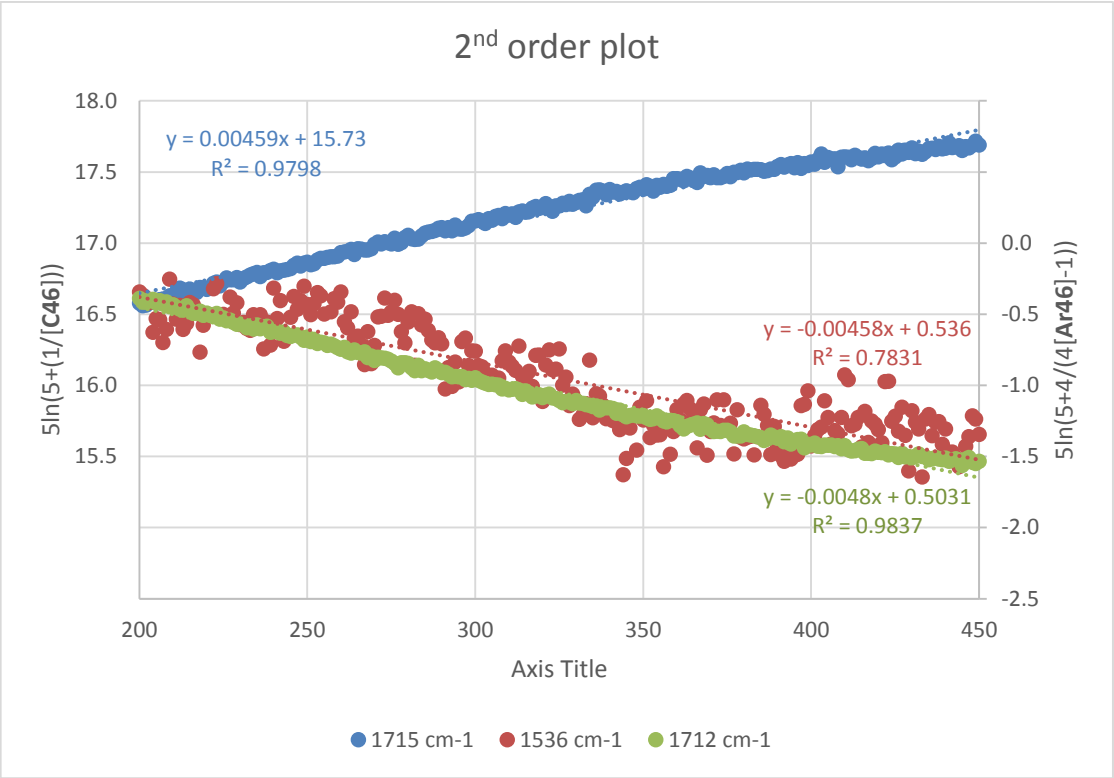

Figure 4-13: 2nd order plots: 5ln(5+(1/[**C46**])) (blue) and 5ln(5+4/(4[**Ar46**]-1)) (red and green) vs time of the arylation in MeCN at 78.0 °C, probed by ReactIR.

v / cm^{-1}	plot equation	linear regression	k / $M^{-1}s^{-1}$
1715	ln[**C46**] = k't + ln(0.05)	y = -0.00109x - 2.91	7.30×10^{-4}
1712	ln(1-20[**Ar46**]) = -k't	y = -0.00114x + 0.12	7.62×10^{-4}
1536	ln(1-20[**Ar46**]) = -k't	y = -0.00110x + 0.12	7.32×10^{-4}
1715	5ln(5+(1/[**C46**])) = kt + 5ln(25)	y = 0.00459x + 15.7	7.65×10^{-4}
1712	5ln(5+4/(4[**Ar46**]-1)) = -kt	y = -0.00478x + 0.50	7.97×10^{-4}
1536	5ln(5+4/(4[**Ar46**]-1)) = -kt	y = -0.00458x + 0.54	7.63×10^{-4}
		average	7.58×10^{-4}

Table 4-2: Linear regression equations and rate constants derived from [**C46**] and [**Ar46**] based on pseudo 1st order and 2nd order.

To overcome the temperature limit of MeCN solvent (b.p. 82 °C), the reaction was monitored in PhCN (b.p. 191 °C), which also enhances the solubility of **C46**. At 110 °C, the solubility of **C46** is above 0.05 M, which is the concentration used in the kinetic screening. The reaction was carried out at 120.0 °C using 0.05 M **C46** and 0.25 M 4-iodoanisole. The sigmoidal curve was no longer observed in the concentration profile (Figure 4-14). However, when monitoring **C46** the

ln[C46] plot is not fitted in with the reaction profile derived from the wavenumber 1560 cm^{-1} for **C46** as the curve bends at 270 – 280 minutes. Due to solvent interference in the C=C / C=O region, the C=O peaks of **C46** and **Ar46** cannot be used. Following recrystallisation of the crude reaction mixture in MeCN/Et_2O, demethylated imidazole **48** (Scheme 4-19) was observed in the filtrate using ^1H NMR spectroscopy and HRMS. Formation of this side-product possibly causes the concentration profile to bend at 300 minutes because of the overlapping of C=O frequencies of **C46** and **48**.

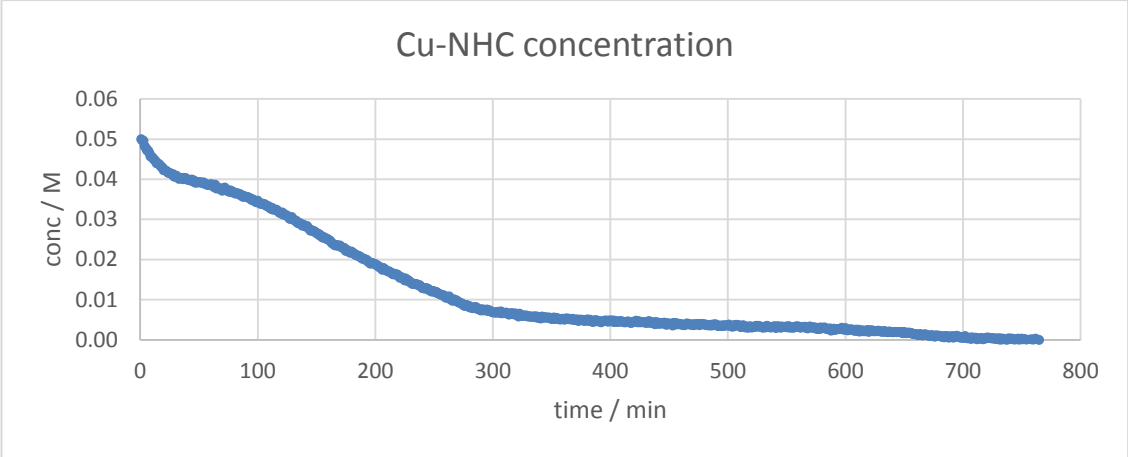

Figure 4-14: Concentration profile of **C46** in PhCN at 120.0 °C, derived from the IR absorptions at 1560 cm^{-1}.

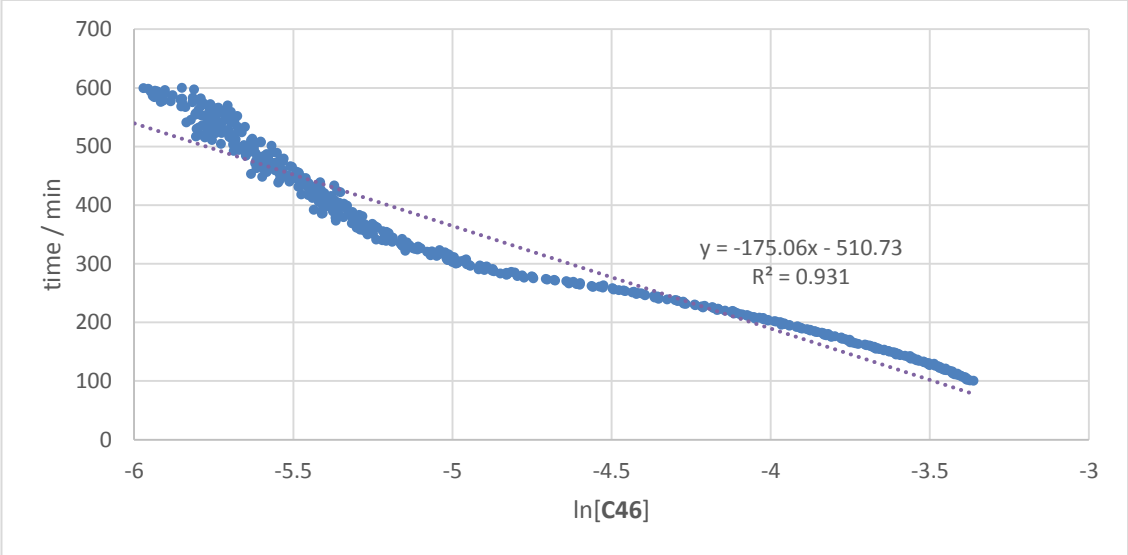

Figure 4-15: ln[**C46**] plot at 100 – 600 minutes

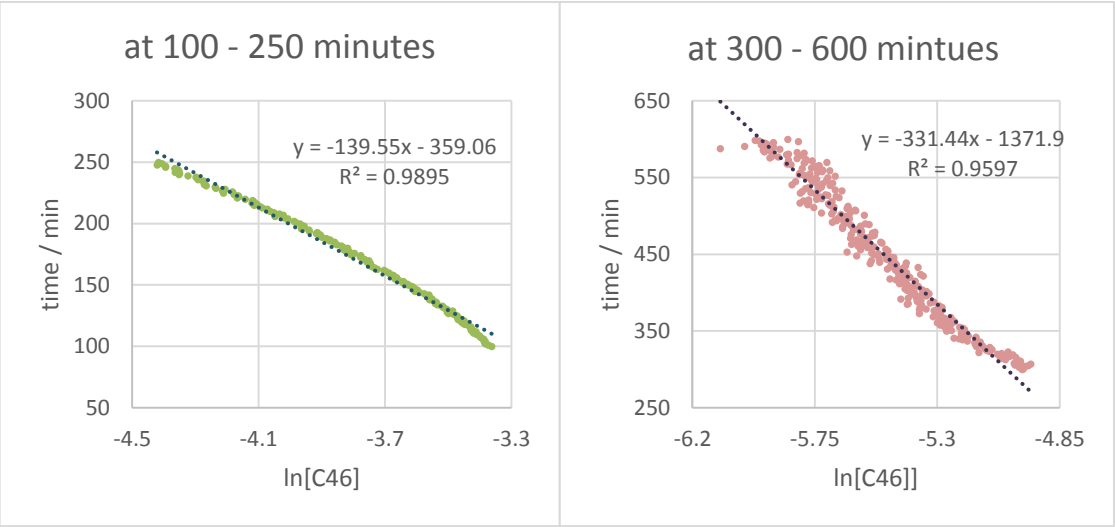

Figure 4-16: Sectioned ln[**C46**] plot at 100 – 250 minutes and 300 – 600 minutes.

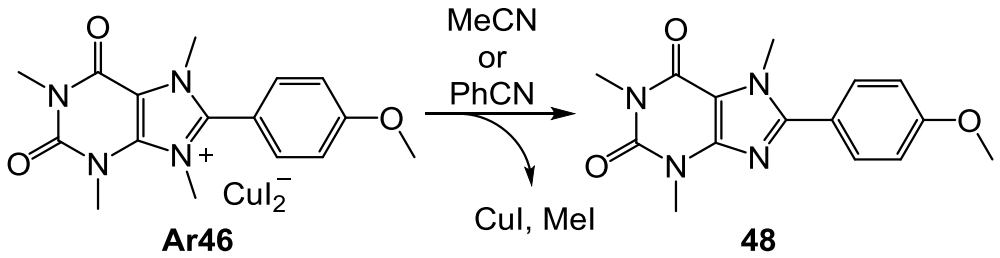

Scheme 4-19: Demethylation reaction of **Ar46**

The solvent was changed to DMAc as this has a higher polarity than MeCN and PhCN and demethylation is less likely to occur. DMAc is more stable at higher temperatures and more electron rich than DMF, which makes the possibility of C-N oxidative addition at Cu and amination less likely to occur. The reaction was screened at 120 °C using 0.05 M **C46** and 0.25 M 4-iodoanisole in DMAc for 270 minutes (Scheme 4-20). Following the reaction, EtOAc was added to precipitate the crude mixture, which was analysed using ^{1}H NMR spectroscopy. The ^{1}H NMR spectrum showed full conversion to **Ar46** and there was no evidence of either aminated (**47**) or demethylated (**48**) product.

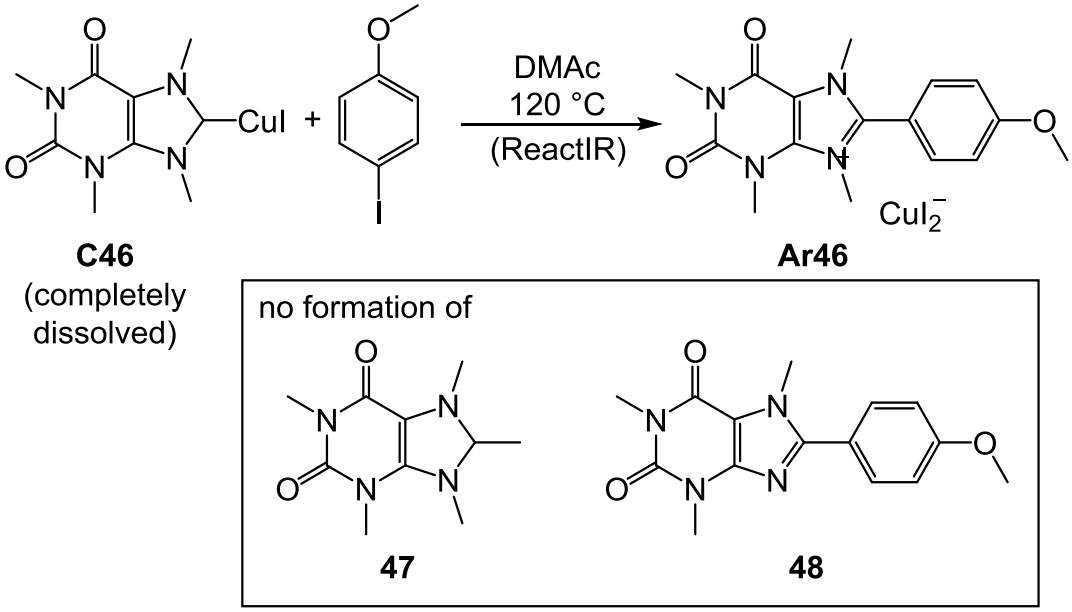

Scheme 4-20: Arylation of **C46** in an *in situ* IR spectroscopy in DMAc at 120 °C

The absorption changes between 1750 – 1220 cm^{-1} were used to determine the concentrations of **C46**, **Ar46** and 4-iodoanisole, which can be divided into 3 regions. C=O stretching frequencies are in the 1st region, between 1740 – 1680 cm^{-1}, the peaks of **C46** at 1719 and 1682 cm^{-1} decreased over time, whereas the peaks of **Ar46** at 1734 and 1701 cm^{-1} increased over time as expected (Figure 4-17). The **C46** peak at 1538 and the **Ar46** peaks at 1562, 1541 and 1523 cm^{-1} are in the region between 1600 – 1520 cm^{-1}, which may be C=C aromatic stretching frequencies (Figure 4-18). In the last region between 1320 – 1230 cm^{-1}, the C-O stretching frequency of 4-iodoanisole at 1246 cm^{-1} decreased slightly over time (Figure 4-19). The **Ar46** peak at 1303 cm^{-1} is also observed in this region, which is likely the C-O or C-N stretching. However, some of these peaks are noisy and therefore omitted from the calculation. In this case (120 °C), the peaks used are 1246 (4-iodoanisole), 1719 (**C46**), 1734 (**Ar46**) and 1303 (**Ar46**) cm^{-1} were used for monitoring.

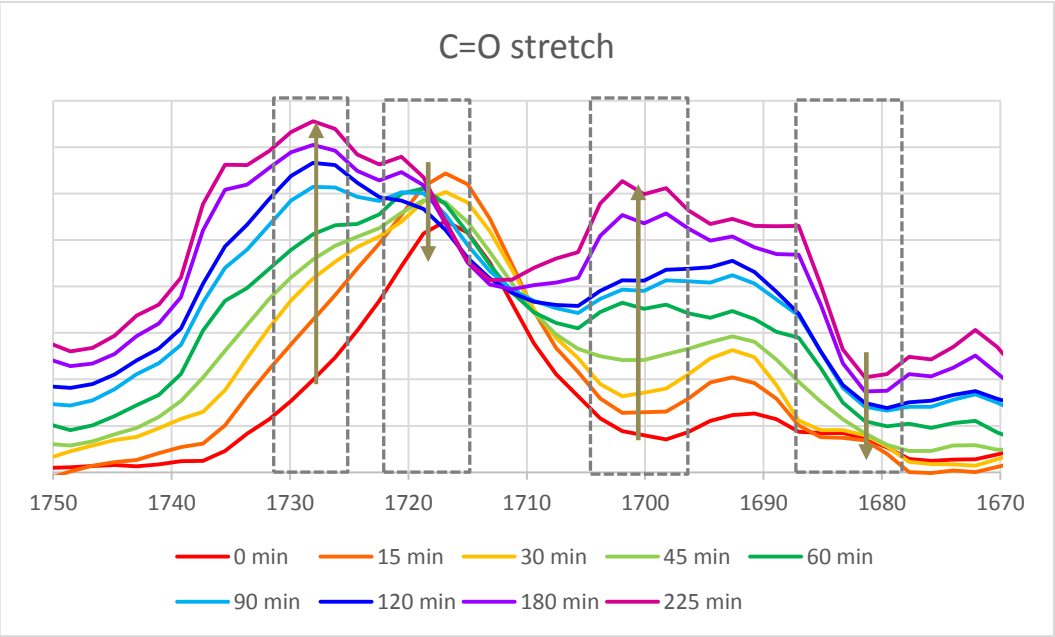

Figure 4-17: IR spectra change between 1750 – 1670 cm^{-1}; 0.05 M **C46** and 0.25 M 4-iodoanisole in DMAc at 120 °C.

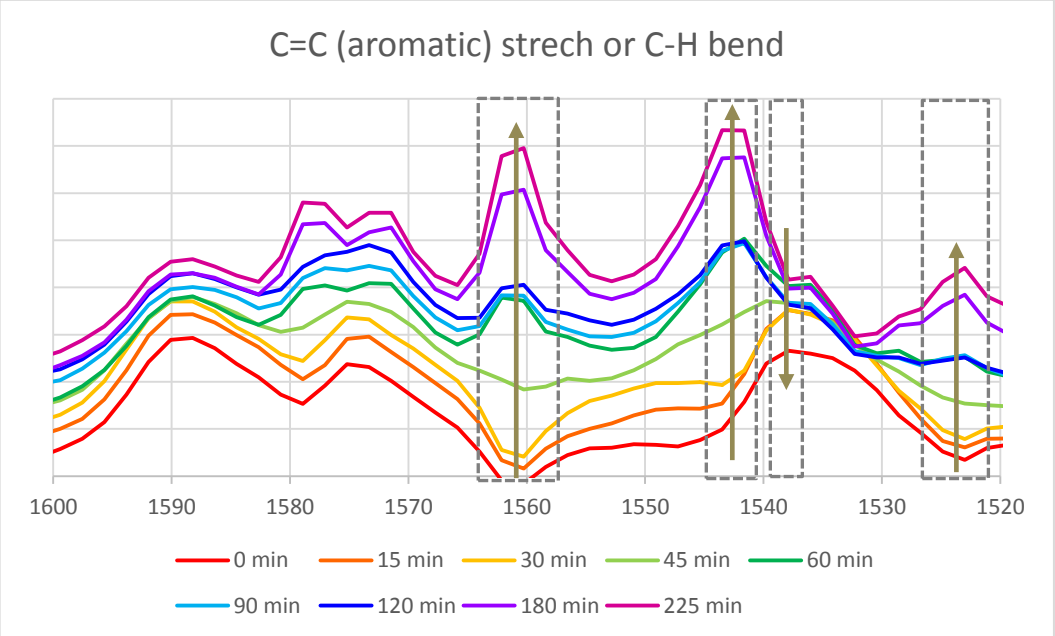

Figure 4-18: IR spectra change between 1600 – 1520 cm^{-1}; 0.05 M **C46** and 0.25 M 4-iodoanisole in DMAc at 120 °C.

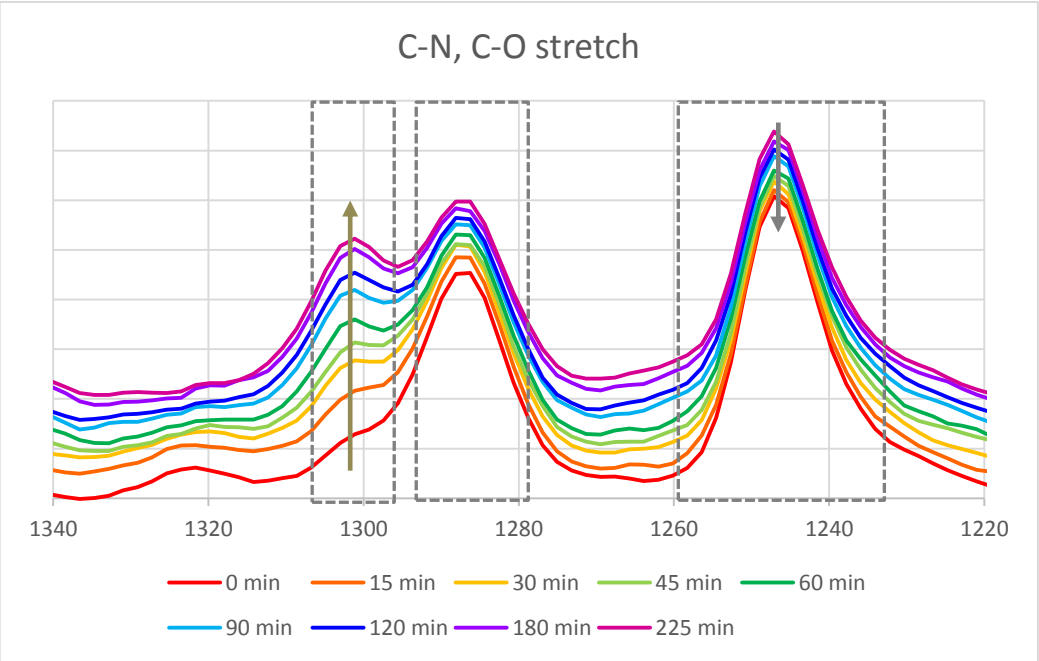

Figure 4-19: IR spectra change between 1340 – 1220 cm^{-1}; 0.05 M **C46** and 0.25 M 4-iodoanisole in DMAc at 120 °C.

The concentration profiles (Figure 4-20) show that there was no induction period observed at 120 °C in DMAc, as **C46** was fully dissolved instantly. The profiles fit the exponential plot and ln[**C46**], ln(1-20[**Ar46**]), 5ln(5+(1/[**C46**])) and 5ln(5+4/(4[**Ar46**]-1)) vs time were plotted (Figure 4-21 and Figure 4-22, see Appendix). These plots fit linear regression and give the rate constant of 1.01, 1.05, 1.11, 1.17, 1.23 and 1.30 × 10^{-3} $M^{-1}s^{-1}$. The rate constant obtained from the pseudo 1st order calculation is lower than that from the 2nd order calculation because in the pseudo 1st order calculation, the [ArI] is constantly at 0.25 M. However, [ArI] decreases from 0.25 to 0.20 M during the reaction and has the average concentration of 0.225 M, which is lower than the concentration used in pseudo 1st order calculation. As the [ArI] of the pseudo 1st order is higher than the more realistic 2nd order that [ArI] decreases over time, the rate constant (k = k' / [ArI]) from pseudo 1st order reaction is lower than 2nd order reaction.

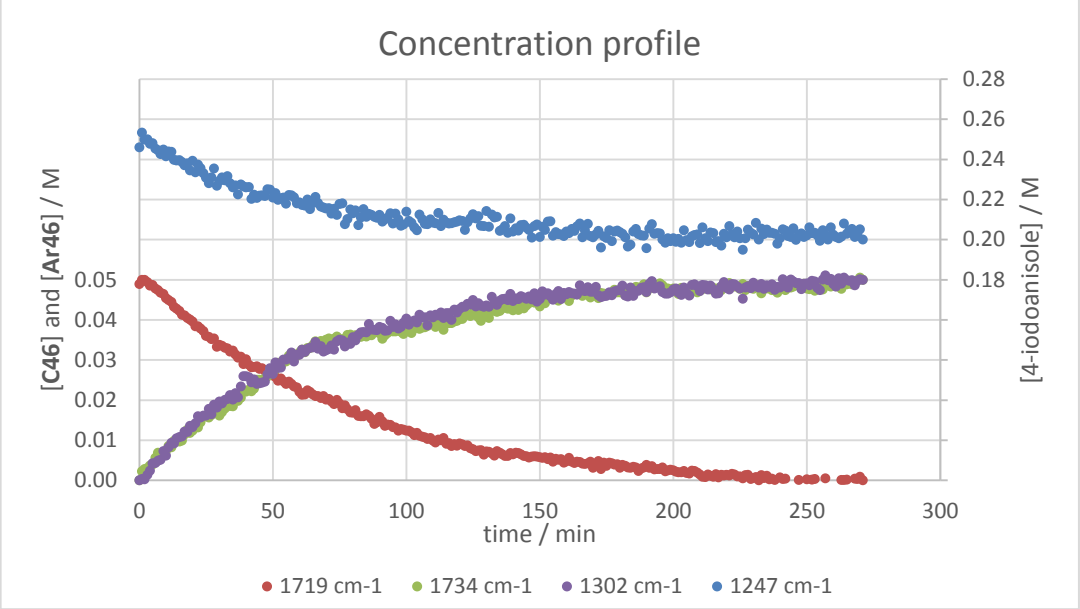

Figure 4-20: Concentration profile of **C46** (red), **Ar46** (green and violet) and 4-iodoanisole (blue) in DMAc at 120.0 °C, probed by ReactIR

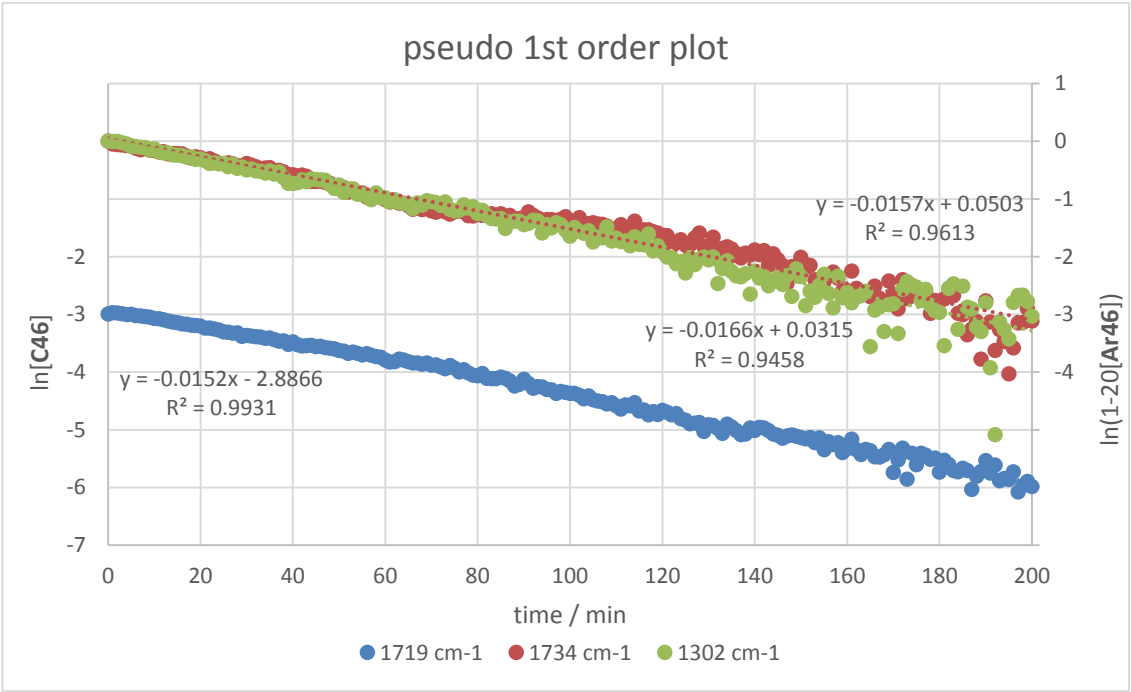

Figure 4-21: Pseudo 1st order plots: ln[**C46**] and ln(1-20[**Ar46**]) vs time of the arylation in DMAc at 120.0 °C, probed by ReactIR.

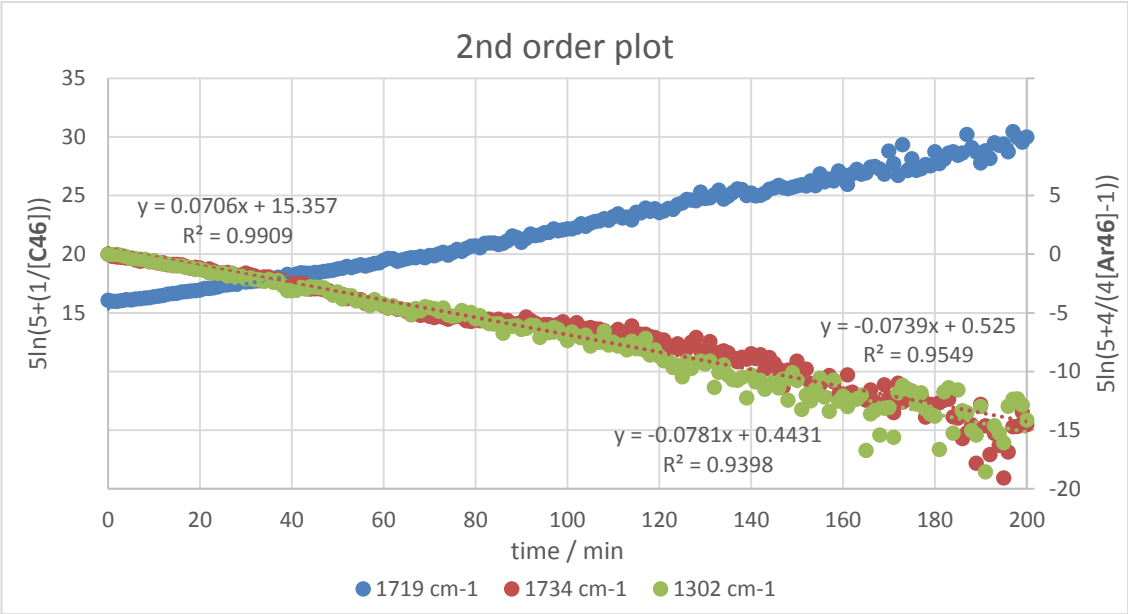

Figure 4-22: 2nd order plots: 5ln(5+(1/[**C46**])) and 5ln(5+4/(4[**Ar46**]-1)) vs time of the arylation in DMac at 120.0 °C, probed by ReactIR.

4.7 Arrhenius plot

The arylation of **C46** in DMAc were repeated at 70, 90, 100 and 140 °C so that the activation energy could be calculated. At 90 °C and above, the concentration profiles were exponential (Figure 4-23) and the same method was utilised to obtain rate constants (Table 4-3). However, at 70 °C, **C46** was not completely dissolved and the sigmoidal curve was observed in the concentration profile (Figure 4-24). In addition, the fluctuation at 250 – 300 minutes was due to liquid nitrogen being filled to the probe. Hence, the calculation is based on the data points after the delay curve (400 – 1200 minutes) and the rate constant (0.9×10^{-4} $M^{-1}s^{-1}$) is similar to the rate constant obtained from the NMR screening in DMF at the same reaction temperature (1.1×10^{-4} $M^{-1}s^{-1}$).

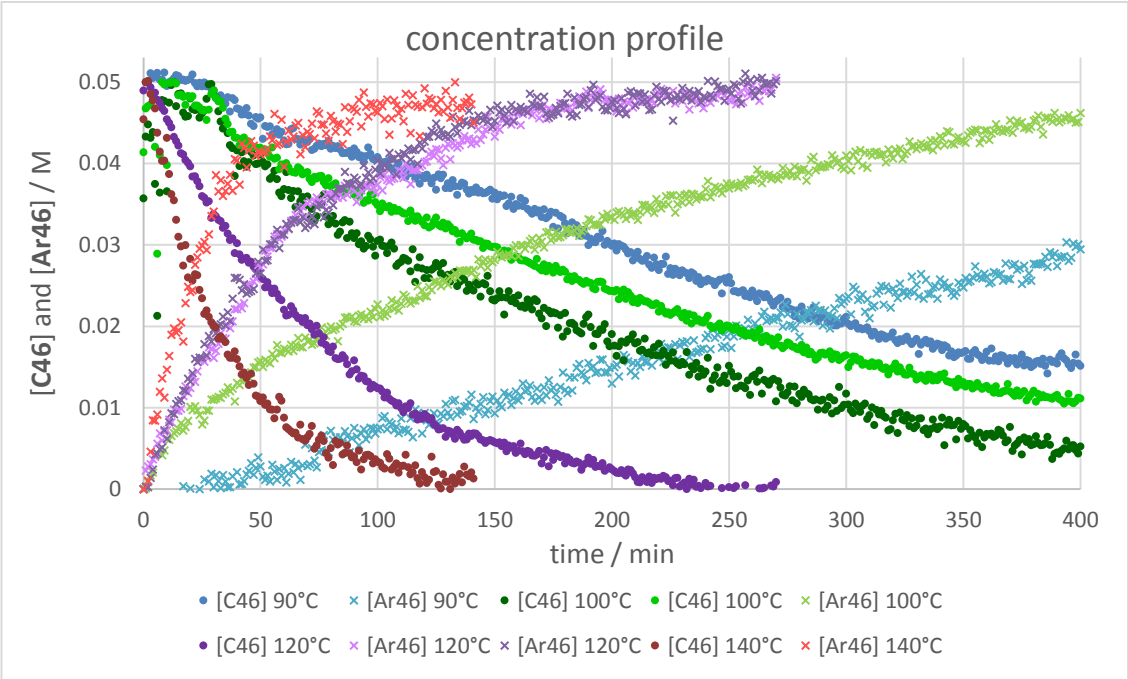

Figure 4-23: Concentration profile of **C46** and **Ar46** in DMAc at 90, 100, 120 and 140 °C, derived from the IR absorptions (see Table 4-3).

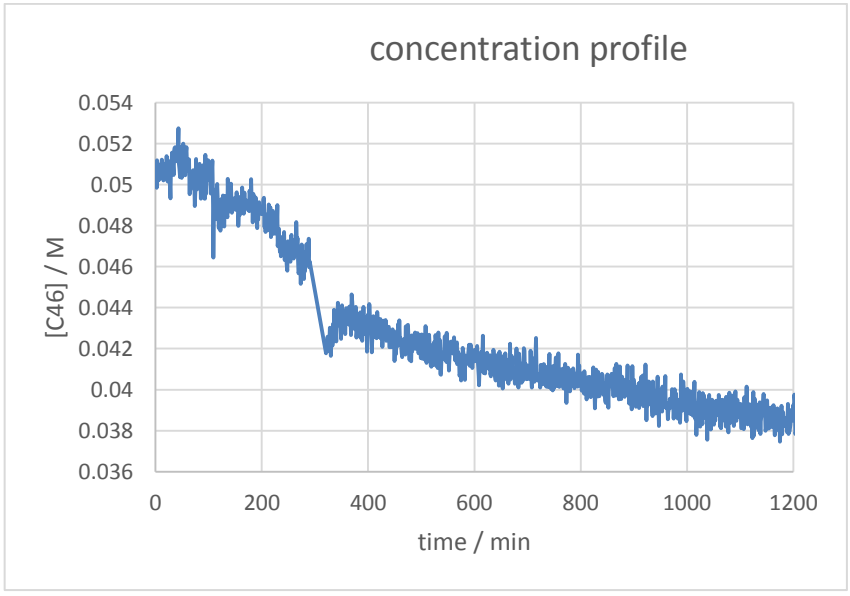

Figure 4-24: Concentration profile of **C46** in DMAc at 70.0 °C, derived from the IR absorptions at 1718 cm^{-1}.

T / °C	used time range / min	v / cm^{-1}	k / $M^{-1}s^{-1}$ (pseudo 1st order)	k / $M^{-1}s^{-1}$ (2nd order)
70*	0 – 900	N/A	1.17×10^{-4}	N/A
70.0	400 – 1200	1718 (**C46**)	9.13×10^{-5}	N/A
90.0	60 – 728	1719 (**C46**)	2.03×10^{-4}	2.32×10^{-4}
		1303 (**Ar46**)	1.92×10^{-4}	2.17×10^{-4}
100.0	30 – 420	1538 (**C46**)	3.96×10^{-4}	4.60×10^{-4}
		1719 (**C46**)	2.64×10^{-4}	2.98×10^{-4}
		1303 (**Ar46**)	3.87×10^{-4}	4.53×10^{-4}
120.0	0 – 200	1719 (**C46**)	1.01×10^{-3}	1.17×10^{-3}
		1734 (**Ar46**)	1.05×10^{-3}	1.23×10^{-3}
		1302 (**Ar46**)	1.11×10^{-3}	1.30×10^{-3}
140.0	0 – 40	1716 (**C46**)	2.06×10^{-3}	2.25×10^{-3}
		1303 (**Ar46**)	2.70×10^{-3}	3.01×10^{-3}

Table 4-3: Rate constants from 0.05 M **C46** and 0.25 M 4-iodoanisole in DMAc at 70 – 140 °C, probed by ReactIR. *Rate constant from the reaction in d_7-DMF, monitored by *in situ* ^{1}H NMR spectroscopy.

Since the rate constants for the arylation of **C46** have been obtained across the temperature range 70 – 140 °C, the activation energy of the reaction was calculated from these values by plotting an Arrhenius graph ($\ln k = E_a/R(1/T) + \ln A$) (Figure 4-25, Table 4-4). When the activation energies are calculated in the temperature range 90 – 140 °C, values of 63.1 (pseudo 1st order) and 62.5 (2nd order) kJ mol^{-1} are obtained, which are very similar to each other. However, when the data point at 70 °C is included in the calculation, the activation energy drops to 58.9 kJ mol^{-1}. The activation energy obtained from the experimental data is significantly higher than the calculated activation energies for the arylation of other Cu-NHC complexes with iodobenzene (**C49**, **C50** and **C51**, Figure 4-26) in toluene (38.5, 39.4 and 27.5 kJ mol^{-1}, respectively).[12] This is likely due to the electron-withdrawing amide backbone of the xanthine-derived ligand **L46**. which stabilises Cu(I) rather than Cu(III). As a result, both oxidative addition of ArI and reductive elimination of **Ar46** become more difficult. Moreover, the DFT calculations cited were based on iodobenzene, whereas 4-iodoanisole was used

in our experimental work. The oxidative addition of a more electron rich 4-iodoanisole is less favourable.

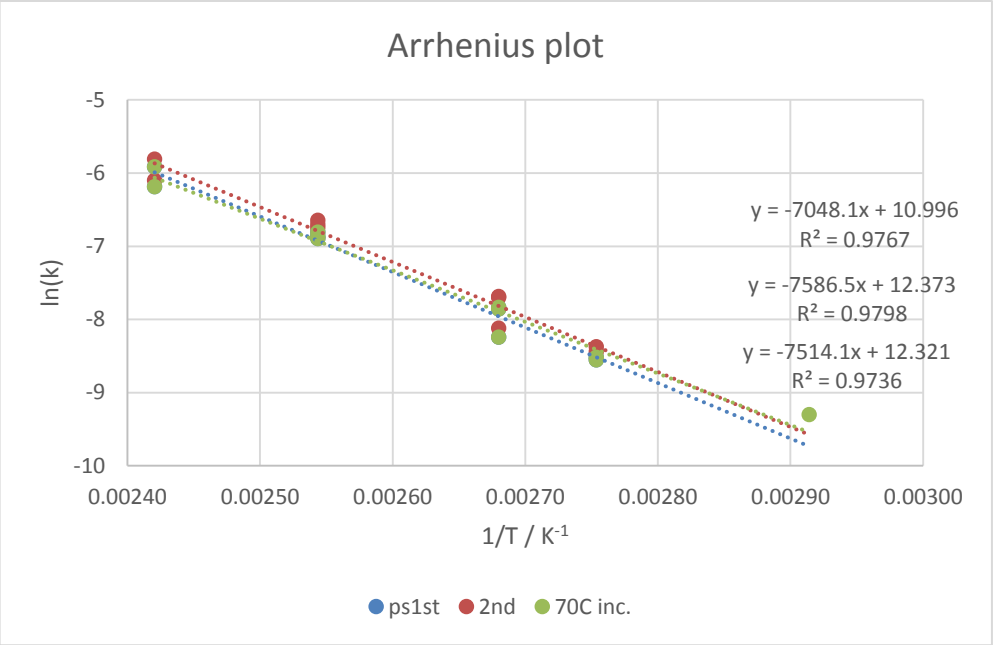

Figure 4-25: Arrhenius plot based rate constants of pseudo 1st and 2nd order reaction of the arylation of **C46** in DMAc at 90 – 140 °C and 1st order reaction at 70 – 140°C.

T / °C	type	E_a / kJ mol^{-1}
70 – 140	pseudo 1st order	58.9
90 – 140	pseudo 1st order	63.1
90 – 140	2nd order	62.5

Table 4-4: The activation energy of the arylation of **C46** from pseudo 1st order and 2nd order data.

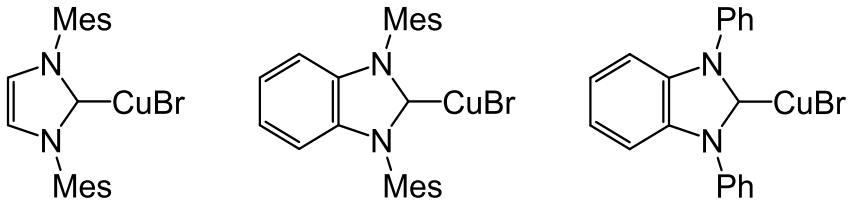

C49 **C50** **C51**

E_a = 38.5 kJ mol $^{-1}$ E_a = 39.4 kJ mol $^{-1}$ E_a = 27.5 kJ mol $^{-1}$

Figure 4-26: Calculated activation energies for the arylation for the arylation of Br-Cu-NHC complexes with iodobenzene in toluene.[12]

4.8 Conclusions

In summary, xanthine-based imidazolium salts can be arylated *via* formation of a Cu-NHC complex, which can be generated electrochemically using Cu electrodes in MeCN. The arylation of Cu-NHC complexes occur efficiently at high temperature in DMF. DMF can also act as a substrate, leading to H-imidazolium and amino-imidazolium side-products. Demethylation of the imidazolium to give an arylated imidazole was also found to occur in some instances. Monitoring the reaction using ^{1}H NMR spectroscopy allows straightforward calculation of the concentrations of each species. Side-products can also be identified using this technique. However, the spectrometer is limited by the temperature and/or large delaying in transferring the sample to the spectrometer. Using *in situ* IR absorption overcomes these issues, though higher concentrations of reaction species are required. IR absorption of C=O, C=C, C-N and C-O stretches were used to calculate rate constants, and the activation energy of the arylation of **C46** in DMAc, which was found to be 58.9 – 63.1 kJ mol^{-1}.

4.9 Future work

The ultimate aim for this work is to find a lower energy pathway to arylate imidazole/imidazolium so that the methodology can be applied to more delicate systems. A potential way to do this could be to use electrochemical reaction *i.e*. arylation of an imidazolium salt under electrochemical conditions *via* a Cu-NHC formed *in situ*. This may also be carried out 'metal free' using inert electrodes which will reduce an imidazolium salt to a free NHC. The NHC may act as a nucleophile and attack aryl iodide to give an aryl-imidazolium ion. Moreover, variation of *N*-substituents, imidazole-backbones and aryl species would potentially give more insights into the arylation reaction.

4.10 Experimental

4.10.1 Preparation of substituted imidazoles

i) Preparation of **P45**

Theophylline (1.5 g, 8.32 mmol) and K_2CO_3 (1.27 g, 9.16 mmol) were added a round-bottomed flask, followed by MeCN (20 mL) and 1-iodobutane (3.8 mL, 33.3 mmol). The reaction mixture was heated and stirred at 80 ºC under N_2 and

hydrous conditions for 48 hours. The mixture was allowed to cool to room temperature and filtered. The solvent was removed from the filtrate *in vacuo*, which resulted in a white solid. Yield: 1.35 g, 5.7 mmol, 69 %

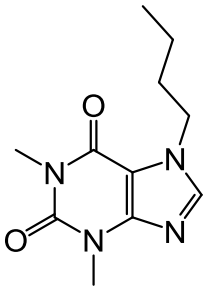

^{1}H NMR (300 MHz, $CDCl_3$) δ (ppm) 7.71 (s, 1H, XnH-8), 4.32 (t, *J* = 7.2 Hz, 2H, N**CH$_2$**$CH_2CH_2CH_3$), 3.68 (s, 3H, NCH_3), 3.41 (s, 3H, NCH_3), 1.86 (quintet, *J* = 7.2 Hz, 2H, NCH_2**CH$_2$**CH_2CH_3), 1.36 (sext, *J* = 7.2 Hz, 2H, NCH_2CH_2**CH$_2$**CH_3), 0.94 (q, *J* = 7.2 Hz, 3H, $NCH_2CH_2CH_2$**CH$_3$**). ^{13}C {^{1}H} (75 MHz, $CDCl_3$) δ (ppm) 115.2 (C), 151.8 (C), 148.7 (C), 140.7 (CH), 110.1 (C), 47.4 (CH_2), 33.0 (CH_3), 30.1 (CH_3), 28.2 (CH_2), 19.7 (CH_2), 13.6 (CH_3). HRMS (ESI^+): *m/z* 237.1356 $[M + H]^+$, calculated $[M + H]^+$ 237.1346.

Consisted with data previously reported.[13]

4.10.2 **Preparation of imidazolium salts**

i) Preparation of H**L45**I

P45 (1.3 g, 5.5 mmol), MeI (2 mL, 32 mmol) and DMF (5 mL) were added to an ampoule and stirred at 70°C in a sealed system for 24 hours. EtOAc (50 mL) was added to precipitate a yellow solid, which was collected by filtration. The solid was recrystallised from DCM / Et_2O and dried *in vacuo*. Yield: 1.69 g, 4.47 mmol, 81 %

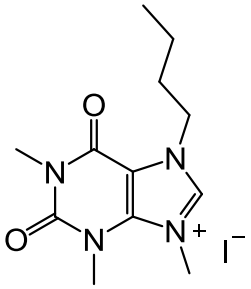

^{1}H NMR (300 MHz, CD_3CN) δ 8.95 (s, 1H, XnH), 4.44 (t, *J* = 7.2 Hz, 2H, N**CH$_2$**$CH_2CH_2CH_3$), 4.07 (s, 3H, NCH_3), 3.68 (s, 3H, NCH_3), 3.27 (s, 3H, NCH_3), 1.82 (quint, *J* = 7.2 Hz, 2H, NCH_2**CH$_2$**CH_2CH_3), 1.33 (sext, *J* = 7.2 Hz, 2H, NCH_2CH_2**CH$_2$**CH_3), 0.90 (t, *J* = 7.3 Hz, 3H, $NCH_2CH_2CH_2$**CH$_3$**). ^{13}C {^{1}H} (75 MHz, CD_3CN) δ 154.3 (C), 151.4 (C), 140.9 (C), 139.2 (C), 139.1 (CH), 50.1 (CH_3), 38.3 (CH_2), 32.4 (CH_3), 32.3 (CH_3), 39.1 (CH_2), 19.8 (CH_2), 13.7 (CH_3). HRMS (ESI^+): *m/z* 251.1522 $[M - I]^+$, calculated $[M - I]^+$ 251.1503.

Consisted with data previously reported.[13]

ii) Preparation of H**L46**I

Caffeine (1.0 g, 5.1 mmol) was added to an ampoule, followed by DMF (10 mL) and MeI (1.6 mL, 25.7 mmol). The reaction mixture was stirred in a sealed system at 90 ºC for 48 hours. The mixture was allowed to cool to room temperature, during which white time a solid was precipitated. EtOAc (60 mL) was added to the mixture and filtered. The solid was

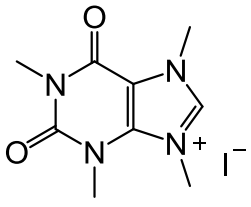

washed with EtOAc(3 × 30 mL) and Et_2O (30 mL), dried *in vacuo* to give the product as an off-white solid. Yield: 0.37 g, 1.1 mmol, 21 %.

^{1}H NMR (300 MHz, CD_3CN) δ 8.67 (s, 1H, XnH), 4.10 (s, 3H, NCH_3), 4.09 (s, 3H, NCH_3), 3.74 (s, 3H, NCH_3), 3.34 (s, 3H, NCH_3). ^{13}C {^{1}H} (75 MHz, CD_3CN) δ 153.0 (C), 150.0 (C), 141.1 (C), 138.0 (CH), 110.0 (C), 36.5 (CH_3), 35.8 (CH_3), 30.3 (CH_3), 25.3 (CH_3). HRMS (ESI^+): *m/z* 209.1031 $[M - I]^+$, calculated $[M - I]^+$ 209.1033.

Consisted with data previously reported.[13]

iii) Preparation of H**L49**Br

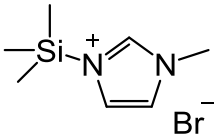

Under Ar, a freshly distilled 1-methylimidazole (1.0 mL, 12.5 mmol) was added dropwise *via* syringe to a stirring solution of bromotimethylsilane (1.7 mL, 12.5 mmol) in Et_2O (5 mL) at 0 °C. A colourless solid as immediately formed. It was collected from cannula filtration, washed with anhydrous Et_2O (2 × 5 mL) and dried *in vacuo*. The colourless solid was stored in a Glovebox. Yield: 2.89 g, 12.2 mmol, 98 %.

^{1}H NMR (300 MHz, CD_3CN) δ 9.05 (s, 1H, imH), 7.50 (s, 1H, imH), 7.41 (s, 1H, imH), 3.91 (s, 3H, NCH_3), 0.58 (s, 9H, $Si(CH_3)_3$). ^{13}C {^{1}H} NMR (75 MHz, CD_3CN) δ 139.6 (N-C-N), 124.9 (N-C-C-N), 123.4 (N-C-C-N), 36.2 (NCH_3), -0.9 ($Si(CH_3)_3$).

Consistent with data previously reported.[26]

4.10.3 Preparation of Cu-NHC complexes

i) Preparation of **C45**

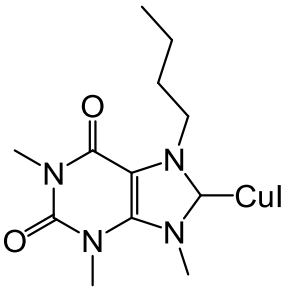

H**L45**I (0.2 g, 0.53 mmol) was added a flame-dried three-necked round-bottomed flask. MeCN (20 mL) was added *via* syringe and two Cu electrodes were inserted. A voltage was applied to achieve a current of 30 mA, which was maintained for 1 hour. The reaction mixture was filtered and washed with excess MeCN. The filtrate was concentrated *in vacuo* and Et_2O was added to precipitate the product, which was collected by filtration as a greyish green solid. Yield: 0.18 g, 0.41 mmol, 77 %.

^{1}H NMR (300 MHz, CD_3CN) δ 4.47 (t, *J* = 7.3 Hz, 2H, N**CH_2**$CH_2CH_2CH_3$), 4.36 (s, 3H, NCH_3), 3.71 (s, 3H, NCH_3), 3.28 (s, 3H, NCH_3), 1.79 (quint, *J* = 7.3 Hz, 2H, NCH_2**CH_2**CH_2CH_3), 1.39 (sext, *J* = 7.3 Hz, 2H, NCH_2CH_2**CH_2**CH_3), 0.93 (t, *J*

= 7.3 Hz, 2H, $NCH_2CH_2CH_2\mathbf{CH_3}$). ^{13}C {^1H} (75 MHz, CD_3CN) δ 210.0 (C), 153.0 (C), 152.0 (C), 151.5 (C), 149.8 (C), 41.1 (CH_3), 38.5 (CH_2), 32.9 (CH_3), 28.0 (CH_3), 21.3 (CH_2), 21.1 (CH_2), 19.9 (CH_3).

Consistent with data previously reported.[13]

ii) Preparation of **C46**

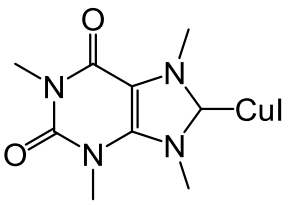

H**L46**I (0.90 g, 2.54 mmol) was added to a flame-dried three-necked round-bottomed flask. MeCN (20 mL) was added *via* syringe and two Cu electrodes were inserted. A voltage was applied to achieve a current of 30 mA, which was maintained for 5 hours. The product was collected by filtration, washed with MeCN (10 mL) and Et_2O (50 mL) and dried *in vacuo* to give pale green solid. Yield: 0.66 g, 1.65 mmol, 65 %.

^1H NMR (300 MHz, d_6-DMSO) δ 4.17 (s, 3H, NCH_3), 4.00 (s, 3H, NCH_3), 3.73 (s, 3H, NCH_3), 3.23 (s, 3H, NCH_3). ^{13}C {^1H} (75 MHz, d_6-DMSO) δ 206.5 (C), 153.1 (C), 150.0 (C), 140.1 (C), 108.2 (C), 64.9 (CH_3), 54.9 (CH_3), 30.6 (CH_3), 28.1 (CH_3).

Consistent with data previously reported.[13]

iii) Cu-metallation of **L49** *via* an electrochemical method

Under Ar, solution of H**L49**Br (0.1 g, 0.42 mmol) in MeCN (5 mL) was transferred to a 3-necked round-bottomed flask. Cu electrodes were inserted into the solution and a voltage was applied to give a current of 30 mA for 46 minutes. The solvent was removed *in vacuo* to give a greyish green solid.

^1H NMR (300 MHz, d_6-DMSO) δ 8.11 (s, 1H, imH), 7.37 (s, 1H, imH), 7.15 (s, 1H, imH), 3.73 (s, 3H, NCH_3). HRMS (ESI^+): *m/z* 227.0348 and 229.0329 $[Cu(methylimidazole)_2]^+$, calculated $[Cu(methylimidazole)_2]^+$ 227.0352 and 229.0334.

iv) Cu-metallation of **L49** *via in situ* silver transmetallation

Under Ar, to freshly activated molecular sieves (4 Å), were added Ag_2O (0.2 g, 0.82 mmol) DCM or MeOH (10 mL) and an solution of H**L49**Br (0.2 g, 0.82 mmol) in DCM (2 mL). The reaction was stirred in the absence of light for 2 hours. CuI (0.16 g, 0.82 mmol) was added and the mixture stirred for a further 1 hour. The reaction mixture was filtered by cannula filtration to give a green solution. The solvent was removed from the filtrate *in vacuo* to give a green solid.

HRMS (ESI$^+$): *m/z* 227.0348 and 229.0329 [Cu(methylimidazole)$_2$]$^+$, calculated [Cu(methylimidazole)$_2$]$^+$ 227.0352 and 229.0334.

4.10.4 Arylation reactions

i) Preparation of **Ar45**

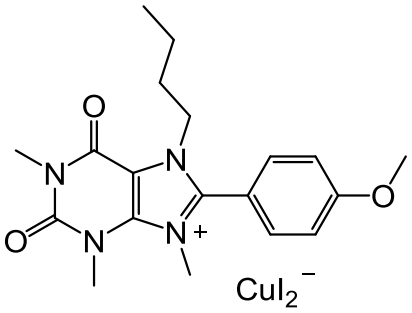

C45 (0.070 g, 0.159 mmol) and 4-iodoanisole (0.372 g, 1.59 mmol) were added to an ampoule. DMF (10 mL) was added *via* a syringe and the reaction mixture was heated at 140 ºC for 24 hours. The mixture was filtered and concentrated in vacuo. Et$_2$O (50 mL) was added to precipitate the light brown solid, which was collected by filtration and washed with Et$_2$O and dried in air. Yield: 0.064 g, 0.095 mmol, 60 %

^{1}H NMR (300 MHz, CD_3CN) δ 7.59 (d, *J* = 9.0 Hz, 2H, ArH), 7.28 (d, *J* = 9.0 Hz, 2H, ArH), 4.32 (t, *J* = 7.2 Hz, 2H, N**CH$_2$**CH$_2$CH$_2$CH$_3$), 3.95 (s, 3H, CH_3), 3.81 (s, 3H, CH_3), 3.80 (s, 3H, CH_3), 3.40 (s, 3H, CH_3), 1.72 (quint, *J* = 7.2 Hz, 2H, NCH$_2$**CH$_2$**CH$_2$CH$_3$), 1.23 (sext, *J* = 7.2 Hz, 2H, NCH$_2$CH$_2$**CH$_2$**CH$_3$), 0.81 (t, *J* = 7.4 Hz, 3H, NCH$_2$CH$_2$CH$_2$**CH$_3$**). HRMS (ESI$^+$): *m/z* 357.1920 [M – CuI$_2$]$^+$, calculated [M – CuI$_2$]$^+$ 357.1921.

ii) Preparation of **Ar46**

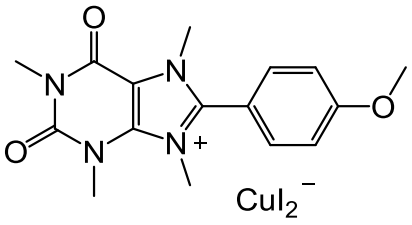

C46 (0.030 g, 0.075 mmol) and 4-iodoanisole (0.175 g, 0.75 mmol) added to an ampoule. Anhydrous and degassed solvent (toluene, MeCN or DMF, 5 mL) was added *via* a syringe. The reaction mixture was heated (35, 90 or 140 ºC) under nitrogen for 24 hours or 168 hours. The mixture was filtered and concentrated *in vacuo*. Et$_2$O (50 mL) was added to precipitate the light brown solid, which was collected from filtration and washed by Et$_2$O and dried in air. Yield (in the case of heating in DMF at 140 ºC for 24 hours): 0.038 g, 0.060 mmol, 80 %

^{1}H NMR (300 MHz, CD_3CN) δ 7.56 (d, *J* = 8.9 Hz, 2H, ArH), 7.26 (d, *J* = 8.9 Hz, 2H, ArH), 3.98 (s, 3H, CH_3), 3.91 (s, 3H, CH_3), 3.83 (s, 3H, CH_3), 3.78 (s, 3H, CH_3), 3.37 (s, 3H, CH_3). ^{13}C {^{1}H NMR (126 MHz, CD_3CN) δ 164.5 (C), 154.9 (C), 151.7 (C), 148.6 (C), 141.0 (C), 134.0 (CH), 116.4 (CH), 112.1 (C), 109.1 (C), 56.8 (CH_3), 37.7 (CH_3), 36.3 (CH_3), 33.3 (CH_3), 29.3 (CH_3). HRMS (ESI$^+$): *m/z* 315.1471 [M – CuI$_2$]$^+$, calculated [M – CuI$_2$]$^+$ 315.1452. Analysis Calculated for $C_{16}H_{19}N_4O_3CuI_2$ + 0.2CuI: C, 28.71; H 2.90; N, 7.93. Found: C, 28.65; H, 2.86;

N, 8.35. IR ν_{max}/cm^{-1} (solid): 1715 (C=O), 1669 (C=O), 1633, 1604, 1542, 1298 (C-N), 1256 (C-O).

4.10.5 ^{1}H NMR monitoring of the arylation reaction

A solution of **C46**, 4-iodoanisole and m-xylene in anhydrous / degassed d_7-DMF was prepared in a Glovebox and transferred into a Young's-tap NMR tube. The reaction mixture was transferred into an NMR spectrometer (500 MHz) and screened with 15-minute interval time for 16 hours at 70 °C.

4.10.6 IR monitoring of the arylation reaction

General procedure. An oven dried, 100 mL three-necked round-bottomed flask equipped with a small stirrer bar was attached to the ReactIR diamond tipped probe, dried and degassed *in vacuo* and back-filled with N_2. A background spectrum was then collected and solvent (MeCN, PhCN or DMAc) (5.5 mL) was added. At this point a reference spectrum was recorded whilst stirring. The solvent was heated to the desired temperature (70, 78, 90, 100, 120, 140 °C), stirred at the temperature for 5 minutes and another reference spectrum was recorded. After that, 4-Iodoanisole (351 mg, 1.5 mmol) was added and more solvent (0.5 mL) was added to rinse the starting material on the side of the flask. The mixture was stirred at the desired temperature for 5 minutes, then **C46** (120 mg, 0.3 mmol) was added. The reaction progress was monitored by measuring the decrease in absorbance of **C46** and 4-iodoanisole, and the increases in absorbance of **Ar46** (specific wavenumbers for each experiment are listed in the table below). All peak absorption data were exported into Excel in three forms: i) with no reference subtraction; ii) after subtraction of a reference spectrum of the solvent at room temperature; iii) after subtraction of a reference spectrum of the solvent at the reaction temperature. All subsequent manipulations were carried out on dataset iii). MeCN/PhCN was removed *in vacuo* and subsequent analysis carried out on the crude reaction mixture. The crude mixture (of the reaction in PhCN) was recrystallised in MeCN/Et_2O and the solvent removed from the filtrate *in vacuo*. Both precipitate and solid obtained from the filtrate were analysed by ^{1}H NMR spectroscopy and HRMS. In the case of reactions in DMAc, EtOAc was added to precipitate a brown solid, which was collected by filtration, washed with EtOAc and Et_2O, dried in air and analysed by ^{1}H NMR spectroscopy.

solvent	T / °C	v / cm^{-1}		
		C46	4-iodoanisole	**Ar46**
MeCN	78	1715	1287	1712, 1536
PhCN	120	1560	1247	(1515, 1567)
DMAc	120	1719	1247	1302, 1734
DMAc	70	1718	-	(1301)
DMAc	90	1719	1245	1303, (1702, 1735)
DMAc	100	1538, 1719	1247	1303
DMAc	140	1716	1246	1303, (1728)

Table 4-5: Wavenumbers used to monitor reactions at different conditions. (wavenumbers) monitored but not used in the calculation of the reaction profile.

4.11 References

(1) Zvilichovsky, G.; Garbi, H.; Nemes, E. *J. Hetero. Chem.* **1981**, *19*, 205.
(2) Che, X.; Zheng, L.; Dang, Q.; Bai, X. *Tetrahedron* **2006**, *62*, 2563.
(3) Chen, X.; Kopecky, D. J.; Mihalic, J.; Jeffries, S.; Min, X.; Heath, J.; Deignan, J.; Lai, S.; Fu, Z.; Guimaraes, C.; Shen, S.; Li, S.; Johnstone, S.; Thibault, S.; Xu, H.; Cardozo, M.; Shen, W.; Walker, N.; Kayser, F.; Wang, Z. *J. Med. Chem.* **2012**, *55*, 3837.
(4) Ye, F.; Chen, L.; Hu, L.; Xiao, T.; Yu, S.; Chen, D.; Wang, Y.; Liang, G.; Liu, Z.; Wang, S. *Bioorg. Med. Chem. Lett.* **2015**, *25*, 1556.
(5) Kovaliov, M.; Weiman, M.; Major, D. T.; Fischer, B. *J. Org. Chem.* **2014**, *79*, 7051.
(6) Gayakhe, V.; Sanghvi, Y. S.; Fairlamb, I. J. S.; Kapdi, A. R. *Chem. Comm.* **2015**, *51*, 11944.
(7) Pivsa-Art, S.; Satoh, T.; Kawamura, Y.; Miura, M.; Nomura, M. *Bull. Chem. Soc. Jpn.* **1998**, *71*, 467.
(8) Potts, K. T. *"Comprehensive Heterocyclic Chemistry"*; Pergamon Press: Oxford, 1984; Vol. 5 and 6.
(9) Ryabov, A. D. *Chem. Rev.* **1990**, *90*, 403.
(10) Bellina, F.; Caurteruccio, S.; Mannina, L.; Rossi, R.; Viel, S. *J. Org. Chem.* **2005**, *70*, 3997.
(11) Bellina, F.; Cauteruccio, S.; Rossi, R. *Eur. J. Org. Chem.* **2006**, 1379.
(12) Williams, T. J.; Bray, J. T. W.; Lake, B. R. M.; Willans, C. E.; Rajabi, N. A.; Ariafard, A.; Manzini, C.; Bellina, F.; Whitwood, A. C.; Fairlamb, I. J. S. *Organometallics* **2015**, *34*, 3497.
(13) Abdelgawad, H., University of Leeds, 2016.
(14) Lake, B. R. M.; Bullough, E. K.; Williams, T. J.; Whitwood, A. C.; Little, M. A.; Willans, C. E. *Chem. Comm.* **2012**, *48*, 4887.
(15) Chapman, M. R.; Shafi, Y. M.; Kapur, N.; Nguyen, B. N.; Willans, C. E. *Chem. Comm.* **2015**, *51*, 1282.
(16) Farhi, M.; Morel, M. *Cavigneaux A* **1968**, *50*, 91.
(17) Hie, L.; Nathel, N. F. f.; Shah, T. K.; Baker, E. L.; Hong, X.; Yang, Y.-F.; Liu, P.; Houk, K. N.; Garg, N. K. *Nature* **2015**, *524*, 79.
(18) Simmons, B. J.; Weires, N. A.; Dander, J. E.; Garg, N. K. *ACS Catal.* **2016**, *6*, 3176.
(19) Pauling, L.; Corey, R. B. *Proc. Natl. Acad. Sci. U. S. A.* **1951**, *37*, 729.
(20) Wan, Y.; Alterman, M.; Larhed, M.; Hallberg, A. *J. Org. Chem.* **2002**, *67*, 6232.

(21) Chen, J.; Feng, J.-B.; Natte, K.; Wu, X.-F. *Chem. Eur. J.* **2015**, *21*, 16370.
(22) Corey, E. J.; Venkateswarlu, A. *J. Am. Chem. Soc.* **1964**, *94*, 1690.
(23) Peng, Y.; Li, Z. *Synlett* **2006**, 1165.
(24) Serrano-Wu, M. H.; Regueiro-Ren, A.; Laurent, D. R. S.; Carroll, T. M.; Balasubramanian, B. N. *Tetrahedron Lett.* **2001**, *42*, 8593.
(25) Orsini, A.; Viterisi, A.; Bodlenner, A.; Weibel, J.-M.; Pale, P. *Tetrahedron Lett.* **2005**, *46*, 2259.
(26) Kockerling, M.; Peppel, T.; Thiele, P.; Verevkin, S. P.; Emelyanenko, V. N.; Samarov, A. A.; Ruth, W. *Eur. J. Inorg. Chem.* **2015**, 4032.

Chapter 5

Higher Oxidation States of Copper-(N-Heterocyclic Carbene) Complexes

5.1 Introduction

Previous chapters have demonstrated the diverse reactivity of Cu(I)-NHCs, as catalysts and through ligand participation in reactivity. To further understand these reaction mechanisms, attempts have been made to prepare Cu(II)-NHC and Cu(III)-NHC complexes,[1] which can potentially be used as reaction intermediate mimics. Due to the unsuitable interaction between Cu in higher oxidation states and a soft basic NHC, reductive elimination of halo-imidazolium often occurs during preparation.[2-4] Arnold achieved the preparation a Cu(II)-NHC in 2004, in which the ligand has an anionic alkoxy group as an *N*-substituent.[5] Later, Nechaev used a neutral NHC ligand together with acetate counterions to successfully prepare a Cu(II)-NHC in 2011.[2] Willans, in 2014, successfully prepared Cu(II)-NHC bromide complexes bearing neutral NHC ligands.[6] In all these (Figure 5-1) chelating ligands were used: anionic-tethered-NHCs, bidentate acetate ligands or pyridyl-tethered-NHCs, which stabilise the Cu centre as 17 or 19 electron complexes. Attempts to prepare Cu(III)-NHC halide complexes have so far proved futile, with one report leading to the reductive elimination of a halo-imidazolium ion.[3]

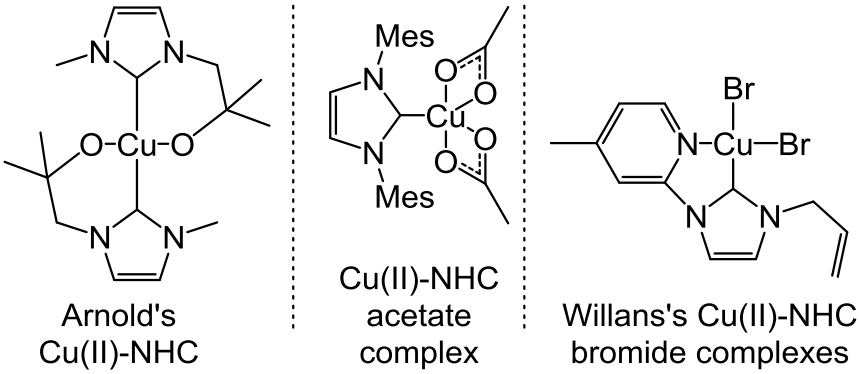

Figure 5-1: Structures of stable Cu(II)-NHC complexes.[2,5,6]

Despite the stability of the Cu(II)-NHC bromide complexes reported by Willans,[6] the outcome of the reaction changed when excess $CuBr_2$ was present. The $CuBr_2$ can form a $(\mu\text{-Br})_2$-bridge with the complex, which results in

disproportionation and reductive elimination of bromo-imidazolium from the Cu(III) centre (Scheme 5-1).[7]

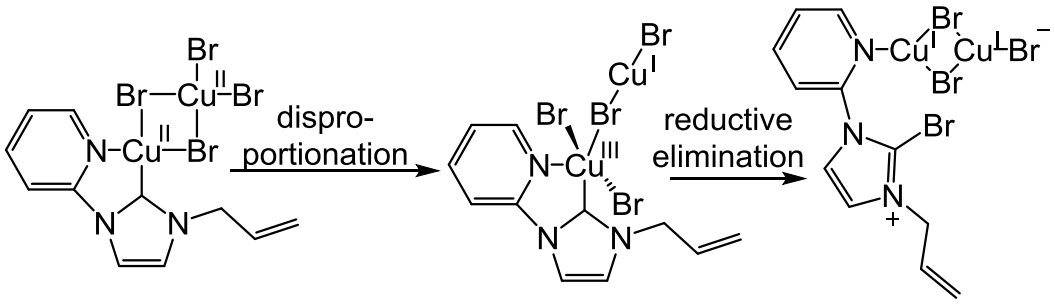

Scheme 5-1: Decomposition of Cu(II)-NHC bromide *via* disproportionation and reductive elimination of bromo-imidazolium salt.[7]

Whilst working with Cu complexes of the pyridyl, allyl substituted NHC shown in Scheme 5-1, a previous group member observed another side-product that appeared to derive from the bromo-imidazolium salt. The structure of this was not fully elucidated, but was thought to be an annulated product. This transformation may be related to a similar Ni-catalysed annulation of an alkenyl-imidazolium salt (Scheme 5-2).[8,9] The Ni-catalysed annulation occurs *via* oxidative addition of $C_{imidazolium}$-H to Ni(0), which formed a Ni(II)-NHC, followed by H-migration and reductive elimination of the annulated product. This part of the project will investigate if the allyl-bromo-imidazolium salt can undergo similar reactions at Cu, where $C_{imidazolium}$-Br is oxidatively added, followed by Br-migration and reductive elimination of a similar annulated product.

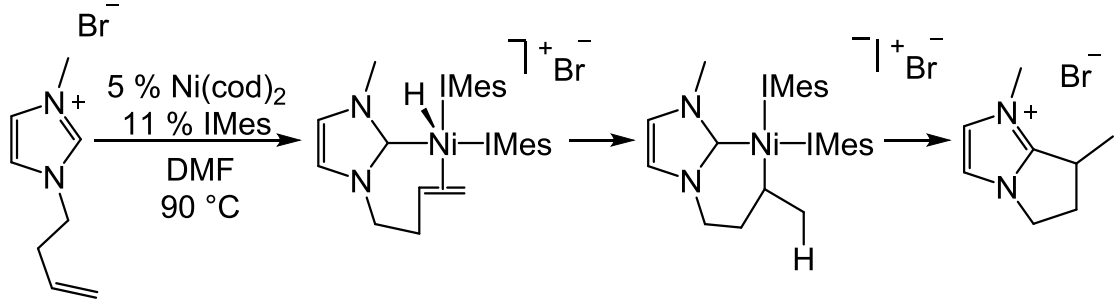

Scheme 5-2: Ni-catalysed annulation of allyl-imidazolium salt.[8]

In addition to adding knowledge to the understanding of higher oxidation state Cu, this transformation could provide a valuable route to annulated compounds that are used in the pharmaceutical and agrochemical industries. For example, α_{1A} adrenoceptor partial agonists have specific imidazole frameworks and are synthesised *via* multiple steps by functionalising a lactam to form an imidazole ring (Scheme 5-3).[10,11]

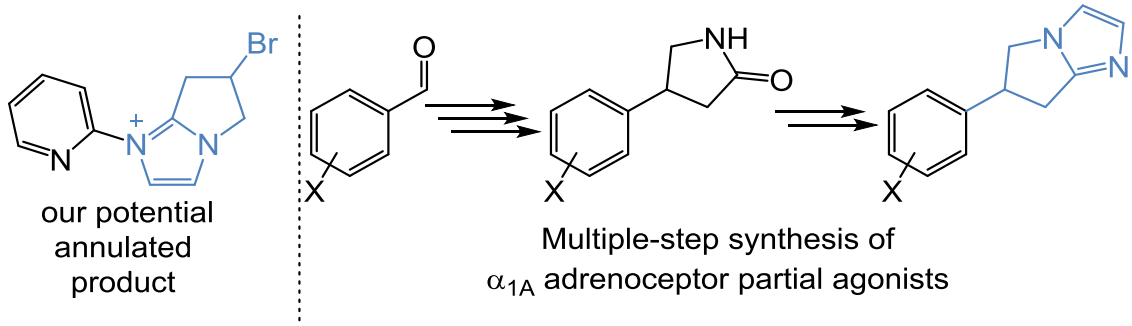

Scheme 5-3: Our predicted annulated product (lef) and synthetic route to α_{1A} adrenoceptor partial agonists.[11]

A further aim of this part of the project is to prepare a Cu(III)-NHC complex, which would be the first example of such type. Based on previous literature, Cu(III) species generally feature square planar and occasionally elongated octahedral geometries.[12-15] In recent times, chelating and macrocyclic ligands have been used to form Cu(III) complexes such as thio-oxalate, alkoxide polyanionic and aryl-amino-macrocyclic ligands (Figure 5-2). Our aim is to design square planar macrocyclic NHC-containing ligands and utilise them in the stabilisation of Cu(III) complexes, with the macrocyclic ligand helping prevent reductive elimination in which the NHC is involved.

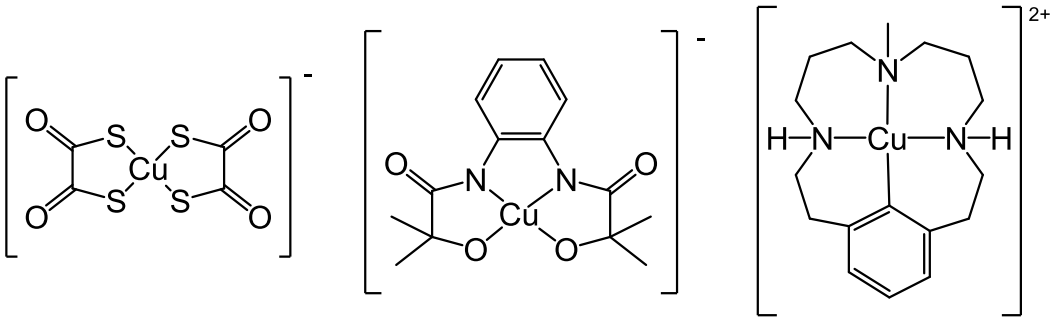

Figure 5-2: Examples of Cu(III) complexes using chelating and macrocyclic ligands.[13-15]

5.2 Reactivity of 1-alkenyl-2-bromo-3-pyridylimidazolium salts

Bromoimidazolium salt **S8.a** was prepared *via* transmetallation from a Ag(I)-NHC complex, Ag**L8**Br, with 2 equivalents of $CuBr_2$ (Scheme 5-4). **S8.a** was obtained as a dark green solid and characterised using HRMS and ^{1}H NMR spectroscopy. The ^{1}H NMR spectrum of the product showed a mixture of **S8.a** and another species, which was later identified (by comparing ^{1}H NMR resonances) as a annulated product **Cy8** (Figure 5-3). However, the elemental analysis of the sample illustrated otherwise, a mixture of a bromoimidazolium ($C_{11}H_{11}BrN_3$) and

H-imidazolium ($C_{11}H_{12}N_3$) (1: 1) were observed with a mixture of $Cu_2Br_3^-$ and $CuBr_2^-$ ions at the ratio of 3: 1. Still the elemental analysis and HRMS cannot distinguish between the **S8** and its annulated product **Cy8** due to the same formula. Single crystals suitable for X-ray diffraction analysis were grown by the vapour diffusion of Et_2O into a concentrated solution of the product in MeCN. **S8.a** crystallised as a dimer of bromo-imidazolium cation with $Cu_4Br_5^-$ counter ion and MeCN in the monoclinic crystal system and the structural solution was performed in the space group $P2_1/n$ (Figure 5-4). As the counter ion results obtained from elemental analysis and x-ray crystallography are different, $Cu_2Br_3^-$ or $Cu_4Br_5^-$ cannot be concluded as the real circumstance. It is likely that the crystallographic data is a result from just one crystal and not the overall product, which might have a mixture of $Cu_xBr_{x+1}^-$ as counter ions (x = 0, 1, 2, …).

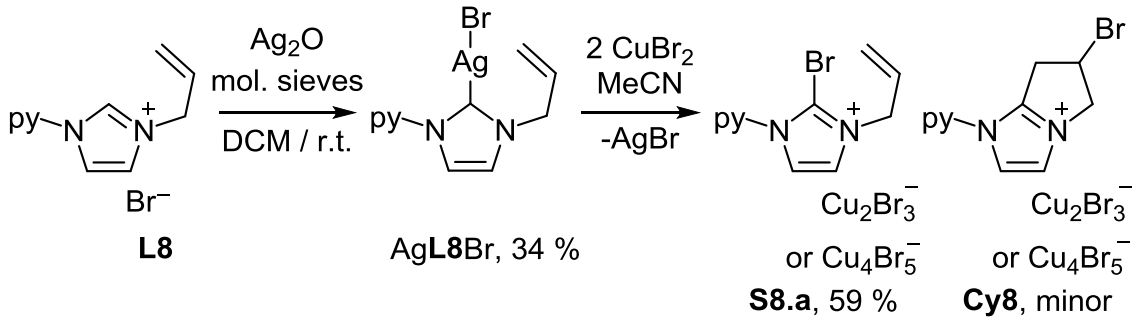

Scheme 5-4: Preparation of **S8.a** *via* Ag**L8**Br transmetallation.

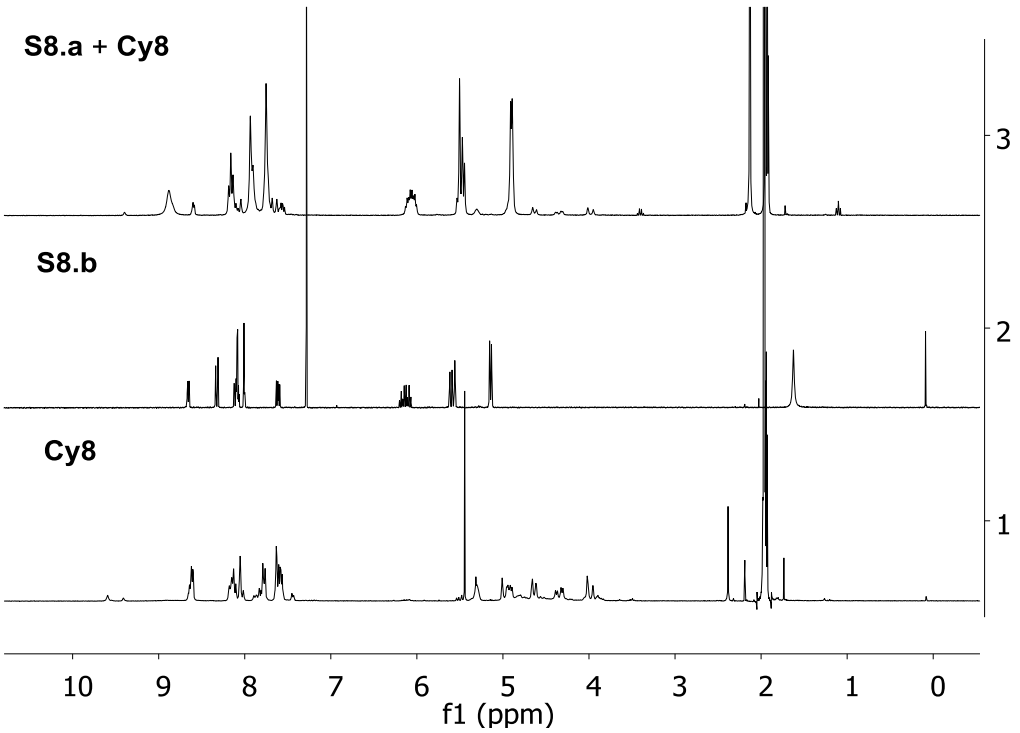

Figure 5-3: ^{1}H NMR spectra of a mixture of **S8.a** and **Cy8** (300 MHz, CD_3CN), **S8.b** (300 MHz, $CDCl_3$) and **Cy8** (300 MHz, CD_3CN). S8.b is a non-Cu containing derivative of **S8.a** *i.e.* with a Br^- counterion.

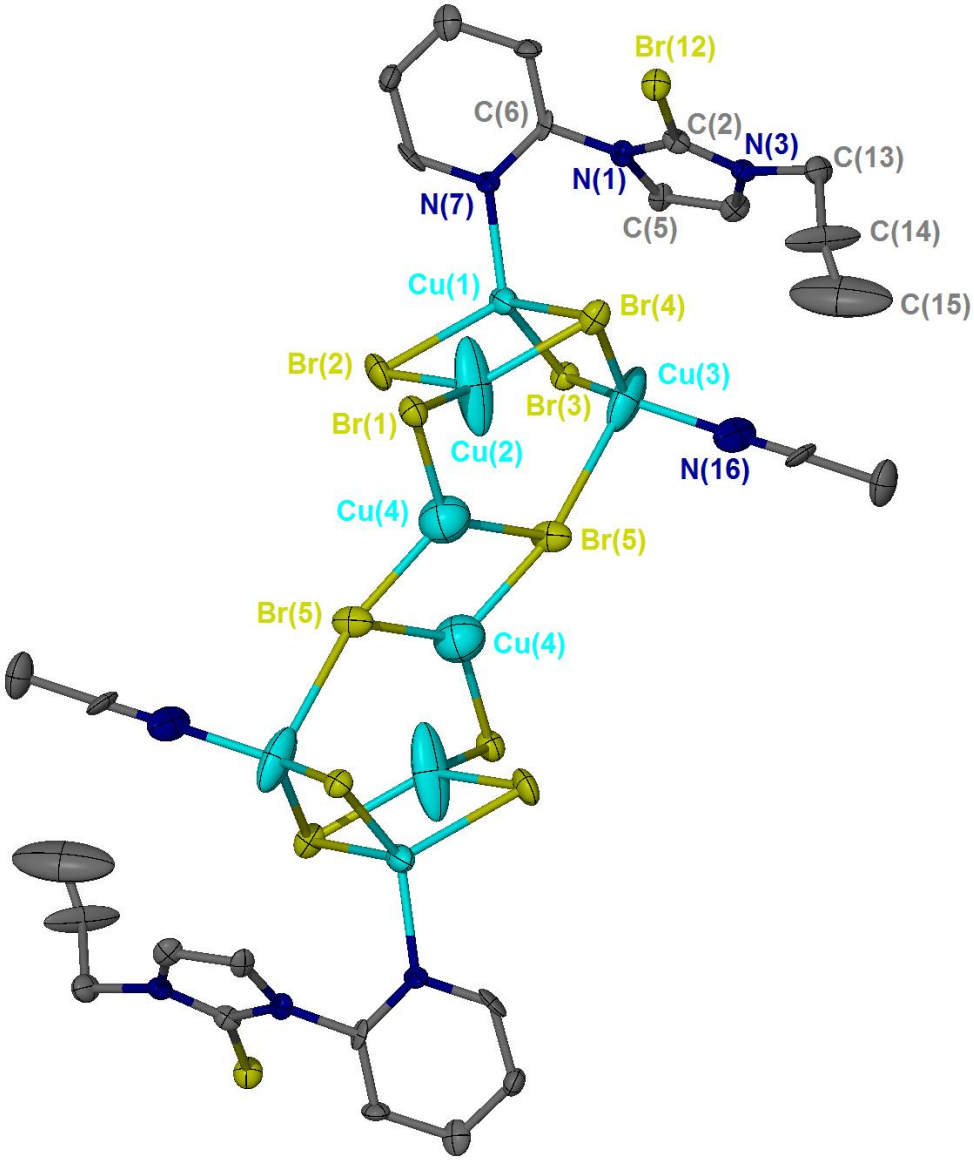

Figure 5-4: Molecular structure of **S8.a**. Ellipsoids are drawn at the 50% probability level and H atoms are omitted for clarity.

C(2)-Br(12)	1.856(13)	N(1)-C(2)-N(3)	110.8(11)
N(1)-C(2)	1.359(17)	N(3)-C(13)-C(14)	111.8(15)
C(2)-N(3)	1.281(17)	C(13)-C(14)-C(15)	144(3)
C(13)-C(14)	1.52(3)	N(7)-C(6)-N(1)-C(5)	-58.6(17)
C(14)-C(15)	1.02(4)		
Cu(1)-N(7)	1.993(17)		
Br(1)-Cu(2)	2.440(8)	Cu(2)-Br(1)-Cu(4)	63.2(2)
Br(1)-Cu(4)	2.382(7)		
Br(2)-Cu(1)	2.503(5)	Cu(1)-Br(2)-Cu(2)	66.3(2)
Br(2)-Cu(2)	2.290(8)		
Cu(1)-Br(3)	2.380(4)	Cu(1)-Br(3)-Cu(3)	68.67(17)
Cu(3)-Br(3)	2.381(7)		
Br(4)-Cu(1)	2.815(5)	Cu(1)-Br(4)-Cu(2)	60.9(2)
Br(4)-Cu(2)	2.286(9)	Cu(1)-Br(4)-Cu(3)	60.73(16)
Br(4)-Cu(3)	2.464(6)	Cu(2)-Br(4)-Cu(3)	84.4(3)
Br(5)-Cu(3)	2.795(7)	Cu(3)-Br(5)-Cu(4)	117.2(2)
Br(5)-Cu(4)	2.332(4)	Cu(3)-Br(5)-Cu(4)'	161.6(3)
Br(5)-Cu(4)'	2.432(4)	Cu(4)-Br(5)-Cu(4)'	61.8(3)

Table 5-1: Selected bond distances (Å) and angles (deg) in the solid-state structure of bromoimidazolium salt **S8.a**.

The C(2)-Br(12) bond length of 1.856(13) Å in **S8.a** is in the normal range for C_{sp^2}-Br bond lengths.[16] A significant difference between **S8.a** and **L8** is that there is a distortion plane between the pyridyl and imidazolium rings in the case of **S8.a**, whereas in **L8** they lie almost coplanar.[6] The cluster of $Cu_8Br_{10}^{2-}$ is a dimer of $Cu_4Br_5^-$, in which most of the Cu-Br-Cu angles are in the range of 60 – 68 °. However, the Cu(2)-Br(4)-Cu(3) and Cu(3)-Br(5)-Cu(4) angles are much larger (84 and 117 ° respectively). The Cu(4)s and Br(5) act as the bridge that connects 2 $Cu_4Br_5^-$ clusters together Hence, the Cu(3)-Br(5)-Cu(4)' is near linear (162 °). This bridging structure is similar to the neutral aggregate of Cu_8I_8 in Feng's work.[17]

S8.a was heated at 95 ºC for 6 days in the absence of solvent with the aim of promoting the annulation reaction. The product was analysed by ^{1}H NMR spectroscopy (Figure 5-5) and was found to contain a dihydropyrrolyl bearing a bromine atom (**Cy8,** Scheme 5-5) in addition to several other decomposition products. ^{1}H COSY NMR experiment was used to determine the geminal and vicinal coupling among the protons of the annulated ring (H_A – H_E) (Figure 5-6). The 2D spectrum shows that H_C couples with H_A, H_B, H_D and H_E as there are four cross peaks corresponding to those protons horizontal to the diagonal peak of H_C. Furthermore, H_A and H_B couple each other (likely geminal) but not the other pair of H_D and H_E and likewise. This illustrates that the methylene pairs are not adjacent to each other as the COSY technique does not take a long range coupling into account. The coupling constants of the region were further analysed from the ^{1}H NMR spectrum. There are two pairs of diastereotopic protons (H_A and H_B, and H_D and H_E), in which ^{2}J coupling constants of 19.5 and 13.5 Hz were observed respectively (Figure 5-7). H_A and H_D each couples with H_C, which is *cis* to them, with a ^{3}J coupling constant 2.9 Hz for both. The small coupling constants resulted in the absence of two cross peaks corresponding to H_C coupled by H_B and H_E. H_B and H_E each couples with H_C with a $^{3}J_{trans}$ coupling constant of 7.2 Hz and 6.4 Hz respectively. When **S8.a** was heated in microwave oven at 90 ºC for 15 minutes, the same reaction took place, with evidence of decomposition in addition to **Cy8** formation.

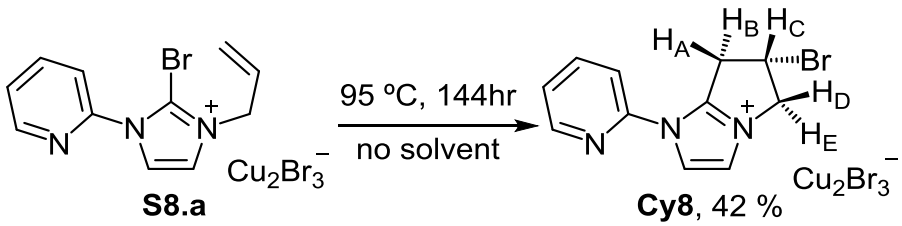

S8.a **Cy8**, 42 %

Scheme 5-5: Annulation reaction of **S8.a**.

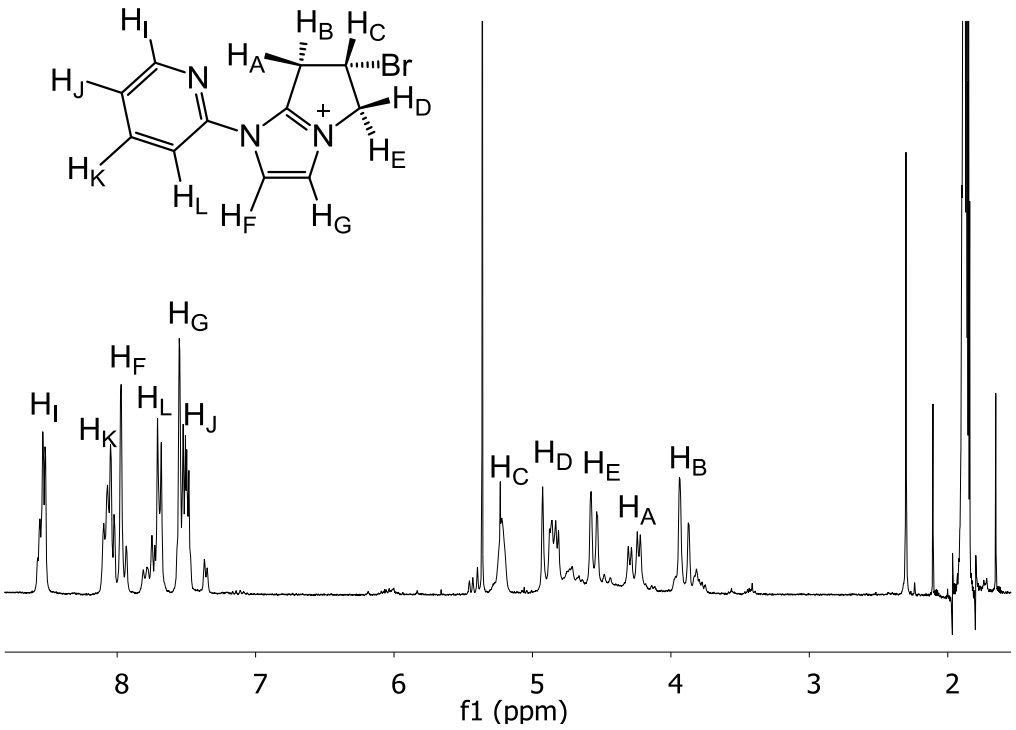

Figure 5-5: ^{1}H NMR spectrum (300 MHz, CD_3CN) of crude **Cy8**.

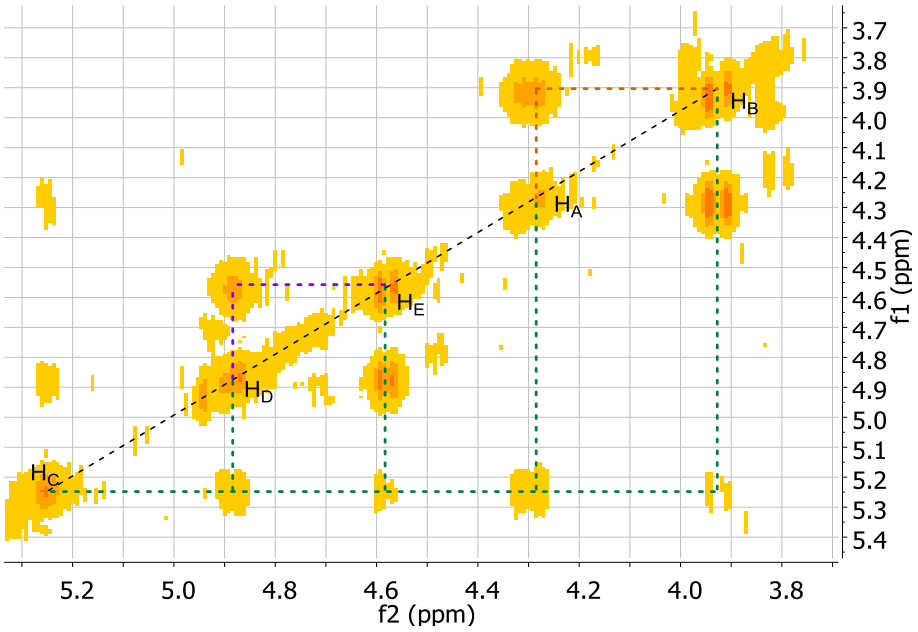

Figure 5-6: 2D ^{1}H COSY spectrum (500 MHz, CD_3CN) of **Cy8**.

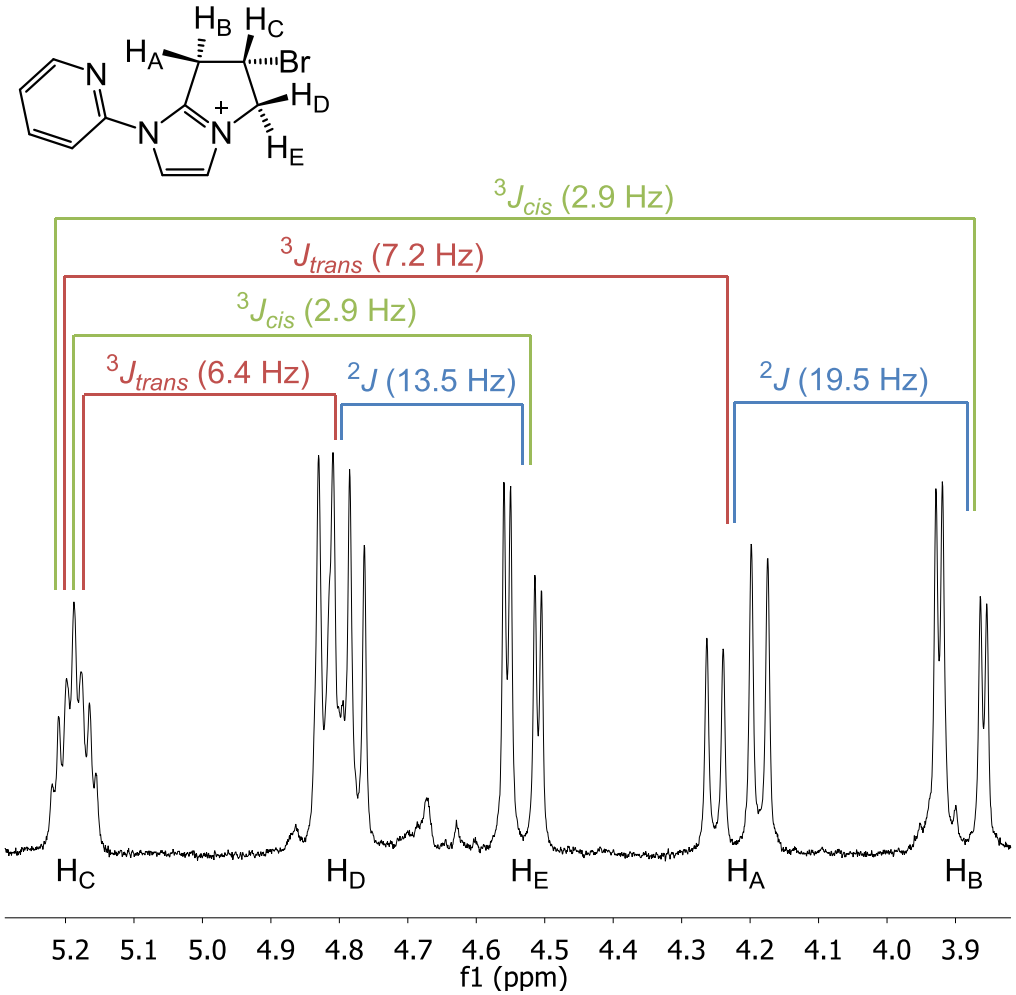

Figure 5-7: Assignment of the ^{1}H spectrum of **Cy8** in the dihydropyrrolyl region, showing ^{2}J and ^{3}J coupling constants (Hz).

To investigate the necessity of Cu in this reaction, a novel Cu-free analogue of **S8.a** was prepared (**S8.b**). Imidazole **P8** was brominated using NBS to give a novel **PS8** (Scheme 5-6a), with the bromination reaction occurring predominantly at the most acidic position (H-2). However, further bromination was observed at other positions, with column chromatography being required to isolate the desired product. **PS8** was allylated to give bromo-imidazolium salt **S8.b** (Scheme 5-6b). In the ^{1}H NMR spectra of **PS8** and **S8.b**, the H-2-imidazole and H-2-imidazolium peaks were no longer observed, compared to **P8** and **L8**, the non-brominated analogues (Figure 5-8). Moreover, the backbone imidazole and imidazolium peaks are more upfield than the non-brominated imidazole/imidazolium analogues.

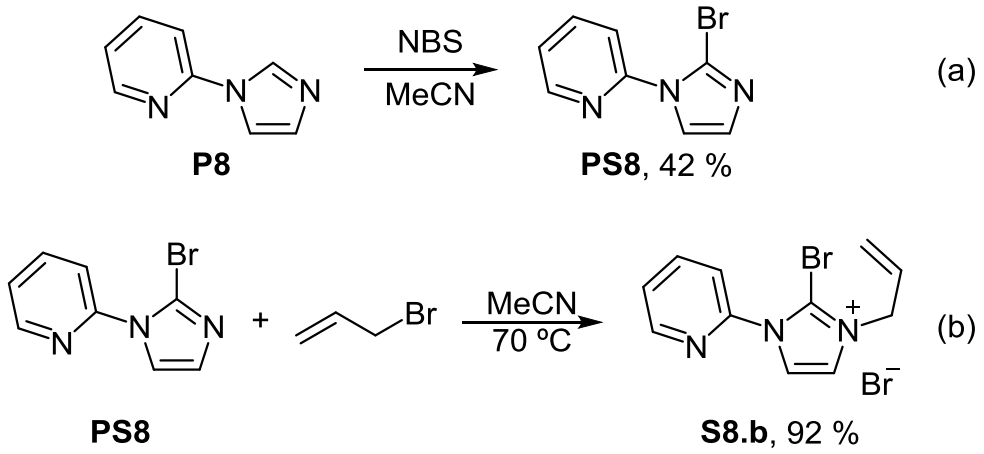

Scheme 5-6: Preparation of **S8.b** *via* bromination of **P8**.

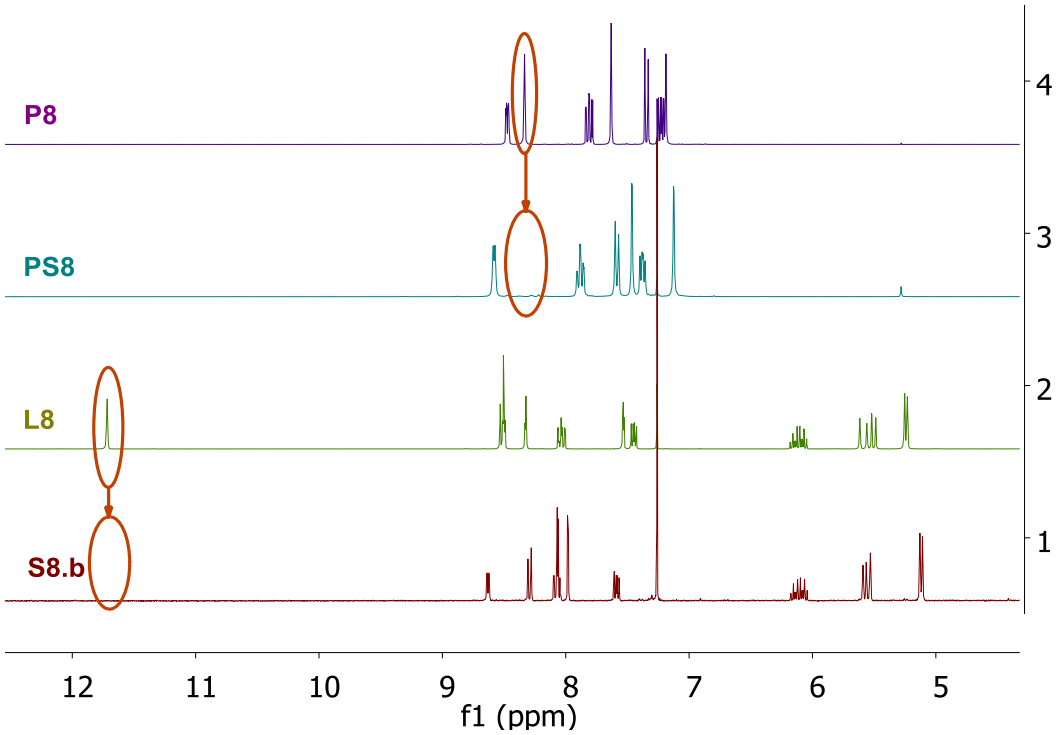

Figure 5-8: ^{1}H NMR spectra (300 MHz, $CDCl_3$) of **P8**, **PS8**, **L8** and **S8.b**.

Crystals suitable for X-ray diffraction analysis were grown of both **PS8** and **S8.b** (Figure 5-9 and Figure 5-10). Single crystals of **PS8** were grown by the vapour diffusion of pentane into a concentrated solution of the product in $CHCl_3$, and those of **S8.b** were grown by the vapour diffusion of Et_2O into a concentrated solution of the product in MeCN/MeOH.

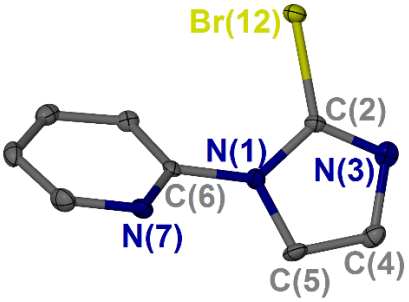

Figure 5-9: Molecular structure of **PS8**. Ellipsoids are drawn at the 50% probability level and H atoms are omitted for clarity.

C(2)-Br(12)	1.870(3)	N(1)-C(2)-N(3)	114.0(3)
N(1)-C(2)	1.374(4)		
C(2)-N(3)	1.304(4)		

Table 5-2: Selected bond distances (Å) and angles (deg) in the solid-state structure of brominated pyridylimidazole, **PS8**.

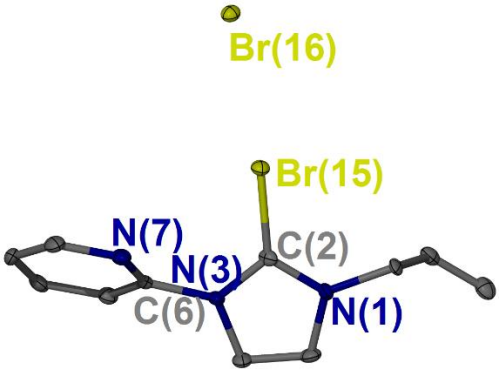

Figure 5-10: Molecular structure of the bromoimidazolium salt **S8.b**. Ellipsoids are drawn at the 50% probability level and H atoms are omitted for clarity.

Br(15)-C(2)	1.862(3)	N(1)-C(2)-N(3)	108.3(3)
N(1)-C(2)	1.337(3)	N(7)-C(6)-N(3)-C(2)	-53.4(4)
C(2)-N(3)	1.333(4)		
Br(15)-Br(16)	3.149		

Table 5-3: Selected bond distances (Å) and angles (deg) of **S8.b**.

In the absence of solvents, the substrate **S8.b** was heated with 0, 1 and 2 equivalents of CuBr for 168 hours. Only when 2 equivalents of CuBr were incorporated in the reaction mixture did the annulation reaction occur to any significant extent (Scheme 5-7). In the presence of 1 equivalent of CuBr, there was only 16 % conversion, as calculated from ^{1}H integrals in ^{1}H NMR spectrum

of the crude product at δ 6.10, 5.50 ppm for **S8.b** and at δ 5.28 ppm for **Cy8** (Figure 5-11).

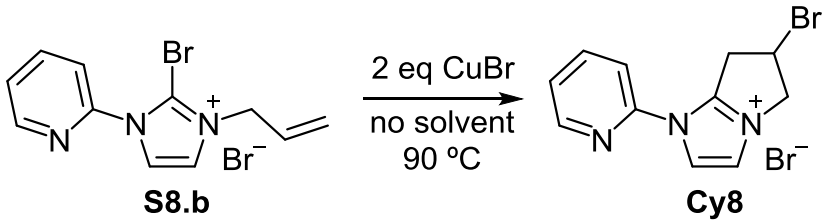

S8.b **Cy8**

Scheme 5-7: Annulation reaction of **S8.b** in the presence of CuBr.

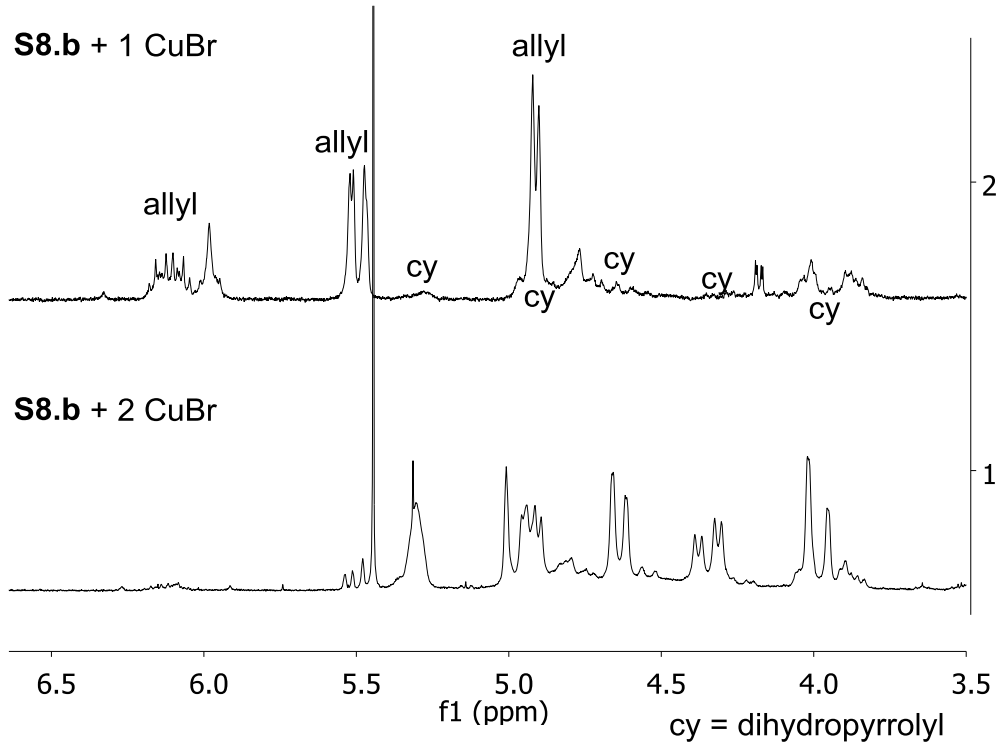

Figure 5-11: ^{1}H NMR spectra (300 MHz, CD_3CN) of a crude mixture when **S8.b** was heated with 1 and 2 equivalents of CuBr at 95 °C for 168 hours in the absence of solvents.

This suggests that C-Br activation through oxidative addition, and alkene coordination occur at different Cu atoms, which are possibly bridged by a bromide ion. Bromide migration to the alkene will form an anionic alkyl ligand, which is a hard base and more suitable to bond to Cu(III) than Cu(I). Hence, the alkyl species coordinates to Cu(III) to form a 6-membered metallacycle. Reductive elimination of **Cy8** would form a 5-membered ring, giving the suggested product (Scheme 5-8). DFT calculations would determine the feasibility of the hypothesised mechanism.

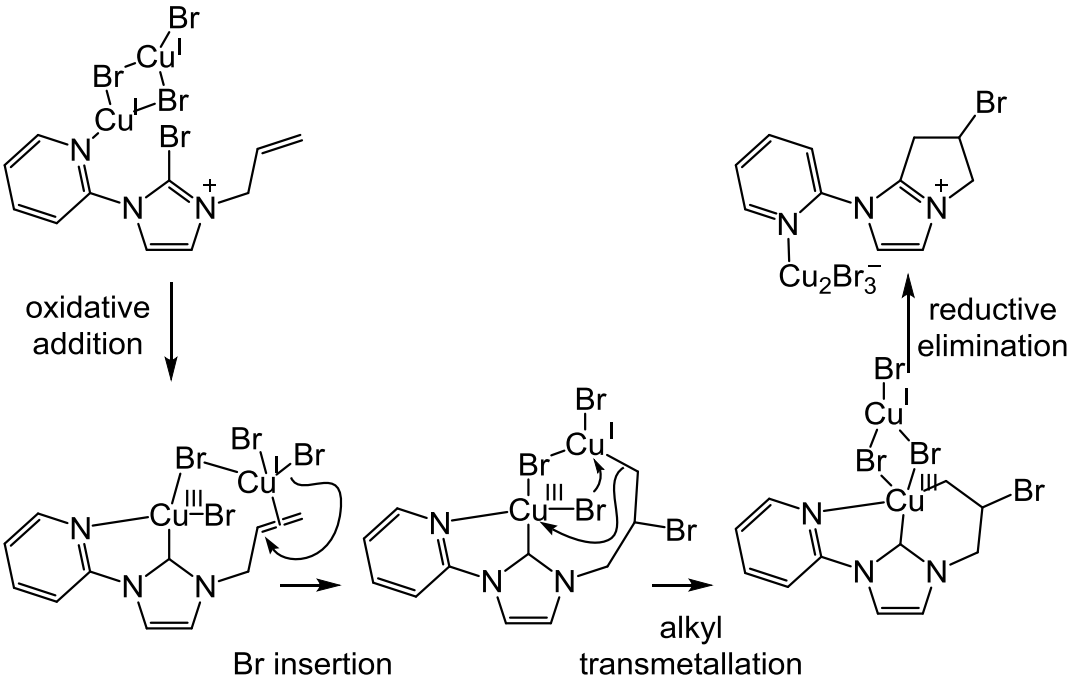

Scheme 5-8: Proposed mechanism for the annulation reaction of **S8**.

5.3 Reactivity of other 2-bromoimidazole derivatives

To compare the Cu-mediated annulation reaction with a reported Rh-catalysed annulation of 1-allylimidazole (Scheme 5-9),[18] the novel brominated imidazoles **S52** and **S53** were to be prepared. The annulated product of 1-allyl-2-bromoimidazole would be neutral, leading to more facile isolation from Cu and other side-products when compared to imidazolium species (*i.e.* **Cy8**).

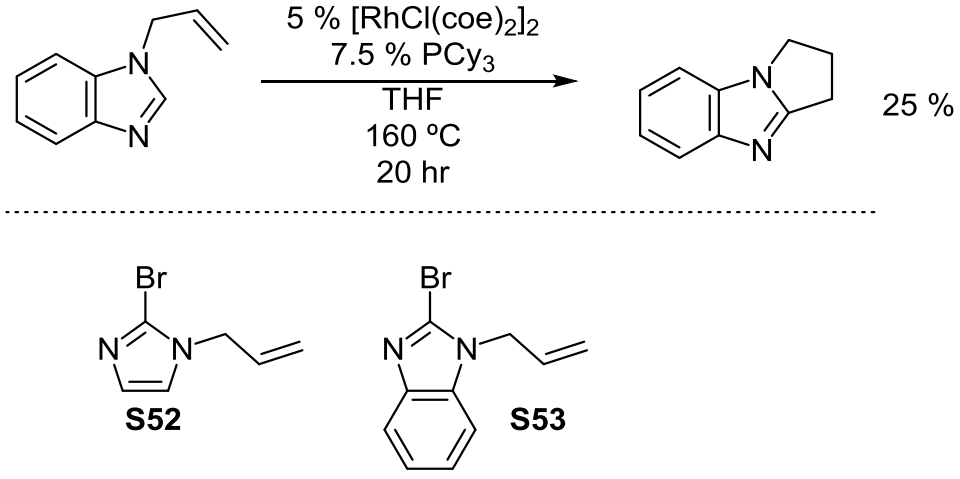

Scheme 5-9: Rh-catalysed annulation of 1-alkenylimidazole (top) [18] and imidazoles **S52** and **S53** prepared to investigate the Cu-mediated process (bottom).

Many methods were attempted to prepare **S52**. Direct bromination of 1-allylimidazole using NBS gave a mixture of various brominated products as

observed by LCMS, with at least 3 bromoimidazole isomers, 2 dibromoimidazole isomers and 1 tribromoimidazole species (Scheme 5-10, Figure 5-12). Mono-brominated isomers can be separated from the starting material, and other brominated species by column chromatography. However, **S52** cannot be separated from other mono-brominated species in the mixture despite using gradient eluents, as they have very similar physical properties.

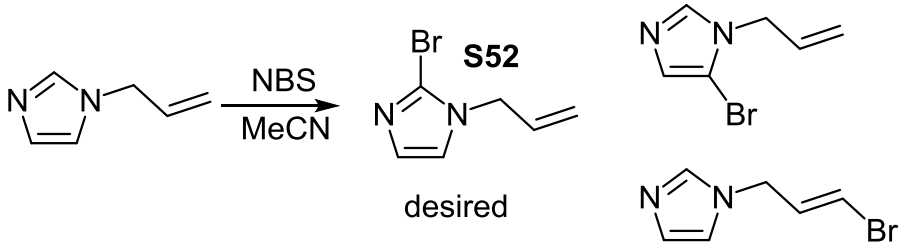

Scheme 5-10: Attempted synthesis of 1-allyl-2-bromoimidazole **S52** and other products formed.

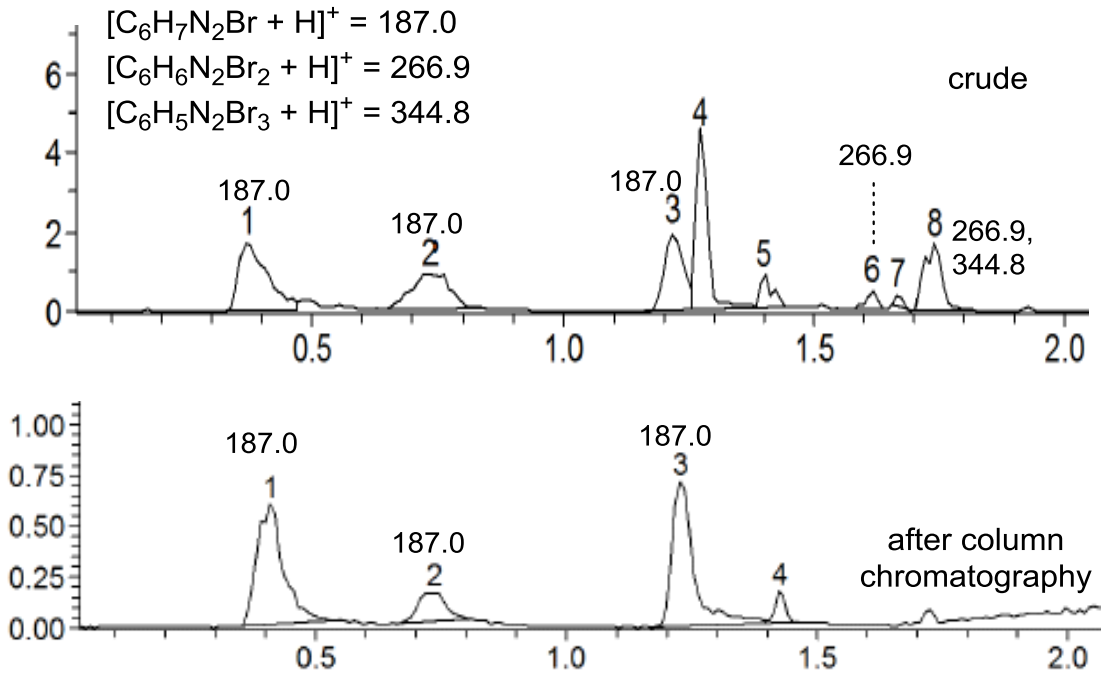

Figure 5-12: LCMS chromatograms of the crude mixture following bromination 1-allylimidazole (top) and a mixture of monobromo-allylimidazole isomers (bottom).

Another approach used was to protect one nitrogen of imidazole using a trityl group,[19,20] or a tetrahydropyranyl (THP) group,[21] and brominate at the C-2 position to afford **55** or **56** (Scheme 5-11). Deprotection of the trityl or THP group in a presence of acid would afford **57**, which would be functionalised to prepare **S52**. However, bromination of these protected imidazoles (**P5'** and **P54**) with *n*-BuLi and NBS was unsuccessful. Expected molecular ions [**55** + H]$^+$, [**56** + H]$^+$ or [**57** + H]$^+$ were not observed in HRMS of either crude products. It is unclear

what occurred in the case of the trityl protected imidazole. However, the ^{1}H NMR spectrum of the crude product from the reaction involving imidazole **P54** indicated that bromination may have occurred on the THP ring, as the proton resonance corresponding to the C-2 position was no longer observed in the crude product. Another possibility is that the protecting group was cleaved to form THP-Br, as the integrations of the imidazole resonances are significantly lower than those of the THP ring (1:7 instead of the expected 1:1).

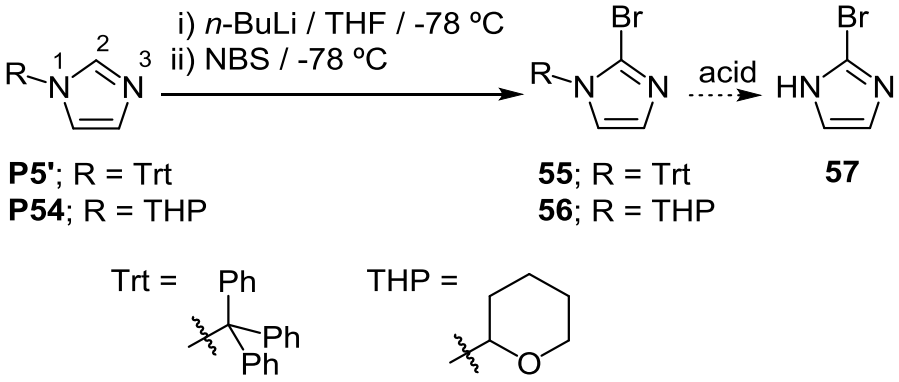

Scheme 5-11: Attempted synthetic route to 2-bromoimidazole using trityl or THP as the imidazole protecting group

Another reported brominating agent is perbromide ionic liquid (**59**), which can also be used as a solvent.[22] This reagent was prepared from addition of a slight excess of Br_2 to 1-butyl-3-methylpyridinium bromide (**58**) (Scheme 5-12a). The excess Br_2 was removed *in vacuo*, while the product was obtained as a bright orange liquid. Addition of a stoichiometric amount of imidazole to the ionic liquid resulted in a formation of tribromoimidazole, as observed in HRMS m/z = 304.7734. A modification of the method involved using ionic liquid **59** in anhydrous MeCN, which was added dropwise to a anhydrous solution of imidazole in MeCN at 0 ºC (Scheme 5-12b). After 15 minutes, water was added to quench the reaction. Following extraction by organic solvent and purification using column chromatography, it was found that the product obtained was 5-bromoimidazole (**60**) rather than the desired 2-bromoimidazole (**57**), characterised using ^{1}H NMR and ^{13}C {^{1}H} NMR spectroscopies and HRMS.

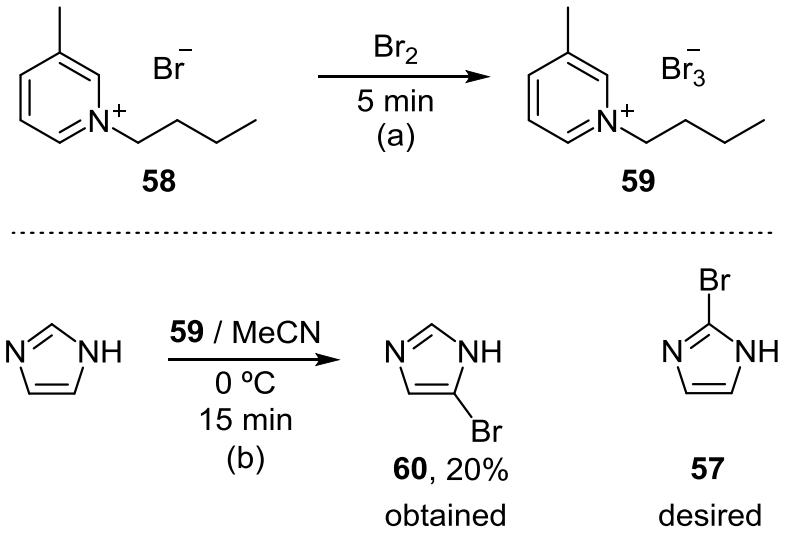

Scheme 5-12: Preparation of the ionic liquid **59** and attempts to apply in the bromination of imidazole.

As bromination by the ionic liquid **59** occurred at the undesired position, benzimidazole was used instead of imidazole, with the rationale that the arene ring will block bromination from taking place at the backbone position. However, the characterisation of the purified product of the reaction of benzimidazole with **59** suggest the formation of 5-bromobenzimidazole or 6-bromobenzimidazole (Scheme 5-13). This suggests that bromination occurs *via* the bromo cation which selectively attacks the aromatic ring with the most electrophilic site.

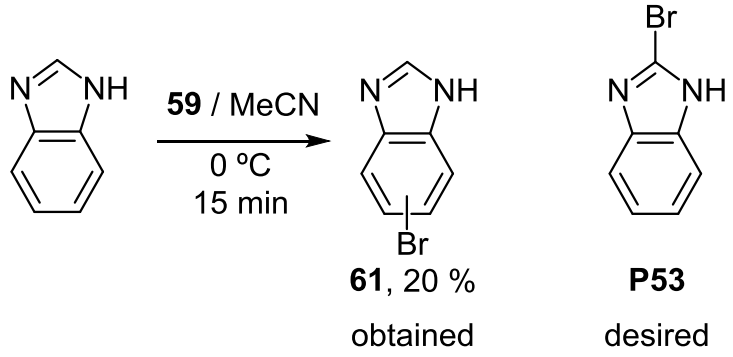

Scheme 5-13: Bromination of benzimidazole by **59**.

Due to difficulties in selective C-2 bromination, 2-bromobenzimidazole (**P53**) was purchased and deprotonated in anhydrous, degassed THF using NaH, followed by nucleophilic substitution with allyl bromide to obtain 1-allyl-2-bromobenzimidazole, which was characterised by ^{1}H and $^{13}C\{^{1}H\}$ NMR spectroscopies and HRMS (**S53**) (Scheme 5-14).

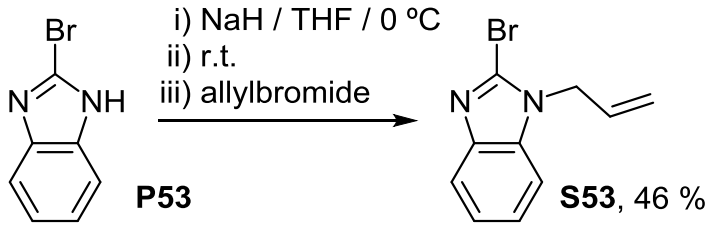

Scheme 5-14: Preparation of **S53**.

To mimic the Rh-catalysed annulation of 1-allylbenzomidazole (Scheme 5-9), **S53** was heated with a catalytic amount (10 mol%) of CuI in CD_3CN at 70 ºC. However, the resonances attributed to a dihydropyrrolyl (*i.e.* the annulated product) were not observed in ^1H NMR spectra (Figure 5-13), whereas the allyl peaks split into more than one set, which suggests that more than one allyl-containing species has been formed. The crude reaction mixture was analysed by LCMS, with the spectra indicating that a benzimidazole-dimer and bis(benzimidazolyl) ether have formed (Scheme 5-15).

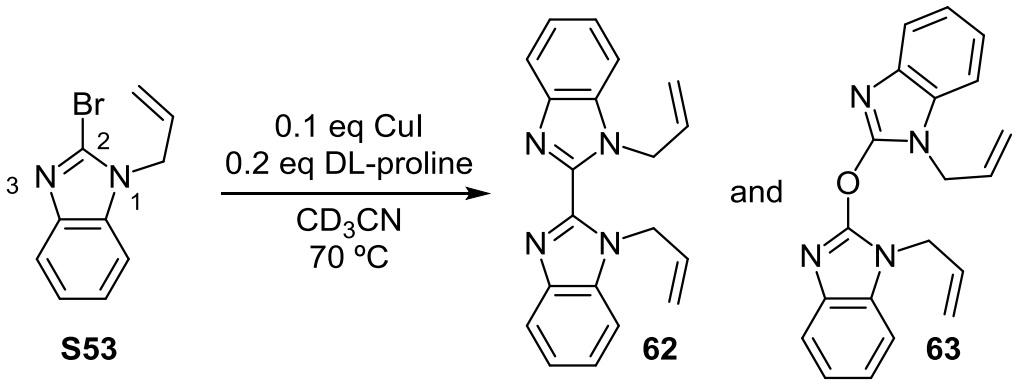

Scheme 5-15: Dimerisation of **S53**.

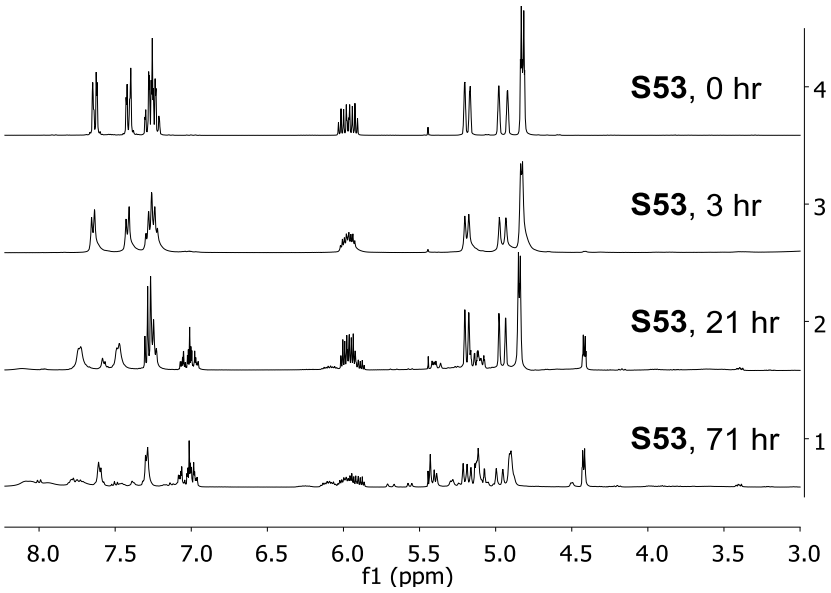

Figure 5-13: ^{1}H NMR spectra (300 MHz, CD_3CN) of **S53** following reaction with 10 % CuI and 20 % DL-proline at 0, 3, 21 and 71 hours.

Although the annulation of 1-allylbenzimidazole by a Rh catalyst (10 % loadings) was successful (25 % yield),[18] the annulation of **S53** did not occur, likely due to the bromine atom replacing the H-2 in benzimidazole. DFT calculations for the Rh-catalysed reaction were performed and the most facile mechanism (152 kJ mol^{-1}) was proposed to take place *via* a stable Rh-NHC intermediate, following concerted proton migration to the N-3 position of the imidazole to form a Rh-NHC complex (Scheme 5-16).[23] However, Br-migration in a similar manner to form an NHC complex might not be possible.

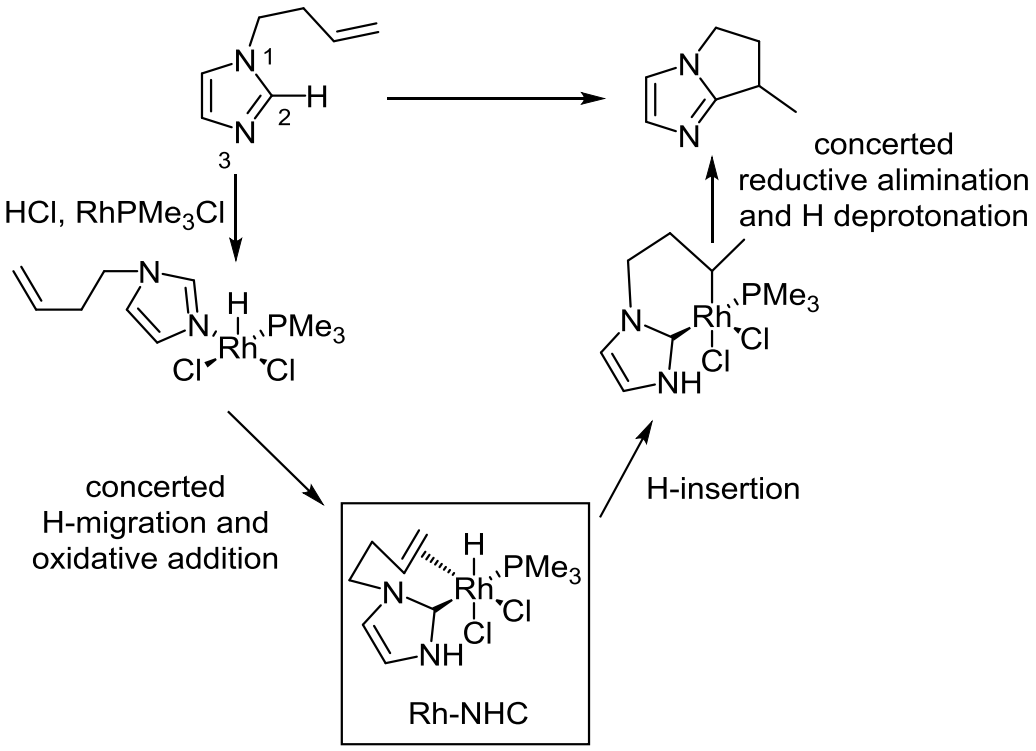

Scheme 5-16: Proposed mechanism of Rh-catalysed annulation of 1-allylbenzimidazole.[18,23]

Another bromo-imidazolium salt, **S64**, in which the pyridyl group of **S8** was replaced by a methyl group, was investigated. **S64** was prepared from the selective bromination of **P3**. Unlike the bromination of **P8** to obtain **PS8**, the bromination of **P3** requires the presence of NaH, otherwise the reaction would occur at the C-5 position instead of the desired C-2 position (Scheme 5-17). Without prior deprotonation, the electrophilic addition occurs at the most electrophilic site, which is the C-5 position of the aliphatic *N*-substituted imidazole and the C-2 position of the aromatic *N*-substituted imidazole. The deprotonation of **P3** occurs at the C-2 position and hence leads to the bromination at the desired position. **S64** was prepared by allylation of **P64** and tested for the annulation reaction in the presence of 2 equivalents of CuBr. However, the expected resonances attributed to the cyclised bromodihydropyrrolyl were not observed in the ^{1}H NMR spectra of the reaction product.

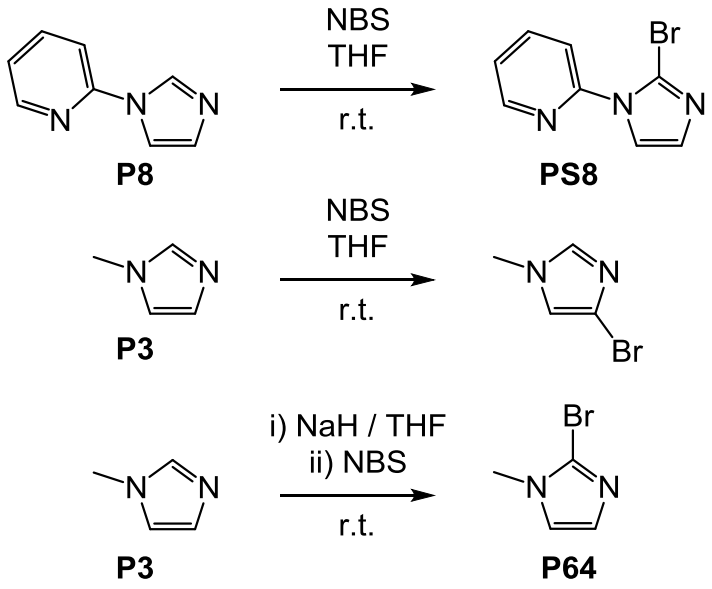

Scheme 5-17: Bromination reactions of **P8** and **P3**.

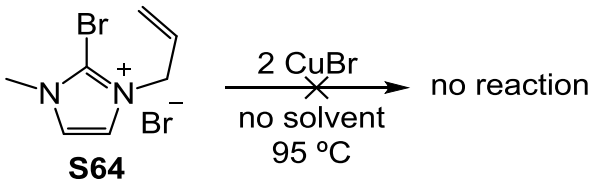

Scheme 5-18: No reactivity of **S64** when heated in the presence of excess CuBr.

The lack of reactivity in **S64** demonstrates that the pyridyl *N*-substituent is essential for the annulation reaction to occur. The pyridine group can co-ordinate to Cu, which brings the Cu into close proximity for the C-Br activation to take place.

5.4 Attempts to synthesise a Cu(III)-NHC *via* oxidative addition

As discussed previously, high-oxidation-state Cu is unsuitable for forming stable complexes with NHC ligands. However, we have endeavoured to overcome this challenge by intelligent ligand design and use of the macrocyclic effect. Cu(III) is d^8 and would usually prefer square planar geometry. One of the literature examples of a Cu(III) organometallic complex utilises an aryl-triamino-macrocyclic ligand, which relies on deprotonation of H-C_{aryl} and dispro-portionation from Cu(II) to form a macrocyclic Cu(III)-aryl complex and a Cu(I) complex (Scheme 5-19).[24] Another report discusses oxidative addition of C_{aryl}-Cl to Cu(I) to form a macrocyclic Cu(III) complex, with DFT calculations supporting the feasibility of such reaction (Scheme 5-20).[25]

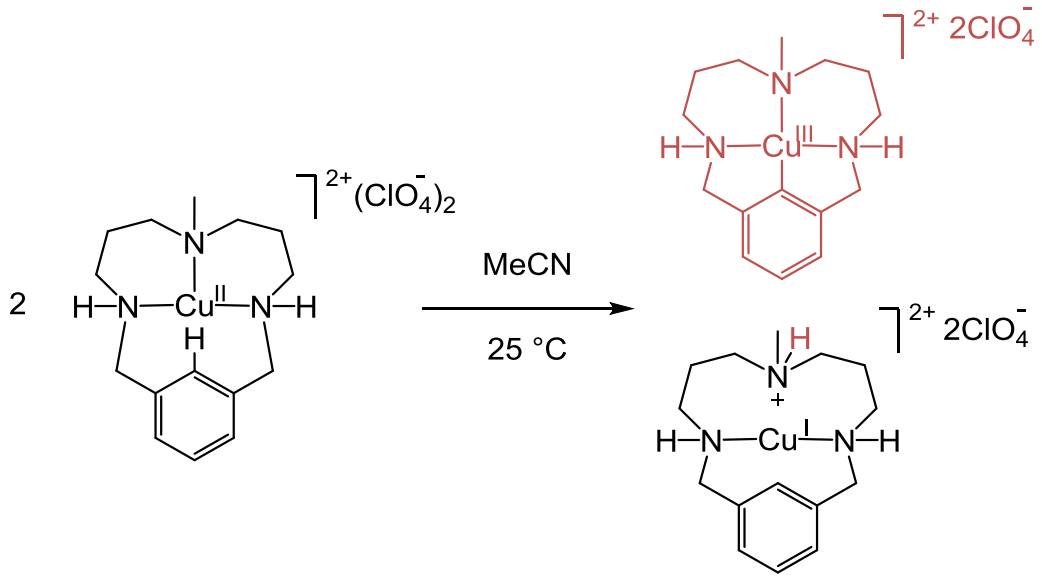

Scheme 5-19: Disproportionation of a Cu(II) complex to form a macrocyclic Cu(III)-aryl complex and a Cu(I) complex.[24]

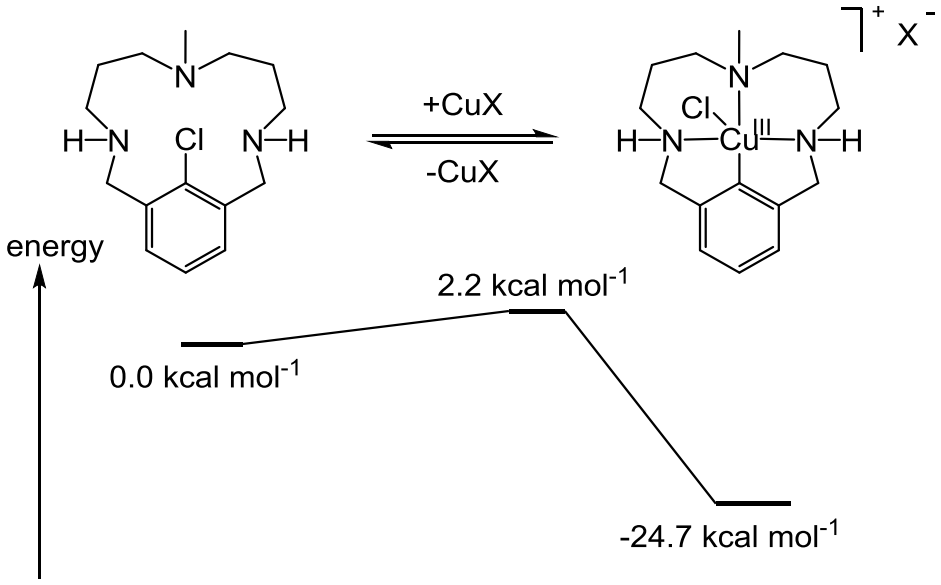

Scheme 5-20: Oxidative addition of a macrocyclic Cl-aryl ligand to Cu(I) to form a macrocyclic Cu(III) complex.[25]

The design of our NHC ligand involves a macrocyclic structure, which contains 4 binding sites for square planar geometry and a C_{aryl}-Br for oxidative addition. The first strategy involved the bromine being at the C-2 position of one of the imidazoliums (H_2**L65**X_2) (Figure 5-14). It was anticipated that Cu(I) coordination would occur from 1 NHC and 2 pyridine sites that are arranged in a T-shape position, with oxidative addition of the $C_{imidazolium}$-Br bond occurring to give the desired Cu(III)-(macrocyclic NHC) complex.

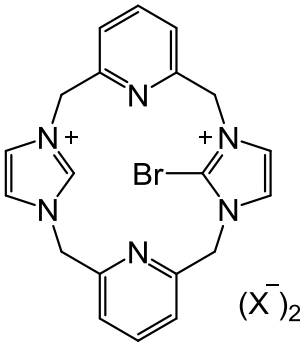

H_2**L65**X_2

Figure 5-14: Structure of the proposed H_2**L65**X_2.

Attempts to prepare the ligand precursor started from transforming pyridine derivative **66** to **67** *via* an S_N1 reaction under acidic conditions. 2 equivalents of imidazole were deprotonated by NaH in THF and reacted with **67** to obtain **68** (53 % yield). The selective bromination of **68** proved challenging. Reacting **68** with NBS in MeCN gave the desired product **P65** in a very small amount (2 %) as the bromination is more selective towards the imidazole backbone positions. Another attempt was carried out using *n*-BuLi to selectively deprotonate the H-2 imidazole ring prior to addition of NBS. However, there was no evidence of either **68**, brominated product or any species containing a bromine atom observed in HRMS. Instead an alternative ligand was proposed.

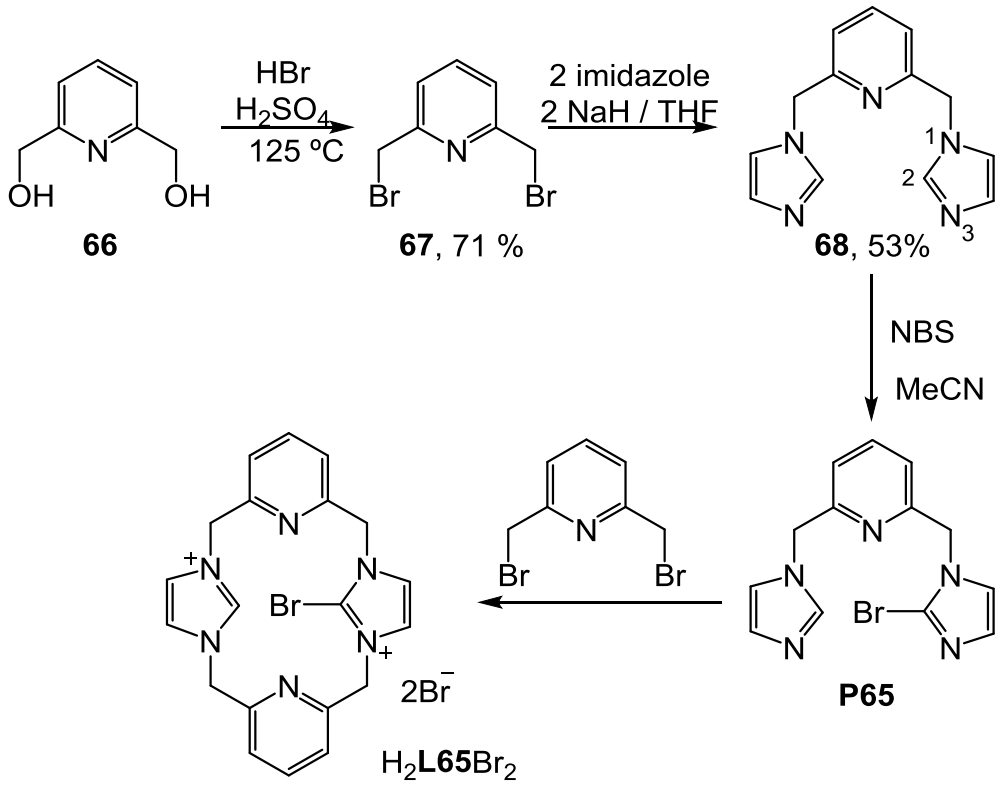

H_2**L65**Br_2

Scheme 5-21: Synthetic route to H_2**L65**Br_2.

Another macrocyclic NHC ligand was proposed, in which a bromo-aryl replaced one of the pyridine rings (Figure 5-15). This ligand is very similar to the macrocyclic ligand in Ribas's work on Cu(III) complexes, which has one anionic aryl and three neutral *N*-coordination sites (**C70**).

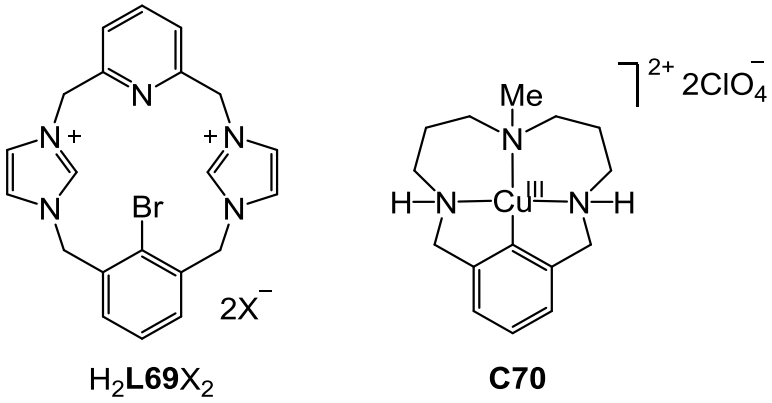

H_2**L69**X_2 **C70**

Figure 5-15: Structures of the proposed H_2**L69**X_2 (NHC ligand precursor, left) and Ribas's Cu(III) complex **C70** (right).

The ligand precursor was prepared stepwise *via* bromination of **71** using radical initiation by heating dibenzoyl peroxide in the presence of NBS to generate a Br• radical. The Br• radicals react with the aliphatic carbon atoms to produce a mixture of **72** and other aliphatically brominated products (Scheme 5-22). The desired product was isolated from the mixture using flash column chromatography (silica gel), eluting with hexane. TLC spotting was used to observe the reaction products, which were characterised by ^{1}H and ^{13}C {^{1}H} NMR spectroscopies (Figure 5-16). The macrocyclic imidazolium bromide salt H_2**L69**Br_2 was precipitated from a dilute mixture of **68** and **72** in anhydrous MeCN. H_2**L69**Br_2 is soluble in water, MeOH and acetone, and was characterised by ^{1}H and ^{13}C {^{1}H} NMR spectroscopy and HRMS.

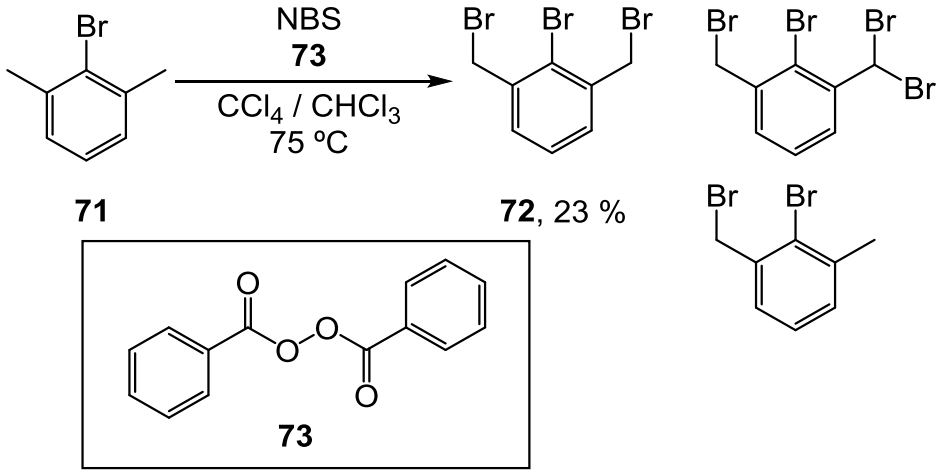

Scheme 5-22: Bromination of **71** to obtain **72**.

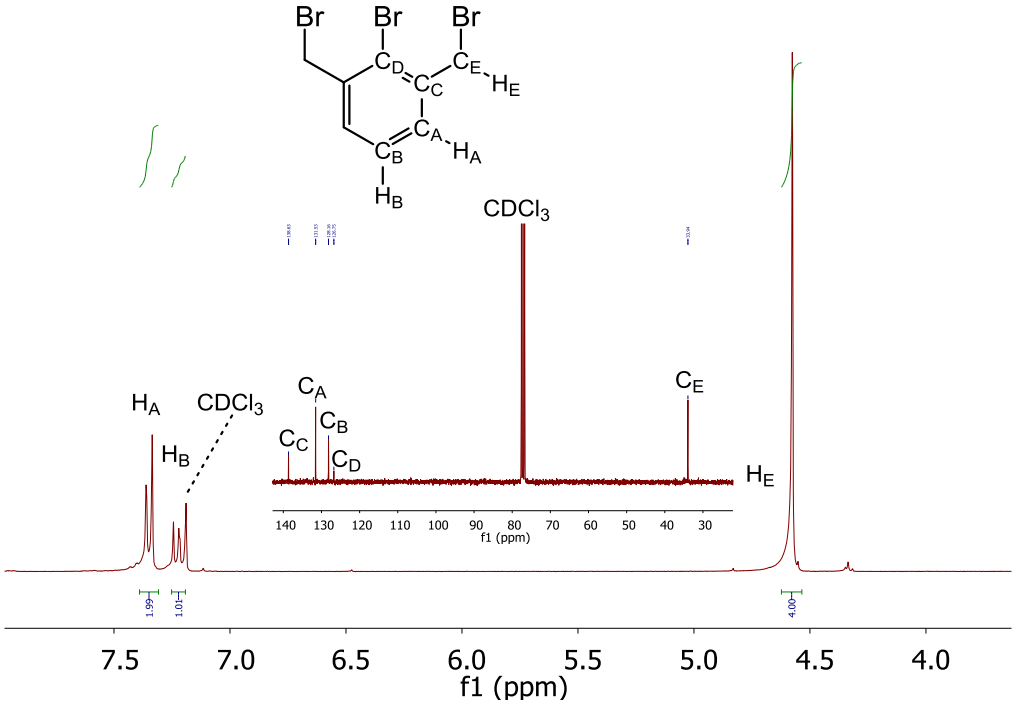

Figure 5-16: ^{1}H (300 MHz, $CDCl_3$) and ^{13}C {^{1}H} NMR (75 MHZ, $CDCl_3$) spectra of **72**.

Metallation of H_2**L69**Br_2 was first attempted by deprotonation with Ag_2O in anhydrous DCM (Scheme 5-23) [Ag**L69**]$^+$ was observed in a HRMS of the reaction sample after 3 hours reaction time. However, isolation of Ag**L69**Br was not possible, and thought that decomposition may occur through C_{aryl}-Br oxidative addition to the Ag centre to form an unstable Ag(III) complex. The reaction was also attempted with the presence of CuI so that silver transmetallation (and potentially oxidative addition of C-Br at Cu(I)) occurs *in situ* to form the desired Cu(I) or Cu(III) products. However, the resonances from HRMS were not assignable to any of the expected products, including [H**L69**]$^+$, [Cu**L69**]$^+$, [Cu**L69** – Br]$^{2+}$ or any Ag derivatives.

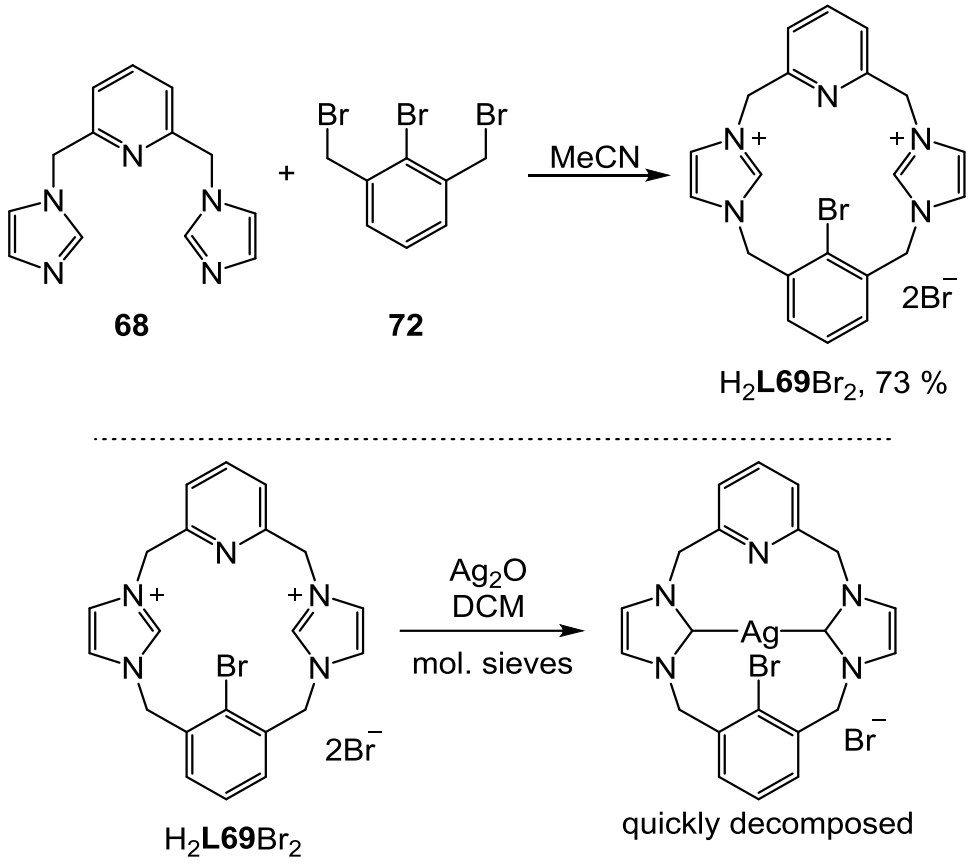

Scheme 5-23: Preparation of H_2**L69**Br_2 and attempted synthesis of Ag**L69**Br.

Another method that can be used for the preparation of Cu-NHC complexes is electrochemical synthesis. These reactions are often conducted in MeCN which stabilises Cu(I). As H_2**L69**Br_2 is not soluble in MeCN, anion exchange was carried out. Excess NH_4PF_6 was added to an aqueous solution of H_2**L69**Br_2 to afford a colourless precipitate and assumed as a complete reaction. H_2**L69**$(PF_6)_2$ was characterised using ^{1}H and ^{13}C {^{1}H} NMR spectroscopies and HRMS (Scheme 5-24). An electrochemical reaction was performed with H_2**L69**$(PF_6)_2$ (0.125 mmol) and Cu electrodes, a voltage was applied to achieve a current of 30 mA, which was maintained for 20 minutes (calculated time = $\frac{0.125\ mmol \times F \times 2}{0.03} = 13\ minues$). At 5 minutes, the solution turned pale yellow and to deep green within 15 minutes. The solvent were removed *in vacuo* and the crude product characterised using ^{1}H NMR spectroscopy (CD_3CN) and HRMS. The ^{1}H NMR spectrum was broad, suggesting the formation of paramagnetic Cu(II), while the MS resonance were not assignable to any of the expected products including [Cu**L69**]$^{+/2+}$, [**L69**]$^{2+}$, [H**L69**]$^+$ or [Cu**L69** – Br]$^{+/2+}$. Another electrochemical reaction was performed with H_2**L69**$(PF_6)_2$ (0.37 mmol) and Cu electrodes at a current of 20 mA for 60 minutes (1.5 times the calculated time *i.e*. 40 minutes),

which gave the yellow and green colour, and the same unassignable analytical results.

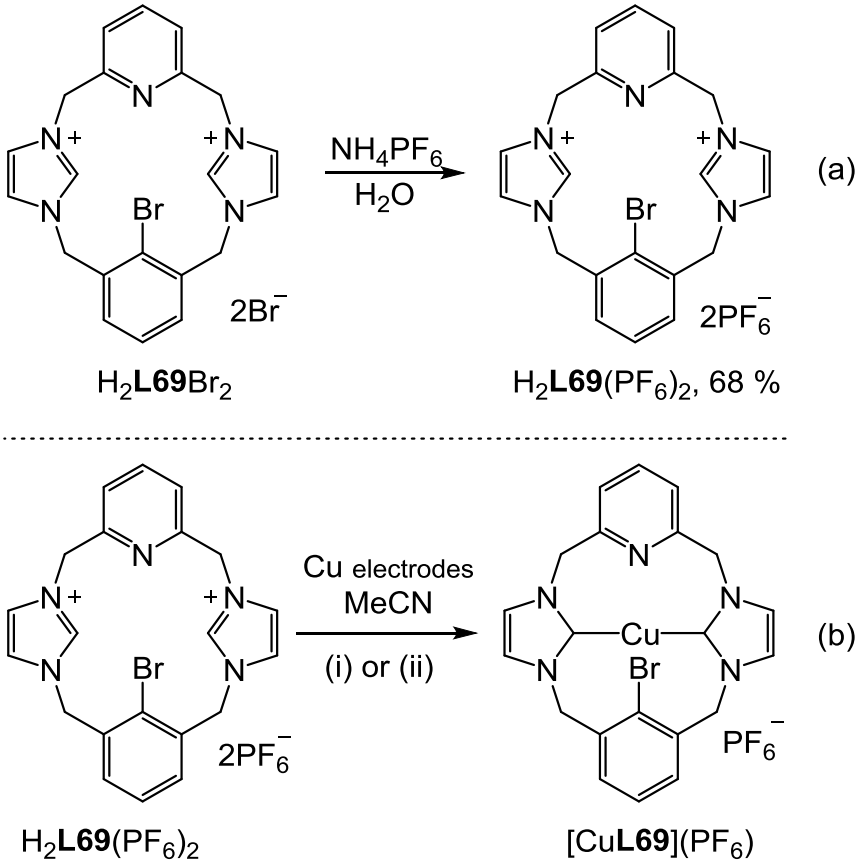

Scheme 5-24: Anion exchange to afford H_2**L69**$(PF_6)_2$ and attempted electrochemical synthesis of [Cu**L69**](PF_6). (i) H_2**L69**$(PF_6)_2$ (0.125 mmol), I = 0.03 A, time = 20 minutes; (ii) H_2**L69**$(PF_6)_2$ (0.269 mmol), I = 0.02 A, time = 60 minutes.

To investigate if the C-Br bond is being activated in these process and potentially leading to decomposition, the C-Br bond was replaced by a C-H bond. **68** was added to 1,3-dibromoethylbenzene **74** in anhydrous MeCN at low concentrations resulting in the precipitation of H_2**L75**Br_2, which was used to prepare H_2**L75**$(PF_6)_2$ by anion exchange (Scheme 5-25). Both Br^- and PF_6^- salts were characterised by ^1H and ^{13}C $\{^1H\}$ NMR spectroscopies and HRMS, where the metathesis was assumed to go to completion by the precipitation of the PF_6^- salt.

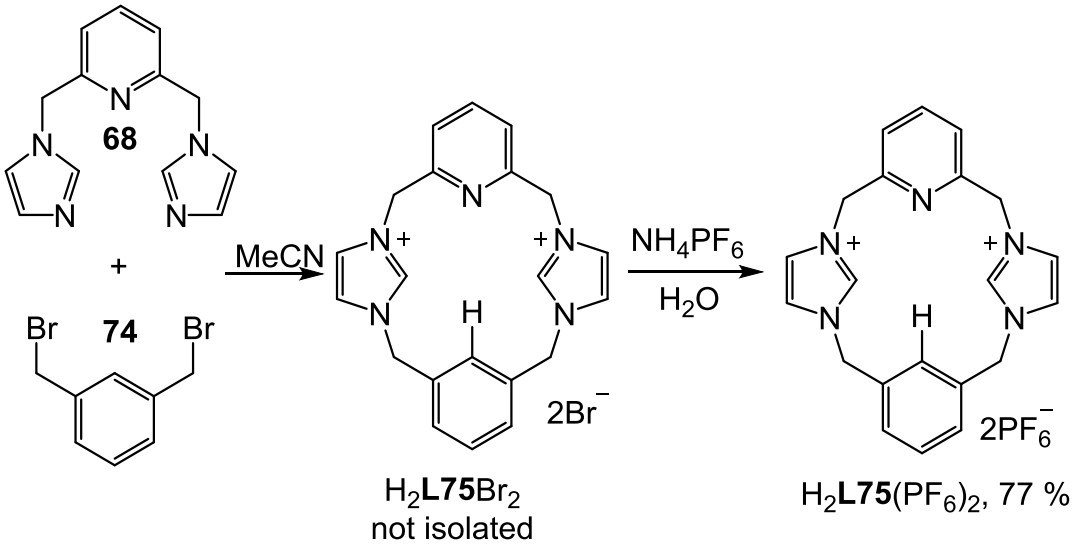

Scheme 5-25: Preparation of macrocycles H_2**L75**Br_2 and H_2**L75**$(PF_6)_2$.

Metallation of H_2**L75**$(PF_6)_2$ was attempted by deprotonation with Ag_2O in MeCN and stirred for 4 hours, after which time [Ag**L75**]$^+$ was not observed. MeOH was added to the reaction mixture and stirred for 20 hours, after which time [Ag**L75**]$^+$ was observed in the HRMS of a reaction sample. The complex [Ag**L75**](PF_6) was isolated as a light brown solid (quantitative yield) and was characterised using ^{1}H NMR spectroscopy and HRMS. The ^{13}C {^{1}H} NMR spectrum was too weak to assign.

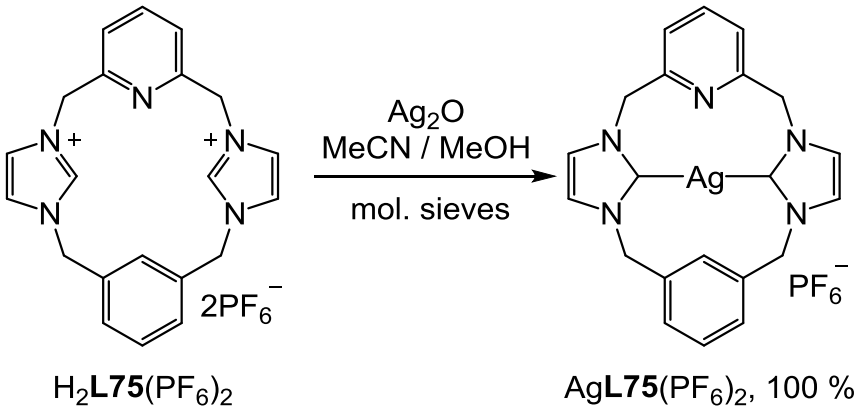

Scheme 5-26: Preparation of [Ag**L75**](PF_6).

The isolated [Ag**L75**](PF_6) was added to CuI in MeCN, with precipitation of AgI being observed. The reaction was filtered, the solvent removed from the filtrate and the green solid was recrystallised in MeCN / Et_2O to afford a pale green solid (57 % yield, Scheme 5-27). The [Cu**L75**](PF_6) was characterised using ^{1}H NMR spectroscopy and HRMS, with [Cu**L75**]$^+$ and [Cu**L75** + H]$^{+2}$ being observed in the mass spectrum.

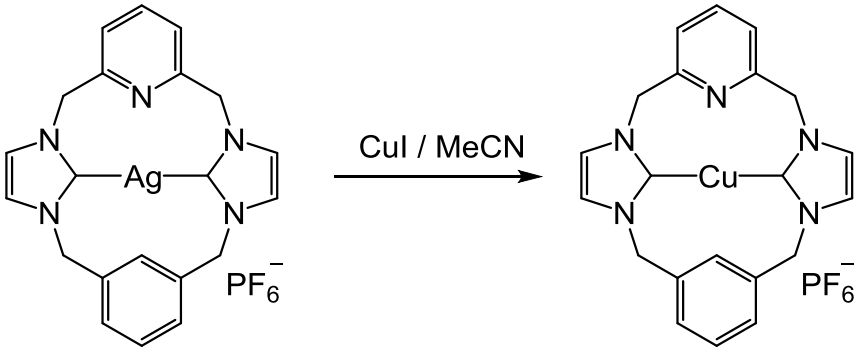

[Ag**L75**](PF$_6$) [Cu**L75**](PF$_6$), 57 %

Scheme 5-27: Preparation of [Cu**L75**](PF$_6$).

The preparation of [Cu**L75**](PF$_6$) was successful, when the C$_{aryl}$-H was utilised whereas when C$_{aryl}$-Br is present (**L69**) the reactions become more complicated. This provides a strong indication that the C-Br is being activated (through either oxidative addition or radical pathway), possibly leading to unstable higher oxidation state species which could not be detected due to decomposition.

5.5 Attempts to synthesise a Cu(III)-NHC *via* oxidation of Cu(II)-NHC

Another potential route to prepare a Cu(III)-NHC involves chemical oxidation of a Cu(II)-(macrocyclic NHC). A macrocyclic ligand precursor void of a C-Br bond was synthesised from **67** and **68** to afford H$_2$**L76**Br$_2$ followed by anion exchanged to obtain H$_2$**L76**(PF$_6$)$_2$ (Scheme 5-28).

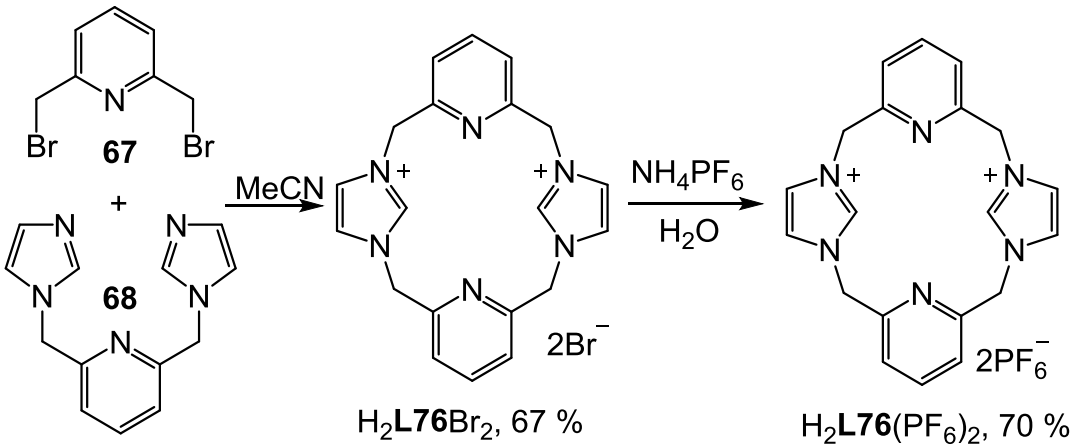

H$_2$**L76**Br$_2$, 67 % H$_2$**L76**(PF$_6$)$_2$, 70 %

Scheme 5-28: Preparation of H$_2$**L76**Br$_2$ and H$_2$**L76**(PF$_6$)$_2$.

H$_2$**L76**(PF$_6$)$_2$ was dissolved in DMSO in the presence of Ag$_2$O and heated at 55 °C for 2 hours to afford Ag**L76**(PF$_6$), with [Ag**L76**]$^+$ being observed in the HRMS after 1 hour of reaction time. The reaction was filtered through Celite. The

filtrate was poured into excess amount of water to afford precipitation of the product Ag**L76**(PF_6), which was collected by filtration and characterised by ^{1}H NMR spectroscopies and HRMS. The data were consistent with literature (Scheme 5-29).[26]

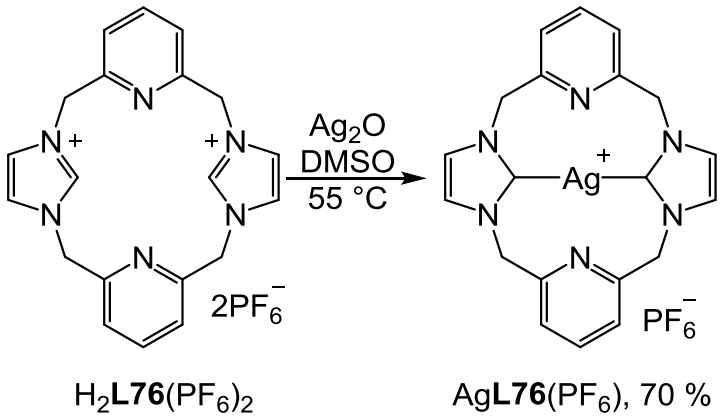

H_2**L76**(PF_6)$_2$ Ag**L76**(PF_6), 70 %

Scheme 5-29: Preparation Ag**L76**(PF_6).

Ag**L76**(PF_6) was added to $CuBr_2$ in MeCN to afford a dark green mixture which, upon addition of $AgPF_6$, immediately changed to purple. The purple solid was precipitated upon addition of Et_2O and collected *via* cannula filtration. Analysis by HRMS revealed the presence of [Cu**L76**]$^{2+}$ (Scheme 5-30).

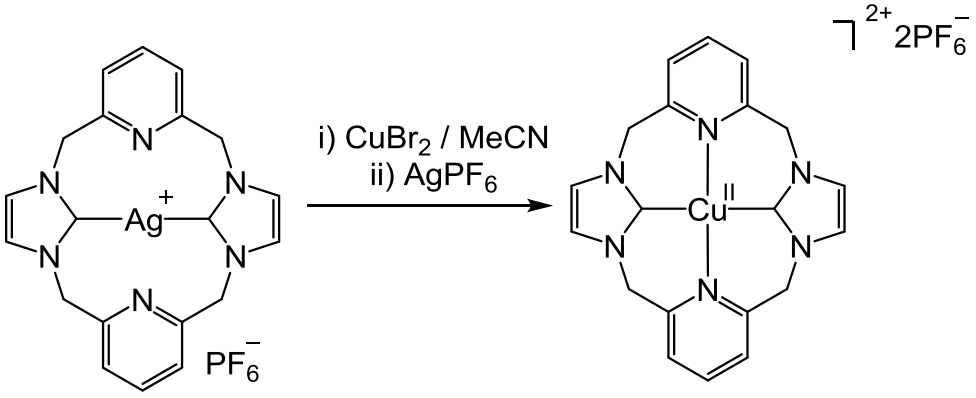

Ag**L76**(PF_6) [Cu**L76**](PF_6)$_2$, 86%

Scheme 5-30: Preparation of [Cu**L76**](PF_6)$_2$.

In addition, a crystal of [Cu**L76**](PF_6)$_2$ suitable for X-ray diffraction analysis was grown *via* vapour diffusion of Et_2O into a concentrated solution in MeCN (Figure 5-17). The crystal structure shows that the complex has a square planar geometry around the Cu(II) (angle C_{NHC}-Cu-$N_{pyridine}$ = 89.92 °, Table 5-4). The Cu-$N_{pyridine}$ distances are 2.14 Å, which are longer than Cu-C_{NHC} distances (1.90 Å). This is similar to previous Cu-NHC-Br_2 complexes reported in the group, which have Cu-$N_{pyridine}$ distances of 2.04 – 2.13 Å and Cu-C_{NHC} distances of

1.93 – 1.98 Å.[6] However, the Cu-C_{NHC} distance in our case is shorter, likely due to **L76** being in a more fixed orientation. Furthermore, when compared to Meyer's [Fe**L76**$(NCMe)_2](PF_6)_2$, which has Fe-C_{NHC} distance (1.94 Å) is also shorter than Fe-$N_{pyridine}$ (2.02 – 2.03 Å). Moreover, in both cases the NHC rings and pyridines are not coplanar, but the macrocyclic ligand is puckered and adopts C_2 symmetry. [Fe**L76**$(NCMe)_2](PF_6)_2$ also complex has 2 NCMe coordinated to Fe^{2+} at the axial positions at 1.93 – 1.94 Å and forms an octahedral complex. Differently, in our case of [Cu**L76**$](PF_6)_2$, there are 2 PF_6^- ions located near the axial position at a further distance of 3.56 Å with the nearest Cu-F(20). The fluoride atom is at 10.831 ° off the axis perpendicular to the plane of ligand coordination.

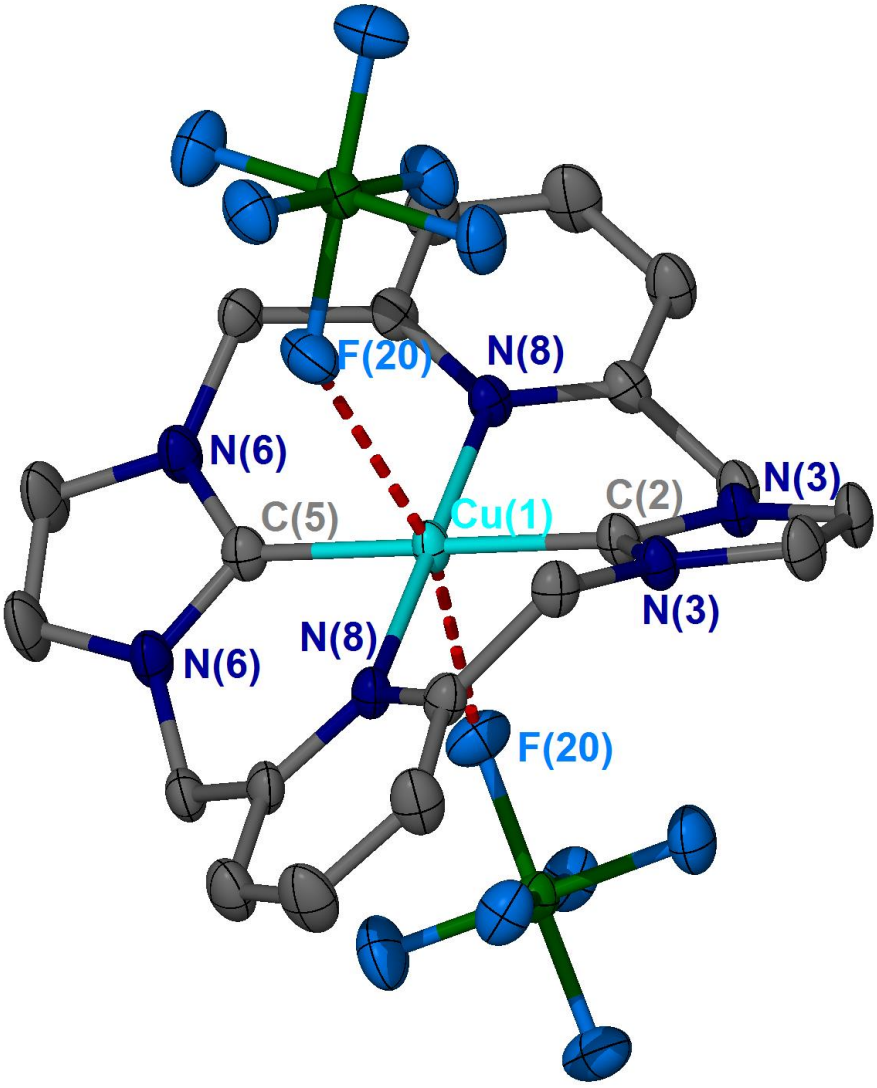

Figure 5-17: Molecular structure of [Cu**L76**$](PF_6)_2$. Ellipsoids are drawn at the 50% probability level, one of 2 PF_6^- ions and H atoms are omitted for clarity.

Cu(1) – C(2)	1.904(3)	C(2) – Cu(1) – N(8)	90.08(4)
Cu(1) – C(5)	1.906(3)	C(2) – Cu(1) – C(5)	180.0(0)
Cu(1) – N(8)	2.1433(16)	N(8) – Cu(1) – C(2) – N(3)	26.546
Cu(1) – N(8')	2.1433(16)	C(2) – Cu(1) – N(8) – C(9)	22.991
C(2) – N(3)	1.339(2)	F(20) – Cu(1) – C(2)	82.049
Cu(1) – F(20)	3.561	F(20) – Cu(1) – C(2) calculated	82.693
		F(20) – Cu(1) – Z-axis	10.831

Table 5-4: Selected bond distances (Å) and angles (deg) in the solid-state structure of the bromoimidazolium salt [Cu**L76**]$(PF_6)_2$.

The [Cu**L76**]$(PF_6)_2$ should have been analysed further using ^{1}H NNR (paramagnetic) spectroscopy and EPR (electron paramagnetic resonance), in order to determine that the Cu centre of the complex has the oxidation state of +2 and would have an unpaired electron regardless of geometry. In addition, magnetic susceptibility would help confirm the one unpaired electron of the Cu(II) centre. The edge peak from X-ray absorption spectroscopy would also allow the determination of the Cu oxidation state.

[Cu**L76**]$(PF_6)_2$ was examined using cyclic voltammetry. The measurements were performed under an atmosphere of Ar using a MeCN solution of [N(*n*-Bu)$_4$]PF_6 as the supporting electrolyte (0.10 M), scanning at 0.10 V•s^{-1} from - 1.3 V to + 2.0 V (Figure 5-18). The cyclic voltammogram shows two irreversible oxidations at E^{ox} = - 0.13 V and + 0.32 V *versus* the Ag/AgCl reference. The latter may be corresponding to the oxidation of Cu(II) to an unstable Cu(III) species, rendering the oxidation irreversible.

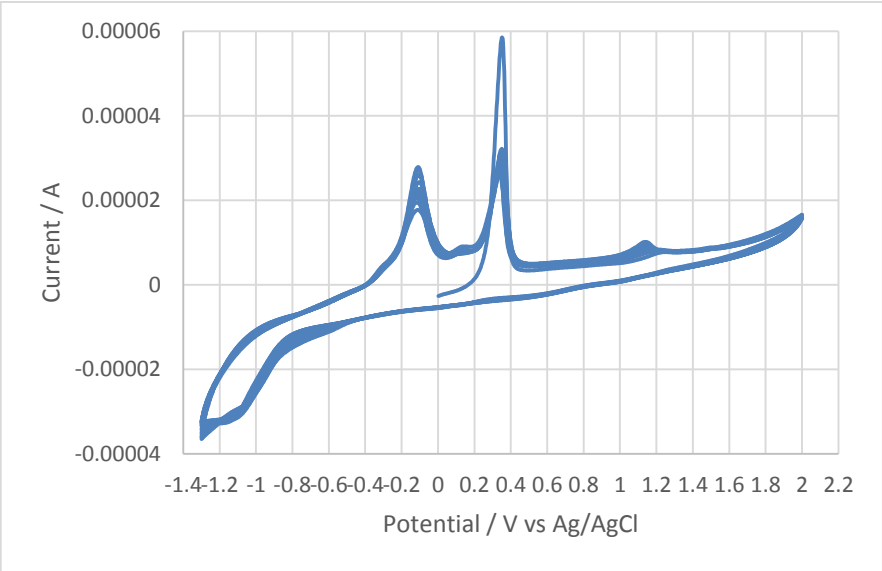

Figure 5-18: Cyclic voltammogram of [Cu**L76**]$(PF_6)_2$ illustrating its irreversible oxidation at -0.13 V and + 0.32 V. Conditions: [[Cu**L76**]$(PF_6)_2$] = 0.4 mM, media = N(*n*-Bu)$_4PF_6$ 0.10 M in MeCN, scan rate = 100 mV•s^{-1}, T = 298 K.

To assess the chemical oxidation of [Cu**L76**]$(PF_6)_2$, an oxidant was selected that would give a neutral product so that the anticipated charged Cu(III) complex could be easily separated. Previously, the Fe(II) complex Fe**L76**$(PF_6)_2$ was oxidised by thianthrenyl PF_6 **77** to yield an Fe(III) complex Fe**L76**$(PF_6)_3$.[27] **77** was prepared by addition of [NO]PF_6 salt to thianthracene in MeCN under an inert atmosphere and obtained as a dark blue solid, which was stored in a Glovebox (Scheme 5-31).

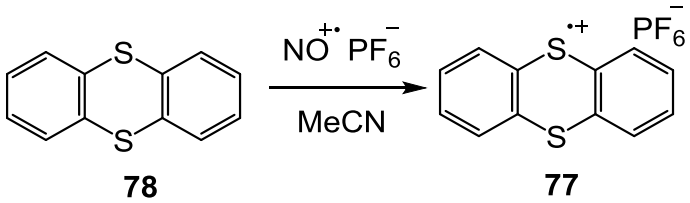

78 **77**

Scheme 5-31: Preparation of the oxidant **77**.

Reaction of [Cu**L76**]$(PF_6)_2$ with **77** in CD_3CN showed that **77** was reduced, as there are sharp peaks corresponding to **78** in the ^{1}H NMR spectrum. Other changes in the ^{1}H NMR spectrum were unassignable. The HR mass spectrum did not give signals corresponding to the starting material [Cu**L76**]$^{2+}$ or anticipated products such as [Cu**L76**]$^{3+}$, [Cu**L76**]$^+$ or [**L76** + H]$^{2+}$, with only [**78** + H]$^+$ being assigned. This suggests that the reduction of **77** to **78** occurred, and it is likely that the oxidation of Cu(II) to Cu(III) also took place but with the desired product being unstable. This was also inferred in the CV studies.

It is possible that the PF_6^- anion is too weak to stabilise the Cu(III)-NHC due to distributed charge among 6 fluoride atoms, with a triflate ion (OTf^-) being used in Ribas's work.[24] H_2**L76**$(OTf)_2$ was prepared *via* anion exchange by addition of 2 equivalents of AgOTf to a stirring suspension of H_2**L76**Br_2 in MeCN. The product was characterised by ^1H and ^{13}C $\{^1H\}$ NMR spectroscopies and HRMS. Attempts were made to prepare a Ag complex for transmetallation, though the desired Ag-NHC did not appear to form (Scheme 5-32).

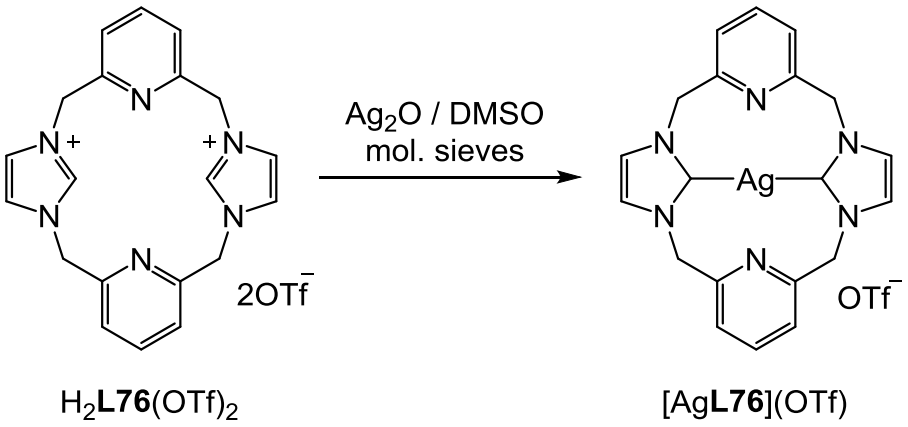

Scheme 5-32: Attempted synthesis of [Ag**L76**](OTf).

Instead, anion exchange was carried out at the last step following transmetallation, and the imidazolium Br^- salt was used as the starting material. The preparation of [Cu**L76**]$(OTf)_2$ was achieved *via* the formation of [Ag_2**L76**$_2$]Br_2 using Ag_2O in MeOH, followed by transmetallation on to $CuBr_2$. AgOTf was added to a MeCN solution of [Cu**L76**Br_2] resulting in a grey mixture, which was filtered and the solvent removed from the filtrate to afford [Cu**L76**]$(OTf)_2$ as a greyish green solid (25 % yield, Scheme 5-33). The complex was characterised by ^1H NMR spectroscopy and HRMS, which showed the [Cu**L76**$(OTf)]^+$ peak in the mass spectrum.

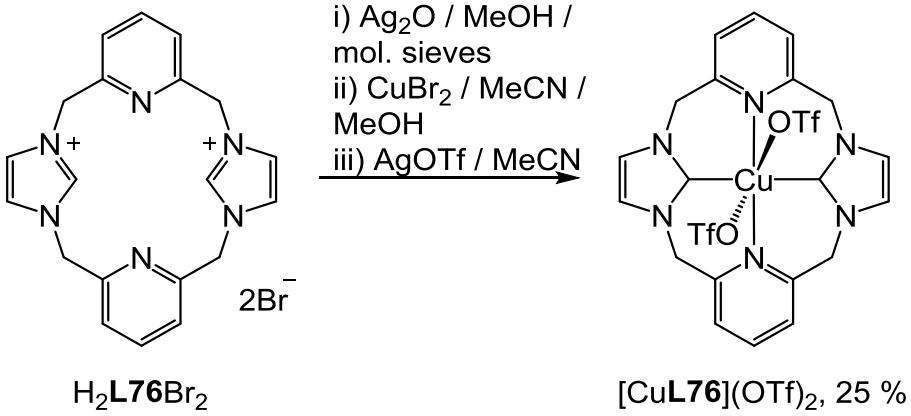

Scheme 5-33: *In situ* preparation of [Cu**L76**$(OTf)_2$.

As previously, Cu**L76**$(OTf)_2$ was reacted with **77** in an NMR tube, resulting in a ^1H NMR spectrum similar to that following the reaction of the PF_6^- derivative with **77**. Therefore, it is likely that the neutral macrocyclic ligand was not stable enough to stabilise the Cu(III) ion and an alternative ligand design is required.

[Cu**L76**]$(OTf)_2$ was examined using cyclic voltammetry. The measurements were performed under an atmosphere of Ar using a MeCN solution of N(*n*-Bu)$_4PF_6$ as the supporting electrolyte (0.10 M), scanning at 0.10 V•s^{-1} from – 2.0 V to + 2.0 V. The cyclic voltammogram shows one oxidation at E_{ox} = + 0.6 V versus the Ag/AgCl reference, which may be corresponding to the oxidation of Cu(II) to a Cu(III) species. However, the reduction at E_{red} = - 0.2 V was unknown. This may be the reversed reduction of Cu(III) to Cu (II) but the chemical oxidation experiments using [Cu**L76**]$(OTf)_2$ with **77** suggested that the Cu(III) was not stable enough.

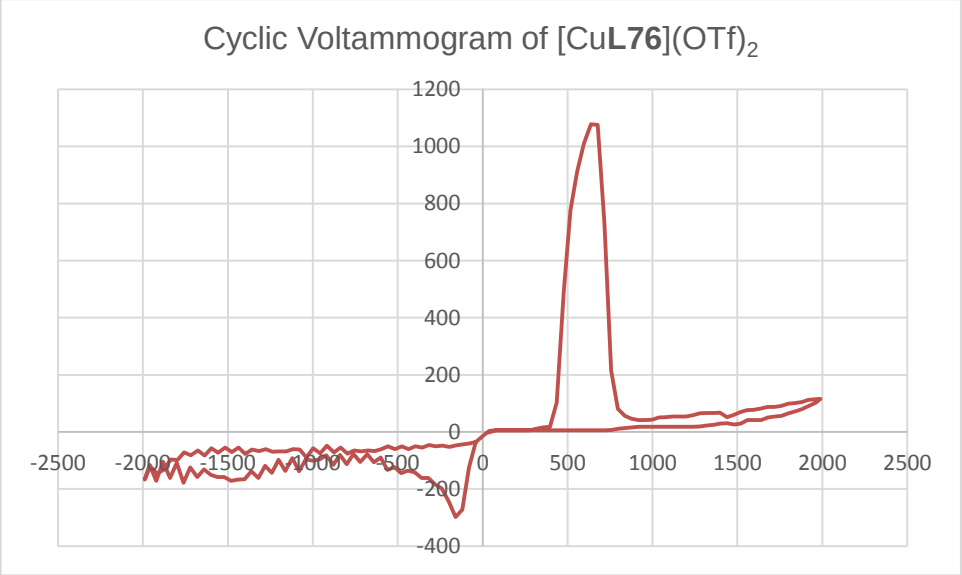

Figure 5-19: A single-round cyclic voltammogram of [Cu**L76**]$(OTf)_2$ using Electrasyn. Conditions: [[Cu**L76**$(OTf)_2$]] = 0.4 mM, media = N(*n*-Bu)$_4PF_6$ 0.10 M in MecN, scan rate = 100 mV•s^{-1}, T = 298 K.

5.6 Conclusions

Previously, Willans had demonstrated that 1-allyl-3-pyridylimidazol-2-ylidene (**L8**) can form an isolable complex with $CuBr_2$ with stabilisation through the pyridyl N-substituent, but undergoes reductive elimination of bromo-imidazolium in the presence of excess $CuBr_2$.[6,7] In this chapter, we have investigated further reactivity of the reductively eliminated bromo-imidazolium salt, which undergoes an annulation reaction. 1-Allyl-2-bromo-3-pyridylimidazolium (**S8**) was prepared by the selective C-2 bromination of pyridyl-imidazole and allylation, and was

examined with the presence and absence of CuBr. This demonstrated that the annulation reaction only occurs when 2 equivalents of CuBr are present. The proposed mechanism involves oxidative addition of the $C_{imidazolium}$-Br bond at one Cu, which is held in close proximity by the coordinated pyridine ring, and alkene coordination at a second Cu centre. DFT calculations are in progress to determine if the proposed mechanism is feasible. Understanding the mechanism provides valuable knowledge for ligand design in catalysis, in addition to potential synthetic route to common scaffolds in pharmaceutical and agrochemical compounds.

Attempts have been carried out to prepare a Cu(III)-NHC using different macrocyclic ligands and various approaches, including oxidative addition of C-Br to Cu(I) and oxidation of preformed Cu(II)-NHC complexes. Preparation of novel Cu(II)-NHC complexes with PF_6^- and OTf^- counterions were successful, although confirming their oxidation was challenging, likely due to the formation of unstable complexes.

5.7 Future work

A new ligand design to stabilise a Cu(II)-NHC may involve an anionic-tethered macrocycle, as the negative charge would help stabilise the hard acid. **L79** (Figure 5-20), which is macrocyclic and has an anionic amide functional group, could be formed by deprotonation of the corresponding secondary amine. However, the preparation of the ligand precursor might be troublesome due to the selectivity of nucleophilic substitution occurring at the sp^3-amine over the sp^2-imidazole. The tertiary amide may be used to form a macrocyclic precursor, which can be reduced to the desired amine with LAH.

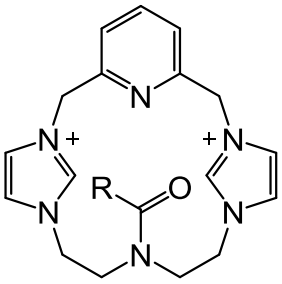

P79

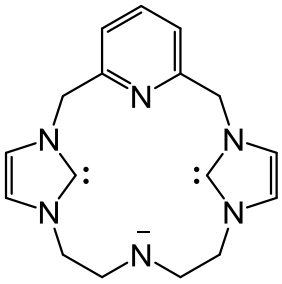

L79

Figure 5-20: Structure of proposed anionic macrocyclic **L79.**

5.8 Experimental

5.8.1 Preparation of S8.a (*via* reductive elimination)

i) Preparation of Ag**L8**Br

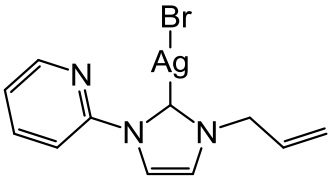

H**L8**Br (1.0 g, 3.76 mmol) and Ag_2O (0.56 g, 2.40 mmol) were added to freshly activated 4Å molecular sieves. DCM (50 mL) was added, and the reaction mixture was stirred at room temperature in the absence of light for 4 hours. The mixture was filtered through Celite, and the solvent was removed from the filtrate *in vacuo* to give a brown oil. The oil was recrystallised in $CHCl_3$ / pentane to obtain a brown solid. Yield: 0.456 g, 1.22 mmol, 34 %.

^{1}H NMR (300 MHz, $CDCl_3$) δ (ppm) 8.53 (dd, *J* = 4.8, 1.1 Hz, 1H, pyH-6), 8.11 (d, *J* = 8.2 Hz, 1H, phH), 7.95 – 7.83 (m, 2H, pyH and imH), 7.38 (ddd, *J* = 7.4, 4.9, 0.8 Hz, 1H, pyH-5), 7.16 (d, *J* = 1.9 Hz, 1H, imH), 6.02 (ddt, *J* = 16.3, 10.3, 6.0 Hz, 1H, **CH**=CH_2), 5.35 (dd, *J* = 24.3, 7.1 Hz, 2H, CH=**CH_2**), 4.89 (dt, *J* = 6.0, 1.3 Hz, 2H, N**CH_2**-vinyl). ^{13}C {^{1}H} NMR (75 MHz, $CDCl_3$) δ (ppm) 150.8, 149.1, 139.4, 132.2, 123.9, 121.5, 120.4, 115.4, 55.3. HRMS (ESI$^+$): *m/z* 477.0844 $[Ag(NHC)_2]^+$, calculated $[Ag(NHC)_2]^+$ 477.0951.

Consistent with data previously reported.[28]

ii) Preparation of **S8.a**

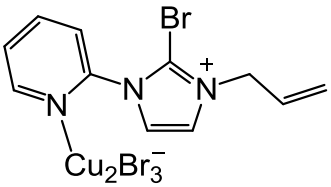

Ag**L8**Br (0.30 g, 0.80 mmol) and $CuBr_2$ (0.36 g) were added to a Schlenk flask, and the mixture dried and degassed *in vacuo*. Anhydrous MeCN (30 mL) was added, and the reaction mixture was stirred at room temperature in the absence of light for 1.5 hours. The mixture volume was reduced *in vacuo* to 10 mL. Et_2O (100 mL) was added to precipitate a dark-green oil-solid. The crude product was recrystallised in $CHCl_3$ / Et_2O. Dark green crystals were collected by filtration and dried *in vacuo* as a mixture. Yield: 0.30 g, 0.48 mmol, (59 %).

HRMS (ESI$^+$): *m/z* 263.9967 [**S8.a** – Cu_2Br_3]$^+$, calculated [**S8.a** – Cu_2Br_3]$^+$ 264.0131. ^{1}H NMR spectrum (300 MHz, CD_3CN) was obtained as a mixture of **S8.a** and **Cy8**. Analysis Calculated for $C_{11}H_{11}N_3BrCu_2Br_3$: C, 20.91; H, 1.75; N, 6.65. Analysis Calculated for $C_{11}H_{11}N_3BrCu_4Br_5$.MeCN: C, 16.27; H, 1.47; N, 5.84. Analysis Calculated for ½ $C_{11}H_{11}N_3Br$ + ½ $C_{11}H_{12}N_3$ + ¾ Cu_2Br_3 + ¼ $CuBr_2$: C, 23.74; H, 2.08; N, 7.55. Found: C, 23.60; H, 2.05; N, 7.30.

Single crystals suitable for X-ray diffraction analysis were grown *via* the vapour diffusion of Et_2O into a concentrated solution of the product in MeCN.

5.8.2 Bromination of imidazoles

i) Preparation of **PS8**

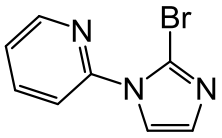

NBS (1.27 g, 7.21 mmol) was added to a Schlenk flask. MeCN (20 mL) was added, followed by **P8** (1.0 g, 6.9 mmol) whilst vigorously stirring. The reaction was heated at 70 ºC for 2 hours and allowed to cool to room temperature. The solvent was removed *in vacuo*. The crude mixture was suspended in DCM (50 mL) and washed with 5% $NaHCO_3$ solution (50 × 5 mL), dried over Na_2SO_4 and solvent removed *in vacuo* to give a dark brown solid. The crude product was purified by fractional column chromatography (silica gel), eluting by EtOAc / petroleum ether 40 (50: 50) to obtain a pale yellow solid. Yield: 0.643 g, 2.86 mmol, 42%.

^{1}H NMR (300 MHz, $CDCl_3$) δ (ppm) 8.52 (ddd, *J* = 4.9, 1.9, 0.9 Hz, 1H, pyH-6), 7.83 (ddd, *J* = 8.1, 7.5, 1.9 Hz, 1H, pyH-4), 7.53 (dt, *J* = 8.1, 0.9 Hz, 1H, pyH-3), 7.41 (d, *J* = 1.6 Hz, 1H, imH), 7.32 (ddd, *J* = 7.5, 4.9, 0.9 Hz, 1H, pyH-5), 7.07 (d, *J* = 1.6 Hz, 1H, imH). ^{13}C {^{1}H} NMR (75 MHz, $CDCl_3$) δ (ppm) 149.4 (C), 138.5 (C), 138.0 (CH), 130.4 (CH), 123.5 (CH), 122.7 (CH), 119.3 (CH), 117.4 (CH). HRMS (ESI$^+$): *m/z* 223.9815 $[M + H]^+$, calculated $[M + H]^+$ 223.9818. Analysis Calculated for $C_8H_6N_3Br$ + 1/8EtOAc : C, 43.43; H 3.00; N, 17.88. Found: C, 43.40; H, 3.00, N, 17.90.

Single crystals suitable for X-ray diffraction analysis were grown *via* the vapour diffusion of pentane into a concentrated solution of the product in chloroform.

ii) Attempted bromination of **P6**

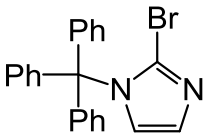

1-Tritylimidazole (**P6**, 0.10 g, 0.32 mmol) was added to an ampoule and THF (3 mL) added. The solution was cooled to -78 ºC. *n*-Buli in hexane (0.34 mL, 1M, 0.34 mmol) was added slowly, which turned the reaction mixture deep red. The reaction mixture was stirred at room temperature for 1.5 hours. It was cooled to -78 ºC again and solution of NBS (0.060 g, 0.34 mmol) in dry/degassed THF (3 mL) was added slowly *via* a syringe. The reaction was stirred for further 30 mins at the low temperature. After that, it was poured into water (10 mL) and concentrated *in vacuo*. The mixture was extracted with Et_2O (3 × 10 mL). The organic extracts were combined, dried over $MgSO_4$ and the solvent removed *in vacuo*. However, either 1-trityl-2-bromoimidazole or 2-bromoimidazole was not observed in LCMS or HRMS.

iii) Preparation of THP-imidazole

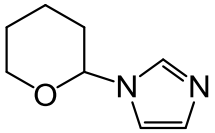

Imidazole (0.2 g, 2.94 mmol) was added to an ampoule. Anhydrous THF (15 mL), 3,4-dihydro-2H-pyran (2.7 mL, 29.4 mmol) and sulfuric acid (7 µL, 0.15 mmol) were added. The colourless reaction mixture was stirred at 60 ºC for 22 hours and the solvent and excess pyran removed *in vacuo*. The crude colourless crystals were dissolved in EtOAc (100 mL), washed with saturated $NaHCO_3$ solution (50 mL), water (50 mL) and brine (50 mL), dried over Na_2SO_4 and solvent removed *in vacuo*. The colourless oil was dissolved in Et_2O (1 mL) and hexane (20 mL) was added slowly to precipitate a colourless oil, which was collected by decanting off the solvents. Yield: 0.060 g, 0.39 mmol, 13%.

^{1}H NMR (300 MHz, $CDCl_3$) δ (ppm) 7.66 (s, 1H, imH-2), 7.07 (s, 2H, imH), 5.55 (d, J = 2.3 Hz, 1H, THP), 4.11 – 3.97 (m, 1H, THP), 3.83 (dd, *J* = 13.9, 7.3 Hz, 1H, THP), 2.34 (ddd, *J* = 23.2, 15.9, 8.0 Hz, 1H, THP), 2.13 – 1.77 (m, 5H, THP). ^{13}C {^{1}H NMR (75 MHz, $CDCl_3$) δ (ppm) 135.1 (CH), 121.7 (CH), 120.0 (CH), 98.3 (CH), 67.3 (CH_2), 33.3 (CH_2), 23.5 (CH_2), 22.2 (CH_2). There were no corresponding peaks in HRMS, likely due to cleavage of the protecting group.

Consistent with data previously reported.[29]

iv) Attempted bromination of THP-imidazole

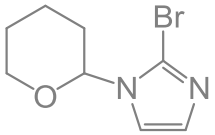

1-THP-imidazole (0.06 g, 0.39 mmol) was added to an ampoule, THF (1 mL) added and the colourless solution was cooled to -78ºC. *n*-BuLi in hexane (0.47 mL, 1M, 0.47 mmol) was added dropwise resulting in a pale yellow solution. The solution was stirred at -78ºC for 25 minutes and a solution of NBS (0.11 g, 0.59 mmol) in THF (1 mL) was added dropwise. The solution was stirred at -78 ºC for 1.5 hr and stirred for a further 1 hour at room temperature. The reaction mixture was quenched with saturated $NaHCO_3$ solution (10 mL) and extracted with DCM (3 × 20 mL). The organic layers were combined, dried over $MgSO_4$ and the solvents removed *in vacuo*. However, there was neither 1-THP-2-bromoimidazole nor 2-bromoimidazole in HRMS.

v) Preparation of ionic liquid **54**

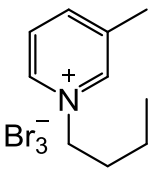

1-Butyl-3-metylpyridinium bromide (1.0 g, 4.3 mmol) was ground and added to a Schlenk flask. Bromine (0.3 mL, 5.81 mmol) was added whilst stirring and the reaction was stirred for 2 hours. Excess bromine was removed *in vacuo* for 3 hours. Due to the viscosity of the product, the ionic liquid was dissolved in MeOH to support the transfer and

collection. The MeOH was removed *in vacuo* to give deep-orange liquid. Yield: 1.41 g, 3.61 mmol, 83 %.

^{1}H NMR ($CDCl_3$, 300 MHz): δ (ppm) 8.64 (s, 1H, pyH-2), 8.62 (d, *J* = 7.8 Hz, 1H, pyH-6), 8.07 (d, *J* =7.8 Hz, 1H, pyH-4), 7.74 (t, *J* = 7.8 Hz, 1H, pyH-5), 4.41 (t, *J* = 7.5 Hz, 2H, N**CH_2**$CH_2CH_2CH_3$), 2.40 (s, 3H, CH_3), 1.72 (m, 2H, NCH_2**CH_2**CH_2CH_3), 1.16 (m, 2H, NCH_2CH_2**CH_2**CH_3), 0.72 (t, J = 7.5 Hz, 3H, $NCH_2CH_2CH_2$**CH_3**). ^{13}C {^{1}H} NMR ($CDCl_3$, 75 MHz): δ (ppm) 145.5 (CH), 143.4 (CH), 141.1 (C), 139.0 (CH), 128.5, 61.3 (CH_2), 32.9 (CH_2), 18.7 (CH_3), 17.9 (CH_2), 12.8 (CH_3).

Consistent with data previously reported.[22]

vi) Attempted bromination of imidazole by brominating reagent **54**

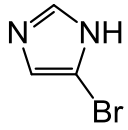

Imidazole (0.70 g, 10.3 mmol) and **54** (2.5 g, 6.4 mmol) were to Schlenk flasks. MeCN (15 mL) was added to the imidazole and MeCN (40 mL) was added to **54**. Both solutions were cooled to 0 ºC and the **54** solution was transferred to the imidazole solution *via* cannula, and the mixture stirred at 0 ºC for 15 minutes. Then water was added and the mixture was concentrated *in vacuo*. Et_2O (100 × 3 mL) were used to extract bromoimidazole species. The solvent was removed from the combined organic solution *in vacuo*. The product was purified by fractional column chromatography (silica gel) eluting by DCM / MeOH (95:5) → DCM / MeOH (90:10). Bromoimidazole was obtained as a colourless solid and analysed to be the compound **60** instead of the desired **57** (2-bromoimidazole). Yield: 0.19 g, 1.29 mmol, 20 %

^{1}H NMR (300 MHz, d_6-DMSO) δ (ppm) 12.39 (s, broad, 1H, **NH**), 7.62 (s, 1H, imH-2), 7.24 (s, 1H, imH-4). ^{13}C {^{1}H} NMR (126 MHz, d_6-DMSO) δ (ppm) 135.9 (CH), 115.6 (CH), 113.5 (C). HRMS (ESI^{+}): *m/z* 146.9546 $[M + H]^{+}$, calculated $[M + H]^{+}$ 146.9552. Analysis Calculated for $C_3H_3BrN_2$ ¼CH_3OH: C, 24.86; H 2.34; N, 18.55. Found: C, 25.10; H, 2.10, N, 18.40.

Inconsistent with reported NMR data (for 2-bromoimidazole): ^{1}H NMR (400 MHz, $CDCl_3$) δ 12.76 (sl, 1H), 7.11 (s, 2H).[30]

vii) Attempted bromination of benziimidazole by brominating reagent **54**

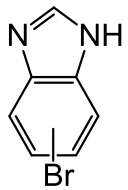

Benzimidazole (0.24 g, 2.05 mmol) and **54** (0.5 g, 1.28 mmol) were separately to Schlenk flask. MeCN (2 mL) was added to the benzimidazole and MeCN (2 mL) was added to **54**. Both solutions were cooled to 0 ºC and the **54** solution was transferred to the imidazole solution, and the mixture stirred at 0 ºC for 1 hour. The reaction mixture

was stirred at room temperature for 1 hour and at 40 °C for 20 hours and the MeCN was removed *in vacuo*. The crude yellow liquid was partitioned in water (25 mL) and Et_2O (25 mL). The organic layer was dried over Na_2SO_4 and solvent removed *in vacuo* to afford an off-white solid. Yield: 0.05 g, 0.25 mmol, 20 %

^{1}H NMR (300 MHz, $CDCl_3$) δ (ppm) 9.35 (s, 1H, **NH**), 8.08 (s, 1H, imH-2), 7.75 (d, *J* = 1.7 Hz, 1H, BzmH), 7.46 (d, *J* = 8.6 Hz, 1H, BzmH), 7.33 (dd, *J* = 8.6, 1.6 Hz, 1H, BzmH). ^{13}C {^{1}H} NMR (75 MHz, $CDCl_3$) δ (ppm) 141.6 (C), 139.0 (CH), 136.7 (C), 126.3 (CH), 118.5 (CH), 116.8 (C), 116.1 (CH). HRMS (ESI$^+$): *m/z* 196.9723 $[M + H]^+$, calculated $[M + H]^+$ 196.9709.

viii) Preparation of **P64**

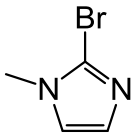

1-Methylimidazole (0.5 mL, 6.3 mmol) and anhydrous THF (10 mL) were added to an ampoule. The reaction mixture was cooled to -78 °C and *n*-BuLi (1.6 M, 4 mL, 6.3 mmol) was added slowly and stirred for 1 hour. A solution of CBr_4 (0.2 g, 0.63 mmol) and NBS (1.12 g, 6.3 mmol) in THF (10 mL) was added. The mixture was stirred at -78 °C for 2 hours, then at room temperature for 1 hour. EtOAc (20 mL) was added and washed with NH_4Cl solution. The organic layer was dried over Mg_2SO_4 and the solvent removed *in vacuo* to give a brown solid. The crude product was purified by fractional column chromatography (silica gel), eluting with EtOAc / petroleum ether 40 (50: 50) to obtain an off-white solid. Yield: 0.47 g, 2.9 mmol, 46 %.

^{1}H NMR (300 MHz, $CDCl_3$) δ (ppm) 6.95 (d, *J* = 1.1 Hz, 1H, imH), 6.92 (d, *J* = 1.1 Hz, 1H, imH), 3.58 (s, 3H, NCH_3). ^{13}C {^{1}H} NMR (75 MHz, $CDCl_3$) δ (ppm) 129.8 (CH), 123.1 (CH), 120.1 (C), 34.6 (CH_3). HRMS (ESI$^+$): *m/z* 160.9710 $[M + H]^+$, calculated $[M + H]^+$ 160.9709.

Consistent with data previously reported.[31]

5.8.3 Preparation of bromo-imidazolium/imidazole substrates

i) Preparation of **S8.b**

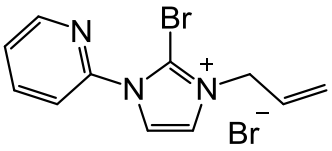

PS8 (0.5 g, 2.23 mmol) was dissolved in MeCN (20 mL) and then allyl bromide (1.0 mL, 11.1 mmol) was added dropwise, and the reaction mixture was stirred at 80 ºC under N_2 and hydrous conditions for 24 hours. The mixture was allowed to cool to room temperature. Et_2O (150 mL) was added to precipitate a pale brown solid which was collected by filtration. The solid was washed with Et_2O (100 mL) and dried *in vacuo*. Yield: 0.71 g, 2.06 mmol, 92 %.

^{1}H NMR (300 MHz, $CDCl_3$) δ (ppm) 8.66 (ddd, *J* = 4.9, 1.9, 0.9 Hz, 1H, py-H6), 8.33 (dt, *J* = 7.8 Hz, 0.9Hz, 1H, pyH-3), 8.10 (td, *J* = 7.8, 1.9 Hz, 1H, pyH-4), 8.03 (d, *J* = 2.3 Hz, 1H, imH), 7.98 (d, *J* = 2.3 Hz, 1H, imH), 7.62 (ddd, *J* = 7.8, 4.9, 0.9 Hz, 1H, pyH-5), 6.14 (ddt, *J* = 16.5, 10.1, 6.3 Hz, 1H, **CH**=CH_2), 5.64 – 5.54 (m, 2H, CH=**CH_2**), 5.13 (dt, *J* = 6.3, 1.2 Hz, 2H, N**CH_2**-vinyl). ^{13}C {^{1}H} NMR (75 MHz, $CDCl_3$) δ (ppm) 149.9 (C), 149.9 (C), 149.8 (CH), 140.2 (CH), 128.5 (CH), 126.3 (CH), 124.6 (CH), 124.2 (CH), 123.3 (CH), 121.3 (terminal CH_2), 53.6 (CH_2). HRMS (ESI$^+$): *m/z* 264.0133 $[M - Br]^+$, calculated $[M - Br]^+$ 264.0131. Analysis Calculated for $C_{11}H_{11}N_3Br_2$: C, 38.29; H 3.21; N, 12.18. Found: C, 37.95; H, 3.10, N, 12.00.

Single crystals suitable for X-ray diffraction analysis were grown by the vapour diffusion of Et_2O into a concentrated solution of the product in MeCN/MeOH.

ii) Preparation of **S53**

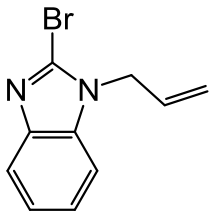

NaH (67 mg, 2.79 mmol) was added to a Schlenk flask and cooled to 0 ºC. Dry THF (1 mL) was added, followed by 2-bromobenzimidazole (0.50 g, 2.53 mmol) while stirring. The white suspension was left to reach room temperature then allyl bromide (0.26 mL) was added, and the reaction mixture was stirred at 60 ºC for 24 hours. Water (10 mL) was added to quench excess NaH. The aqueous solution was extracted with DCM (3 × 20 mL), which were combined, dried over $MgSO_4$ and the solvents removed *in vacuo*. The product was obtained as a pale yellow solid. Yield: 0.60 g, 2.53 mmol, 100 %

^{1}H NMR (400 MHz, $CDCl_3$) δ (ppm) 7.73 – 7.58 (m, 1H, BzmH), 7.31 – 7.11 (m, 3H, BzmH), 5.85 (ddt, J = 17.1, 10.3, 5.2 Hz, 1H, **CH**=CH_2), 5.18 (dtd, J = 10.3, 1.6, 0.8 Hz, 1H, CH=**CH_2** *trans*), 5.00 (dtd, J = 17.1, 1.8, 0.7 Hz, 1H, CH=**CH_2** *cis*), 4.73 (dt, J = 5.1, 1.7 Hz, 2H, N-**CH_2**-vinyl). ^{13}C {^{1}H} NMR (101 MHz, $CDCl_3$) δ (ppm) 143.0 (C), 135.4 (C), 130.8 (CH), 129.9 (C), 123.3 (CH), 122.8 (CH), 119.4 (CH), 118.3 (CH_2), 109.8 (CH), 47.6 (CH_2). HRMS (ESI$^+$): *m/z* 237.0020 $[M + H]^+$, calculated $[M + H]^+$ 237.0022. Analysis Calculated for $C_{10}H_9N_2Br$: C, 50.66; H 3.83; N, 11.82. Found: C, 50.30; H, 3.80, N, 11.60.

iii) Preparation of **S64**

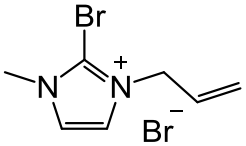

PS64 (0.47 g, 2.9 mmol) was dissolved in MeCN (20 mL) and allyl bromide (1.25 mL, 14.5 mmol) was added dropwise, and the reaction mixture was stirred at 80 ºC under N_2 and hydrous conditions for 24 hours. The mixture was allowed to reach room temperature and Et_2O (150 mL) was added to precipitate a pale

brown solid which was collected by filtration. The solid was washed in Et_2O (100 mL) and dried *in vacuo*. Yield: 0.53 g, 1.88 mmol, 67 %.

^{1}H NMR (300 MHz, CD_3CN) δ (ppm) 7.73 (s, 1H, imH), 7.71 (s, 1H, imH), 6.02 (ddt, J = 16.7, 10.6, 5.7 Hz, 1H, **CH**=CH_2), 5.44 (d, J = 10.6 Hz, 1H, CH=**CH_2** *trans*), 5.33 (d, J = 16.7 Hz, 1H, CH=**CH_2** *cis*), 4.86 (d, J = 5.7 Hz, 2H, N**CH_2**-vinyl), 3.87 (s, 3H). ^{13}C {^{1}H} NMR (CD_3CN) δ (ppm) 130.3 (CH), 125.7 (C), 124.1 (CH), 123.8 (CH), 120.7 (CH_2), 52.8 (CH2), 37.6 (CH_3). HRMS (ESI$^+$): *m/z* 201.0033 [M – Br]$^+$, calculated [M – Br]$^+$ 201.0022.

5.8.4 Reactivity of bromo-imidazoliums/imidazole at Cu

i) Annulation of **S8.a** to afford **Cy8**

S8.a (0.05 g, 79 mmol) was added an ampoule and the solid was heated at 95 ºC for 6 days (above melting point). When the system was cooled to room temperature, the solid stuck to the glassware. The solid was collected by suspension in MeCN and the solvent removed *in vacuo*. Yield: 0.042 g, 84 %. The product was obtained as a mixture of **Cy8** and **S8.a**.

iv) Annulation of **S8.b** to afford **Cy8** (with 2 equivalents of CuBr)

S8.b (0.12 g, 0.35 mmol) and CuBr (0.1 g, 0.70 mmol) were added, followed by MeCN (1 mL). The green reaction mixture was stirred at room temperature for 30 mins and the solvent was removed *in vacuo*. The dark solid was heated at 90 ºC for 7 days. The crude mixture was recrystallised in MeCN / Et_2O to obtain a dark green-grey solid. Yield: 0.14 g, 0.22 mmol, 64%.

^{1}H NMR (501 MHz, CD_3CN) δ (ppm) 8.64 (d, *J* = 4.7 Hz, 1H, pyH-6), 8.12 (t, *J* = 7.4 Hz, 1H, pyH-4), 8.06 (s, 1H, imH), 7.80 (d, *J* = 7.4 Hz, 1H, pyH-3), 7.63 (s, 1H, imH), 7.58 (dd, *J* = 7.4, 4.7 Hz, 1H, pyH-5), 5.37 – 5.28 (m, 1H, pyrrolH-6), 4.95 (dd, *J* = 13.5, 6.4 Hz, 1H, pyrrolH-5 *trans*), 4.66 (dd, *J* = 13.5, 2.9 Hz, 1H, pyrrolH-5 *cis*), 4.37 (dd, *J* = 19.5, 7.2 Hz, 1H, pyrrolH-7 *trans*), 4.01 (dd, *J* = 19.5, 2.9 Hz, 1H, pyrrolH-7 *cis*). ^{13}C {^{1}H} NMR (126 MHz, CD_3CN) δ (ppm) 150.6 (C), 150.2 (CH), 147.9 (C), 141.4 (CH), 126.0 (CH), 124.3 (CH), 120.3 (CH), 115.8 (CH), 59.4 (CH_2), 44.3 (CH), 40.4 (CH_2). HRMS (ESI$^+$): *m/z* 264.0127 [**Cy8** – Cu_2Br_3]$^+$, calculated [**Cy8** – Cu_2Br_3]$^+$ 264.0131.

v) Cu-catalysed reaction of **S53** (to give **62** and **63**)

To a solution of **S53** (30 mg, 0.19 mmol) in CD_3CN (0.4 mL) in a Young's-tap NMR tube was added CuI (3.6 mg, 0.019 mmol) and DL-proline (4.4 mg, 0.038 mmol). The reaction was heated at 75 °C for 24 hours and samples were analysed using ^1H NMR spectroscopy and HRMS. Multiple allyl peaks were observed in the ^1H NMR spectrum and **62** and **63** were observed in HRMS.

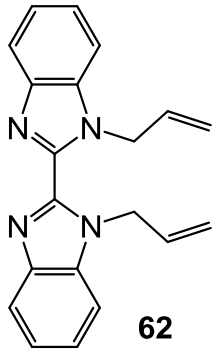

62

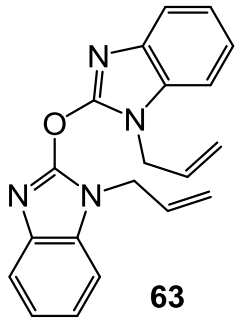

63

vi) Reactivity of **S64** (no reaction)

S64 (0.1 g, 0.35 mmol) was added to an ampoule and CuBr (0.102 g, 0.71 mmol) was added, folllowed by MeCN (3 mL). The green reaction mixture was stirred at room temperature for 30 mins, the solvent was removed *in vacuo* and the resulting oily solid was heated to 90 ºC for 169 hours. The crude mixture was dissolved in CD_3CN for NMR analysis.

^1H NMR (300 MHz, CD_3CN) δ (ppm) 7.61 (d, *J* =1.8 Hz, 1H, imH), 7.58 (d, *J* = 1.8 Hz, 1H, imH), 6.00 (ddt, *J* = 17.3, 10.2, 5.7 Hz, 1H, **CH**=CH_2), 5.44 (d, *J* = 10.2 Hz, 1H, CH=**CH_2** *trans*), 5.33 (d, *J* = 17.3 Hz, 1H, CH=**CH_2** cis), 4.81 (d, *J* = 5.7 Hz, 1H, N**CH_2**-vinyl).

Data was the same as the starting material (**S64**), suggesting there was no change in the imidazolium cation.

5.8.5 Preparation of ligand precursors

i) Preparation of **67**

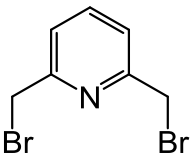

An HBr solution (≥ 48 %w, 20 mL) was added slowly to **66** (2.0 g, 14.4 mmol), followed by addition of H_2SO_4 (5 mL) and NaBr (4.0 g) to the stirring solution. The reaction mixture was heated at 120 °C for 24 hours. The reaction mixture was allowed to cool to room temperature and poured into deionised water (20 mL). A saturated $NaHCO_3$ solution was added dropwise until pH = 8 was reached. The mixture was extracted with DCM (4 × 50 mL) and the organic layers were combined, dried over Na_2SO_4 and the solvent removed *in vacuo* to give a pale pink solid. The crude product was purified by flash column chromatography (silica gel),

eluting with EtOAc / hexane (1: 9) → EtOAc / hexane (1: 4) to give a colourless solid. Yield: 2.7 g, 10 mmol, 71 %.

^{1}H NMR (300 MHz, $CDCl_3$) δ (ppm) 7.64 (t, *J* = 7.7 Hz, 1H, pyH-4), 7.31 (d, *J* = 7.7 Hz, 2H, pyH-3 and pyH-5), 4.47 (s, 4H, 2(py-**CH_2**-Br)). ^{13}C {^{1}H} NMR (75 MHz, $CDCl_3$) δ (ppm) 156.8 (C), 138.1 (CH), 122.8 (CH), 33.5 (CH_2). HRMS (ESI^+): *m/z* 265.8989 $[M + H]^+$, calculated $[M + H]^+$ 265.8996.

Consistent with data previously reported.

ii) Preparation of **68**

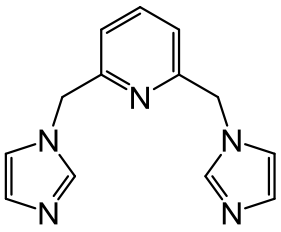

Imidazole (0.61 g, 8.98 mmol) was added to an ampoule, followed by THF (5 mL). NaH (0.22 g, 8.98 mmol) was slowly added to the stirring imidazole solution and the reaction mixture was stirred for a further 1 hour. **67** (1.19 g, 4.49 mmol) was added and stirred for at room temperature 20 hours. The reaction mixture was filtered and the solvent was removed from the filtrate *in vacuo* to afford the product as an off-white solid. Yield: 0.56 g, 2.37 mmol, 53 %.

^{1}H NMR (300 MHz, $CDCl_3$) δ (ppm) 7.54 (t, J = 7.8 Hz, 1H, pyH-4), 7.51 (s, 2H, imH), 6.99 (s, 2H, imH), 6.89 (s, 2H, imH), 6.83 (d, J = 7.8 Hz, 2H, pyH-3 and pyH-5), 5.12 (s, 4H, 2(py-**CH_2**-im)). ^{13}C {^{1}H} NMR (75 MHz, $CDCl_3$) δ (ppm) 156.2, 138.5, 137.6, 129.7, 120.4, 119.5, 52.1. HRMS (ESI^+): *m/z* 240.1245 $[M + H]^+$, calculated $[M + H]^+$ 240.1244; 120.5655 $[M + 2H]^{2+}$, calculated $[M + 2H]^{2+}$ 120.5658; 479.2420 $[2M + H]^+$, calculated $[2M + H]^+$ 479.2415.

Consistent with data previously reported.

iii) Bromination of **68** (preparation of **P65**)

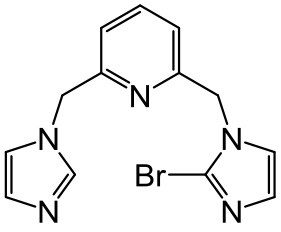

68 (0.30 g, 1.25 mmol) was added to a Schlenk flask, followed by MeCN (5 mL) *via* syringe and slow addition of a solution of NBS (0.23 g, 1.32 mmol) in MeCN (10 mL) *via* cannula transfer. The reaction was stirred at room temperature for 24 hours and the solvent was removed *in vacuo* and the crude product was suspended in DCM (50 mL) and washed with 5 % $NaHCO_3$ solution (3 × 50 mL), dried over Na_2SO_4 and the solvent removed *in vacuo* to afford a dark brown solid. The solid was purified by fractional column chromatography (silica gel), eluting with 5 % MeOH in DCM to obtain a light brown solid. Yield: 8 mg, 0.025 mmol, 2 %.

^{1}H NMR (500 MHz, $CDCl_3$) δ (ppm) 7.76 (s, 1H, imH), 7.65 (t, *J* = 7.7 Hz, 1H, pyH-4), 7.14 (s, 1H, imH), 7.07 (s, 1H, imH), 7.06 (s, 1H, imH), 7.00 (s, 1H, imH), 6.95 (d, *J* = 7.7 Hz, 1H, pyH), 6.90 (d, *J* = 7.7 Hz, 1H, pyH), 5.24 (s, 2H, N**CH$_2$**-py), 5.21 (s, 2H, N**CH$_2$**-py). ^{13}C {^{1}H} NMR (126 MHz, $CDCl_3$) δ (ppm) 156.4 (C), 156.4 (C), 155.8 (C), 138.7 (CH), 138.6 (CH), 130.7 (CH), 122.9 (CH), 122.9 (CH), 121.2 (CH), 120.8 (CH), 120.7 (CH), 52.8 (CH_2), 52.6 (CH_2). HRMS (ESI^+): *m/z* 318.0362 $[M + H]^+$, calculated $[M + H]^+$ 318.0349; 637.0612 $[2M + H]^+$, calculated $[2M + H]^+$ 637.0604.

iv) Preparation of **72**

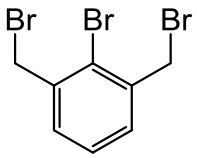

In air, a mixture of **71** (5 mL, 37.5 mmol), NBS (13.4 g, 75.1 mmol) and **73** (0.50 g, 1.88 mmol) in CCl_4 (20 mL) and $CHCl_3$ (50 mL) was heated at 75 °C under hydrous conditions for 24 hours. The reaction mixture was allowed to cool to room temperature and the solvents removed *in vacuo*. The crude colourless oil was suspended in $CHCl_3$ (20 mL) and filtered. The filtrate was washed with water (3 × 20 mL) and the aqueous layers were combined and extracted with $CHCl_3$ (3 × 60 mL). The combined organic layers were dried over Na_2SO_4 and the solvent removed *in vacuo*. The crude product was purified by fractional column chromatography eluting with hexane to obtain a colourless solid. Yield: 2.9 g, 8.5 mmol, 22 %.

^{1}H NMR (300 MHz, $CDCl_3$) δ (ppm) 7.35 (d, *J* = 7.8 Hz, 2H, ArH-4 and ArH-6), 7.22 (dd, *J* = 8.3, 7.0 Hz, 1H, ArH-5), 4.58 (s, 4H, N**CH$_2$**Br). ^{13}C {^{1}H} NMR (75 MHz, $CDCl_3$) δ (ppm) 138.6, 131.5, 128.2, 126.8, 33.9. There were no relevant peaks observed in HRMS as **72** is unlikely to be ionised with either Na^+ or K^+ ion.

Consistent with data previously reported.

5.8.6 Preparation of macrocyclic imidazolium salts

General procedure for preparation of imidazolium Br$^-$ salts. Corresponding dibromide (1 equivalent) and **68** (1 equivalent) were added separately to Schlenk flasks. MeCN (10 mL) was added to each flask. The solution of dibromide was slowly transferred into the **68** solution *via* a syringe. The reaction mixture was stirred for 16 hours, during which time a colourless solid. The colourless solid was collected by filtration, washed with Et_2O and dried *in vacuo*.

i) Preparation of H_2**L69**Br_2

68 (0.090 g, 0.38 mmol) and **72** (0.129 g, 0.38 mmol) were reacted according to the general procedure to afford a colourless solid. Yield: 0.16 g, 0.275 mmol, 73 %.

^{1}H NMR (300 MHz, d_6-DMSO) δ (ppm) 8.71 (s, 2H, imH-2), 8.03 – 7.28 (m, 10H, ArH, pyH and imH), 5.57 – 5.50 (m, 8H, N**CH$_2$**-py and N**CH$_2$**-Ar). ^{13}C {^{1}H} NMR (75 MHz, d_6-DMSO) δ (ppm) 158.0 (C), 140.9 (C), 138.3 (CH), 135,8 (CH), 128.5 (CH), 127.3 (C), 127.1 (CH), 122.9 (CH), 122.7 (CH), 120.5 (CH), 58.4 (CH_2), 54.3 (CH_2). HRMS (ESI$^+$): *m/z* 210.5461, 211.5451 $[M – 2Br]^{2+}$, calculated $[M – 2Br]^{2+}$ 210.5446, 211.5435.

ii) Preparation of H_2**L75**Br_2

68 (0.6 g, 2.5 mmol) and **74** (0.66 g, 2.5 mmol) were reacted according to the general procedure to afford a sticky solid, on which anion exchange was subsequently carried out to afford H_2**L75**$(PF_6)_2$ (see below).

iii) Preparation of H_2**L76**Br_2

67 (1.33 g, 5.01 mmol) and **68** (1.20 g, 5.01 mmol) were reacted according to the general procedure to afford a colourless solid. Yield: 1.70 g, 3.37 mmol, 67 %.

^{1}H NMR (300 MHz, d_4-MeOH) δ (ppm) 8.95 (t, *J* = 1.4 Hz, 2H, imH-2), 7.86 (t, *J* = 7.6 Hz, 2H, pyH-4), 7.53 (d, *J* = 7.6 Hz, 4H, pyH-3 and pyH-5), 7.43 (d, *J* =1.4 Hz, 4H, imH-4 and imH-5), 5.50 (s, 4H, N**CH$_2$**-py). ^{13}C {^{1}H} NMR (75 MHz, d_d-MeOH) δ (ppm) 154.0, 140.3, 133.3, 124.6, 122.8, 54.2. HRMS (ESI$^+$): *m/z* 172.0869 $[M – 2Br]^{2+}$, calculated $[M – 2Br]^{2+}$ 172.0869.

General procedure for anion exchange to form imidazolium PF_6^- salts. The corresponding bromide salt (1 equivalent) was dissolved in a minimum volume of water, followed by addition of NH_4PF_6 (10 equivalents) whilst vigorously stirring in air under hydrous conditions, to afford a colour less solid. The solid was collected by filtration, washed with MeOH and Et_2O, and dried *in vacuo*. The process was assumed to go to completion as the precipitation of

i) Preparation of H_2**L69**$(PF_6)_2$

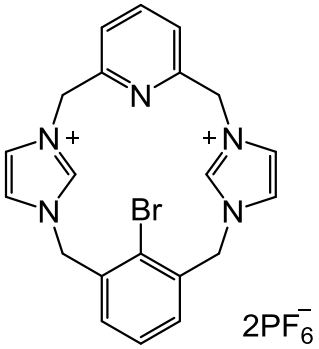

H_2**L69**Br_2 (0.10 g, 0.14 mmol) and NH_4PF_6 (0.22 g, 1.4 mmol) were reacted according to the general procedure to afford a colourless solid. Yield: 0.060 g, 0.095 mmol, 68 %.

^{1}H NMR (300 MHz, CD_3CN) δ (ppm) 8.15 (s, 2H, imH-2), 7.92 (t, *J* = 7.8 Hz ,1H, pyH-4), 7.83 (d, *J* = 7.8 Hz, 2H, pyH-3 and pyH-5), 7.70 (t, *J* = 7.8 Hz ,1H, ArH-4), 7.56 (d, *J* = 7.8 Hz, 2H, ArH-3 and ArH-5), 7.49 (d, *J* = 1.7 Hz, 2H, imH), 7.42 (d, *J* = 1.7 Hz, 2H, imH), 5.55 (d, *J* = 14.6 Hz, 2H, N**CH$_2$**-py), 5.34 (d, *J* = 15.1 Hz, 2H, N**CH$_2$**-Ar), 5.32 (d, *J* = 14.6 Hz, 2H, N**CH$_2$**-py), 5.17 (d, *J* = 15.1 Hz, 2H, N**CH$_2$**-Ar). ^{13}C {^{1}H} NMR (75 MHz, CD_3CN) δ (ppm) 154.3 (C), 140.2 (C), 136.5 (CH), 135.9 (CH), 135.5 (CH), 130.6 (CH), 125.0 (C), 124.9 (CH), 124.9 (CH), 123.8 (CH), 55.3 (CH_2), 54.7 (CH_2). HRMS (ESI$^+$): *m/z* 210.5485, 211.5476 $[M - 2PF_6]^{2+}$, calculated $[M - 2PF_6]^{2+}$ 210.5446, 211.5435.

ii) Preparation of H_2**L75**$(PF_6)_2$

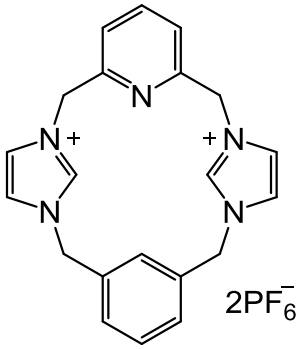

The sticky H_2**L75**Br_2 was dissolved in water and NH_4PF_6 (3.9 g, 25 mmol) was added. The mixture was reacted according to the general procedure to afford a colourless solid. Yield: 1.22 g, 1.92 mmol, 77 %.

^{1}H NMR (300 MHz, CD_3CN) δ (ppm) 8.5 (s, 2H, imH-2), 7.97 (t, *J* = 7.7 Hz, 1H, pyH-4), 7.60 – 7.35 (m, 10 H, pyH, ArH and imH), 5.43 (s, 4H, N**CH$_2$**-py), 5.39 (s, 4H, N**CH$_2$**-Ar). ^{13}C {^{1}H} NMR (75 MHz, CD_3CN) δ (ppm) 154.0 (C), 140.0 (CH), 139.7 (C), 137.1 (CH), 136.5 (CH), 135.7 (CH), 131.1 (CH), 130.6 (CH), 130.2 (CH), 130.0 (CH), 129.5 (CH), 125.1 (CH), 124.6 (CH), 124.3 (CH), 123.9 (CH), 123.4 (CH), 123.1 (CH), 118.3 (CH), 54.4, 54.2, 53.4, 53.1. HRMS (ESI$^+$): *m/z* 171.5901 $[M - 2PF_6]^{2+}$, calculated $[M - 2PF_6]^{2+}$ 171.5893.

iii) Preparation of H_2**L76**$(PF_6)_2$

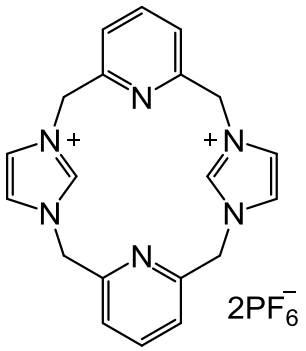

H_2**L76**Br_2 (1.30 g, 2.6 mmol) and NH_4PF_6 (4.2 g, 26 mmol) were reacted according to the general procedure to afford a colourless solid. Yield: 1.158 g, 1.83 mmol, 70 %.

^{1}H NMR (300 MHz, CD_3CN) δ (ppm) 8.55 (s, 2H, imH-2), 7.96 (t, *J* = 7.7 Hz, 2H, pyH-4), 7.54 (d, *J* = 7.7 Hz, 4H, pyH-3 and pyH-5), 7.34 (s, 4H, imH-4 and imH-5), 5.44 (s, 8H, N**CH$_2$**-py). ^{13}C {^{1}H} NMR (75 MHz, CD_3CN) δ (ppm) 153.8 (C), 139.7 (CH), 137.6 (CH), 124.1 (CH), 123.7 (CH), 54.0 (CH_2). HRMS (ESI$^+$): m/z 172.0867 $[M - 2PF_6]^{2+}$ calculated $[M - 2PF_6]^{2+}$ 172.0869.

Preparation of an imidazolium OTf salt.

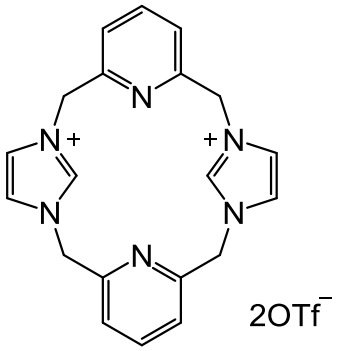

H_2**L76**Br_2 (0.40 g, 0.79 mmol) was added to ampoule. MeCN (10 mL) was added, followed by AgOTf (0.41 g, 1.59 mmol) whilst vigorously stirred and the mixture stirred for a further 1 hour, during which time a yellow precipitate was observed. The precipitate was removed by cannula filtration and the volume of the filtrate was reduced to about 2 mL *in vacuo*. Et_2O (50 mL) was added to precipitate a colourless solid, which was collected *via* cannula filtration. The colourless product was washed with anhydrous Et_2O (10 mL) and dried *in vacuo*. Yield: 0.40 g, 0.66 mmol, 84 %.

^{1}H NMR (300 MHz, CD_3CN) δ (ppm) 8.65 (t, *J* = 1.5 Hz, 2H, imH-2), 7.92 (t, *J* = 7.7 Hz, 2H, pyH-4), 7.52 (d, *J* = 7.7 Hz, 4H, pyH-3 and pyH-5), 7.34 (d, *J* = 1.5 Hz, 4H, imH-4 and imH-5), 5.44 (s, 8H, N**CH$_2$**-py). ^{13}C {^{1}H} NMR (75 MHz, CD_3CN) δ (ppm) 153.2 (C), 138.6 (CH), 136.6 (CH), 124.0 (CH), 123.4 (CH), 53.8 (CH_2). HRMS (ESI$^+$): m/z 172.0871 $[M - 2OTf]^{2+}$ calculated $[M - 2OTf]^{2+}$ 172.0869.

5.8.7 Preparation of complexes using the electrochemical method

i) Preparation of [Cu**L69**](PF_6): 1st attempt

H_2**L**$(PF_6)_2$ (80 mg, 0.126 mmol) was added to a flame-dried three-necked round-bottomed flask. MeCN (20 mL) was added *via* syringe and two Cu electrodes were inserted into the solution. A voltage was applied to achieve a current of 30 mA, which was maintained for 15 minutes. The solvent was removed *in vacuo* to

give a green solid, which was analysed in anhydrous CD_3CN or MeCN prepared in a Glovebox.

ii) Preparation of [Cu**L69**](PF_6): 2nd attempt

H_2**L69**(PF_6)$_2$ (235 mg, 0.37 mmol) was added to a flame-dried three-necked round-bottomed flask. MeCN (20 mL) was added *via* syringe and two Cu electrodes were inserted into the solution. A voltage was applied to achieve a current of 20 mA, which was maintained for 60 minutes. The solvent was removed *in vacuo* to give a green solid, which was analysed in anhydrous CD_3CN or MeCN prepared in a Glovebox.

5.8.8 Preparation of complexes *via* silver transmetallation

i) Attempted preparation of [Ag**L69**](PF_6)

H_2**L69**(PF_6)$_2$ (0.2 g, 0.28 mmol) and Ag_2O (0.065 g, 0.28 mmol) were added to freshly activated 4Å molecular sieves. In the absence of light, DCM (5 mL) was added *via* syringe and the mixture stirred for 3 hours, after which time a HRMS of the reaction sample showed the formation of [Ag**L69**]$^+$ ion. The reaction mixture was filtered *via* cannula filtration. The solvent was removed from the filtrate *in vacuo* and recrystallised by DCM / hexane to obtain a sticky light brown solid. Yield: undetermined. The [Ag**L69**]$^+$ was no longer observed from the product sample.

ii) Attempted preparation of Cu**L69**Br *via in situ* [Ag**L69**]$^+$

H_2**L69**(PF_6)$_2$ (0.05 g, 0.070 mmol) and Ag_2O (0.016 g, 0.070 mmol) were added to freshly activated 4Å molecular sieves and dried *in vacuo*. In the absence of light, DCM (5 mL) was added *via* syringe and the mixture stirred for 1 hour. CuBr (0.010 g, 0.070 mmol) was added and the mixture stirred for 2 hours. Neither [Ag**L69**]$^+$ nor [Cu**L69**]$^+$ was observed in the HRMS of the reaction sample.

iii) Preparation of [Ag**L75**](PF_6)

H_2**L75**(PF_6)$_2$ (0.2 g, 0.32 mmol) and Ag_2O (0.073 g, 0.32 mmol) were added to the freshly activated 4Å molecular sieves. In the absence of light, MeCN (10 mL) was added *via* syringe and stirred for 4 hours. MeOH (10 mL) was added and stirred for 16 hours. The mixture was filtered through Celite and the solvents were removed from the filtrate *in vacuo* to afford a brown oil. The crude brown oil was recrystallised in MeCN (3 mL) / Et_2O (50 mL) to give a light brown solid. Yield: 0.20 g, over theoretical yield (likely with a trace of Ag(PF_6))

^{1}H NMR (300 MHz, CD_3CN) δ (ppm) 7.91 – 6.85 (m, 11H), 5.48 – 5.00 (m, 8H). 13 C {1H} NMR (126 MHz, CD_3CN) resonance was too weak and noisy despite

6000-scan experiment. HRMS (ESI)$^{+}$: *m/z* 448.0682 [Ag**L75**]$^{+}$, calculated [Ag**L75**]$^{+}$ 448.0691.

iv) Preparation of [Cu**L75**](PF_6)

In the absence of light, [Ag**L75**](PF_6) (0.050 g, 0.084 mmol) and CuI (0.016 g, 0.084 mmol) were mixed in MeCN (50 mL) for 24 hours. The mixture was filtered through Celite. The filtrate was concentrated to about 2 mL in volume and Et_2O (70 mL) was added to precipitate a pale green solid, which was collected by cannula filtration and dried *in vacuo*. Yield: 0.0265 g, 0.048 mmol, 57 %.

^{1}H NMR (300 MHz, CD_3CN) δ (ppm) 7.91 – 6.85 (m, 11H), 5.48 – 5.00 (m, 8H). ^{13}C {^{1}H} NMR (126 MHz, CD_3CN) resonance was too weak and noisy despite 6000-scan experiment. HRMS (ESI)$^{+}$: *m/z* 404.0932 [Cu**L75**]$^{+}$, calculated [Cu**L75**]$^{+}$ 404.0931; 202.5509 [Cu**L75** + H]$^{+2}$, calculated [Cu**L75** + H]$^{+2}$ 202.5502.

v) Preparation of [Ag**L76**](PF_6)

H_2**L76**(PF_6)$_2$ (1.0 g, 1.58 mmol) and Ag_2O (0.37 g, 1.58 mmol) were added to the freshly activated 4Å molecular sieves. In the absence of light, DMSO (5 mL) was added *via* a syringe and stirred for 3 hours at 55 °C. The mixture was filtered through Celite and the filtrate poured into water (100 mL) to afford a colourless precipitate. The solid was collected by filtration and dried *in vacuo*. Yield: 0.66 g, 1.11 mmol, 70 %.

^{1}H NMR (300 MHz, *d*$_6$-DMSO) δ (ppm) 7.99 (t, J = 7.7 Hz, 2H), 7.77 (s, 4H, imH), 7.69 (d, *J* = 7.7 Hz, 4H), 5.52 (s, 8H). ^{13}C {^{1}H} NMR resonances were very weak despite at 126 MHz (500 MHz machine). HRMS (ESI^{+}): *m/z* 449.0796 [M – PF_6]$^{+}$, calculated [M – PF_6]$^{+}$ 449.0644.

Consistent with data previously reported.

vi) Preparation of [Cu**L76**](PF_6)$_2$

In the absence of light, [Ag**L76**](PF_6) (0.30 g, 0.50 mmol) and $CuBr_2$ (0.113 g, 0.51 mmol) were stirred at room temperature in MeCN (10 mL) under Ar for 2 hours. $AgPF_6$ (0.127 g, 0.51 mmol) was added, with the colour immediately changing to purple. The reaction mixture was filtered *via* cannula filtration. The filtrate was concentrated to about 2 mL *in vacuo* and anhydrous Et_2O (70 mL) was added to precipitate a purple solid, which was collected by cannula filtration and dried *in vacuo*. Yield: 0.30 g, 0.43 mmol, 86 %.

^{1}H NMR (300 MHz, CD_3CN) δ (ppm) 7.98 (t, *J* = 7.7 Hz, 2H), 7.77 (s, 4H, imH), 7.69 (d, J = 7.7 Hz, 4H), 5.54 – 5.46 (m, 4H), 5.46 – 5.36 (m, 4H). ^{13}C {^{1}H} NMR resonances were very weak despite at 126 MHz (500 MHz machine). HRMS

(ESI$^+$): *m/z* 202.5437 $[M - 2PF_6]^{2+}$, calculated $[M - 2PF_6]^{2+}$ 202.5439. Analysis Calculated for $C_{20}H_{18}N_6CuP_2F_{12}$ + 2/5CuP_2F_{12}: C, 28.69; H 2.17; N, 10.04. Found: C, 28.66; H 2.20; N, 10.24.

Single crystals suitable for X-ray diffraction analysis were grown *via* the vapour diffusion of Et_2O into a concentrated solution of the product in MeCN.

vii) Attempted preparation of [Ag**L76**(OTf)]

H_2**L76**$(PF_6)_2$ (1.0 g, 1.58 mmol) and Ag_2O (0.37 g, 1.58 mmol) were added to freshly activated 4Å molecular sieves. In the absence of light, DMSO or MeCN (5 mL) was added *via* syringe and stirred for 3 hours at 55 °C.

viii) Preparation of [Cu**L76**$(OTf)_2$]

H_2**L76**Br_2 (0.50 g, 1.0 mmol) and Ag_2O (0.23 g, 1.0 mmol) were added to freshly activated 4Å molecular sieves. In the absence of light, MeOH (20 mL) was added and stirred at 50 °C under Ar for 4.5 hours. The reaction mixture was filtered *via* cannula and concentrated to about 5 mL *in vacuo*. MeCN (10 mL) was added followed by $CuBr_2$ (0.22 g, 1.0 mmol) and the reaction mixture stirred at room temperature for 4.5 hours. The yellow precipitate was removed by cannula filtration and the solvents removed from the filtrate *in vacuo*. MeCN (10 mL) was added, followed by AgOTf (0.51 g, 2.0 mmol) to afford a grey mixture. The mixture was stirred for 30 minutes, filtered *via* cannula and the solvent removed i*n vacuo* to obtain a greenish grey solid. Yield: 0.25 g, 0.36 mmol, 36 %.

^{1}H NMR spectrum resonances were very weak (300 MHz and 500 MHz, CD_3CN) but approximately at δ 7.97 – 7.72, 7.62 – 7.38 and 5.55 – 5.35. HRMS (ESI$^+$): *m/z* 554.0397 $[M - Otf]^+$, calculated $[M - OTf]^+$ 554.0404.

5.8.9 Preparation of oxidant 77

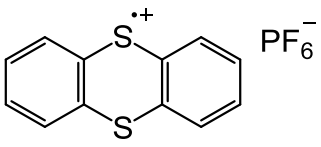

78 (0.20 g, 0.92 mmol) and $NOPF_6$ (0.16 g, 0.92 mmol) were added to an ampoule. Under Ar, MeCN (5 mL) was added and stirred at room temperature for 2 hours, during which time a brown fume was observed and the colour of the mixture changed to beep blue. Et_2O (100 mL) was added to precipitate a deep blue solid, which was collected by cannula filtration, washed with Et_2O (2 × 25 mL) and dried *in vacuo*. Yield: 0.19 g, 0.52 mmol, 57 %.

^{1}H NMR spectrum (300 MHz and 500 MHz, CD_3CN) was very weak. HRMS (ESI$^+$): *m/z* 216.0057 $[M - PF_6]^+$, calculated $[M - PF_6]^+$ 216.0067.

5.8.10 Oxidation of Cu-L76 complexes

Chemical Oxidation Procedure. [Cu**L75**]$(PF_6)_2$ or [Cu**L75**$(Otf)_2$] (0.05 mmol) was dissolved in CD_3CN (0.4 mL). A solution of **77** (0.05 mmol) in CD_3CN (0.5 mL) was added in portions of 0.1, 0.15 and 0.25 mL and analysed using ^1H NMR spectroscopy after each addition.

i) [Cu**L76**]$(PF_6)_2$ (35 mg, 0.05 mmol) was reacted with **77** according to the oxidation procedure, with colour changed from purple to orange. HRMS (ESI^+): *m/z* 404.0800 [Cu**L76** – H]$^+$, calculated [Cu**L76** – H]$^+$ 404.0805; 436.0695 [Cu**L76** – H + 2O]$^+$, calculated [Cu**L76** – H + 2O]$^+$ 436.0695.

ii) [Cu**L76**$(Otf)_2$] (34 mg, 0.05 mmol) was reacted with **77** according to the oxidation procedure, with the grey colour being bleached. HRMS (ESI^+): *m/z* 554.9120, 556.9114 [Cu**L76** + OTf + H]$^+$, calculated [Cu**L76** + OTf + H]$^+$ 555.0482; 570.9070, 572.9065 [Cu**L76** + OTf + H + O]$^+$, calculated [Cu**L76** + OTf + H + O]$^+$ 571.0431. However, those m/z peaks were not corresponding to Cu isotope ratio pattern (^{63}Cu: ^{65}Cu = 2.2: 1).

5.9 References

(1) Peters, M.; Breinbauer, R. *Tetrahedron Lett.* **2010**, *51*, 6622.
(2) Kolychev, E. L.; Shuntikov, V. V.; Khrustalev, V. N.; Bush, A. A.; Nechaev, M. S. *Dalton Trans.* **2011**, *40*, 3074.
(3) Lin, B.-L.; Kang, P.; Stack, T. D. P. *Organometallics* **2010**, *29*, 3683.
(4) Hu, X.; Castro-Rodriguez, I.; Meyer, K. *J. Am. Chem. Soc.* **2003**, *125*, 12237.
(5) Arnold, P. L.; Rodden, M.; Davis, K. M.; Scarisbrick, C.; Blake, A. J.; Wilson, C. *Chem. Comm.* **2004**, 1612.
(6) Lake, B. R. M.; Willans, C. E. *Organometallics* **2014**, *33*, 2027.
(7) Lake, B. R. M.; Ariafard, A.; Willans, C. E. *Chem. Eur.* **2014**, *20*, 12729.
(8) Normand, A. T.; Hawkes, K. J.; Clement, N. D.; Cavell, K. J.; Yates, B. F. *Organometallics* **2007**, *26*, 5352.
(9) Normand, A. T.; Yen, S. K.; Huynh, H. V.; Hor, T. S. A.; Cavell, K. J. *Organometallics* **2008**, *27*, 3153.
(10) Roberts, L. R.; Fish, P. V.; Storer, R. I.; Whitlock, G. A. *Bioorg. Med. Chem. Lett.* **2009**, *19*, 3113.
(11) Whitlock, G. A.; Brennan, P. E.; Roberts, L. R.; Stobie, A. *Bioorg. Med. Chem. Lett.* **2009**, *19*, 3118.
(12) Casitas, A.; King, A. E.; Parella, T.; Costas, M.; Stahl, S. S.; Ribas, X. *Chem. Sci.* **2010**, *1*, 326.
(13) Casitas, A.; Poater, A.; Sola, M.; Stahl, S. S.; Ribas, X. *Dalton Trans.* **2010**, *39*, 10458.
(14) Casitas, A. *RSC Catalysis Series* **2013**, *11*, 46.
(15) Housecroft, C. E.; Sharpe, A. G. *Inorganic Chemistry*; Pearson Education Limited: Harlow, 2008.
(16) Allen, F. H.; Kennard, O.; Watson, D. G. *J. Chem. Soc., Perkin Trans. 2* **1987**, S1.

(17) Bi, M.; Li, G.; Hua, J.; Liu, Y.; Liu, X.; Hu, Y.; Shi, Z.; Feng, S. *Crystal Growth and Design* **2007**, *7*, 2066.
(18) Tan, K. l.; Bergman, R. G.; Ellman, J. A. *J. Am. Chem. Soc.* **2001**, *123*, 2685.
(19) Kirk, K. L. *J. Org. Chem.* **1978**, *43*, 4381.
(20) Figueiredo, R. M. d.; Thoret, S.; Huet, C.; Dubois, J. *Synthesis* **2007**, *4*, 529.
(21) Primas, N.; Bouilon, A.; Lancelot, J.-C.; Santos, J. S.-d. O.; Lohier, J.-F.; Rault, S. *Lett. Org. Chem.* **2008**, *5*, 8.
(22) Borikar, S. P.; Daniel, T.; Paul, V. *Tetrahedron Lett.* **2009**, *50*, 1007.
(23) Hawkes, K. J.; Cavell, K. J.; Yates, B. F. *Organometallics* **2008**, *27*, 4758.
(24) Ribas, X.; Jackson, D. A.; Donnadieu, B.; Mania, J.; Parella, T.; Xifra, R.; Hedman, B.; Hodgson, K. O.; Llobet, A.; Stack, T. D. P. *Angew. Chem., Int. Ed.* **2002**, *41*, 2991.
(25) Casitas, A.; Canta, M.; Sola, M.; Costas, M.; Ribas, X. *J. Am. Chem. Soc.* **2011**, *113*, 19386.
(26) Garrison, J. C.; Simons, R. S.; Talley, J. M.; Wesdemiotis, C.; Tessier, C. A.; Youngs, W. J. *Organometallics* **2001**, *20*, 1276.
(27) Klawitter, I.; Anneser, M. R.; Dechert, S.; Meyer, S.; Demeshko, S.; Haslinger, S.; Pothig, A.; Kuhn, F. E.; Meyer, F. *Organometallics* **2015**, *34*, 2819.
(28) Lake, B. R. M.; Willans, C. E. *Chem. Eur. J.* **2013**, *19*, 16780.
(29) Jawor, M.; Ahmed, B. M.; Mezei, G. *Green Chem.* **2016**, *18*, 6209.
(30) Rault, S.; Primas, N.; Bouillon, A.; Lancelot, J.-C.; Santos, J. S.-d. O.; Lohier, J.-F. *Lett. Org. Chem.* **2008**, *5*, 8.
(31) Boga, C.; Vecchio, E. D.; Forlani, L.; Todesco, P. E. *J. Organomet. Chem.* **2000**, *601*, 233.

Conclusions

N-Heterocyclic carbenes (NHCs) are examples of stable singlet carbenes, which can be used in coordination chemistry. Their unique structural, steric and electronic properties can enhance the catalytic performance such as Grubbs II catalyst. However, there has also been non-innocent reactivity that such ligand get involved in reactions, for example, reductive elimination of aryl-imidazolium or halo-imidazolium ions.

In this project, a great variety of NHC ligands, *N*,*N*'-donors and *O*,*O*'-donors were investigated for their catalytic activity when coordinated with Cu(I) *in situ* in an Ullmann-type etherification reaction. The Cu complex that were observed to show good activity are with 1-allyl-3-picolylbenzimidazol-2-ylidene. We proposed that it was due to the balance of electronic and structural properties of the ligand that enhance all nucleophilic substitution, oxidative addition and reductive elimination steps assuming that the catalytic cycle takes place *via* such Cu(I)/Cu(III) mechanism.

Further investigations were carried out on side reactions during the catalysis, which aryl-imidazolium formation, dehalogenation and homocoupling reactions were explored under variations of nucleophile, base and metal/ligand concentrations. The etherification is favoured by a sufficient amount of nucleophile and metal/ligand, and can be increased with excess base. However, the aryl-imidazolium formation is favoured by a minimal base and excess metal/ligand.

We had then exploit the side reaction of aryl-imidazolium formation to selectively functionalise xanthine-based imidazolium compounds, which were activated electrochemically to form Cu-NHC complexes. The arylation reactions were monitored by *in situ* 1H NMR and IR spectroscopy, which the activation energy of the arylation was calculated to be 58.9 – 63.1 kJ mol^{-1}. Further investigation on the reaction mechanism is under process to understand the rate determining step of the reaction and thence the activation energy may be lowered so that the arylation reaction may be performed efficiently at lower temperatures.

Other part of the project inspected the further reaction of the 1-allyl-2-bromo-3-pyridyl imidazolium dicuprate(I)tribromide, which was generated by reductive elimination when excess CuBr2 is present with the Cu(NHC)Br_2 complex of 1-allyl-3-picolylimidazol-2-ylidene. The bromo-imidazolium salt can undergo

annulation reaction to form 7-bromo-5,6-dihydro-3-pyridyl-pyrolloimidazolium salt, which excess of Cu and pyridyl group were observed to be essential for the reaction.

As most of the reactions discussed in the project were proposed to proceed via a Cu(III) intermediate, attempts were made to stabilise a Cu(III)-NHC using the macrocyclic effect. The attempt to synthesise Cu(III) complexes *via* either oxidative addition of C-X bond to Cu(I) complexes or oxidation of preformed Cu(II)-NHC complexes was not successful. However, the cyclic voltammetry data suggested that the oxidation of Cu(II) to Cu(III) is possible but still lack of sufficient stabilisation.

Appendix

Supplementary Information on Compound NMR Analysis

P14*

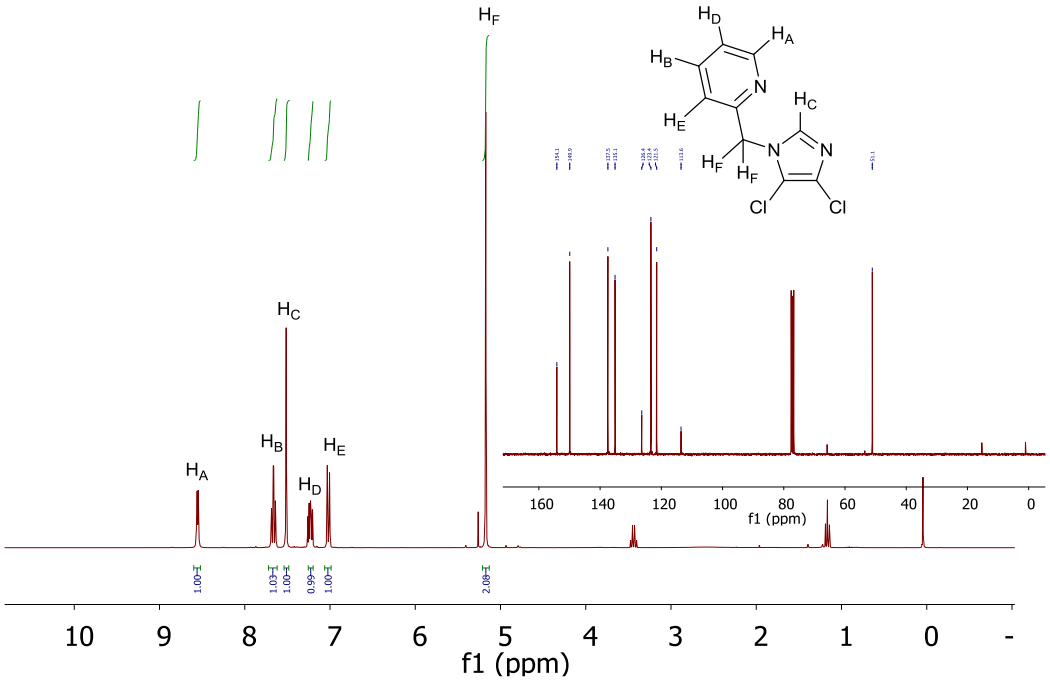

P14*: ^{1}H & ^{13}C $\{^{1}H\}$ NMR (300/75 MHz, $CDCl_3$)

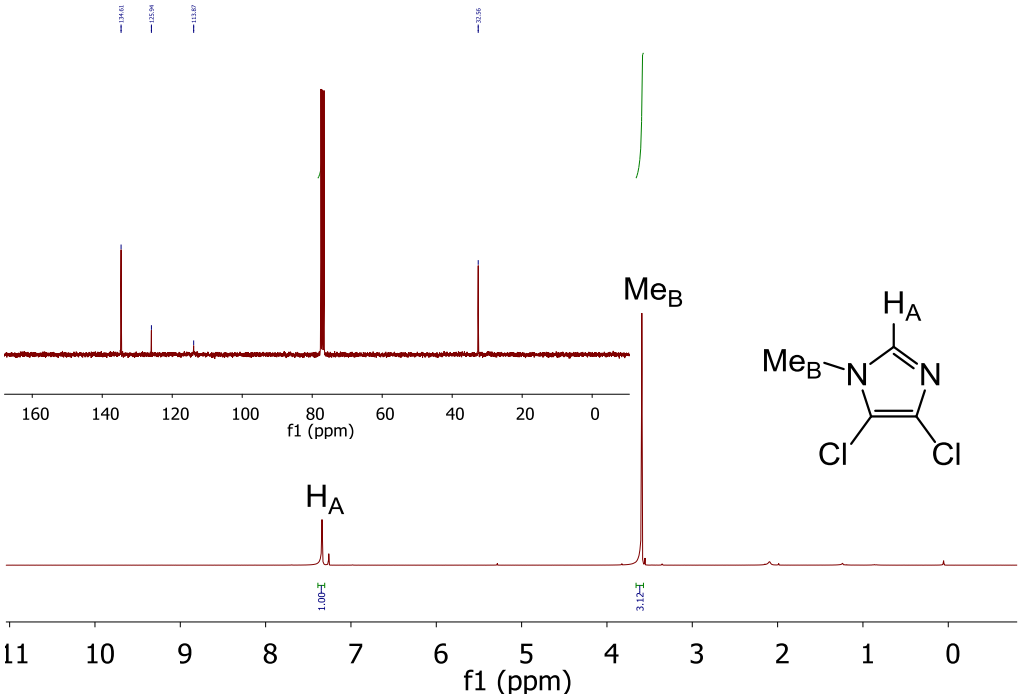

P14: ^{1}H and ^{13}C $\{^{1}H\}$ NMR (300/75 MHz, $CDCl_3$)

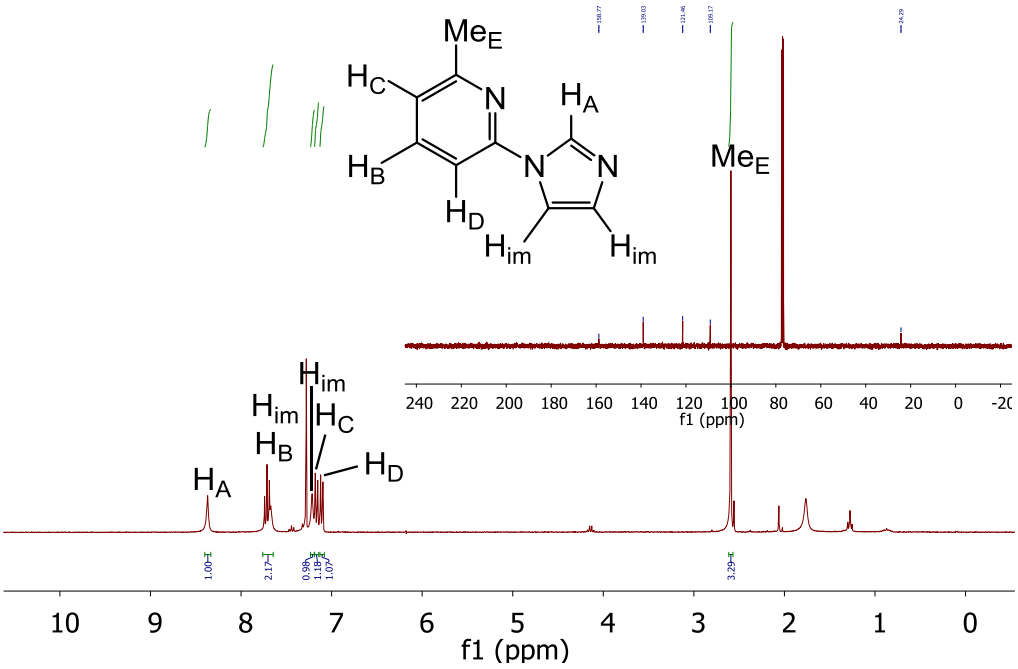

P17: ^{1}H and ^{13}C $\{^{1}H\}$ NMR (300/75 MHz, $CDCl_3$)

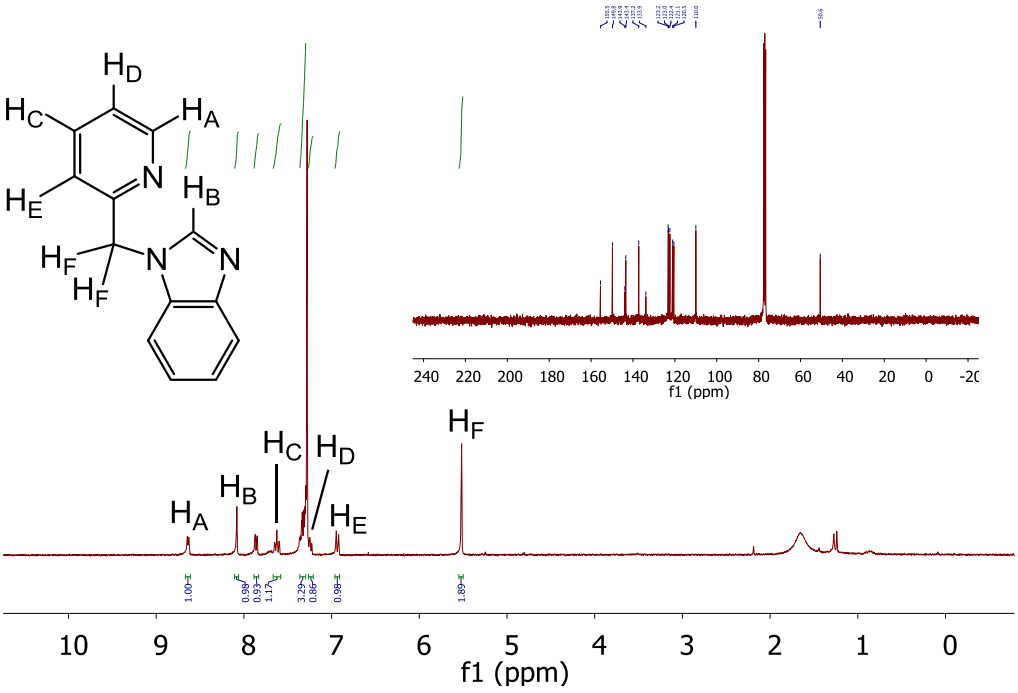

P23: ^{1}H and ^{13}C $\{^{1}H\}$ NMR (300/75 MHz, $CDCl_3$)

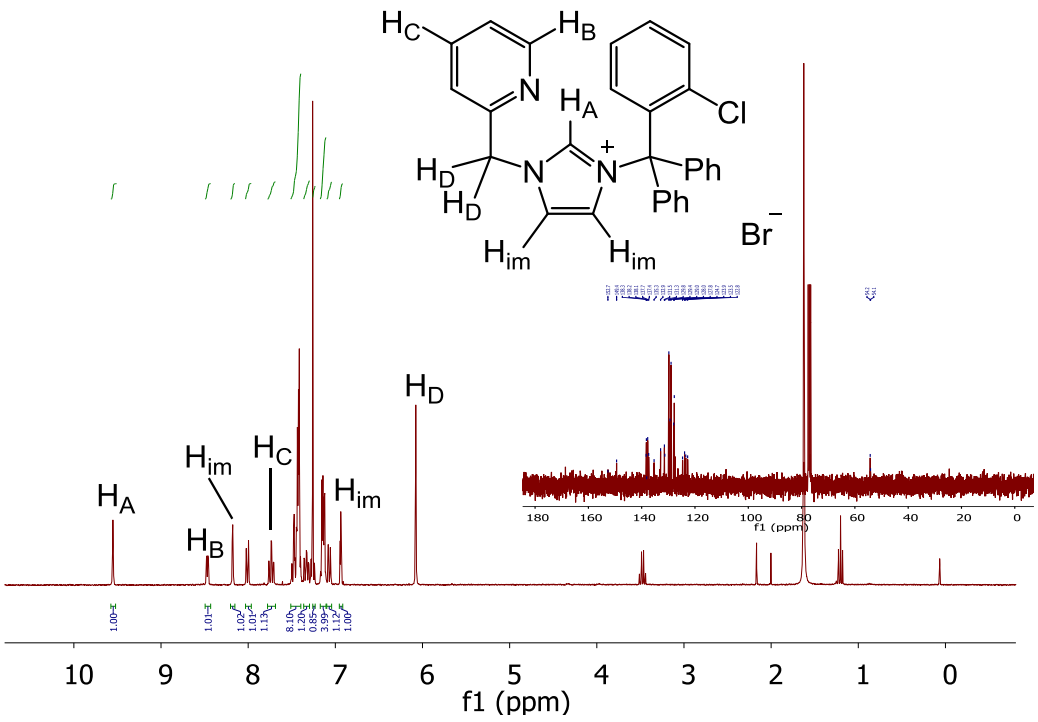

H**L5**Br: ^{1}H and ^{13}C $\{^{1}H\}$ NMR (300/75 MHz, $CDCl_3$)

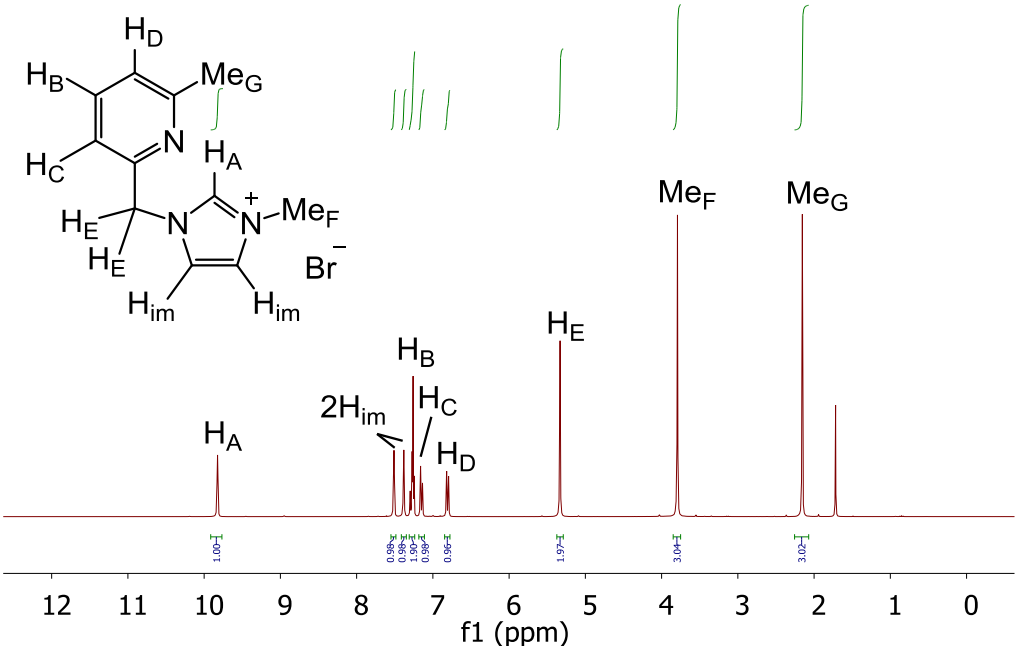

H**L7**Br: ^{1}H NMR (300 MHz, $CDCl_3$)

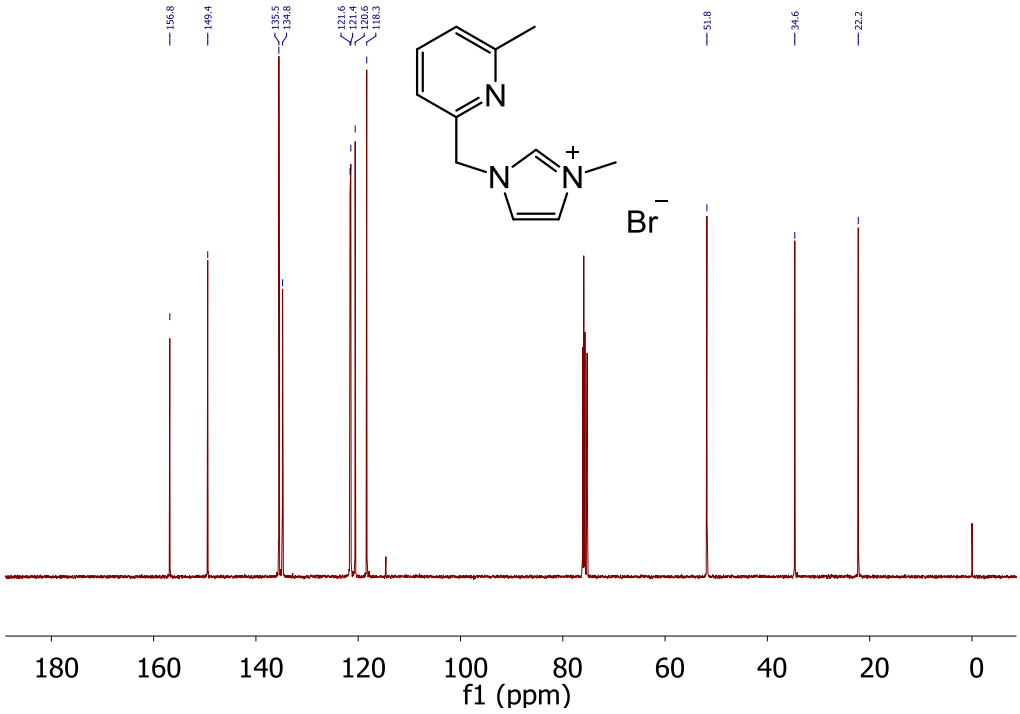

H**L7**Br: ^{13}C {^{1}H} NMR (75 MHz, $CDCl_3$)

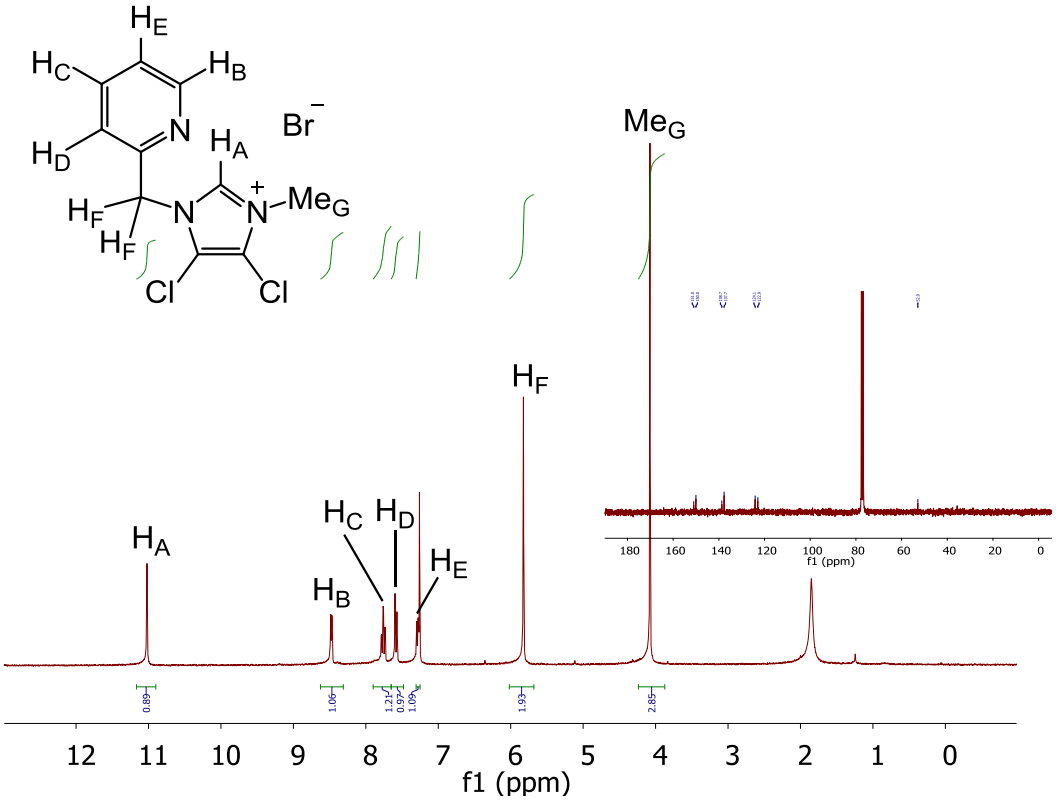

H**L14**Br: ^{1}H and ^{13}C {^{1}H} NMR (300/75 MHz, $CDCl_3$)

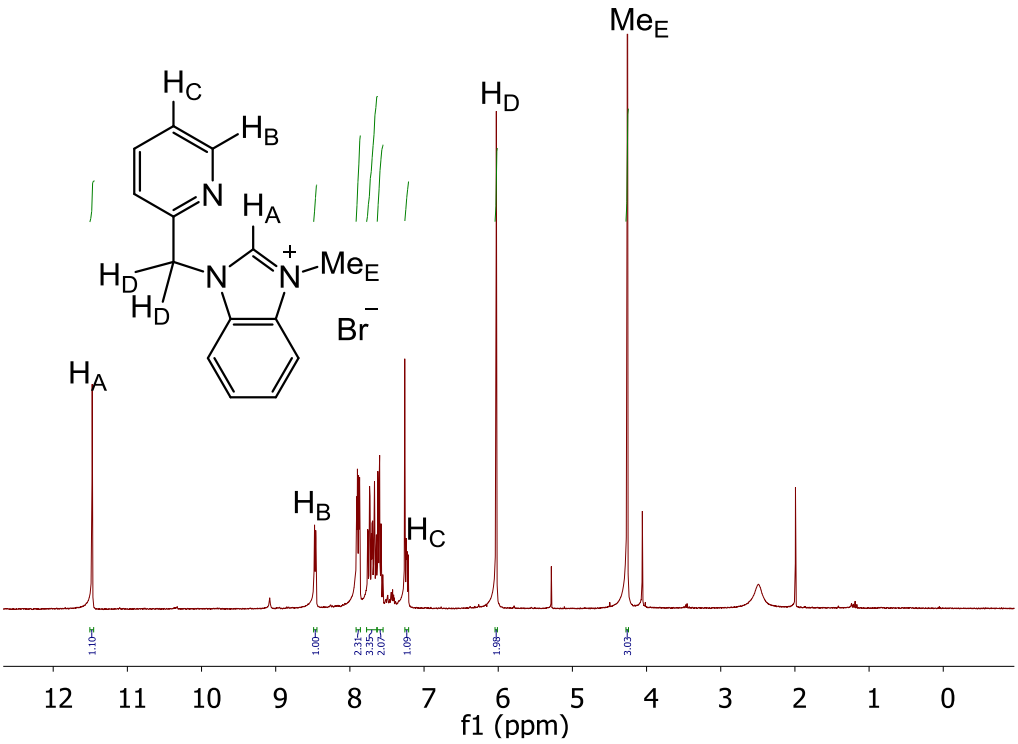

H**L15**Br: ^{1}H NMR (300 MHz, $CDCl_3$)

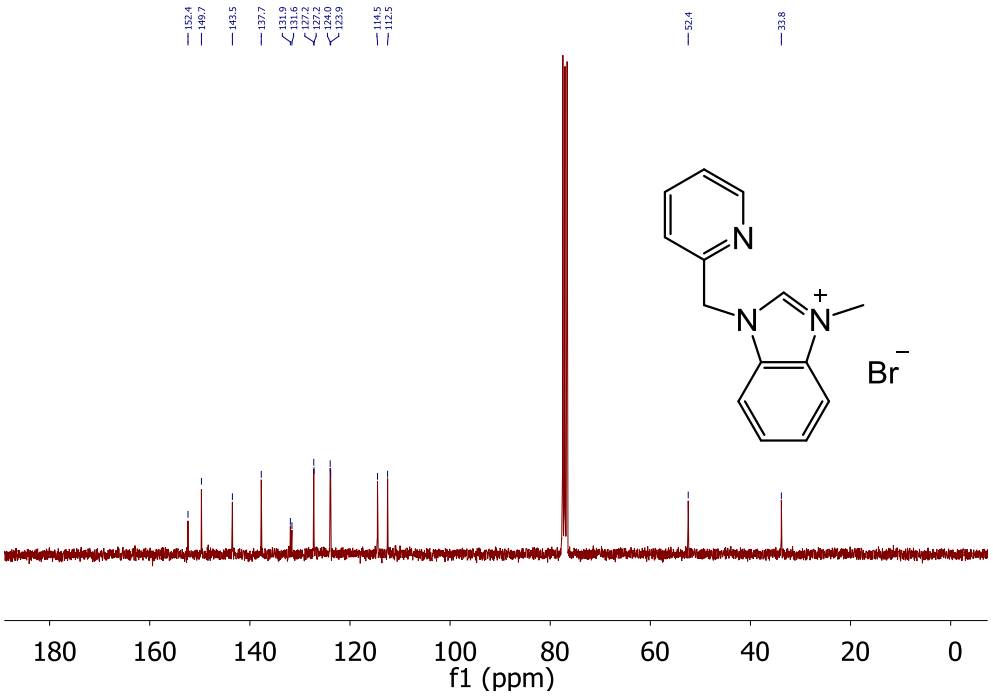

H**L15**Br: ^{13}C {^{1}H} NMR (75 MHz, $CDCl_3$)

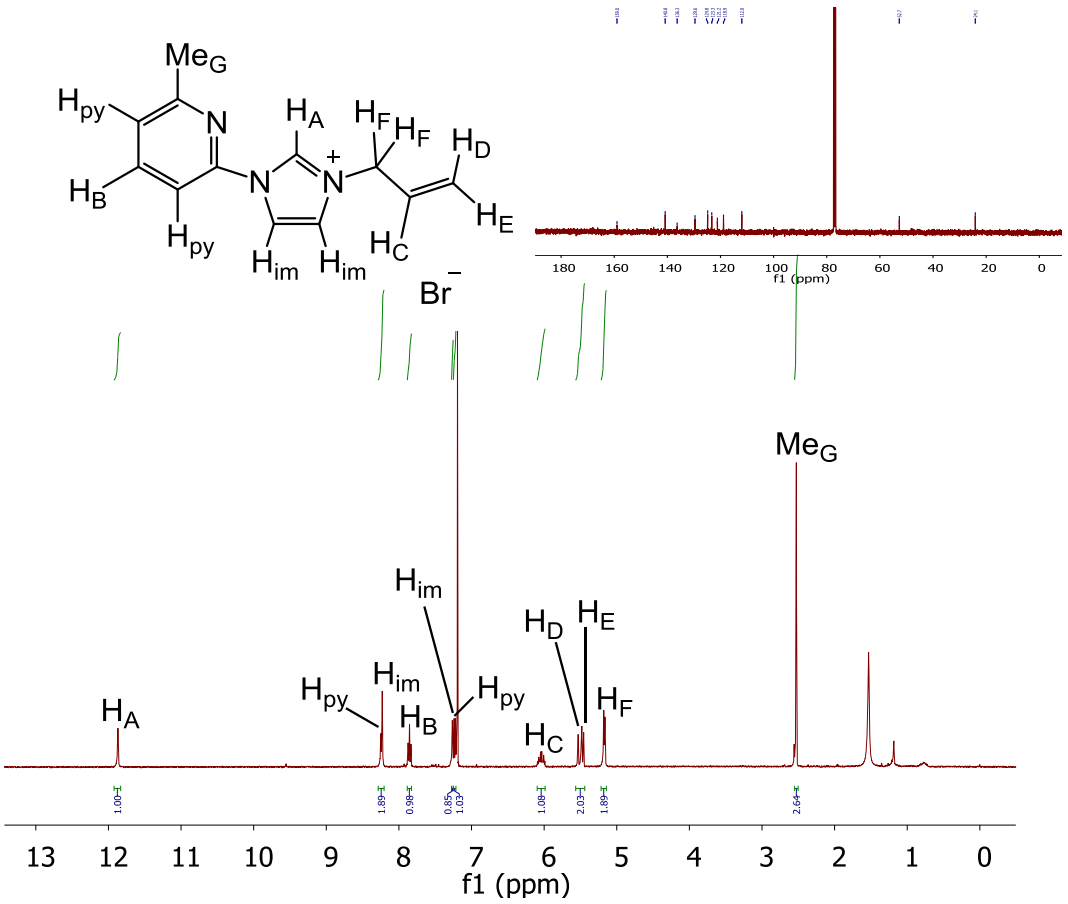

H**L17**Br: ^{1}H and ^{13}C $\{^{1}H\}$ NMR (400/101 MHz, $CDCl_3$)

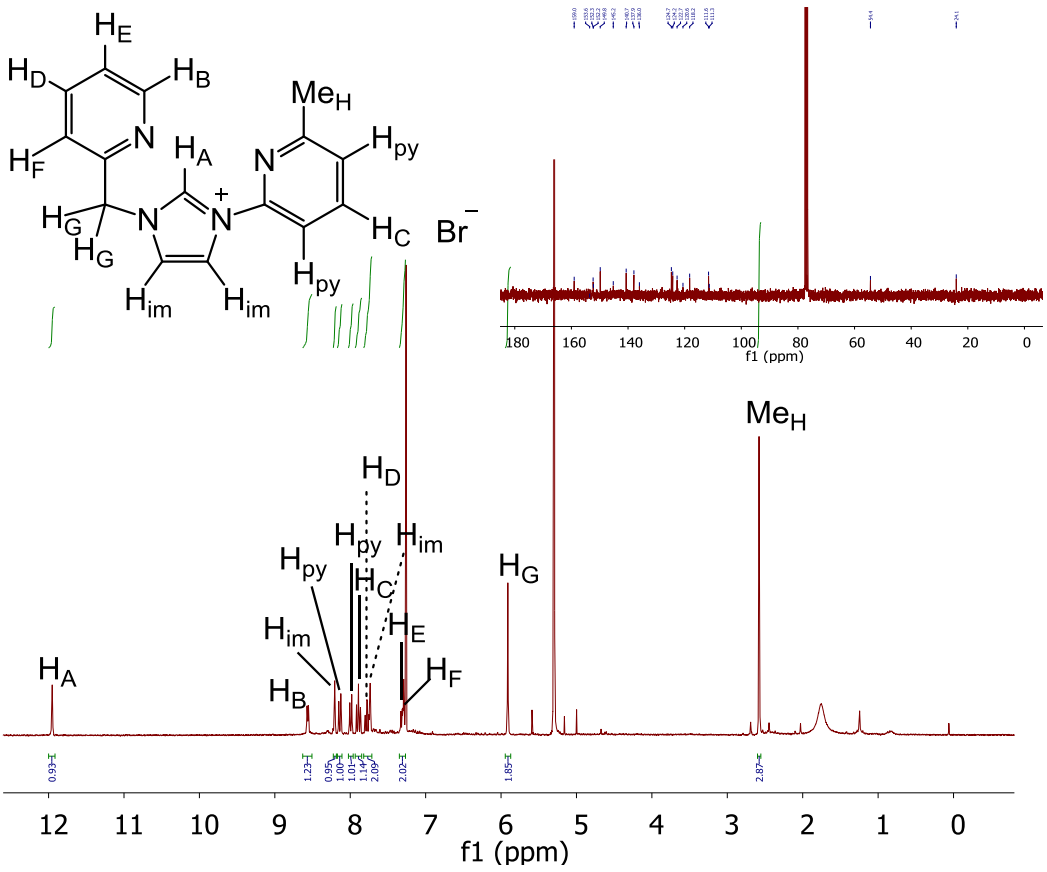

H**L21**Br: ^{1}H and ^{13}C {^{1}H} NMR (300/75 MHz, $CDCl_3$)

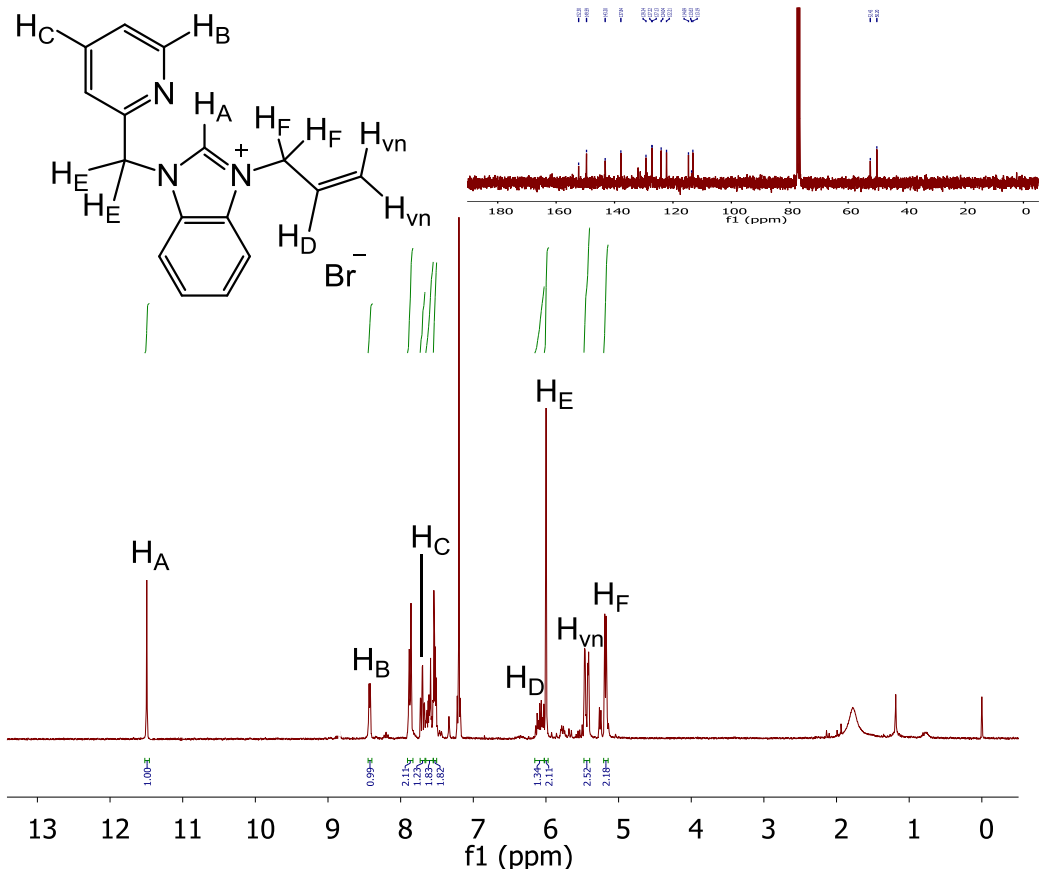

H**L23**Br: ^{1}H and ^{13}C {^{1}H} NMR (300/75 MHz, $CDCl_3$)

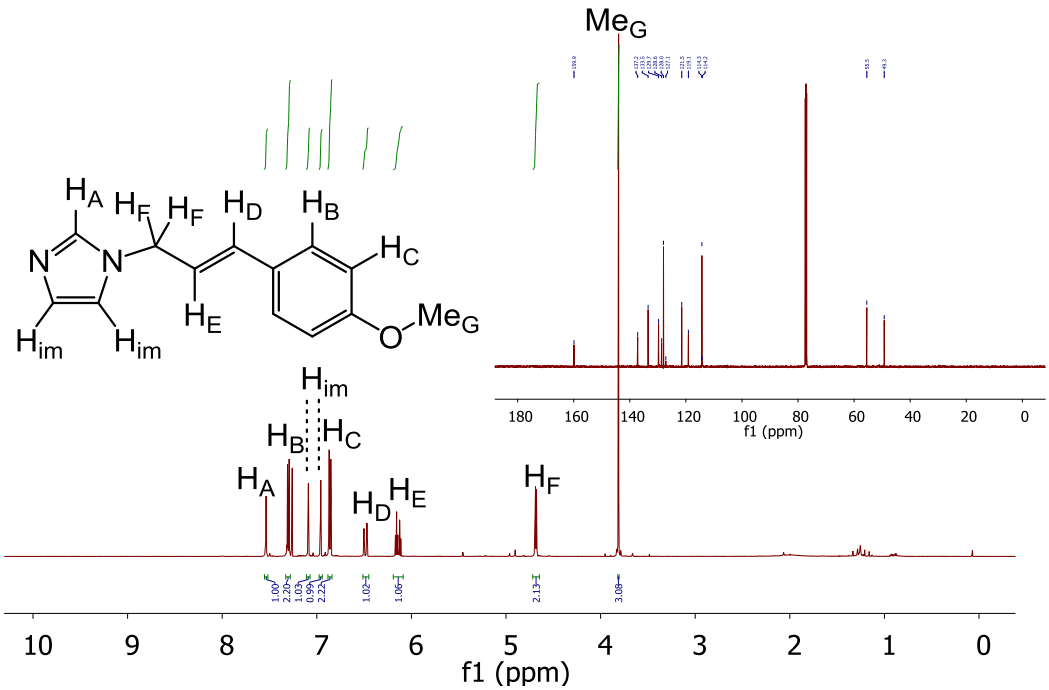

39: ^{1}H and ^{13}C {^{1}H} NMR (500/126 MHz, $CDCl_3$)

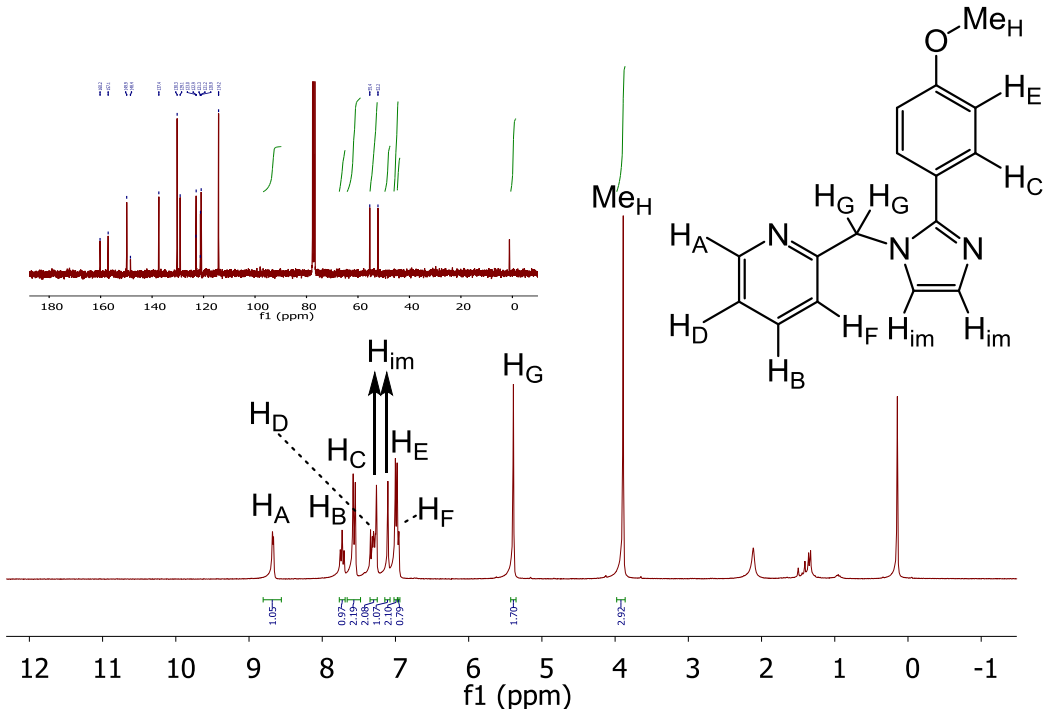

40: ^{1}H and ^{13}C {^{1}H} NMR (300/75 MHz, $CDCl_3$)

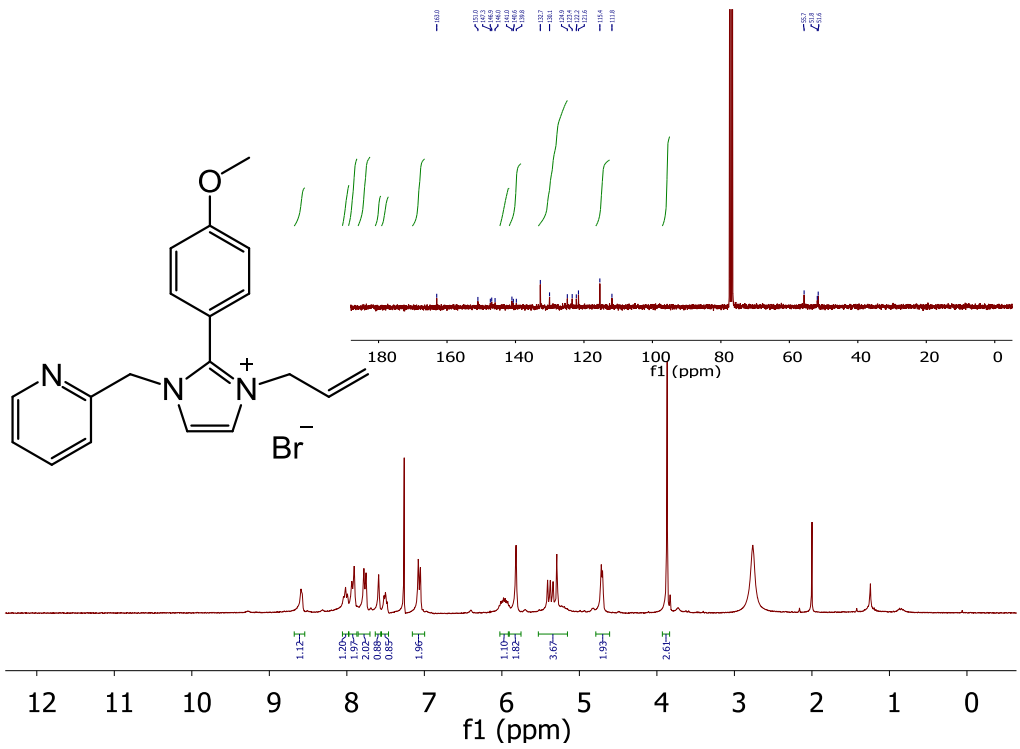

Ar1: ^{1}H and ^{13}C $\{^{1}H\}$ NMR (300/75 MHz, $CDCl_3$)

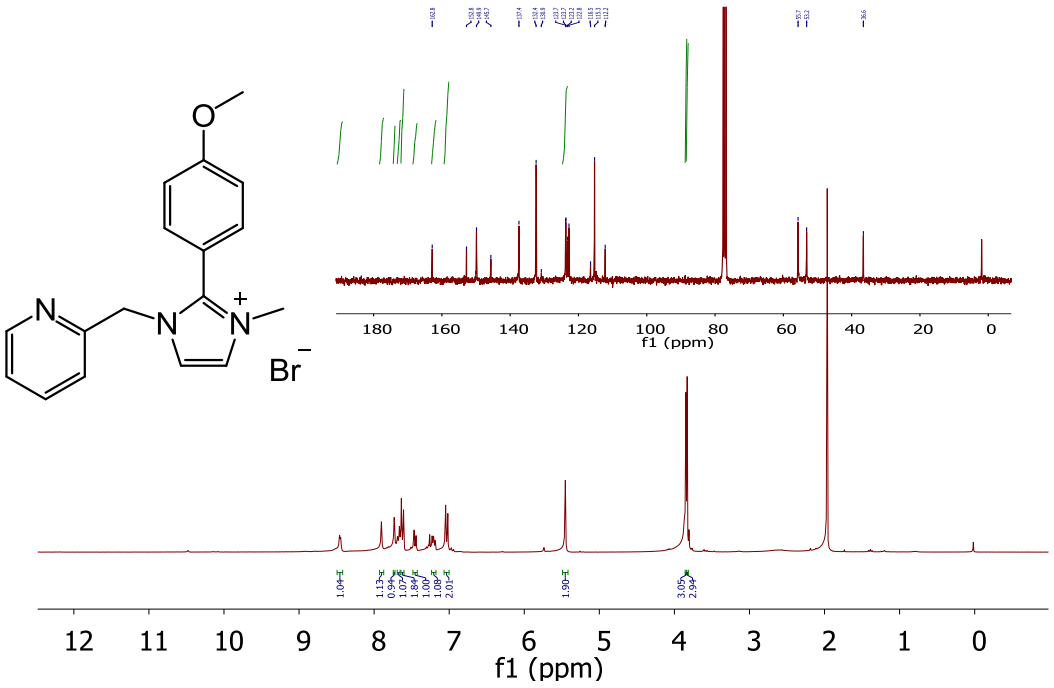

Ar3: ^{1}H and ^{13}C $\{^{1}H\}$ NMR (300/75 MHz, $CDCl_3$)

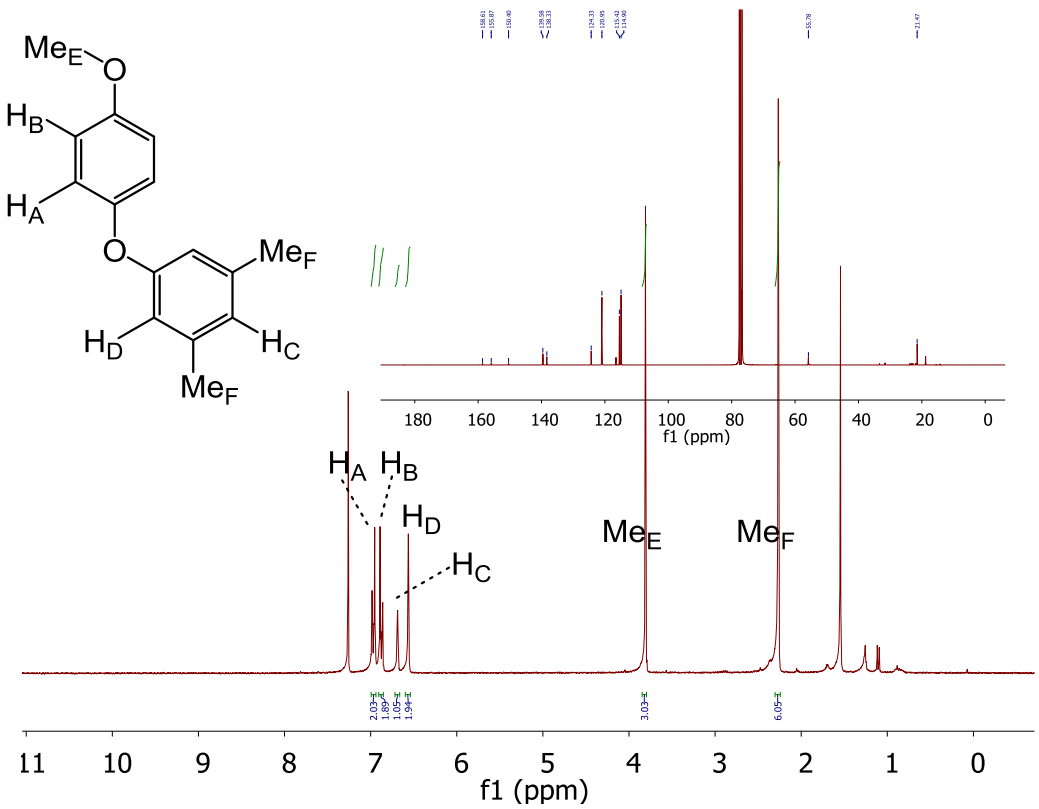

ArNu: ^{1}H and ^{13}C $\{^{1}H\}$ NMR (300/75 MHz, $CDCl_3$)

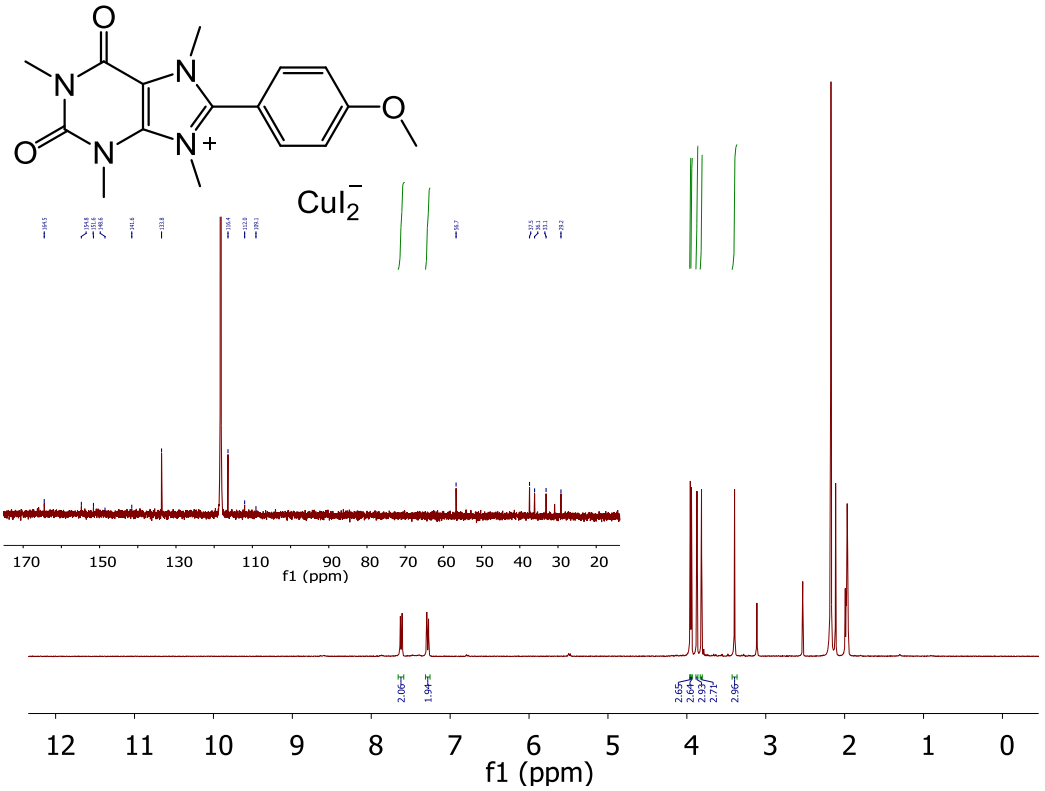

Ar46: ^{1}H and ^{13}C $\{^{1}H\}$ NMR (300/126 MHz, CD_3CN)

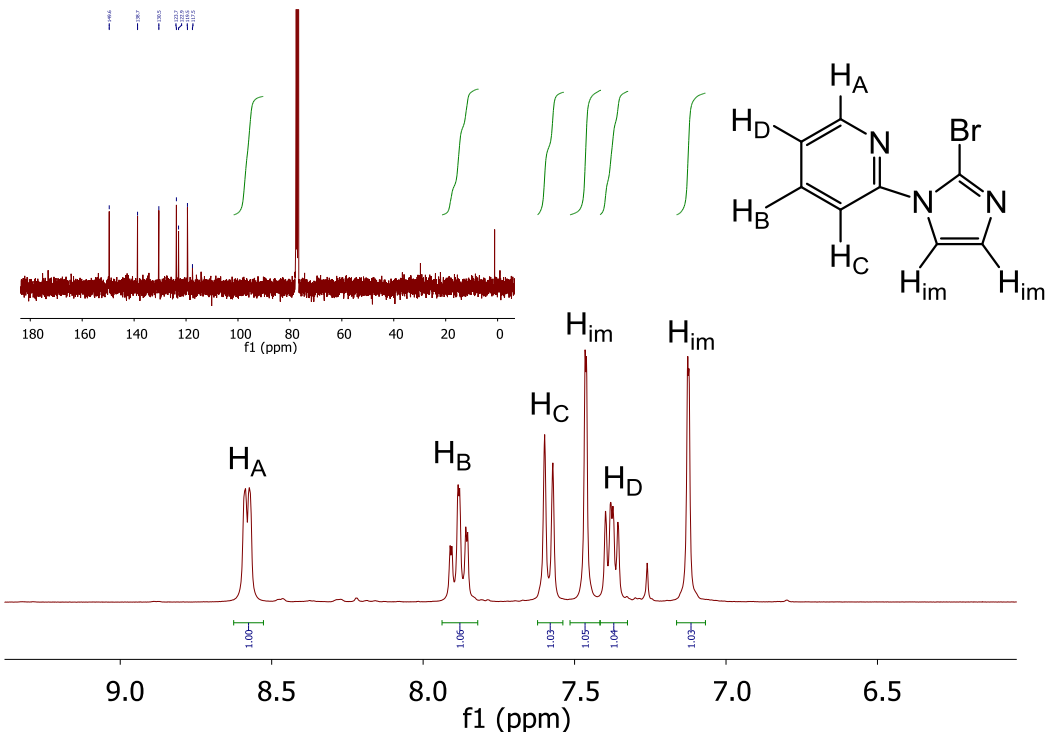

PS8: ^{1}H and ^{13}C $\{^{1}H\}$ NMR (300/75 MHz, $CDCl_3$)

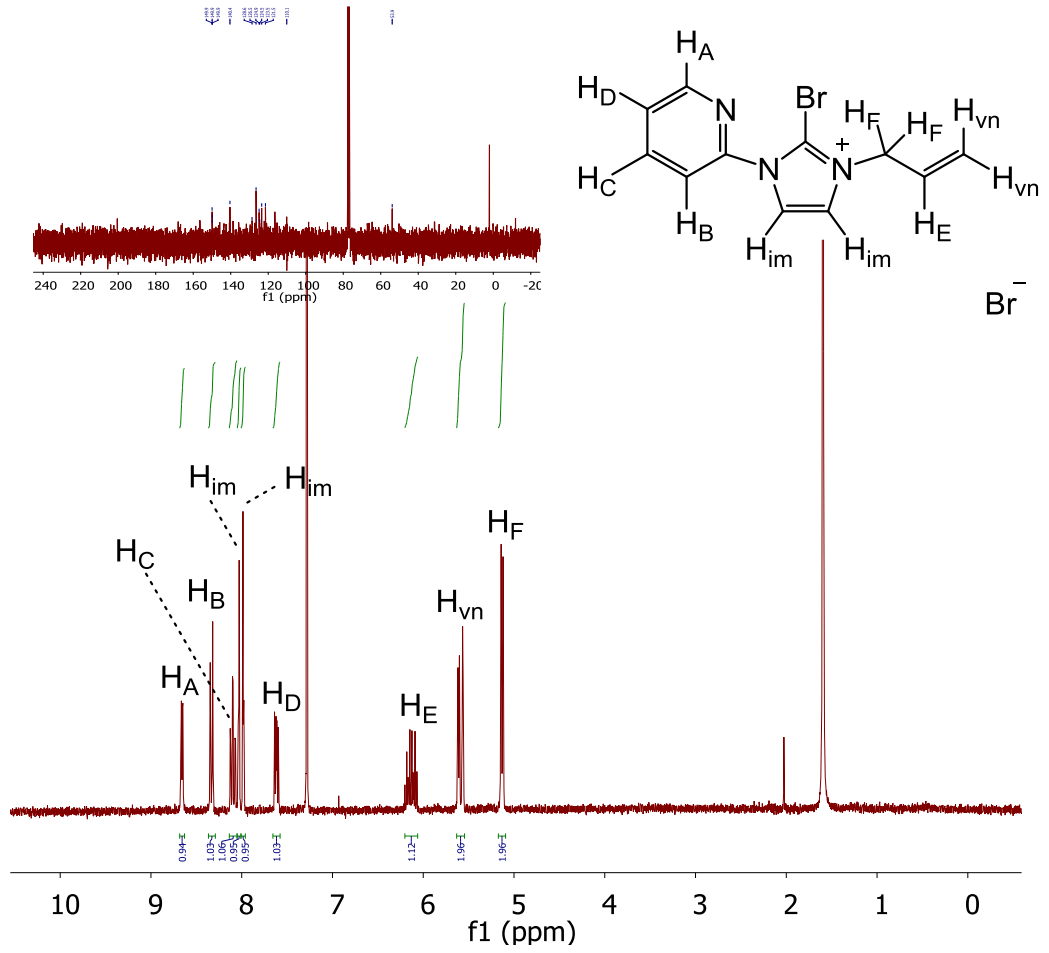

S8.b: ^{1}H and ^{13}C $\{^{1}H\}$ NMR (300/75 MHz, $CDCl_3$)

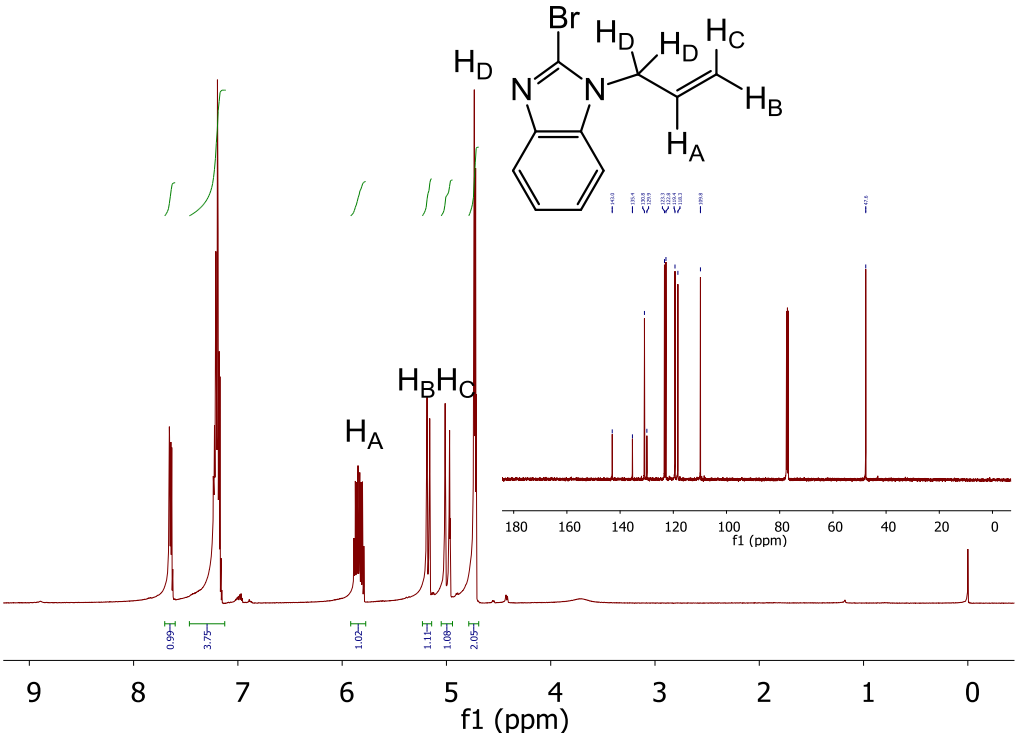

S8.b: ^{1}H and ^{13}C $\{^{1}H\}$ NMR (400/101 MHz, $CDCl_3$)

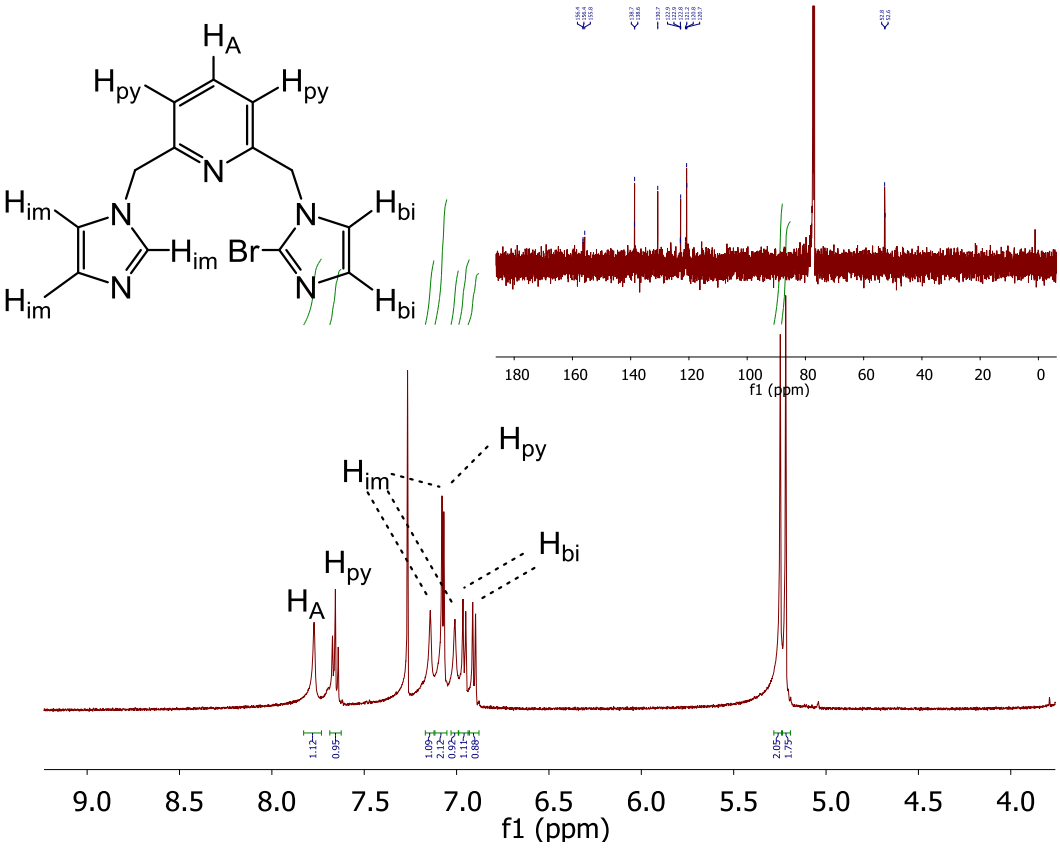

P65: ^{1}H and ^{13}C $\{^{1}H\}$ NMR (500/126 MHz, $CDCl_3$)

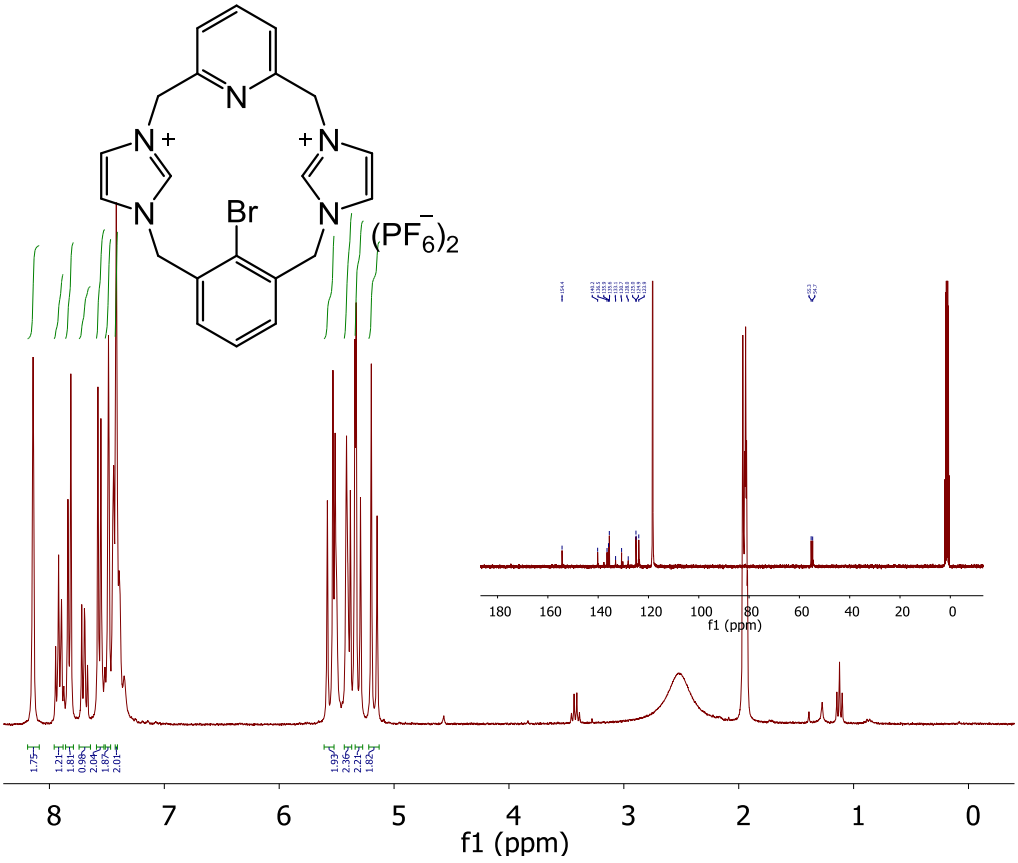

H_2**L69**$(PF_6)_2$: ^1H and ^{13}C $\{^1H\}$ NMR (300/126 MHz, CD_3CN)

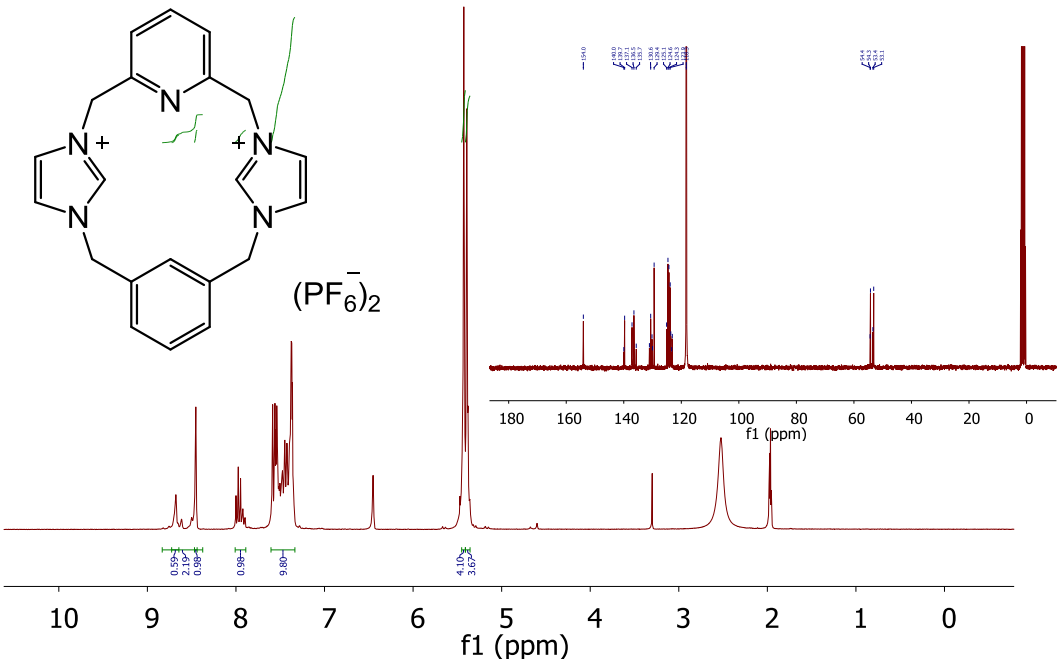

H_2**L75**$(PF_6)_2$: ^1H and ^{13}C $\{^1H\}$ NMR (300/126 MHz, CD_3CN)

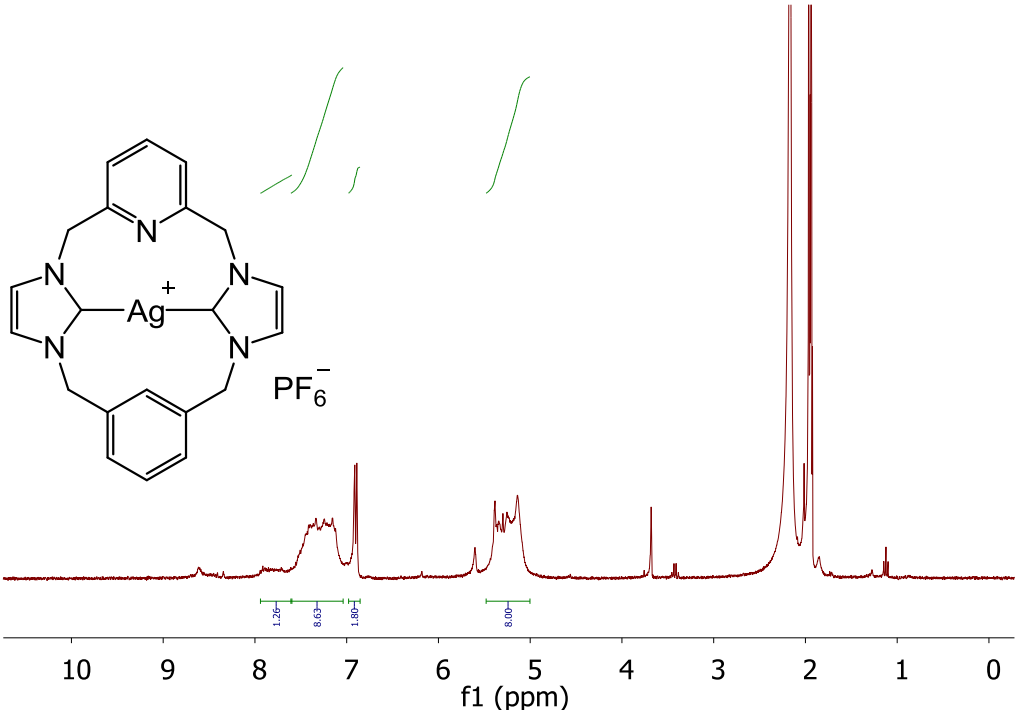

Ag**L75**(PF_6): ^1H = NMR (300 MHz, CD_3CN)

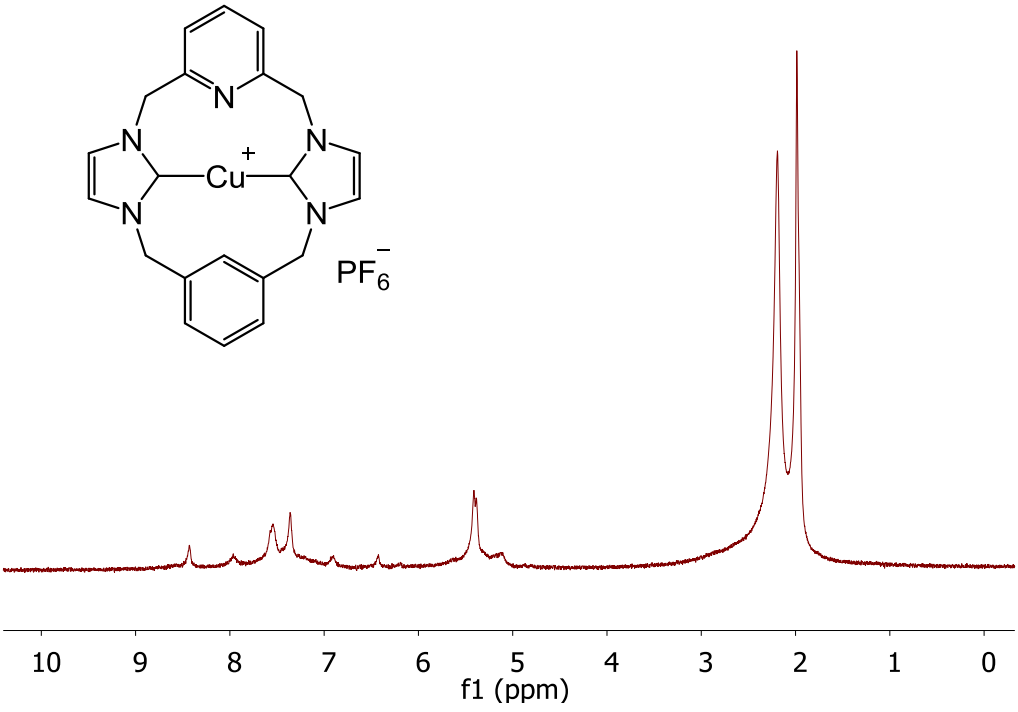

Cu**L75**(PF_6): ^1H = NMR (300 MHz, CD_3CN)

Supplementary Information on Compound X-ray Crystallography Analysis

S8.a:

Identification code	RW49a
Empirical formula	$C_{14.33}HN_{11.33}Cu_2Br_{4.67}$
Formula weight	830.92
Temperature/K	120.0(2)
Crystal system	monoclinic
Space group	$P2_1/n$
a/Å	10.0973(4)
b/Å	18.5632(7)
c/Å	12.1813(5)
α/°	90.00
β/°	102.343(4)
γ/°	90.00
Volume/Å^3	2230.46(15)
Z	6
ρ_{calc}g/cm^3	3.712
μ/mm^{-1}	15.444
F(000)	2320.0
Crystal size/mm^3	? × ? × ?
Radiation	MoKα (λ = 0.71073)
2Θ range for data collection/°	6.3 to 62.4
Index ranges	-14 ≤ h ≤ 13, -26 ≤ k ≤ 26, -16 ≤ l ≤ 17
Reflections collected	17703
Independent reflections	6356 [R_{int} = 0.0586, R_{sigma} = 0.0862]
Data/restraints/parameters	6356/0/244
Goodness-of-fit on F^2	1.766

Final R indexes [I>=2σ (I)]	R_1 = 0.1166, wR_2 = 0.2891
Final R indexes [all data]	R_1 = 0.1660, wR_2 = 0.3124
Largest diff. peak/hole / e Å^{-3}	8.45/-7.66

PS8:

Identification code	RW37
Empirical formula	$C_8H_6BrN_3$
Formula weight	224.07
Temperature/K	120.1(4)
Crystal system	monoclinic
Space group	$P2_1/n$
a/Å	3.85834(19)
b/Å	17.1193(12)
c/Å	11.9087(5)
α/°	90.00
β/°	90.029(4)
γ/°	90.00
Volume/Å^3	786.60(8)
Z	4
ρ_{calc}g/cm^3	1.892
μ/mm^{-1}	5.164
F(000)	440.0
Crystal size/mm^3	? × ? × ?
Radiation	Mo Kα (λ = 0.71073)
2Θ range for data collection/°	6.84 to 62.42
Index ranges	-5 ≤ h ≤ 5, -22 ≤ k ≤ 23, -17 ≤ l ≤ 13
Reflections collected	5035

Independent reflections	2203 [R_{int} = 0.0507, R_{sigma} = 0.0782]
Data/restraints/parameters	2203/0/109
Goodness-of-fit on F^2	1.024
Final R indexes [I>=2σ (I)]	R_1 = 0.0470, wR_2 = 0.0763
Final R indexes [all data]	R_1 = 0.0743, wR_2 = 0.0838
Largest diff. peak/hole / e $Å^{-3}$	0.66/-0.58

S8.b:

Identification code	RW38
Empirical formula	$C_{11}H_{11}Br_2N_3$
Formula weight	345.05
Temperature/K	119.97(16)
Crystal system	monoclinic
Space group	$P2_1/c$
a/Å	10.2246(7)
b/Å	7.7322(4)
c/Å	15.8412(7)
α/°	90.00
β/°	103.205(6)
γ/°	90.00
Volume/$Å^3$	1219.27(12)
Z	4
$\rho_{calc}g/cm^3$	1.880
μ/mm^{-1}	6.624
F(000)	672.0
Crystal size/mm^3	0.21 × 0.08 × 0.03
Radiation	MoKα (λ = 0.71073)

2Θ range for data collection/°	6.68 to 56.56
Index ranges	-12 ≤ h ≤ 13, -10 ≤ k ≤ 10, -21 ≤ l ≤ 20
Reflections collected	7751
Independent reflections	3037 [R_{int} = 0.0380, R_{sigma} = 0.0500]
Data/restraints/parameters	3037/0/145
Goodness-of-fit on F^2	1.058
Final R indexes [I>=2σ (I)]	R_1 = 0.0342, wR_2 = 0.0641
Final R indexes [all data]	R_1 = 0.0536, wR_2 = 0.0708
Largest diff. peak/hole / e $Å^{-3}$	0.46/-0.67

[Cu**L76**]$(PF_6)_2$:

Identification code	RW302-1
Empirical formula	$C_{20}H_{18}CuF_{12}N_6P_2$
Formula weight	695.88
Temperature/K	119.97(17)
Crystal system	monoclinic
Space group	C2/c
a/Å	13.5194(6)
b/Å	11.8103(3)
c/Å	17.2239(7)
α/°	90
β/°	111.094(5)
γ/°	90
Volume/$Å^3$	2565.83(19)
Z	4
ρ_{calc}g/cm^3	1.801
μ/mm^{-1}	3.438

F(000)	1388.0
Crystal size/mm^3	0.1572 × 0.1072 × 0.0709
Radiation	CuKα (λ = 1.54184)
2Θ range for data collection/°	10.26 to 147.326
Index ranges	-16 ≤ h ≤ 14, -13 ≤ k ≤ 14, -18 ≤ l ≤ 21
Reflections collected	4598
Independent reflections	2509 [R_{int} = 0.0174, R_{sigma} = 0.0232]
Data/restraints/parameters	2509/0/223
Goodness-of-fit on F^2	1.074
Final R indexes [I>=2σ (I)]	R_1 = 0.0307, wR_2 = 0.0818
Final R indexes [all data]	R_1 = 0.0331, wR_2 = 0.0836
Largest diff. peak/hole / e $Å^{-3}$	0.33/-0.40

Calculations on ln plots for the kinetics of the arylation of C46

i) Pseudo 1st order on [**C46**] using [**C46**] versus time

$$[\boldsymbol{C46}] = x$$
$$-\frac{dx}{dt} = k'x$$
$$\int_0^t k'dt = -\int_{x_0}^{x} \frac{1}{x}dx$$
$$k't - 0 = lnx_0 - lnx$$
$$lnx = -k't + lnx_0$$

ii) Pseudo 1st order on [**C46**] using [**Ar46**] versus time

$$[\boldsymbol{Ar46}] = y$$
$$[\boldsymbol{C46}] = 0.05 - y$$
$$\frac{dy}{dt} = k'(0.05 - y)$$
$$\int_0^t k'dt = \int_0^y \frac{1}{0.05 - y}dy$$
$$k't - 0 = \ln(1 - 20y) - \ln(1)$$
$$\ln(1 - 20y) = -k't$$

iii) 2nd order on [**C46**] and [4-iodoanisole] using [**C46**] versus time

$$[\boldsymbol{C46}] = x$$
$$[ArI] = 0.25 - 0.05 + x = 0.2 + x$$
$$-\frac{dx}{dt} = k(x)(0.2 + x)$$
$$\int_0^t kdt = -\int_{0.05}^{x} \frac{1}{x(0.2 + x)}dx$$
$$kt - 0 = -\left(-5\ln\left(5 + \frac{1}{x}\right) + 5\ln(100)\right)$$
$$kt = 5\ln\left(5 + \frac{1}{x}\right) - 5\ln(100)$$
$$5\ln\left(5 + \frac{1}{x}\right) = kt + 5\ln(100)$$

iv) 2nd order on [**C46**] and [4-iodoanisole] using [**Ar46**] versus time

$$[\boldsymbol{Ar46}] = y$$
$$[\boldsymbol{C46}] = 0.05 - y$$
$$[ArI] = 0.25 - y$$
$$\frac{dy}{dt} = k(0.05 - y)(0.25 - y)$$
$$\int_0^t kdt = \int_0^y \frac{1}{(0.05 - y)(0.25 - y)}dy$$

$$kt - 0 = -5\ln\left(5 + \frac{4}{4y-1}\right) + 5\ln(1)$$

$$5\ln\left(5 + \frac{4}{4y-1}\right) = -kt$$

Calculation on structures of $[CuL76](PF_6)_2$

$$known; \text{‹}(NHC - Cu - py) = \theta = 90.08°$$

$$\text{‹}(NHC - Cu - F) = \varphi = 82.049°$$

$$\text{‹}(py - Cu - F) = \omega = 82.693°$$

$$assume; \quad Cu - F = a$$

$$x = a\ cos\varphi$$

$$y = a\ cos\omega sin\theta$$

$$z^2 = a^2sin^2\varphi - a^2cos^2\omega sin^2\theta$$

$$z = \sqrt{a^2sin^2\varphi - a^2cos^2\omega sin^2\theta}$$

$$XY = \sqrt{a^2cos^2\varphi + a^2cos^2\omega sin^2\theta}$$

$$\text{‹}(Z - Cu - F) = tan^{-1}\frac{\sqrt{a^2cos^2\varphi + a^2cos^2\omega sin^2\theta}}{\sqrt{a^2sin^2\varphi - a^2cos^2\omega sin^2\theta}}$$

$$= 10.831°$$